NTIA Report 83-136

Computation of Linear Communication Antennas

J. L. Lloyd

U.S. DEPARTMENT OF COMMERCE
Malcolm Baldrige, Secretary
David J. Markey, Assistant Secretary
for Communications and Information

October 1983

PREFACE

This report concerns antenna models and computer subroutines intended to be used with a larger program, the IONospheric Communications Analysis and Prediction (IONCAP) program. This introductory section is a general description of the larger program. The body of this report is arranged to agree with the reports describing the IONCAP program.

For many years, numerous organizations have been employing the high frequency (HF) spectrum to communicate over long distances. It was recognized, in the late thirties, that these communication systems were subject to marked variations in performance. The effective operation of long distance HF systems increased in proportion to the ability to predict variations in the ionosphere, since such an ability permitted the selection of optimum frequencies, antennas, and other circuit parameters. A worldwide network of ionosondes was established to measure ionospheric parameters. Worldwide noise measurement records were taken, and variations in signal amplitudes were recorded over various HF paths. The results of this research established that most variations in HF system performance are directly related to changes in the ionosphere, which in turn are related in a complex manner by solar activity, seasonal and diurnal variations, as well as latitude and longitude.

By 1948, a treatise on ionospheric radio propagation was published by the Central Radio Propagation Laboratory (CRPL) of the National Bureau of Standards. This document (CRPL, 1948) outlined the state of the art in HF propagation. Manual techniques were given for analyzing HF circuits of short, intermediate, and long distances. Because the manual methods were laborious and time consuming, various organizations developed computer programs to analyze HF circuit performance. All these programs were based on manual methods for short or intermediate distances and used various numerical representations of the ionospheric data. The program described here is a direct descendant of these programs. Use of such an HF prediction program and required input parameters and output options is described in OT Report 76-102 (Haydon et al., 1976).

The Ionospheric Communications Analysis and Prediction Program (IONCAP) was designed in modular form and coded in simple FORTRAN following as much as possible the ANS Standard. The modular form allows any subsection to be replaced without affecting the rest of the program. As much as possible, table look-up techniques were used to reduce computer run time, to facilitate the modular structure, and to determine the possible pitfalls of any subsection. In particular, iterative search procedures were eliminated as these tend to become unstable under some ionospheric conditions. The program is divided into seven largely independent sections:

1. input subroutines,
2. path geometry subroutines,
3. antenna subroutines,
4. ionospheric parameter subroutines,
5. maximum usable frequency subroutines,
6. system performance subroutines, and
7. output subroutines.

This report describes the revisions to the antenna subroutines.

The input subroutines handle the various input options. There are three kinds of input: card images, a long-term data tape image, and an antenna tape image. The card images contain various circuit parameters and control run options. The long-term data tape contains numerical coefficients for ionospheric parameters and for atmospheric noise as well as various tables of parameters needed for circuit performance. The antenna tape contains optional antenna patterns which can be generated by the IONCAP program or from some other source. Simplification of the input card images, along with greater input flexibility as well as extended and newly developed input features, provide significant improvements in this section over previous models.

The path geometry subroutines determine the circuit geometry, select optimum areas to sample the ionosphere, and evaluate the magnetic field at these sample areas. There are no significant improvements in this section over previous models.

The antenna subroutines process antenna data input cards, calculate antenna gains, and output antenna patterns. These subroutines assume the antennas are associated with existing systems that have been properly designed.

The ionospheric parameter subroutines evaluate all ionospheric parameters needed by the program. The old programs assumed an implicit two parabola ionosphere. A complete explicit electron density profile is used in this program. The profile includes a D-E region starting at 70 km, an F2 region, an F1 ledge, and an E-F valley. [A method of including the top side is given in a Radio Science article (Haydon and Lucas, 1968)]. Any electron density profile subroutine could be substituted for this one and not affect the operation of the program. It has been found that traditional empirical absorption equations using the secant law will not work at those lower frequencies with corresponding heights from an electron density profile lower than 90 km. This problem has been corrected in this program.

The Maximum Usable Frequency (MUF) subroutines evaluate MUFs and Optimum Traffic Frequencies (FOT). The method is a direct evaluation of the junction frequency (for 50 percent of the days) rather than an iterative search. A corrected form of Martyn's theorem is used. The E, F1, and F2 layer MUFs are considered. There is also a separate sporadic-E MUF calculation. The program also includes the old manual nomogram method as an option (Lucas and Haydon, 1961).

The system performance subroutines evaluate all needed circuit parameters. There are two separate sets of subroutines, one for shorter distances (less than 10000 km) and one for long distances. The models for the shorter distances are replacements for previous computer programs. The long path models have not previously been incorporated into a computer program. The short path models correspond to the manual method in ITS-81 (Haydon et al., 1969). A manual method corresponding to the long path models is given in NBS Report 462, (CRPL, 1948). The user may run either set of subroutines for any given distance (overriding the 10000 km breakpoint). Somewhat pardoxically the two models are identical for one-hop circuits. The short path model evaluates each possible ray path for the circuit; high and low angle, E, F1, and F2 modes, possible over-the-MUF modes, and sporadic-E modes. Losses include regular D-E absorption (CCIR-252 loss), deviative losses, and sporadic-E losses. The CCIR-252 loss was only for F2 modes. For E-layer modes, an additive corrective factor was developed and used. For lower frequencies, which have low reflection heights (less than 90 km), a correction to the frequency dependence was added. The noise at the receiver site is evaluated as well as the mode, signal, and noise statistics.

The short distance model applied to long paths would lead to the expectation that failure of propagation at any of the reflection areas would cause propagation to fail altogether. Empirically, however, it has been found that propagation does not fail until the ionosphere at control areas about 2000 km from each end of the path fails to support propagation. The long-distance model evaluates the optimum radiation angle at the transmitter and the optimum reception angle at the receiver, using an antenna-gain-minus-ionosphere-loss function. Losses are as for the short paths at each end of the path with a loss-per-kilometer function used to fill in the path. Noise and signal statistics are as for the short paths.

A complete HF communications systems performance program has been rewritten. The chief limitations to improvements are not primarily those of the computer state-of-the-art nor of theoretical, physical, or mathematical ignorance, but of lack of better statistical knowledge of the circuit parameters and their interrelations. Approximately six areas of research were incorporated into this revision of the program. Much of the improvements result from the combined efforts of various laboratories, both government and private, and both domestic and foreign.

1. The description of the ionosphere is now more complete.
2. The loss equations have been supplemented. This includes E-mode adjustments, sporadic-E effects, over-the-MUF losses, and losses for low reflection heights.
3. Revision was made to the ray path geometry calculations. This was an empirical adjustment of Martyn's theorem.
4. Revision of the loss statistics was made to include the effects of sporadic-E layer, and of over-the-MUF modes.
5. A separate long-path model was developed.
6. Revisions made to the antenna gain models are described in this report.

Although this program was coded so that revision of any subpart is relatively easy, the hardest part of joining so many diverse submodels is to assure consistency and continuity of the entire program. The whole in this case is much more than a sum of the parts.

TABLE OF CONTENTS

LIST OF FIGURES

LIST OF FIGURES

LIST OF FIGURES

LIST OF TABLES

LIST OF TABLES

LIST OF MAJOR SYMBOLS

The more frequently used symbols appear here. These symbols that are grouped together by definition are first shown.

(R, θ, ϕ)	Spherical coordinate system, see Figure 6.
(x, y, z)	Cartesian coordinate system.
R_V	Vertical reflection coefficient.
C_V	Absolute value of R_V.
ψ_V	Phase of R_V; check normalization in text.
ψ'_V	$\psi_V + 2kh \cos \theta$; phase including height, h, above ground.
R_H	Horizontal reflection coefficient
C_H	Absolute value of R_H.
ψ_H	Phase of R_H, check normalization in text.
ψ'_H	$\psi_H + 2kh \cos \theta$; phase including height, h, above ground.

GREEK LETTERS:

γ	Euler's constant, 0.5721^+.
Δ	Angle of elevation measured from tangent to earth's surface.
ε_r	Relative dielectric constant.
η	Impedance of free space ($\sim 120\pi \sim 377$).
θ	Angle of elevation, measured from normal to earth's surface; used in spherical coordinate system.
λ	Wavelength.
μ	Permeability.
π	3.14^+.
ϕ	Angle between x-axis and reference point; used in spherical coordinate system.
ψ_a	Angle between antenna wire and far field reference point.
ψ'_a	Angle between image of antenna wire and far field reference point.
ω	Angular frequency.

LIST OF MAJOR SYMBOLS

ROMAN LETTERS:

a	Radius of the earth.
C_i	Cosine integral.
C_{in}	Modified cosine integral $C_{in}(\alpha) = \gamma + \log_e \alpha - c_i(\alpha)$.
D	Ground distance.
E	Field strength, dBu.
e	Field strength, volts/meter.
e_o	Reference field strength isotropic antenna in free space.
e_p	Primary field; used to gather constants into one symbol in antenna equations.
E_θ	Theta component of far field.
E_ϕ	Phi component of far field.
F_{cs}	Absolute value of cymomotive force; used by CCIR to describe antenna gain. $G = 20 \log_{10} (F_{cs}/173.2)$, dBI.
f	Operating frequency, MHz.
G	Gain of antenna, dBI.
g	Gain of antenna. $G = 10 \log_{10} g$.
H, h	Height of antenna.
I	Current on antenna.
I_m	Maximum value of antenna current.
L	Length of antenna wire or dipole.

COMPUTATION OF LINEAR COMMUNICATION ANTENNAS

John L. Lloyd*

This report contains a consolidation of practical engineering equations for linear communication antennas suitable for use in the prediction and analysis of the system performance of high frequency communication equipment. The theoretical background and the nature of the approximations are discussed. Complete equations are provided. Examples of the computations are given for each type of antenna.

SECTION I - THEORY

1. INTRODUCTION

The Institute for Telecommunication Sciences (ITS) undertakes studies of the ionosphere in order to predict ionospheric propagation effects. The basic prediction program used for assessing ionospheric propagation conditions was intended to provide the necessary data for the design of HF communication systems and for selection of frequency complements for such systems. The computer program, Ionospheric Prediction and Analysis Program (IONCAP) is described elsewhere in an unpublished document by J. L. Lloyd, D. L. Lucas, G. W. Haydon, and L. R. Teters entitled "Estimating the performance of telecommunication systems using the ionospheric transmission channel--Techniques for analyzing ionospheric effects upon HF systems." This report describes the antenna models and program code to be used with the IONCAP program.

The intention of this work was to create an antenna package to be used with the HF skywave predictions. The radio waves considered here have been reflected from the ionosphere and thus have traveled a considerable distance. This allows the separation of the problem into two parts: the local effect of the ground at the transmitting site on the antenna, and similarly the local effect of the ground at the receiving site on the antenna. Further, the assumption of plane wave reflection is justified for this skywave case. While many workers have studied this problem over the last 50 years, the basic references and sources for the models used here are depicted in Figure 1. The plane wave reflection method and appropriate experiments are described in Feldman (1933). A general method of analyzing antennas was described by Schelkunoff (1939). Laitinen (1957) combined

*The author is with the U.S. Department of Commerce, National Telecommunications and Information Administration, Institute for Telecommunication Sciences, Boulder, Colorado 80303

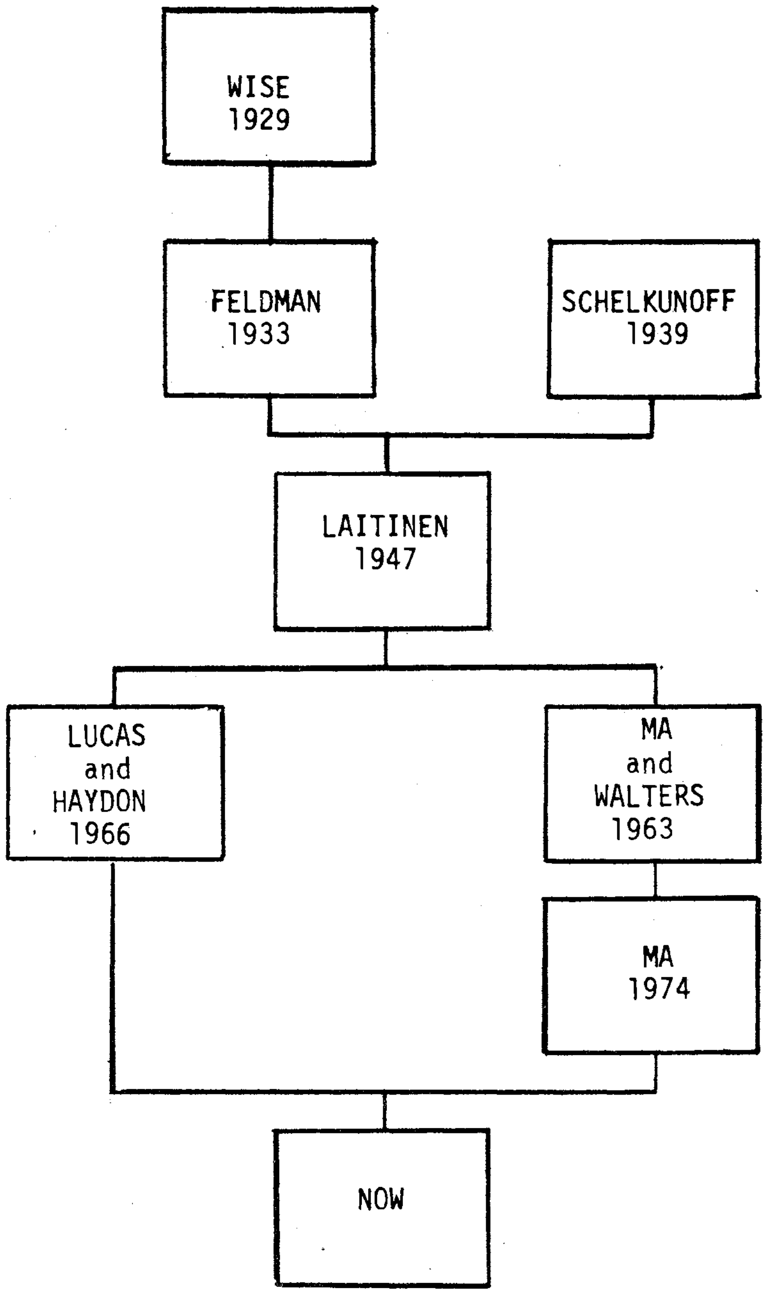

Figure 1. General flow of development of antenna models.

these methods into a general analysis of skywave atennas. Ma (1974) continued the work in a series of reports, most of which is included in the monograph referenced. Since the report by Laitinen is not generally available, the development of the general integral equations used is reproduced as Section 3 of this report. The theoretical development then continues as in the monograph by Ma (1974), page 243, ff. No ground wave effects are to be included in the antenna patterns included here. The appropriate patterns for use with the ground wave will depend on the ground wave model used (see e.g., Norton, 1941, Bremmer, 1949, or Okumura et al., 1968).

No new theory is included in this report, the effort was directed to development of a simple, reasonably accurate submodule to be used with skywave predictions in which the overwhelming uncertainties are in the effect of the ionosphere, and which are described only on a statistical basis over monthly or seasonal periods. The analysis of the antenna models was broken into two logical subdivisions (Carrel, 1964):

(1) the exterior (radiation) problem that deals with the interaction of the antenna with the propagation medium, and

(2) the interior (circuit) problem that deals with the interaction of currents, voltage, etc., within the antenna system itself.

The solution to the interior problem is implemented as precalculated curves or measured curves where available. The exterior problem is implemented using the full equations as developed by Ma (1974). For arrays of dipoles, the practice used by Uda of expressing the array equations as that of the resonant dipole element and a reduced array factor (Uda and Mushiake, 1954) is introduced. This procedure results in computer code that is quite stable and fast in running time. There are no matrix inversion routines nor any use of the complex arithmetic routines.

The revised code includes all the antenna types previously included with the IONCAP program. The old antenna submodules were designated as ITSA-1 (Rev. 1977), which corresponded to the ITSA-1 prediction program (Lucas and Haydon, 1966) and as ITS-78 (Rev. 1977) which corresponded to the ITS-78 prediction program (Barghausen et al., 1969). A version of the ITSA-1 code Appendix F of Lucas and Haydon, 1966 was used as the basis of the revised code since this contained more antenna types and more stable code. The code was subdivided into separate modules and then additional antenna types added. The initial version of the revised code is designated as IONCAP VERSION 82.02 (second version completed in 1982). The primary simplification used was to solve the interior problem in free space. The resulting antenna patterns are reasonably accurate when the antenna systems are well designed, and the frequency complement specified is within the design limits.

2. FIELDS AND POWER GAIN

The antenna subroutine included in the program is a modification of the one from the ITSA-1 program (Lucas and Haydon, 1966). This subroutine is relatively fast and contains simple models which assume that the antennas were well designed.

Basically there are three quantities in the evaluation of the antenna gain: the power gain as a function of elevation and azimuth angles (and frequency, of course), the input resistance looking into the antenna feed point (i.e., the radiation resistance), and the ability of the antenna to radiate the power supplied to it (i.e., the antenna efficiency). Both the power pattern and the radiation resistance depend greatly upon the current distribution along the antenna, the environmental conditions, and the mutual interaction among antennas if there are more than one in the system. The antenna model follows the common convention of assuming a sinusoidal current distribution on all the wire antennas. With this assumption, the calculation of power patterns including the ground effect is rather straightforward. Evaluation of radiation resistances with the ground influence included is, however, still somewhat difficult for some antenna models. The basic reference for the models used has been taken as the ITS-74 report (Ma and Walters, 1969). Any questions of difficulties with the equations have been resolved by taking the values given in that report as standard.

2.1 Basic Definitions and Standards

In this section, some basic equations and standards used for both skywave and ground wave propagation are collected. The standard reference antenna for skywave propagation is the isotropic antenna in free space. For ground wave propagation, the standard reference antenna is the short vertical over a perfectly conducting ground. The equations to be used for these antennas are given. The skywave antennas are to be used with the calculation of system loss so a short description of this is given also.

The isotropic antenna in free space is an omnidirectional antenna, i.e., radiates equally in all directions, and is placed in free space, a homogeneous, nonabsorbing medium of dielectric constant unity. This is, of course, a fictitious situation, unrealizable in practice, but used to standardize the antenna gains and transmitted power. The field intensity or power density in free space is given by (Norton, 1959)

$$\frac{e^2}{\eta} = \frac{p_r}{4\pi D^2} \quad (1)$$

where

- e is the field strength, volts/meter
- η is the impedance of free space, ohms
- p_r is the radiated power, watts
- D is the distance from the antenna, meters.

The $4\pi D^2$ reflects the use of a sphere and the η reflects the use of free space. The impedance is given by:

$$\eta = 4\pi c 10^{-7} \text{ ohms ;} \quad (2)$$
$$= 120\pi$$

where

- c is the velocity of light in free space.

The primary field from an isotropic antenna is then

$$e_o = \sqrt{30}\,\sqrt{p_r}/D \quad ; \text{ V/m.} \quad (3)$$

Here p_r is the actual radiated power, not the power output of the transmitter nor the power input to the antenna.

At a standard distance of 1 km and a power of 1 kW, the field strength is

$$e_o = 173.2 \text{ mV/m or } 104.8 \text{ dBu.}$$

This is for a full sphere; if a half-sphere, i.e., over a perfectly conducting plane, the field intensity is doubled

$$e_o = 245 \text{ mVm or } 107.8 \text{ dBu.}$$

Following Ramo and Whinnery (1960), the gain, g, relative to an isotropic source is defined as the ratio of power required from the isotropic source to produce the given intensity in the desired direction to that required from the actual antenna:

$$g = \frac{4\pi r^2 P_{AV}}{W} = \frac{4\pi D^2 P_{AV}}{\frac{1}{2} R I^2} , \quad (4)$$

where

$P_A V$ = the time average Poynting vector, i.e., power flow through a reference sphere,

D = the distance from the origin of the coordinate system to point in space,

W = the total radiated power in free space,

R = the radiation resistance of the antenna, ohms, and

I = the input current to the antenna, amperes.

Here $P_A V$ is related to the radiated power, p_r, (equal when reference antenna and units are added as below):

$$p_r = I^2 R . \tag{5}$$

When the efficiency factor is used to account for heating losses, the antenna input power is (Laitinen, 1957):

$$p_i = I^2 (R_{radiation} + R_{loss}). \tag{6}$$

The antenna subroutines as used here and HF prediction methods used at ITS and the CCIR 252-2 method required the antenna input power.

The HF prediction methods are based on the concept of system loss. The system loss (Rice et al., 1965) of a radio circuit consisting of a transmitting antenna, receiving antenna, and the intervening propagation medium is defined as the dimensionless ratio, p_r/p_a, where

p_r is the radio frequency power input into the terminals of the transmitting antenna, and

p_a is the resultant radio frequency signal power available at the terminals of the receiving antenna. The system loss is usually expressed in decibles:

$$L_s = 10 \log_{10} (p_r/p_a). \tag{7}$$

From transmitter output to receiver input, the situation is depicted in Figure 2.

L_{et} is power radiation efficiency for the transmitting antenna.

L_{er} is power reception efficiency for the receiving antenna.

$L_{\ell t}$ is the loss from transmitter to antenna and includes both transmission line and mismatch losses.

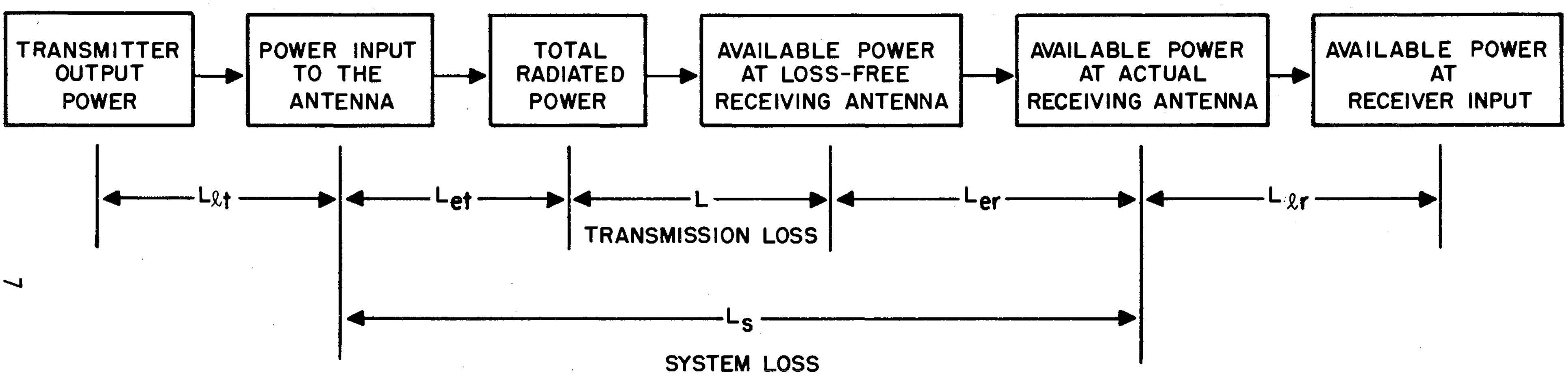

Figure 2. System loss for a radio circuit.

$L_{\ell r}$ is the loss from the transmitter to the receiver antenna and includes the transmission line loss between the antenna and the receiver, but not the mismatch losses.

L is the transmission loss defined as the ratio of the total radiated power to the available power from an equivalent loss-free antenna.

Two other loss terms are (1) basic transmission loss, L_b, which is system loss when the real antennas are replaced by isotropic antennas, and (2) free space basic transmission loss, L_{bf}, the loss occurring when only the spreading loss in free space is considered (but with isotropic antennas). The reception area of an isotropic antenna is

$$\text{area} = \frac{\lambda^2}{4\pi} \tag{8}$$

where

λ is the wavelength in same units as the distance D.

This gives the free space basic loss as (CCIR 252-2, 1970):

$$L_{bf} = 10 \log_{10} \left[\frac{p_r}{p_r \, \lambda^2/(4\pi D)^2} \right]$$

$$= 32.44 + 20 \log_{10} f + 20 \log_{10} D \tag{9}$$

where

f is the operating frequency in MHz

and

D is the distance in kilometers.

The inclusion of medium losses and dielectric losses and antenna circuit losses in the system loss, L_s, provides a quantity which can be directly and accurately measured. Transmission loss and basic transmission loss are theoretical values which can be used to compare radio circuit performance.

Another measure used to evaluate radio circuit performance is the incident field intensity at a specified distance from a transmitter. This is commonly called field strength (although it is e^2 not e). The receiver antenna is by definition taken as an isotropic antenna. The relation between field strength and basic transmission loss is (Norton, 1959):

$$p_a = \frac{p_r}{\ell_b} = \frac{e^2}{\eta} \frac{\lambda^2}{4\pi} \tag{10}$$

where the variables are as in equation (1), and

$$L_b = 10 \log_{10} \ell_b \ . \tag{11}$$

Solving for e^2:

$$e^2 = p_r \, \eta \left(\frac{4\pi}{\lambda^2}\right) \frac{1}{\ell_b} \ ; \quad (V/m)^2$$

$$= p_r \left[\frac{(120\pi)\ (4\pi)}{(c^2/f^2)}\right] \left(\frac{1}{\ell_b}\right);$$

$$= p_r \left[\frac{480\pi^2}{(300)^2}\right] f^2 \left(\frac{1}{\ell_b}\right); \quad (V/m)^2 \ .$$

The units of frequency, f, were taken as MHz and changing the intensity to squared μV/m

$$e^2 = p_r \left[\frac{480\pi^2}{(300)^2}\right] f^2 \quad \frac{10^{12}}{\ell_b} \qquad ; \quad (\mu V/m)^2 \ .$$

Now change to decibels above a μV/m;

$$E = 107.21 + 20 \log_{10} f + P_r - L_b \ . \tag{12}$$

Changing to a real transmitting antenna:

$$E = 107.21 + 20 \log_{10} f + P_t + G_t - L_b \tag{13}$$

where

- E is rms field strength in dBu,
- f is frequency in MHz,
- P_t is antenna input power, dBu,
- G_t is transmitter antenna gain, dBI (decibels above an isotropic antenna) with efficiency factor included.
- L_b basic transmission loss, dB.

The HF prediction methods as well as the CCIR method use equation (13) in this form and units. Evaluating equation (13) for a standard power of 1 kW and distance of 1 km for only free space losses [equation (9)].

$$E = 107.2 - 20 \log_{10} f + 30. + 0.$$
$$-32.44 - 20 \log_{10} f - 20 \log_{10} 1.$$

$$E = 104.8 \text{ dBu, i.e., } e_o = 173.2 \ \text{mV/m},$$

which are the same numbers as evaluated with equation (3).

The ground wave reference standard is a short, vertical antenna over perfect ground radiating 300 mV/m at 1 km [compare with equation (3)].

$$e_0 = 3\sqrt{10}\,\sqrt{p_r}/D \quad ; \quad V/m . \qquad (14)$$

For a standard power of 1 kW and distance of 1 km,

$$e_0 = 300 \text{ mV/m or } 109.54 \text{ dBu}.$$

The 300 is not arbitrary; it is an approximation of $\sqrt{3c10^{-8}}$ 100,

c is the speed of light (Norton, 1959).

The gain of this antenna is 4.8 dBI. This antenna is used with the CCIR ground-wave curves, the methods in Bremmer (1949) and one of the ground wave programs used at ITS (GW78, L. Berry, private communication).

Using equation (13) for this antenna, the field strength is

$$\begin{aligned} E &= 107.21 + 20 \log_{10} f + 30. + 4.8 - L_b \\ &= 142 + 20 \log_{10} f - L_b \qquad (15) \end{aligned}$$

which is identical to the equation given in CCIR Report 252-2.

The confusion between the ground-wave reference antenna and the skywave reference antenna arises from the old skywave standard of effective radiated power (CRPL, 1948):

"The effective radiated power, P, radiated in a particular direction from a transmitting antenna is, for the purpose of calculations in this chapter, defined as 1/3 gp_r.

The factor 1/3 is introduced for the sake of convention, so that 1 kw of effective radiated power corresponds to a field intensity of 300,000 μv/m at 1 km, which is the field produced at 1 km in the horizontal direction by a short vertical antenna over a perfect earth, with one end on the ground, radiating 1 kw total power. The gain g of such an antenna in the horizontal plan is 3.

The effective radiated sky-wave power determines the field intensity for sky-wave propagation. Calculations of incident field intensity described later in this chapter are based upon a standard effective radiated power of 1 kw, i.e., a field intensity of 300,000 μv/m at a distance of 1 km, which, as seen from the above, corresponds to an isotropic antenna radiating 3 kw total power in free space."

The situation can then be described as either a different reference antenna or as different powers. The graphical methods in R.P.U. 9 (Laitinen, and Haydon, 1950) and NBS Circular 462 (CRPL, 1948) as well as the FTZ method (Beckmann, 1965) expect power as effective radiated power, i.e., 1/3 the radiated power of an isotropic antenna, or are referenced to a short dipole over perfect ground. The method used with computers at ITS as well as the CCIR 252-2 method require power, P_t, input to the antenna and gain, including efficiency factor, referenced to an isotropic antenna in free space. The difference, neglecting efficiency factors, is 4.8 dBW in power or 4.8 dBI in antenna gain.

One more reference is used by the CCIR (ITU, 1978), "the value of cymomotive force (c.m.f.) on a half-sphere above the ground centered at the antenna and of radius which is large compared to the physical and electrical dimensions of the antenna."

The electric field, e, in mV/m at a distance of 1 km for 1 kW radiated power is numerically equal to c.m.f. F_{cs}. The maximum value of F_{cs} is given as

$$F_{cs}(\max) = \frac{200\sqrt{3\pi}}{\sqrt{\int_0^{2\pi}\int_0^{\pi/2} F^2(\phi, \theta)\cos\theta \, d\theta d\phi}} \quad ; \text{ volts} \tag{16}$$

where

F is the normalized radiation pattern, maximum value is 1.

(ϕ, θ) are the spherical coordinate angles.

For an isotropic antenna, F is identically 1, so

$$F_{cs}(\max) = \frac{200\sqrt{3\pi}}{\sqrt{2\pi}} \quad ; V$$

$$= \left(\frac{2}{\sqrt{2}}\right)\sqrt{3}\,(100) \quad ; V$$

$$= (\sqrt{2})(\sqrt{3})(100) \quad ; V.$$

The integration with respect to θ, was over a half-sphere, so halve for free space (half the intensity)

$$F_{cs}(\max) = \sqrt{3}\,100 \quad ; V$$

$$= 173.2 \quad ; V$$

which is numerically equal to e_0 for p_r = 1 kW and D = 1 km [equation (3)]. So to convert from F_{cs}(max) to gain, dBI,

$$G = 20 \log_{10}\left(\frac{F_{cs}\ (\max)}{173.2}\right)\ , \text{dBI.} \tag{17}$$

For the short vertical antenna; F_{cs} = 300 volts.

Some care must be taken in distinguishing the skywave pattern from the ground-wave pattern. The skywave antenna pattern is intended for waves that are reflected from the ionosphere, and thus it is proper to separate the antennas (transmitting and receiving) and consider only the effects of the ground at each antenna site and to consider the propagation as that of plane waves (Feldman, 1933). The procedure is then to use the reflection coefficient method, described later, and to integrate over the antenna structure. This method is not intended to be an evaluation of the ground wave field, although it corresponds to one of the possible approximations to the ground wave. For short distances, the ground wave consists of three factors: the direct wave, the reflected wave, and the surface wave. Although the skywave antenna patterns as given in this report were developed independently of the ground wave methods, the relationship has been described:

> "For small angles and short distances, the third term must be used together with the first order terms. As the distance is increased, the first order terms are sufficient for the specification of the field down to a very small angle which is inversely proportional to the distance. This latter property of the first order terms is very useful in computing the sky-wave radiation from antennas. In this case we are interested in the total field at the ionosphere where the waves are reflected or refracted back to earth. At high angles, the distance to the ionosphere is of the order of 100 miles, but at high angles the first order terms may be used at very short distances; at lower angles, the distance to the ionosphere becomes inversely proportional to the angle (neglecting the curvature of the earth) in just the manner required to make possible the use of the first order terms for computing the sky-wave radiation," (Norton, 1937).

The ground-wave pattern is to be used with some method of calculation that has been normalized to a standard antenna [e.g., equation (14)]. The variation of the pattern with elevation angle for the short dipole was omitted above. The equation (14) becomes

$$e_0 = (3\sqrt{10}\,\sqrt{p_r}/D)\cos\Delta \quad, \text{V/m} \tag{18}$$

where

Δ is the elevation angle (measured from the earth's surface).

The user needs to check to determine if the cosine term is in the program or curves being used.

It is possible, of course, to determine the ground-wave field from the antenna by integrating the ground-wave equations over the antenna structure. This is a complicated and expensive method, although programs exist which attempt this (e.g., Strait, 1980). The more common method is to determine the pattern of the antenna as normalized to the standard reference antenna and to compute the field strength (or system loss) using the reference antenna. When this approximation is used, the height of the antenna is the mean electrical height, $\bar{L}$, (Laitinen, 1957). This height is defined as the height at which the current can be considered to be concentrated. For a vertical antenna (Figure 3),

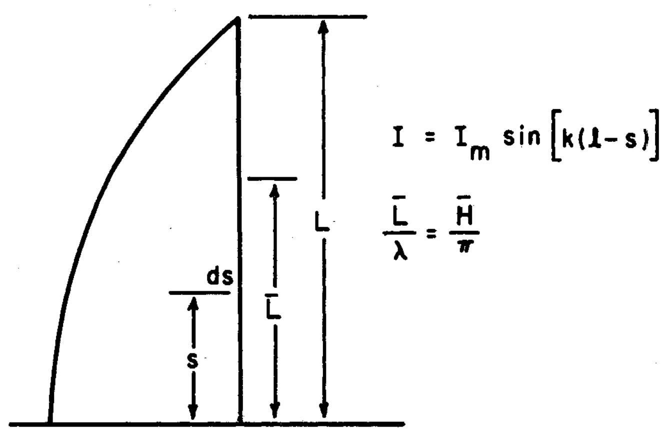

Figure 3. Mean electrical height of a vertical antenna.

$$\bar{H} = \frac{\int_0^L k\, I\, ds}{\int_0^L I\, ds} \quad, \text{radians} \tag{19}$$

where

I is the current distribution,

L is the length of the antenna,

$k = 2\pi/\lambda$, λ is wavelength.

The units are the old units, the transformation to $\bar{L}$ is

$$\bar{L} = \left(\frac{1}{\pi}\right)\bar{H}\ \lambda\ . \tag{20}$$

The results for a vertical antenna and an inverted L is given in Figure 4.

2.2 Antenna Efficiencies

The efficiency of an antenna or its ability to radiate the power supplied to it (Laitinen, 1957) is assumed in these methods to be 100 percent for horizontal non-terminated antennas, and 67 percent (1.7 dB reduction) for terminated horizontal antennas. The efficiency (F_ℓ) of an inverted "L" antenna (Figure 5) is represented by the following polynomial

$$F_\ell = 20\log_{10}(6.335\ X + 67.95\ X^2 - 693.00\ X^3 + 1600.00\ X^4)$$

$$X = \text{physical height}/\lambda \tag{21}$$

where

λ = wavelength of the operating frequency

F_ℓ = theoretical power gain to be reduced by this amount--dB.

The efficiency (F_v) of the grounded vertical antenna (Figure 5) is represented by the following polynomial

$$F_v = 25.646 - 364.817\ X + 2179.89\ X^2 - 6091.33\ X^3 + 6416.702\ X^4 \tag{22}$$

(variables are identical to above).

The above efficiencies are for a matched system; i.e., there is no mismatch loss between the antenna and the transmission line (Wolfe, 1967). The measured and theoretical values differ due to the ground system used and to antenna heat losses. The curve of Figure 5 is taken from measured and theoretical values of efficiencies (Laitinen (1957).

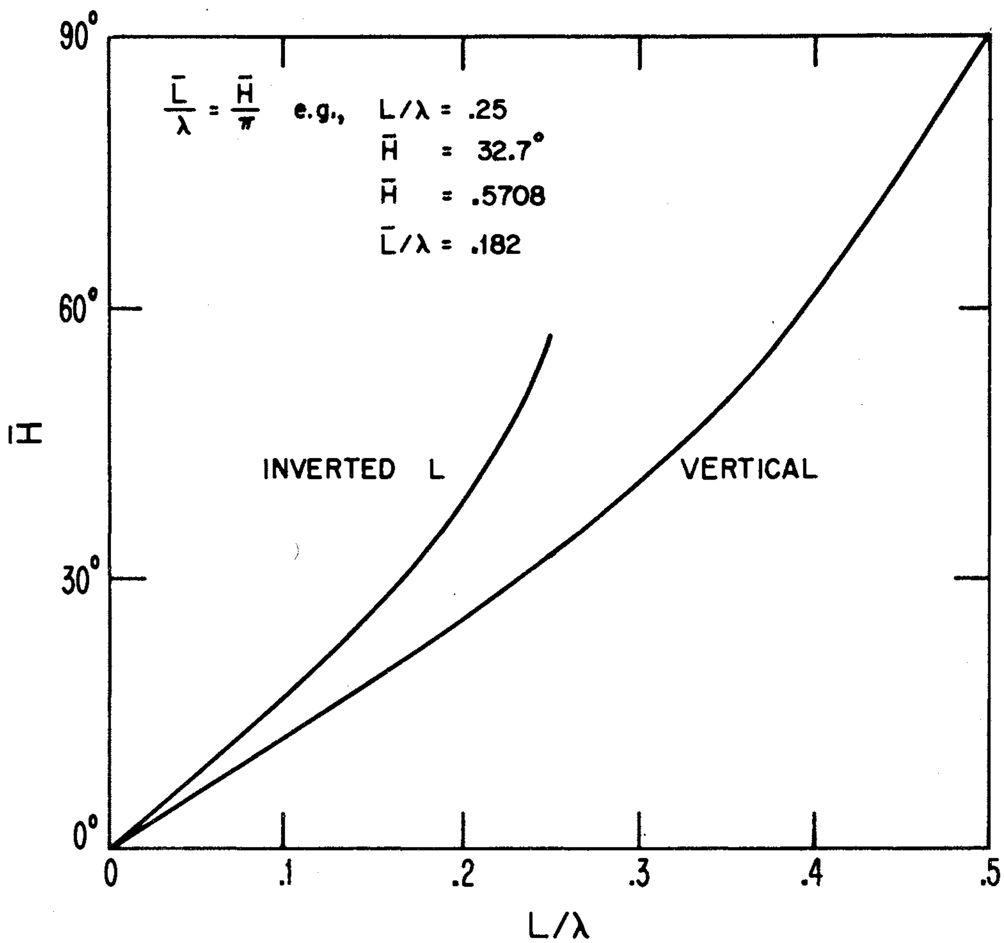

Figure 4. Mean electrical height, H, vs. physical height in fractions of one wavelength, L, grounded vertical antenna, inverted "L" antenna.

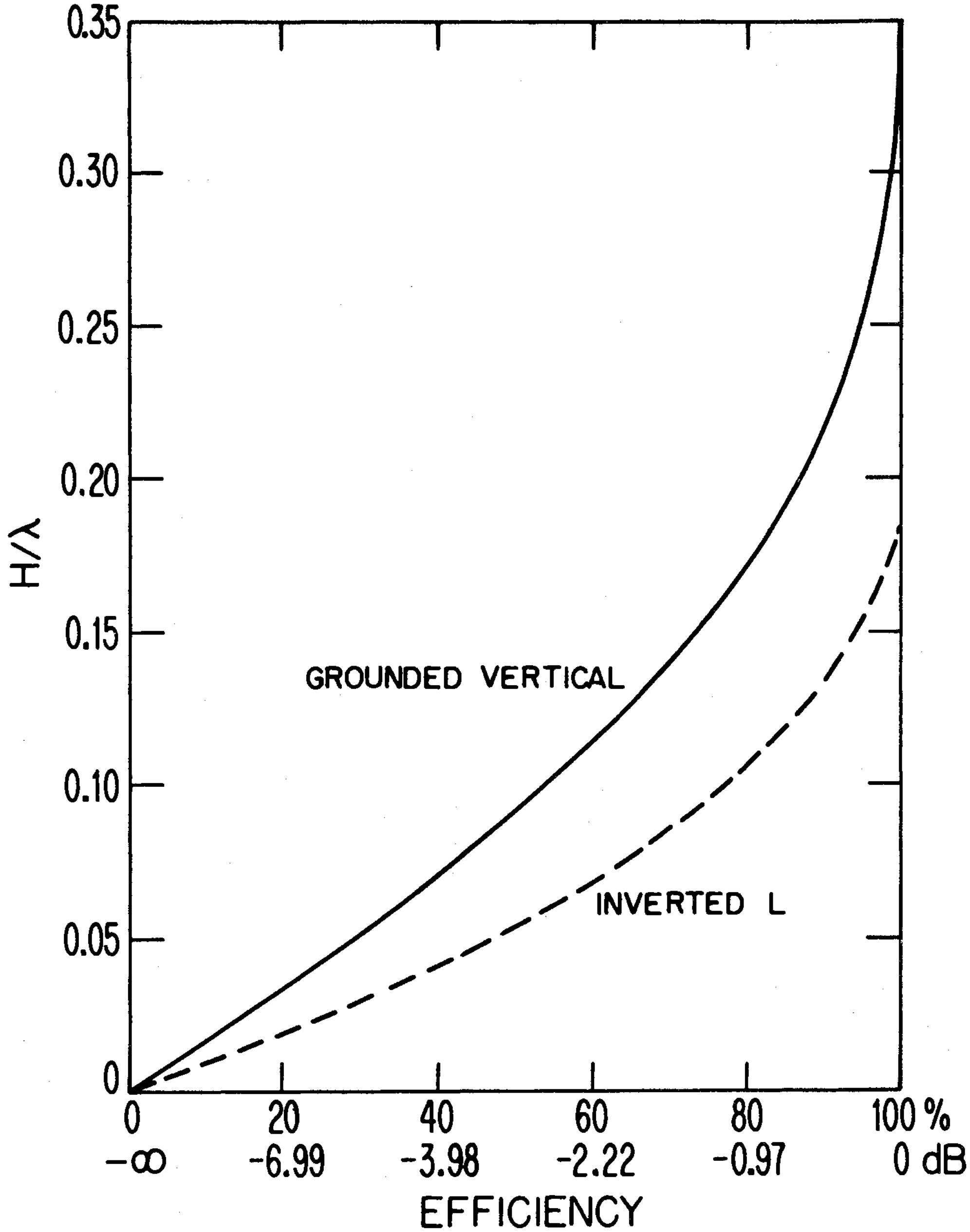

Figure 5. Efficiency of the inverted "L" and grounded vertical antennas.

For the reception of high frequency signals, the ability of the antenna to discriminate between the signal and the noise is the important consideration, since the major noise sources--atmosphere, man-made, and cosmic--are external to the antenna system. In the absence of better information, it is assumed that this external noise arrives equally from all directions, and the receiving antenna gain (performance of the antenna in the reception of this signal relative to its performance in the reception of noise) is the directive gain of the antenna; i.e., antenna efficiency is not considered in the receiving antenna gain.

The directive gain may be applied to signal-to-noise ratio predictions; however, power gain should be used when predicting system loss or receiver input power.

2.3 Reflection Coefficients

If an electromagnetic wave in air is incident on the ground, then the reflection coefficient of the wave is defined as the ratio of the field strength of the reflected wave to the field strength of the incident wave. Since the incident and reflected waves have phase as well as amplitude, the reflection coefficient is, in general, a complex number. For waves polarized parallel to the plane of incidence of the wave (vertical polarization) the reflection coefficient is (Schelkunoff and Friis, 1952)

$$R_v = \frac{(\varepsilon_r - jx)\sin\Delta - \sqrt{(\varepsilon_r - jx) - \cos^2\Delta}}{(\varepsilon_r - jx)\sin\Delta + \sqrt{(\varepsilon_r - jx) - \cos^2\Delta}} \qquad (23)$$

and for waves polarized perpendicular to the plane of incidence (horizontal polarization)

$$R_H = \frac{\sin\Delta - \sqrt{(\varepsilon_r - jx) - \cos^2\Delta}}{\sin\Delta + \sqrt{(\varepsilon_r - jx) - \cos^2\Delta}} \qquad (24)$$

where $\sqrt{\ }$ denotes the principal branch of the complex square root function, and

ε_r ≡ relative dielectric constant of earth

$$x \equiv \frac{\sigma}{\omega\varepsilon_\nu} = 18 \times 10^3\ \sigma/f \quad (25)$$

ε_ν ≡ dielectric constant of free space (farad/meter)

σ ≡ conductivity of earth (mhos/meter)

ω ≡ angular frequency

f ≡ frequency in megahertz

Δ ≡ angle of elevation in degrees, and

$j \equiv \sqrt{-1}$.

If, using the appropriate subscript V or H on R, one writes R in the form $R = |R|\ e^{i\gamma}$, then $|R|$ is the amplitude of the reflection coefficient and γ the phase. Since the function $e^{i\gamma}$ is periodic with $2\pi i$, the expression given here does not uniquely define the phase. It will, however, always be clear from the context which value of γ is being used. Letting $\psi = \gamma \pm \pi$,

$$R = -\ K\ e^{j\psi} \quad (26)$$

It is the purpose of this section to obtain K and ψ for both vertically and horizontally polarized waves. Letting $A = (\varepsilon_r - ix) - \cos^2 \Delta$, one finds that

$$A = \rho e^{j\alpha} \quad , \quad (27)$$

where

$$\rho = [(\varepsilon_r - \cos^2 \Delta)^2 + x^2]^{1/2} \quad , \quad (28)$$

and

$$\alpha = -\mathrm{Tan}^{-1}\left[\frac{x}{(\varepsilon_r - \cos^2 \Delta)}\right] . \quad (29)$$

Equation (26) can now be written as

$$R_v = \frac{(\varepsilon_r - jx)\sin\Delta - \rho^{1/2} e^{j\alpha/2}}{(\varepsilon_r - jx)\sin\Delta + \rho^{1/2} e^{j\alpha/2}} \tag{30}$$

The reduction of (23) to the form (26) gives

$$K_v = \frac{\left[\rho^2 + (\varepsilon_r^2+x^2)^2\sin^4\Delta - 2\rho(\varepsilon_r^2+x^2)\sin^2\Delta\cos\left(\alpha + 2\sin^{-1}\left[\frac{x}{(\varepsilon_r^2+x^2)^{1/2}}\right]\right)\right]^{1/2}}{\left[\rho + (\varepsilon_r^2+x^2)\sin^2\Delta + 2\rho^{1/2}(\varepsilon_r^2+x^2)^{1/2}\sin\Delta\cos\left(\frac{\alpha}{2} + \sin^{-1}\left[\frac{x}{(\varepsilon_r^2+x^2)^{1/2}}\right]\right)\right]} \tag{31}$$

The analysis of ψ_v yields the following three cases:

1. If $(\varepsilon_r^2 + x^2)\Delta - \rho = 0$, then

   a. If $\sin\Delta\sin(\mathrm{Tan}^{-1}\frac{x}{\varepsilon_r} + \frac{\alpha}{2}) = 0$, then $\psi_v = 0$. (32)

   b. If $\sin\Delta\sin(\mathrm{Tan}^{-1}\frac{x}{\varepsilon_r} + \frac{\alpha}{2}) > 0$, then $\psi_v = \frac{\pi}{2}$. (33)

   c. If $\sin\Delta\sin(\mathrm{Tan}^{-1}\frac{x}{\varepsilon_r} + \frac{\alpha}{2}) < 0$, then $\psi_v = -\frac{\pi}{2}$. (34)

2. If $\rho - (\varepsilon_r^2 + x^2)\sin^2\Delta > 0$, then

$$\psi_v = \mathrm{Tan}^{-1}\left[\frac{2\rho^{1/2}\sqrt{\varepsilon_r^2 + x^2}\sin\Delta\sin(\tan^{-1}\frac{x}{\varepsilon_r} + \frac{\alpha}{2})}{\rho - (\varepsilon_r^2 + x^2)\sin^2\Delta}\right] \tag{35}$$

3. If $\rho - (\varepsilon_r^2 + x^2)\sin^2\Delta < 0$, then

$$\psi_v = \mathrm{Tan}^{-1}\left[\frac{2\rho^{1/2}\sqrt{\varepsilon_r^2 + x^2}\sin\Delta\sin(\tan^{-1}\frac{x}{\varepsilon_r} + \frac{\alpha}{2})}{\rho - (\varepsilon_r^2 + x^2)\sin^2\Delta}\right] + \pi \tag{36}$$

A similar analysis leads to

$$K_H = \frac{\left[\rho^2 + \sin^4\Delta - 2\rho \sin^2\Delta \cos\alpha\right]^{1/2}}{\left[\rho + \sin^2\Delta + 2\rho^{1/2} \sin\Delta \cos \frac{\alpha}{2}\right]} \tag{37}$$

and

$$\psi_H = \text{Tan}^{-1} \frac{2\rho^{1/2} \sin\Delta \sin\alpha/2}{\rho - \sin^2\Delta} \tag{38}$$

The normalization of these parameters is as was done in ITSA-1 program (Lucas and Haydon, 1966). In order to compare with the complex numbers R_V, R_H (Ma, 1974) subtract π and add π.

$$R_V = K_V \exp(j(\psi_V - \pi)) \tag{39}$$

$$R_H = K_H \exp(j(\psi_H + \pi)) \tag{40}$$

3. GENERAL ANTENNA EQUATIONS

The general form of the equations describing linear antennas over lossy ground are given in this section. The coordinate systems used are described. Then the general antenna equations are given. These will be applied to specific antenna systems in the following sections of the report.

Three coordinate systems are used: (1) the mathematical model the antenna is placed in, (2) the circuit between the transmitter and receiver, and (3) the computer code used. The model coordinate system will be a spherical one as depicted in Figure 6. The three coordinate surfaces are:

(1) The sphere, R = constant, ≥ 0.

(2) The cone, θ = constant, $0 \leq \theta \leq \pi$.

(3) The plane, ϕ = constant, $0 \leq \phi \leq 2\pi$.

The relationship with Cartesian coordinate is given by the equations

$$\begin{aligned} x &= R \sin\theta \cos\phi \\ y &= R \sin\theta \sin\phi \\ z &= R \cos\theta \\ R &= \sqrt{x^2 + y^2 + z^2} \\ \theta &= \text{arc cos } (Z/\sqrt{x^2 + y^2 + z^2}) \\ \phi &= \text{arc tan } (y/x). \end{aligned} \tag{41}$$

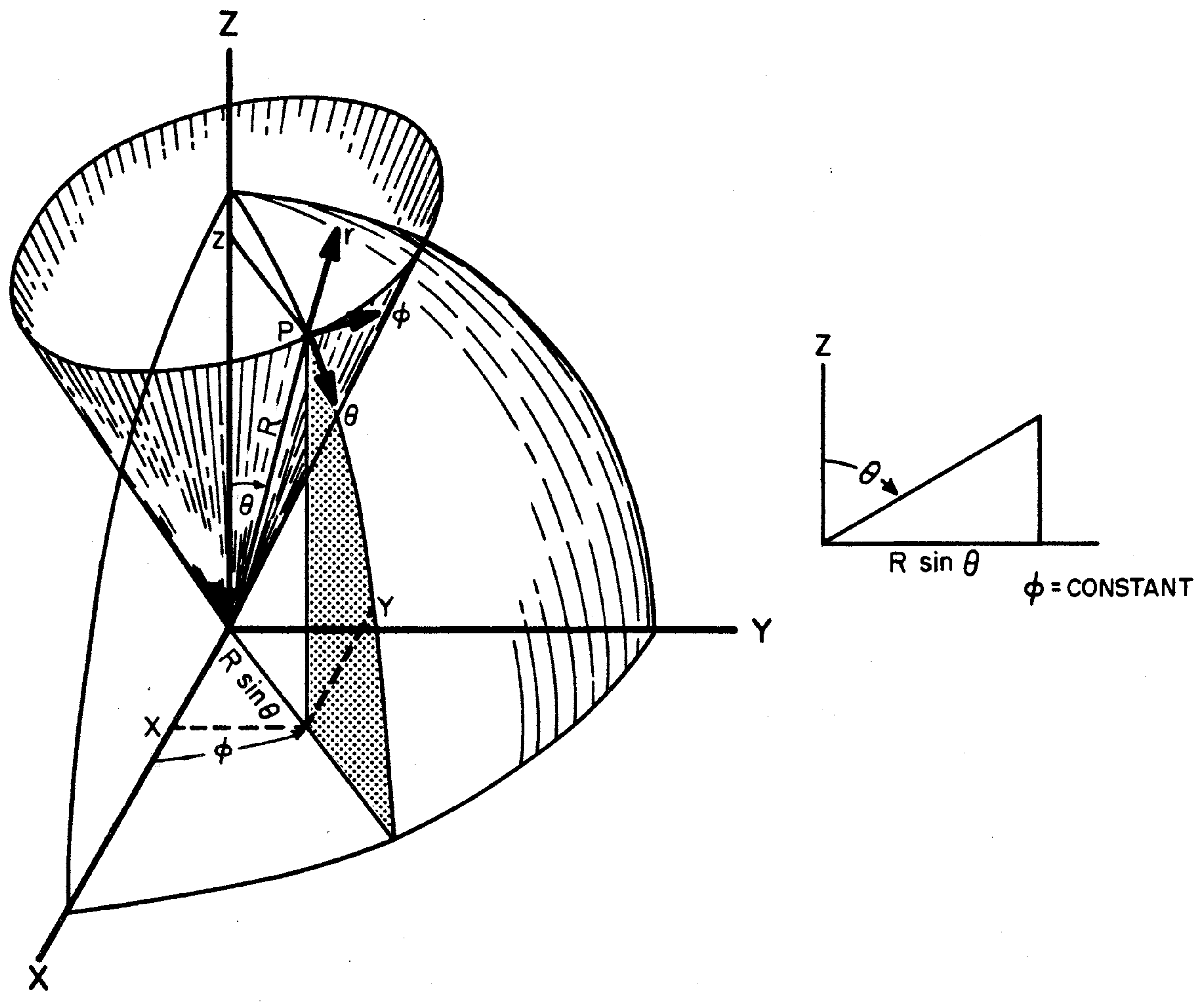

Figure 6. Spherical coordinates. The unit vectors lie in the lines of intersection of three pairs of coordinate surfaces. The differential element of volume is shown at the right of the figure.

The ground plane is taken as the x-y plane. The basic problem is to determine the field from a wire element placed arbitrarily above the ground at an observation point P (Figure 7). Two angles that will recur throughout the antenna models are the angle ψ_a between the wire element and the observation point and the angle ψ'_a between the image of the wire element and the observation point. Using the inner product formula and equations (41), the angles are

$$\cos\psi_a = (\sin\theta \cos\phi, \sin\theta \sin\phi, \cos\theta)\ (\sin\theta_a \cos\phi_a, \sin\theta_a \sin\phi_a, \cos\theta_a)$$

$$= \sin\theta \cos\phi \sin\theta_a \cos\phi_a + \sin\theta \sin\phi \sin\theta_a \sin\phi_a + \cos\theta \cos\theta_a$$

$$\cos\psi_a = \cos\theta \cos\theta_a + \sin\theta \sin\theta_a \cos(\phi - \phi_a) \tag{42}$$

and

$$\cos\psi_a = -\cos\theta \cos\theta_a + \sin\theta \sin\theta_a \cos(\phi - \phi_a)\ . \tag{43}$$

In this report the antenna system will be placed so that the desired main beam of the antenna will be placed in the direction of the positive x axis. This convention is not followed in the references so some care must be exercised when comparing equations.

The coordinate system used to describe the circuit between transmitter and receiver is centered on the transmitter site and uses ground distance from the transmitter, azimuth angle east of north, and vertical distance from the earth's surface. While normally the main beam of the antenna is in the same azimuth as that of the circuit, this is not always the case. The computer code uses the mathematical model coordinate system and converts the circuit coordinates into this spherical system.

The power gain of the antenna is defined using equation 4 (IEEE, 1965):

$$g = \frac{4\pi R^2\ P_{AV}}{W} = \left(\frac{R^2}{30\ W_{in}}\right)(|E_\theta|^2 + |E_\phi|^2) \tag{44}$$

where

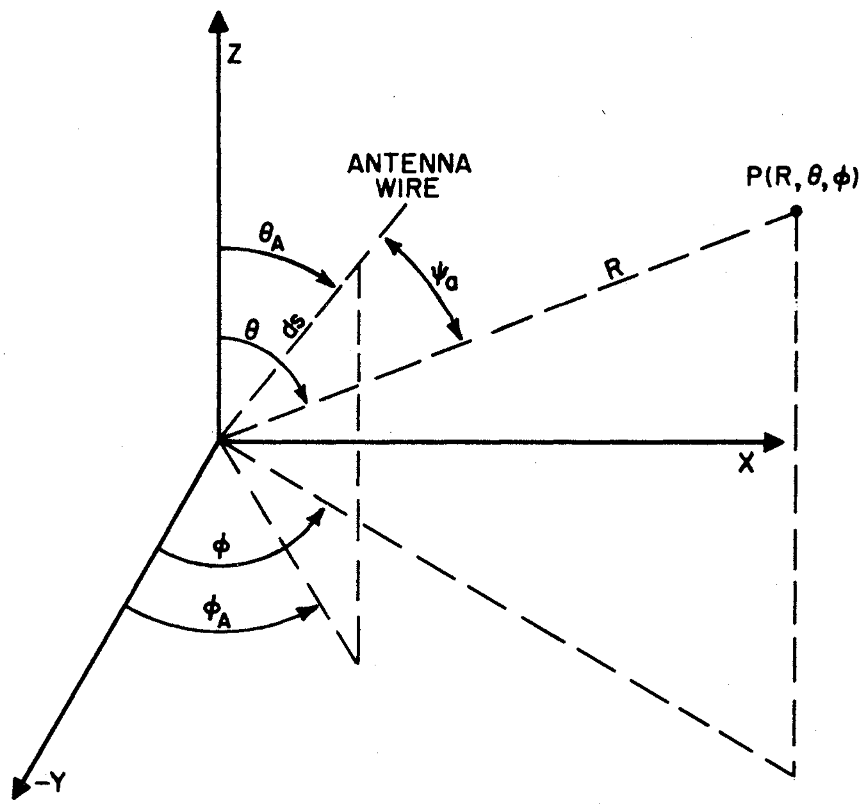

Figure 7. Arbitrarily oriented antenna above a flat earth.

E_θ and E_ϕ are the field in the indicated direction;

$W_{in} = |I_{in}|^2 R_{in}$

where

I_{in} is the input current at the feeding point and

R_{in} is the input resistance.

The calculations are simplified using the general radiation formulas (Schelkunoff, 1939; Laitinen, 1957) for traveling waves

$$E_\theta = k\ e_p \sin\theta \int_0^L I_{in}\ e^{-jks\ (1 - \cos\theta)}\ ds \qquad (45)$$

and for standing waves

$$E_\theta = k\ e_p \sin\theta \int_0^L F(s)\ e^{\ jks \cos\theta}\ ds \qquad (46)$$

where

$$e_p = j\ \omega\mu_o \frac{e^{-jkR}}{kR} \sim j30k\ \frac{e^{-jkR}}{R}\ . \qquad (47)$$

The factor $k = 2\pi/\lambda = \omega\sqrt{\mu_o\ \varepsilon_o}$ has been included within e_p here. This factor will come from the integration of the standing wave current distribution over a thin wire. The revaluation

$$\frac{1}{4\pi}\sqrt{\frac{\mu_o}{\varepsilon_o}} \cong 30$$

is used in equation (47). L is the length of the antenna and F(s) is the standing wave.

For an antenna over a lossy ground, the effect of the ground reflection must be accounted for. The horizontally and vertically polarized fields produced by a linear antenna are found by projecting the horizontal and vertical projection of the radiation vectors in the θ and ϕ directions. For horizontal polarization (Ma, 1974)

$$\begin{aligned} E_H &= \text{total horizontal component} \\ &= E_i(R_1) + E_r(R_2) \\ &= E_i(R_1) + R_H E_i(R_2) \end{aligned} \qquad (48)$$

where

E_i is the incident field,

E_r is the reflected field,

R_1 is the distance between the antenna feed and the far field point,

R_2 is the distance between the image of the antenna feed and the far field point, and

R_H is the horizontal Fresnel reflection coefficient.

For vertical polarization

$$E_H' = \text{total horizontal component}$$

$$= E_i(R_1) - R_V E_i(R_2)$$

$$E_V = E_i(R_1) + R_V E_i(R_2) \quad (49)$$

where

R_V is the vertical Fresnel reflection coefficient.

So the equation for the fields are

$$E_\theta = k\, e_p[\cos\alpha \cos(\phi - \phi_a) \cos\theta \int_0^L I(s)$$

$$\exp(jks \cos\psi_a)\ [1 - R_V \exp(-2jk\ h_s \cos\theta)]\ ds$$

$$-\sin\alpha \sin\theta \int_0^L I(s) \exp(jks \cos\psi_a)$$

$$[1 + R_V \exp(-2jk\ h_s \cos\theta)]\ ds] \quad (50)$$

and

$$E_\phi = -e_p\, k \cos\alpha \sin(\phi - \phi_A) \int_0^L I(s)$$

$$\exp(jks \cos\psi_a)\ [1 + R_H \exp(-2jk\ h_s \cos\theta)]\ ds \quad (51)$$

where

$\alpha = \pi/2 - \theta_a$,

$I(s)$ is the current distribution.

The term $\exp(jks \cos\psi_a)$ is the phase advance of the element ds at s over the origin.

h_s is the height of the antenna above ground.

The equations (50) and (51) are based on the assumption of plane wave reflection over a lossy earth and are the basis of the antenna equations formulated by Laitinen (1957) and Ma (1974).

In order to finish the calculations, the radiation resistance, R_{in}, must be determined. This can be calculated by viewing the antenna and its image as a coupled two-port network.

$$V_1 = Z_{11} I_1 + Z_{12} I_2 \tag{52}$$

where

V_1 is the impressed voltage, volts,

I_1 is the input current of the antenna, amperes,

Z_{11} is the self impedance, ohms,

Z_{12} is the mutual impedance between the antenna and its image, and

I_2 is the image current of I_1.

$$I_2 = R_H I_1 \quad \text{; evaluated with } \theta = 0 \text{ for horizontal elements and} \tag{53}$$

$$I_2 = R_v I_1 \quad ; \quad \theta = 0 \text{ for vertical elements.} \tag{54}$$

From equation (52), then the radiation resistance is

$$R_{in} = Re(Z_{11}) + Re(C\ Z_{12}) \tag{55}$$

where

Re is real part,

C is R_v or R_H calculated with $\theta = 0$.

The antenna pattern can now be calculated using equations (44), (50), (51), and (55). There are three basic levels of approximation:

(1) Numerical integration using method of moments. The current distribution I(s) is expanded into base functions to carry out the integrations. The use of Sommerfeld integrals is sometimes used to find the current relationships and the radiation resistance (see e.g., Strait, 1980).

(2) Analytic integration using a 3-term current expansion and using complex matrix inversion methods for the current relationships and radiation resistance (Ma, 1974).

(3) Using the simple 1-term current expansion (sinusoidal) and solving for the current relationships and radiation resistances either in free space or over perfect ground. This is the classical method of finding patterns for skywave fields.

To each of these approaches, the efficiency factor of the antenna must be added [see equations (6)]. The approach followed here is to use free space, or perfect ground conditions, or to use precalculated or measured curves to find the current relationship and radiation resistances and to do an analytic integration of equations (50) and (51) with a sinusoidal current distribution.

For convenience in referencing, a standard integral that appears in the formula for particular antennas is evaluated here. From standard integral tables (or verify by integration by parts) it is known that

$$\int e^{AX} \sin (Bx+C) = \frac{e^{AX}}{A^2+B^2} [A \sin (Bx+C) - B \cos (Bx+C)] \; . \qquad (56)$$

where A, B, C are dummy variables. For a wire of length, L, the integral will be of the form:

$$\left(\frac{1}{k}\right)[C + j D] = \int_0^Z e^{jks \cos\psi_a} \sin [k(L - s)] \, ds$$

$$= \left(\frac{1}{k}\right) \frac{1}{\sin^2\psi_a} \left[e^{jks \cos\psi_a} \left(\cos[k(L - s)] + j \cos\psi_a \sin [k(L - s)] \right) \right]_0^Z \qquad (57)$$

$$C + j D = \frac{1}{\sin^2\psi_a} \left[e^{jkZ \cos\psi_a} \left(\cos [k(L - Z)] + j \cos\psi_a \sin [k(L - Z)] \right) - (\cos kL + j \cos\psi_a \sin kL) \right] . \qquad (58)$$

The factor $\left(\frac{1}{k}\right)$ that appears in equation (57) is combined into the factor e_p, equation (47). For a straight wire, the integration limit, Z, is taken as L. Z = L:

$$C = \frac{1}{\sin^2\psi_a} [\cos(kL \cos\psi_a) - \cos kL]$$

$$D = \frac{1}{\sin^2\psi_a} [\sin(kL \cos\psi_a) - \cos\psi_a \sin kL] \; . \qquad (59)$$

For a bent wire like the inverted L antenna, L is H + ℓ and the integration limit is Z = H.

$$C = \cos(kH \cos\psi_a) \cos k\ell - \cos\psi_a \sin kL \sin(kH \cos\psi_a)$$

$$- \cos [k(H + \ell)]$$

$$D = \cos\psi_a \sin kP \cos[kH \cos\psi_a] + \cos k\ell \sin[kH \cos\psi_a)$$

$$- \cos\psi_a \sin[k[\ell + H)] \ . \qquad (60)$$

For a dipole, the required integral is

$$\int_{-L/2}^{L/2} e^{jks \cos\psi_a} \sin [k(L - s)] \, ds = \frac{1}{k} (C + jD) \ . \qquad (61)$$

The integration of equation (61) is easily accomplished by using the symmetry of the sine term, an even function, the symmetry of the real part of the exponential term, an even function, and the anti-symmetry of the imaginary part of the exponential term, an odd function. These functions are depicted in Figure 8. The real part of the integral is a symmetric (even) function, so the total integral is twice the integral of the positive integral (i.e., equation (59). The imaginary part of the integral is an anti-symmetric (odd) function, so the total integral is zero. From equation (59)

$$C = \frac{2}{\sin^2\psi_a} \left[\cos \left[k\left(\frac{L}{2} \cos\psi_a\right)\right] - \cos \left(k \frac{L}{2}\right)\right]$$

$$D = 0. \qquad (62)$$

The above equations (59), (60), and (62) will recur with some of the antennas described below.

4. VERTICAL MONOPOLES AND STANDING WAVE WIRE ANTENNAS

The equations and approximations used in the computer code will be given in this and the following sections for various antenna types as specified. The derivation of the equations follows from the general formulae given in the last section. Since most of the equations have been derived elsewhere (Laitinen, 1957; Ma and Walters, 1969; or Ma, 1974) only a compilation of the results is given, unless the form of the approximations is not published elsewhere.

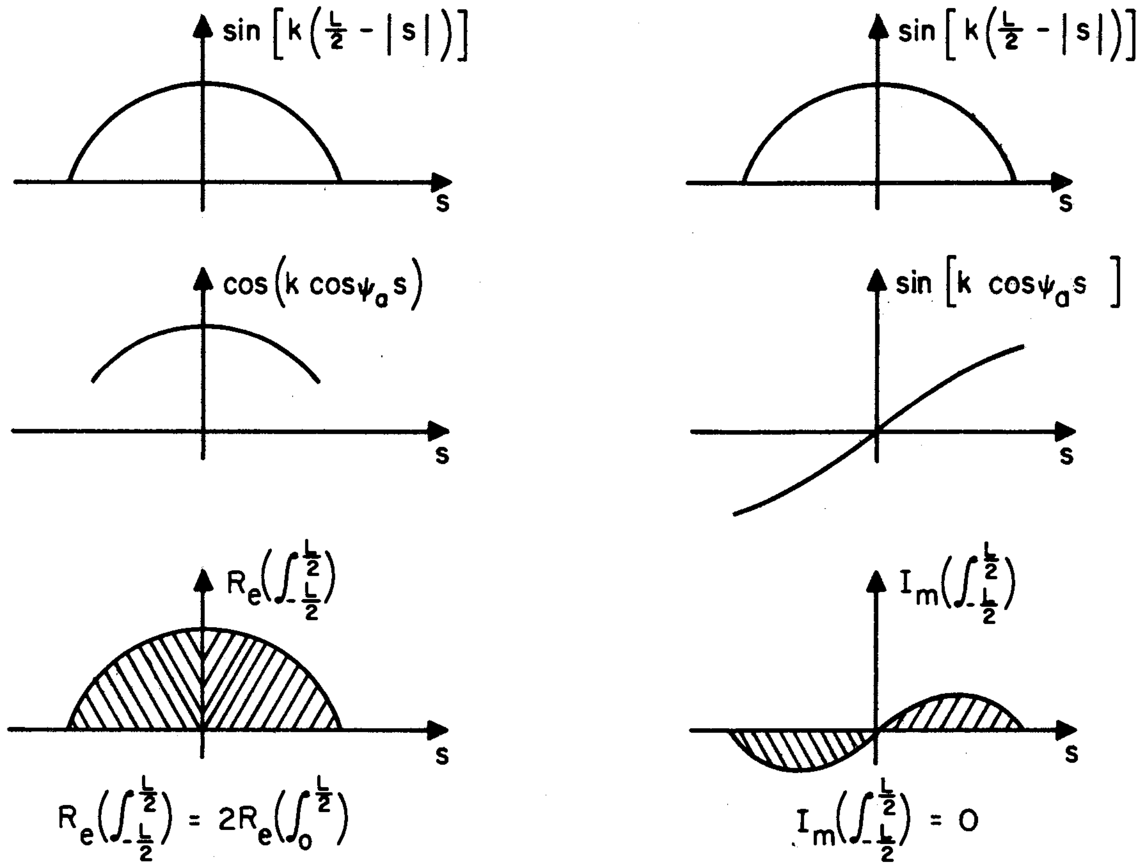

Figure 8. Integration of current for a dipole using symmetry.

Vertical monopole, antenna 2 and 17 (Antenna numbers refer to numbering with computer code)

The vertical monopole has the geometry as indicated in Figure 3. This antenna is usually placed over a ground screen. No direct explicit account is made here for the ground screen. The efficiency factor (Section 2.3) is for a monopole over a properly designed ground screen. The current distribution is

$$I(s) = I_m \sin (k(L - z)), \quad z > 0 . \tag{63}$$

The field components are

$$E_\theta = - e_p \, k \, I_m \, [C + jD + R_v(C - jD)] \tag{64}$$

$$E_\phi = 0. \tag{65}$$

where

$$C = (\cos(k\ell \cos\theta) - \cos k\ell)/\sin\theta$$

$$D = (\sin(k\ell \cos\theta) - \cos\theta \sin k\ell)/\sin\theta \tag{66}$$

$(\cos\psi_a = \cos\theta$ here.)

Let

$$b = \text{Arctan } (D/C) \tag{67}$$

then

$$g = \frac{30 \, (C^2 + D^2) \, [1 + K_v^2 - 2K_v \cos(\psi_v - 2b)]}{R_{in}} \tag{68}$$

where

K_v is the magnitude of the reflection coefficient,

ψ_v is the phase of the reflection coefficient. $(= \arg(R_v) - \pi$ as given in Ma (1974) so the change in sign in equation (61).)

The substitution (from Laitinen)

$$C^2 + D^2 = C^2/\cos^2 b \tag{69}$$

is made into equation (61) for use in the computer code.

The radiation resistance is calculated assuming a perfect earth. The equations used are taken from Jordan (1950) as these are already separated into real and imaginary parts.

$$R_{in} = 30 \, [(1 + \cos\beta) \, C_{in}(\beta) - 0.5 \cos\beta \, C_{in} \, (2\beta) - \sin\beta \, S_i(\beta) + 0.5 \sin\beta \, S_i(2\beta)] \tag{70}$$

where

$$\beta = 2\left(\frac{2\pi}{\lambda}\right)L = 2kL$$

$$C_{in}(\beta) = \gamma + \log_e \beta - C_i(\beta)$$

$$C_i(\beta) = \text{cosine integral}$$

$$S_i(\beta) = \text{sine integral}$$

$$\gamma = 0.577$$

For short antennas, $L/\lambda \leq 0.181$, the short antenna formula is used. $R_{in} = 10(kL)^2$.

Vertical log periodic monopole array, antenna 19

The vertical log periodic monopole array is a simple approximation intended for an azimuth (i.e., main beam) use. This is modeled as a quarter-wave monopole with additional gain as specified by the user.

Sloping long wire, antenna number 11

The sloping long wire is a tilted monopole when placed on the ground (Figure 9). This can also be elevated. When horizontal, this configuration is a long wire. The radiation resistance formula used assumes that the base of the wire is on the ground. The assumed orientation of the wire is that the acute angle of the slope, α, is along the positive x-axis (Figure 8). Thus, the geometric relationships are

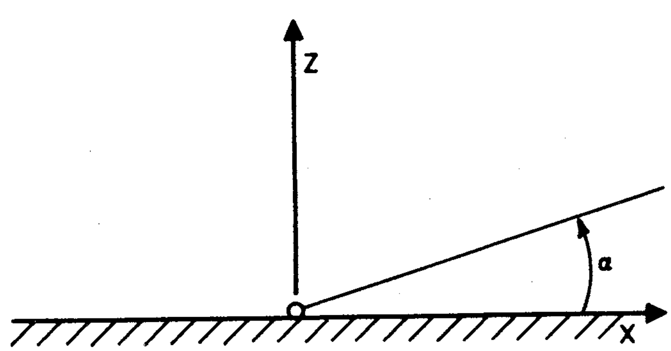

Figure 9. Orientation of sloping long wire antenna.

$$\cos\psi_a = \cos\theta \sin\alpha + \sin\theta \cos\alpha \cos\phi$$

$$\cos\psi_a' = -\cos\theta \sin\alpha + \sin\theta \cos\alpha \cos\phi$$

$$h_s = h + (\sin\alpha)\, s. \qquad (71)$$

Since this is a standing wave antenna, the current is

$$I(s) = I_m \sin[k(L - s)]. \qquad (72)$$

Using equations (50) and (51), the field components are

$$E_\theta = e_p\, k\, I_m \Bigg[\cos\alpha \cos\phi \cos\theta \int_0^L \sin[k(L - s)]\, e^{jks \cos\psi_a} (1 - R_v\, e^{-2jk\,(h + \sin\alpha\, s) \cos\theta})\, ds$$

$$- \sin\alpha \sin\theta \int_0^L \sin[k(L - s]\, e^{jks \cos\psi_a} \left[1 + R_v\, e^{-2jk\,(h + \sin\alpha\, s) \cos\theta}\right] ds\Bigg]$$

$$= e_p\, I_m\, [F_3 + j\, G_3] \qquad (73)$$

$$E_\phi = e_p\, k\, I_m \cos\alpha \sin\phi \int_0^L \sin[k(L - s)]\, e^{jks \cos\psi_a} \left[1 + R_H\, e^{-j2k\,[h + \sin\alpha\, s] \cos\theta}\, ds\right]$$

$$= e_p\, I_m\, (F_4 + j\, G_4)\;. \qquad (74)$$

The required integrals are

$$\int_0^L \sin[k(L - s)]\, e^{jks \cos\psi_a}\, ds = \frac{1}{K} (C_1 + j\, D_1) \qquad (75)$$

and

$$\int_0^L \sin[k(L - s)]\, e^{jks \cos\psi_a}\, e^{-2jk \sin\alpha\, s \cos\theta}\, ds$$

$$= \int_0^L \sin[k(L - s)]\, e^{jks \cos\psi_a'}\, ds = (C_2 + j\, D_2)\, \frac{1}{K} \qquad (76)$$

where

$$C_1 = [\cos(kL\cos\psi_a) - \cos kL]/\sin^2\psi_a$$

$$D_1 = [\sin(kL\cos\psi_a) - (\cos\psi_a)(\sin kL)]/\sin^2\psi_a$$

$$C_2 = [\cos(kL\cos\psi_a') - \cos kL]/\sin^2\psi_a'$$

$$D_2 = [\sin(kL\cos\psi_a') - (\cos\psi_a')(\sin kL)]/\sin^2\psi_a' \quad . \tag{77}$$

It is convenient to combine the height phase term with the phase of the reflection coefficients.

$$\psi_V' = \psi_V + 2kh\cos\theta$$

$$\psi_H' = \psi_H + 2kh\cos\theta \ .$$

The field components are then

$$F_3 = (\cos\alpha\cos\phi\cos\theta - \sin\alpha\sin\theta)\, C_1 - (\cos\alpha\cos\phi\cos\theta + \sin\alpha\sin\theta)\, |R_V| \, [C_2\cos\psi_V' - \sin\psi_V'\, D_2] \tag{78}$$

$$G_3 = (\cos\alpha\cos\phi\cos\theta - \sin\alpha\sin\theta)\, D_1 - (\cos\alpha\cos\phi\cos\theta + \sin\alpha\sin\theta)\, |R_V|\, [D_2\cos\psi_V' + C_2\sin\psi_V'] \tag{79}$$

$$F_4 = (\cos\alpha\sin\phi\, [C_1 + (C_2\cos\psi_H' - D_2\sin\psi_H')\, |R_H|] \tag{80}$$

$$G_4 = \cos\alpha\sin\phi\, [D_1 + (D_2\cos\psi_H' + C_2\sin\psi_H')\, |R_H|]. \tag{81}$$

The gain is

$$g = 30(F_3^2 + G_3^2 + F_4^2 + G_4^2)/R_{in} \quad . \tag{82}$$

The radiation resistance is calculated assuming the antenna is on the ground (h = 0) and perfect ground conditions (Shelkunoff and Friis, 1952).

$$\begin{aligned} R_a = {} & 60\, C_{in}(2kL)\sin\alpha \\ & + 30\, [2\, C_{in}(2kL) - C_{in}(2kL)(1 - \sin\alpha) \\ & \quad - C_{in}(2kL)(1 + \sin\alpha)]\cos(2kL) \\ & + 30\, [-2\, S_i(2kL) + S_i(2kL)(1 - \sin\alpha) \\ & \quad + S_i(2kL)(1 + \sin\alpha)]\sin(2kL) \ . \end{aligned} \tag{83}$$

This variable, R_a, is calculated in the subroutine RWIRE. For the sloping wire R_{in} is 0.5 R_a. For a vertical wire, $\alpha = 90°$, the factors become

$$C_1 = C_2 = C$$

$$D_2 = -D_1 = D$$

and

$$E_\phi = 0.$$

So the field components are identical to those for a monopole [equations (62) and (63)]. Also the radiation resistance .5 R_a, equation (81), becomes R_{in}, equation (68). The only difference is the efficiency factor, which is zero for the long wire.

Inverted L, number 8

The inverted L is a bent wire orientated for the computer model as in Figure 10. The assumed current distribution is shown also in Figure 9.

$$I(s) = I_m \sin [k(L + H - s)] .$$

The field derivation is divided into that for the vertical portion and that for the horizontal portion. For the vertical portion

$\alpha = 90°$; $\cos\psi_a = \cos\theta$ and $h_s = h_o + s$.

$E_\phi = 0.$

$$E_\theta = -e_p\, k \sin\theta \int_0^L I_m \sin [k(L + H - s)]\, e^{jks \cos\psi_a}$$

$$[1 + R_v\, e^{-2jk\, h_o \cos\theta}\, e^{-2jk\, s \cos\theta}]\, ds. \qquad (84)$$

As for the monopole

$$\int_0^H \sin [k(L + H - s)]\, e^{jks \cos\psi_a}\, ds = (A_4 - j\, B_4)\, \frac{1}{k} \left(\frac{1}{\sin^2\theta}\right). \qquad (85)$$

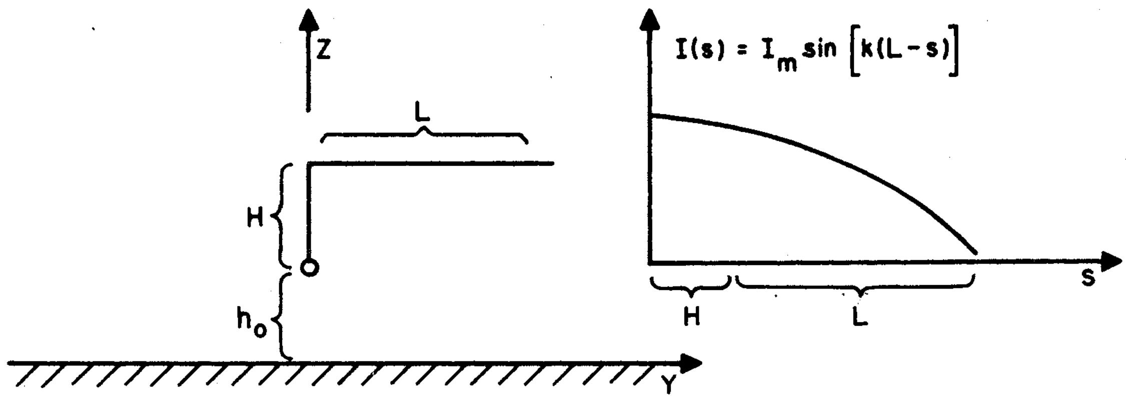

Figure 10. Orientation and current distribution of inverted "L."

Using equation (60)

$$A_4 = [\cos(kL)\cos(kH\cos\theta) - \cos\theta\sin(kL)\sin(kH\cos\theta) - \cos[k(H + L)]]$$

$$B_4 = [\cos\theta\sin kL\cos[k(H\cos\psi_a) + \cos kL\sin[kH\cos\theta] - \cos\theta\sin[k(L + H)]] \; . \tag{86}$$

so,

$$E_\theta = -e_p\left(\frac{I_m}{\sin\theta}\right)(A_4 + j\,B_4) + \left(R_v e^{-2jkh_o\cos\theta}\right)(A_4 - j\,B_4) \tag{87}$$

$$= -e_p\left(\frac{1}{\sin\theta}\right)\sqrt{A_4^2 + B_4^2}\,e^{jb}\left(1 + R_v\,e^{-2j(b + k\,h_o\cos\theta)}\right)$$

$$E_\theta = -(F_{11} + j\,G_{11})\,I_m\,e_p \tag{88}$$

$$b = \text{Arctan}\,(B_4/A_4)$$

$$F_{11} = \frac{\sqrt{A_4^2 + B_4^2}}{\sin\theta}\,[\cos b + C_v \cos\psi_v']$$

$$G_{11} = \frac{\sqrt{A_4^2 + B_4^2}}{\sin\theta}\,[\sin b + C_v \sin\psi_v'] \qquad (89)$$

$$C_v = |R_v|$$

$$\psi_v' = \psi_v - b - 2kh_o \cos\theta \;.$$

For the horizontal portion

$$\alpha = 0°, \; \cos\psi_a = \sin\theta \sin\phi$$

$$I(s) = I_m \sin[k(L - s)]$$

$$E_\theta = + e_p\, k \sin\phi \cos\theta\, I_m \int_o^L \sin(k(L - s))$$

$$e^{jks \sin\phi \sin\theta}\,[1 - R_v\, e^{-2jk(h_o + H)\cos\theta}]\, ds \qquad (90)$$

$$E_\phi = -e_p\, k \cos\phi\, I_m \int_o^L \sin[k(L - s)]\, e^{jks \cos\phi \sin\theta}$$

$$[1 + R_H\, e^{-2jk(h_o + H)\cos\theta}]\, ds. \qquad (91)$$

The integnal is

$$\int_o^L \sin[k(L - s)]\, e^{jks \cos\psi_a} = \frac{A_5 + j\, B_5}{k \sin 2\psi_a} \qquad (92)$$

$$A_5 = \cos[kL \cos\psi_a] - \cos kL$$

$$B_5 = \sin[kL \cos\psi_a] - \cos\psi_a \sin kL \;. \qquad (93)$$

So,

$$E_\theta = \frac{e_p \sin\phi \cos\theta \; I_m}{\sin 2\psi_a} [(A_5 + j\,B_5)\,(1 - R_v\, e^{-2jk(h_o + H)\cos\theta})]$$

$$= e_p\, I_m\, [F_{12} + j\, G_{12}] \tag{94}$$

$$E_\phi = \frac{-e_p \cos\phi \; I_m}{\sin 2\psi_a} [(A_5 + j\,B_5)\,(1 + R_H\, e^{-2jk(h_o + H)\cos\theta})]$$

$$= e_p\, (F_2 + j\, G_2)\,. \tag{95}$$

The total field is

$$E_\theta = e_p\, I_m\, [(F_{12} - F_{11}) + j(G_{12} - G_{11})]$$

$$= e_p\, I_m\, (F_1 + j\, G_1) \tag{96}$$

$$E_\phi = e_p\, I_m\, (F_2 + j\, G_2) \tag{97}$$

$$g = 30\, \frac{[F_1^2 + G_1^2 + F_2^2 + G_2^2]}{R_{in}} \tag{98}$$

$$F_1 = \frac{\sin\phi \cos\theta}{\sin^2\psi_a} \sqrt{A_5^2 + B_5^2}\; [\cos b' - C_v \cos\psi_v'']$$

$$- \frac{1}{\sin\theta} \sqrt{A_4^2 + B_4^2}\; (\cos b + C_v \cos\psi_v') \tag{99}$$

$$G_1 = \frac{\sin\phi \cos\theta}{\sin^2\psi_a} \sqrt{A_5^2 + B_5^2}\; [\sin b' - C_v \sin\psi_v'']$$

$$- \frac{1}{\sin\theta} \sqrt{A_4^2 + B_4^2}\; (\sin b + C_v \sin\psi_v') \tag{100}$$

$$b = \text{Arctan}\,(B_4/A_4)$$

$$\psi_v' = \psi_v - b - 2kh_o \cos\theta$$

$$b' = \text{Arctan}\,(B_5/A_5)$$

$$\psi_v'' = \psi_v + b' - 2k(h_o + H)\cos\theta$$

$$F_2 = \frac{\sin\phi}{\sin^2\psi_a} \sqrt{A_5^2 + B_5^2} \; [\cos b' + C_H \cos\psi_H']$$

$$G_2 = \frac{\sin\phi}{\sin^2\psi_a} \sqrt{A_5^2 + B_5^2} \; [\sin b' + C_H \cos\psi_H'] \qquad (101)$$

$$\psi_H' = \psi_H + b' - 2k(h_o + H) \cos\theta \; . \qquad (102)$$

The radiation resistance is calculated using the equation (70) with L replaced by the total length of the antenna, H + L. To this is added the maximum of 0. or $R_{in,H}$, where (Ma and Walters, 1969)

$$R_{in,H} = 60 \; [\log_e L - C_i(2kL) - \frac{\sin(2kL)}{2kL} - 0.423]. \qquad (103)$$

The practice of restricting $R_{in,H}$ to positive values was a programming convention since it is not well defined for small values of L and meaningless for negative values. The problem arises when H + L nears 0.7λ. The term $R_{in,H}$ is actually a difference term rather than an independent radiation resistance term (Schelkunoff and Friis, 1952), which is negative when L/λ is more than .25λ.

For L = 0, the radiation pattern is identical to that for a vertical monopole, as $A_5 = B_5 = 0$, and E_θ for the vertical portion is the same as for the monopole. When the height and length of the inverted L are selected so that the contributions to the magnitude of E_θ are equal except for the azimuth term sinϕ; the preferred direction of radiation is at an azimuth of -90°. This corresponds to the antenna used by Marconi in 1906 (Sommerfeld, 1964).

5. DIPOLES AND ARRAYS OF DIPOLES

The patterns for a vertical dipole are like those for a monopole over perfect ground. The equations for a tilted dipole will be derived; then the equations for a horizontal dipole and arrays of horizontal dipoles will be given. The vertical dipole and arrays of vertical dipoles will follow. These are all standing wave antennas.

Tilted dipole, number 14

The assumed orientation of the tilted dipole is shown in Figure 11. The geometric relationships are: $\phi_a = 90°$, $\theta_a = 90° - \alpha$.

$$\cos\psi_a = \sin\alpha \cos\theta + \sin\theta \cos\alpha \cos(\phi - 90°)$$

$$= \sin\alpha \cos\theta + \sin\theta \cos\alpha \sin\phi \quad (104)$$

$$\cos\chi_a' = - \sin\alpha \cos\theta + \sin\theta \cos\alpha \sin\phi \quad (105)$$

$$h_s = h + (\sin\alpha)s, \; -\frac{L}{2} \leq s \leq \frac{L}{2} \quad (106)$$

and the current distribution is

$$I(s) = I_m \sin [k (\frac{L}{2} - |s|)] \quad (107)$$

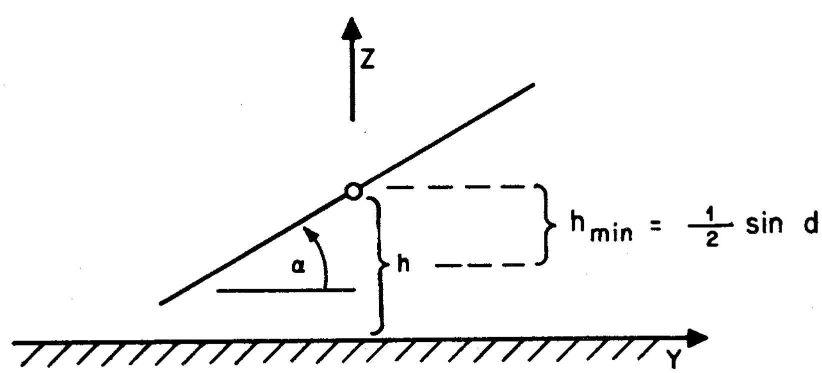

Figure 11. Orientation of a tilted dipole.

$$E_\theta = k\ e_p\ I_m\ [\cos\alpha\ \sin\phi\ \cos\theta \int_{-\frac{L}{2}}^{\frac{L}{2}} \sin\ [k\ (\frac{L}{2} - |s|]\ e^{jks\ \cos\psi_a}$$

$$[1 - R_v\ e^{-2jkh\ \cos\theta}\ e^{-2jks\ \sin\alpha\ \cos\theta}]\ ds$$

$$- \sin\alpha\ \sin\theta \int_{-\frac{L}{2}}^{\frac{L}{2}} \sin\ [k\ \frac{L}{2} - |s|)]\ e^{jks\ \cos\psi_a}$$

$$[1 + R_v\ e^{-2jkh\ \cos\theta}\ e^{-2jks\ \sin\alpha\ \cos\theta}]\ ds] \qquad (108)$$

$$E_\theta = e_p\ I_m\ [\cos\alpha\ \sin\phi\ \cos\theta\ [(C_1 + j\ D_1)$$

$$- R_v\ e^{-2jkh\ \cos\theta}\ (C_2 + j\ D_2)]$$

$$- \sin\alpha\ \sin\theta\ [(C_1 + j\ D_1) + R_v\ e^{-2jkh\ \cos\theta}(C_2 + j\ D_2)]] \qquad (109)$$

$$E_\phi = e_p\ I_m\ \cos\alpha\ \cos\phi \int_{-\frac{L}{2}}^{\frac{L}{2}} \sin\ [k\ (\frac{L}{2} - |s|)]\ e^{jks\ \cos\psi_a}$$

$$[1 + R_H\ e^{-2jkh\ \cos\theta} e^{-2jks\ \sin\alpha\ \cos\theta}]\ ds$$

$$= e_p\ I_m\ \cos\alpha\ \sin\phi\ [(C_1 + j\ D_1) + R_H e^{-2jkh\ \cos\theta}(C_2 + j\ D_2)] \qquad (110)$$

The required integrals are given using equation (62)

$$\frac{1}{k}\,(2C_1 + j\,D_1) = \int_{-\frac{L}{2}}^{\frac{L}{2}} e^{jks\cos\psi_a} \sin\left[k\left(\frac{L}{2} - |s|\right)\right] ds$$

$$= 2C_1\left(\frac{1}{k}\right)$$

$$= \frac{2}{\sin^2\psi_a}\left[\cos\left[k\left(\frac{L}{2}\cos\psi_a\right)\right] - \cos\left(k\,\frac{L}{2}\right)\right] \tag{111}$$

and

$$\frac{1}{k}\,(2C_2 + j\,D_2) = \int_{-\frac{L}{2}}^{\frac{L}{2}} e^{jks\cos\psi'_a} \sin\left[k\left(\frac{L}{2} - |s|\right)\right] ds$$

$$= 2C_2\left(\frac{1}{k}\right)$$

$$= \frac{2}{\sin^2\psi'_a}\left[\cos\left[k\left(\frac{L}{2}\cos\psi'_a\right)\right] - \cos\left(k\,\frac{L}{2}\right)\right] . \tag{112}$$

So

$$E_\theta = 2\,e_p\,I_m\,[(\cos\alpha\,\sin\phi\,\cos\theta - \sin\alpha\,\sin\theta)\,C_1$$

$$- R_v\,e^{-j2kh\cos\theta}\,(\cos\alpha\,\sin\phi\,\cos\theta + \sin\alpha\,\sin\theta)\,C_2]$$

$$= 2\,e_p\,I_m\,(F_3 + j\,G_3) \tag{113}$$

$$E_\phi = 2\,e_p\,I_m\,\cos\alpha\,\cos\phi\,[C_1 + R_H\,\bar{e}^{2jkh\cos\theta}\,C_2]$$

$$= 2\,e_p\,I_m\,(F_4 + j\,G_4) \tag{114}$$

where

$$F_3 = (\cos\alpha \sin\phi \cos\theta - \sin\alpha \sin\theta)\, C_1$$

$$-|R_V|\, (\cos\alpha \sin\phi \cos\theta + \sin\alpha \sin\theta)\, C_2 \cos\psi_V' \tag{115}$$

$$G_3 = -|R_V|\, (\cos\alpha \sin\phi \cos\theta + \sin\alpha \sin\theta)\, C_2 \sin\psi_V' \tag{116}$$

$$F_4 = \cos\alpha \cos\phi\, (C_1 + |R_H|\, C_2 \cos\psi_H') \tag{117}$$

$$G_4 = \cos\alpha \cos\phi\, |R_H|\, C_2 \sin\psi_H' \tag{118}$$

$$\psi_V' = \psi_V - 2kh \cos\theta \tag{119}$$

$$\psi_H' = \psi_H - 2kh \cos\theta \;. \tag{120}$$

The gain is then,

$$g = \frac{[F_3^2 + G_3^2 + F_4^2 + G_4^2]\,(120)}{R_{in}} \;. \tag{121}$$

The radiation resistance, R_{in}, is calculated using equation (70) with a length of L/2 and doubling the result.

Horizontal dipole number 3

For the horizontal dipole, the geometry becomes:

$\alpha = 0,\ \phi_a = 90$

$\cos\psi_a = \sin\theta \sin\phi$

$\cos\psi_a' = \cos\psi_a$.

The equations simplify to:

$$F_3 = \sin\phi \cos\theta \; C_1 \; (1 - |R_V| \cos\psi'_V)$$

$$G_3 = -\sin\phi \cos\theta \; C_1 \; |R_V|$$

(122)

$$F_4 = \cos\phi \; C_1 \; (1 + |R_H| \cos\psi'_H)$$

$$G_4 = \cos\phi \; C_1 \; |R_H| \sin\psi'_H \; .$$

The radiation resistance of the horizontal dipole is taken as in free space, equation (70), with length as one-half the length of the dipole and radiation resistance twice the calculated value (73.2 ohms for a halfwave dipole). For a perfectly conducting ground and a horizontal antenna on the ground (h = 0), the radiated field is zero (Sommerfeld, 1964). The dipole and its image will cancel out. The use of the approximation of the radiation resistance used here will result in the gain going from the perfect ground case of 8.2 dBI to the free space gain of 2.2 dBI as the height of the antenna approaches zero. The effect of the ground can be added by using the calculation of mutual resistance. Following a suggestion by Uda (Uda and Mushiake, 1954), we write the mutual resistance as relative to that for a halfwave antenna, and then as relative to the self impedance

$$R_{11} = b \; R_{11}$$

where R_{11} is given as described above by equation (70) and b is given by Table 1 [generated using values of R_{21} in Kraus (1950)].

Then equation (55) and R_H evaluated at $\theta = 0$:

$$R_{in} = R_{11} + R_H \; b \; R_{11}$$

$$= R_{11} \; (1 + R_H \; b) \; . \qquad (123)$$

For perfect ground, $R_H = -1$, the radiation resistance approaches zero as the height approaches zero; i.e., the field becomes zero. This can be effected within the computer code by making $R_{in} = R_{11} \; (1 - b)$ have a minimum value of (0.000120).

Table 1. Mutual Resistance of Parallel Dipoles Relative to That of Two Halfwave Dipoles

Height, h/λ	Relative Mutual Resistance, b
0.00	1.000
.05	.923
.10	.706
.15	.402
.20	.086
.25	-.174
.30	-.320
.35	-.339
.40	-.254
.45	-.098
.50	.052
.60	.216
.70	.079
.80	-.113
.90	-.131
1.00	.015

The computer code follows Ma and Walters (1969) and so uses

$$A^2 = C_1 \, (F_3^2 + G_3^2)$$

$$B^2 = C_1 \, (F_4^2 + G_4^2) \tag{124}$$

$$A^2 = [1 + |R_V|^2 - 2|R_V| \cos\psi_V'] \sin^2\phi \cos^2\theta$$

$$B^2 = [1 + |R_H|^2 + 2|R_H| \cos\psi_H'] \cos^2\phi \tag{125}$$

$$g = \left(\frac{120}{R_{in}}\right) C_1^2 \, (A^2 + B^2) \; . \tag{126}$$

Vertical dipole, number 5

For the vertical dipole, the geometry becomes

$$\alpha = 90°$$

$$\cos\psi_a = \cos\theta \quad , \quad \sin^2\psi_a = \sin^2\theta$$

$$\cos\psi_a' = - \cos\theta$$

The equations simplify to

$$F_3 = - \sin\theta \; C_1 \; (1 + |R_V| \cos\psi_V)$$

$$G_3 = + \sin\theta \; C_1 \; |R_V| \sin\psi_V \tag{127}$$

$$F_4 = G_4 = 0.$$

Yagi array of horizontal dipoles, number 4

The geometry of the Yagi array is shown in Figure 12. A dipole array is aligned with one or more parasitic elements. The elements usually consist of a reflector, the dipole, and one or more directors in the desired direction.

The program code will handle two or more elements. The geometry as in Figure 12 gives the relationship

$$\theta_A = \frac{\pi}{2}$$

$$H_s = H$$

$$\cos\psi_a = \sin\theta \sin\phi.$$

The distance from the base of the mth element to the observation point is approximated by

$$r_m \cong r_1 - x_m \sin\theta \cos\phi.$$

The current in the dipole is taken as the standing wave sinusoidal current

$$I_s(y) = I_m \sin[k \frac{L}{2} - |y|]. \qquad (128)$$

The current maximum on each element, I_m, is required for the solution of the interior problem. Following the procedure used by Uda and Mushiake (1954) for this array, the gain can be written as that of the driven element plus correction factors for the array. This procedure will smooth the computer calculations.

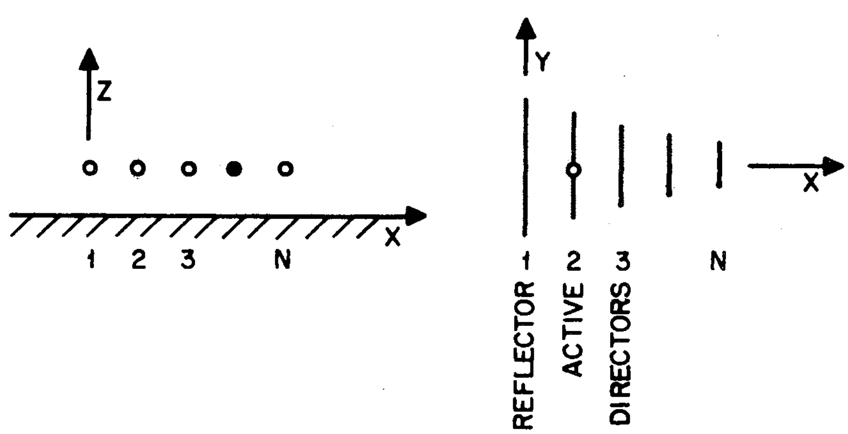

Figure 12. Geometry of a Yagi array.

This procedure will also be used for other arrays such as the log periodic array. The gain is then

$$g = g_2 \; |S|^2/\delta R_{in}$$

$$g_2 = \frac{120}{R_{in}} \left(|E_{\theta_2}|^2 + |E_{\phi_2}|^2 \right) \qquad (129)$$

where

g_2 is the gain of the driven element as given above, equation (126).

S is the array factor.

δR_{in} is the change in radiation resistance given by the presence of the additional elements.

The solution for the array factor is straightforward assuming the interior problem for the current distribution is solved. The currents are normalized to that for the driven element, number 2. To simplify the notation, use I_m for the ratio of the current of the mth element to the driven. (So, $I_2 = 1$.) Then

$$S = \sum_{1}^{N} S_m \quad .$$

S_1 is the reflector

$$S_1 = I_1 \left(\frac{C_1}{C_2}\right) e^{jk(x_1 - x_2) \sin\theta \cos\phi} \qquad (130a)$$

S_2 is the driven element

$S_2 = 1.$

The other elements are the directors,

$$S_m = I_m \left(\frac{C_m}{C_2}\right) e^{jk(x_m - x_2) \sin\theta \cos\phi} \quad . \qquad (130b)$$

The C_m are the dipole factors given by equation (111). The interior problem for the current distribution is given here under the assumption that the Yagi array is well designed and for the HF/VHF bands (e.g., Ma, 1974, or Uda and Mushiake, 1954). Thus the element lengths are near $\lambda/2$. Note also under these assumptions the dipole factor ratios C_m/C_2 are nearly one. The theoretical solution for the current distribution and radiation resistance can be formulated as a matrix inversion problem (Ma, 1974). Rather than using this procedure in the computer code, a precalculated curve is used here. The values are given in Table 2 and plotted in Figure 13. For two elements, the theoretical solution is reasonably simple (Kraus, 1950), and the relative current maximums are given by Table 1. For elements near $\lambda/2$ in length, the numbers in Table 2 are reasonable. For other lengths (and frequencies) the curves will have the same shape as in Figure 13, but will vary. The solution as calculated by the method of moments for a long array is added to Figure 13 (Thiele, 1969).

With this many elements, the relative current amplitudes reach a minimum (or vary about a minimum curve). This is caused by the presence of a traveling wave along the array (Mailloux, 1966). The equations used here assume a first order solution for the standing wave on each individual element [equation (128)]. A set of curves similar to Figure 13 is calculated using the second order, King-Sandler approximation, and compared to measured values by Mailloux (1966). The third-order approximation used by Ma (1974) is discussed and compared to those curves by King (1967). The curves given here (Figure 13) agree with the third-order approximation for free space (Ma, 1974). The radiation resistance factor (δR_{in}) is taken from these calculations as (1/1.358).

In summary, the calculation procedure is to calculate the gain of a single dipole, number 2. Then calculate the array factor for the reflector, number 1, using equation (130a) and Table 2. If any directors are present, equation (130b) is used with Table 2 to include their effect. Finally, the somewhat ad hoc correction, δR_{in}, to the radiation resistance is used. The program will do a single element array (as a check on the computer code), a two-element array with a single reflector (or a single director if the azimuth is specified as 180°), or an array with an arbitrary number of elements. For arrays not designed with elements nearly $\lambda/2$ in length, the curve of Figure 13 needs to be replaced by an appropriate curve or set of curves.

Table 2. Relative Current for a Yagi Antenna

d/λ	$\|I_m\|/\|I\|_2$	$+(\alpha_n - \alpha_2)$
0.	1.00	0.
.12	.95	-70.
.20	.644	-130.
.25	.263	-220.
.65	.1565	-720.
1.357	.00002	-1470.

a. Values used in the calculation.

	d/λ	$\|I_2\|/\|I\|_m$	$+(\alpha_n - \alpha_2)$ Degrees	Radians
Free Space	0.	1.	0.	0.
	.2	.6435	-150.	-2.6
	.25	.2639	-247.	-4.3
Sea	.0	1.	0.	0.
	.2	.7153	140.	-2.44
	.25	.291	-231.	-4.0
Land	0.	1.	0.	0.
	.2	.758	-139.	-2.43
	.25	.313	-234.	-4.1

b. Values as calculated in Ma (1974).

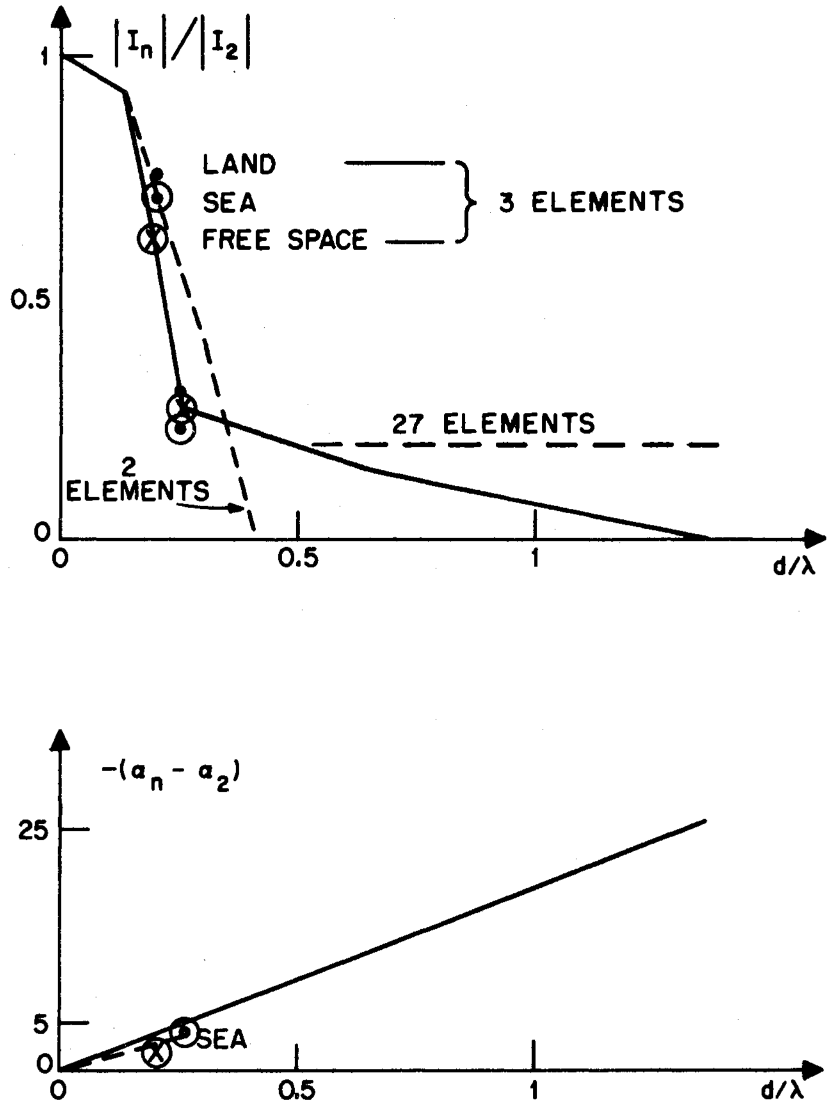

Figure 13. Relative current for a Yagi antenna.

Curtain array, number 6

The curtain array is a two-dimensional array of horizontal dipoles (Figure 14). There are N bays of M stacked dipoles. A reflecting screen is placed in back of the array. This array is modeled using the results for a single horizontal dipole, the array factors for a two-dimensional array, and the effect of the reflecting screen (Stewart et al., 1964).

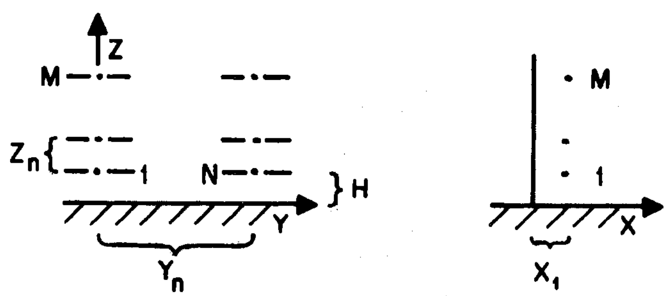

Figure 14. Geometry of a curtain array.

The gain is given as

$$g = \left(\frac{480}{R_{in}}\right) |C_1|^2 \; |S_x|^2 \; |S_y|^2 \; (|S_V|^2 + |S_H|^2) \tag{131}$$

C_1 is the element factor, equation (111).

S_x is a screen factor. Assuming equal current distribution in a perfect image of each element, the factor is

$$1 - e^{-j2kx_s \cos\psi_x} = 2j \; e^{-jkx_1 \cos\psi_x} \sin(kx_s \cos\psi_x)$$

or

$$4 \; |S_x|^2 = \sin^2 (k \; x_s \cos\psi_x) \tag{132}$$

where

x_s is the distance to the screen and

$\cos x_s = \cos\phi \; \sin\theta.$

The effect of the number of bays is given by the width factor

$$S_y = \sum_{1}^{N} A_m \exp[jky_m (\sin\theta \sin\phi - \delta)] \qquad (133)$$

where

N is the number of bays,

A_m is the relative current in the mth bay (the current is $I_{mm} = A_m B_m$, B_m as below),

y_m is the distance to the mth bay,

δ is the phase delay.

The main beam of the curtain array can be steered in azimuth by the application of a progressive phase delay between the bays of the array. For a desired direction specified by the angles, the phase delay is (Ma, 1974, page 188)

$$\delta = \sin\theta_0 \sin\phi_0$$

where

θ_0 is the desired angle for elevation ($90° - \Delta_0$)

ϕ_0 is the desired azimuth angle.

The effect of the number of elements in each bay, the height above ground, the polarization, and the ground reflection is given by the factors

$$S_V = \left[\frac{\sin\phi \cos\theta}{\sqrt{\cos^2\phi + \sin^2\phi \cos^2\theta}}\right] \sum_{1}^{M} B_m e^{jkz_m \cos\theta}$$

$$[1 - R_V e^{-2kz_m \cos\theta}]$$

$$S_H = \left[\frac{\cos\phi}{\sqrt{\cos^2\phi + \sin^2\phi \cos^2\theta}}\right] \sum_{1}^{M} B_m e^{jkz_m \cos\theta}$$

$$[1 + R_H e^{-2kz_m \cos\theta}] . \qquad (134)$$

B_m is the relative current in the mth element of the bay (the current is $I_{mm} = A_m B_m$, A_m as above).

z_m is the height of the mth element.

The polarization terms are normalized by the factor under the square root sign in the denominator of equation (134).

The radiation resistance term, R_{in}, is approximated by the value [0.5 M N (73.2)]. The solution for R_{in} as a matrix inversion problem using self and mutual impedances is given by Ma (1974). For a large array, which is the intended application, the field appears to radiate from the center. Considering the array as a large conducting sheet, the radiation resistance of "elements" near the center is $480/\pi$. Near the edges, the resistance is different (Schelkunoff and Friis, 1952).

For broadcast use it is common to designate the array by the symbols (CCIR, 1978) HR N/M/H, where

HR denotes horizontal array of halfwave elements a halfwave apart, with a reflecting screen spaced a quarterwave behind the elements,

N is the number of bays,

M is the number of elements per bay, and

H is the height of the lowest element.

The patterns are given for perfect ground. In this case,

$$(|S_V|^2 + |S_H|^2) = 2\,|S_z|^2$$

$$S_z = \sum_{1}^{M} B_m\, e^{jkz_m \cos\theta}\,[1 - e^{-2jkz_m \cos\theta}]\,, \qquad (135)$$

the gain becomes

$$g(\phi,\theta) = \frac{960}{R_{in}}\,|C_1|^2\,|S_x|^2\,|S_y|^2\,|S_z|^2$$

$$= |F(\phi,\theta)|^2 \qquad (136)$$

where $F(\phi, \theta)$ is the radiation pattern function normally plotted.

$$F(\phi,\theta) = \sqrt{\frac{960}{R_{in}}}\; C_1\, S_x\, S_y\, S_z\ . \qquad (137)$$

Contours of normalized values of F along with the maximum value in cymomotive force [equation (16)], and the radiation angle of the maximum are given in the CCIR Antenna Diagrams (1978). A rough estimate of the gain can be given by multiplying the number of elements in the array by two (for the reflecting screen) and by the gain for an individual element, (1.64 = 120/73.2). To this gain in dB should be added 6 dB for reflection from perfect ground (Stewart et al., 1964). The equation is

$$g = [(M \times N \times 2) (\frac{120}{73.2})] \times 4$$

$$= (\frac{960}{73.2}) MN \tag{138}$$

For a 4 by 4 array, this is 32 (16 plus 16) times 1.64, giving a gain of 17.2 dBI. Adding 6 dB for the perfect ground, this gives a total gain of 23.2 dBI.

The computer code used is that of the ITSA-1 program (Lucas and Haydon, 1966). The phase retardation, δ, is not included ($\delta = 0$). The current terms A_m and B_m are omitted ($A_m = B_m = 1$). The normalization of the polarization terms in equation (134) are omitted (no difference in main beam directions, $\phi = 0$). The full equations were given here as a reference to possible future incorporation into the code and for comparison with other formulations of the curtain antenna.

Log periodic array of horizontal dipoles, number 13

Log periodic dipole arrays are the result of the application of log periodic principles to the design of arrays of conventional elements. This technique was reported by D. E. Isbell (1959).

If frequency independent operation is sought from a structure composed of resonant elements, the resonances must be staggered so that as the frequency is varied, the function of the resonant element is transferred smoothly from one element to the next. Figure 15 is a drawing of an array made up of dipole elements. The length of the elements and the spacings between the elements are related to the design ratio τ.

Excellent information on the design of log periodic dipole arrays has been done by Carrel (1961). Carrel made a mathematical analysis of log periodic dipole arrays which takes into account the mutual impedances between dipole elements. He has reduced this information to a set of nomographs which may be used in the design of these arrays.

An antenna is generally designed to have a certain directivity and input impedance over a given frequency range. Physical size and the number of

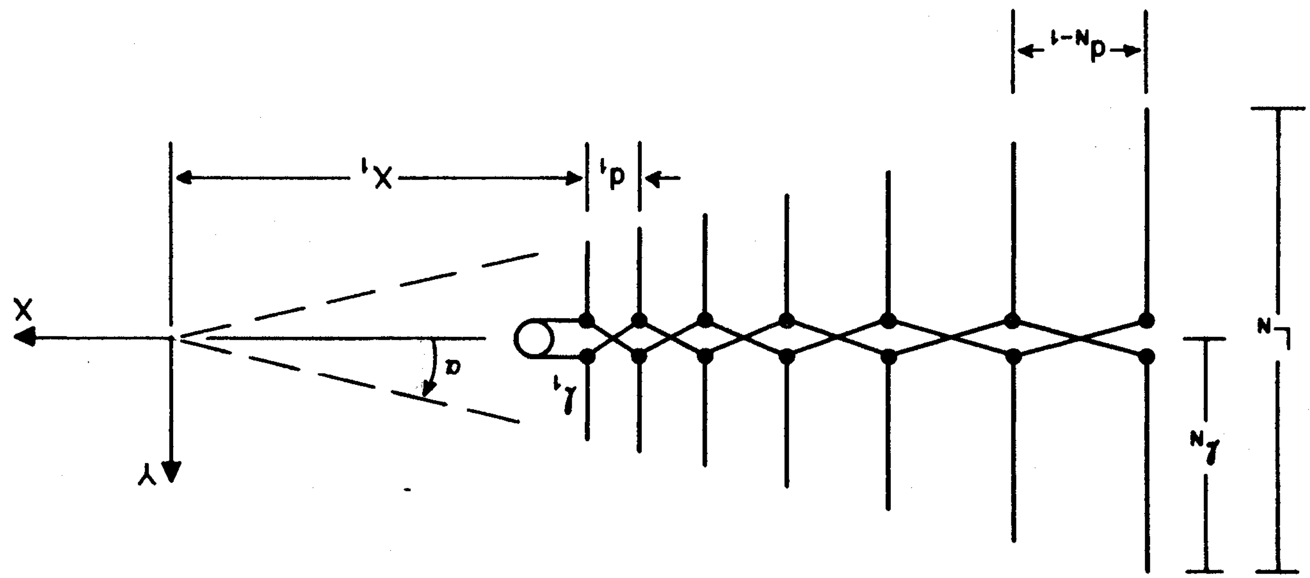

Figure 15. Log periodic array.

elements are also of interest since they govern the weight and complexity of manufacture. A repeat of Carrel's set of nomographs and the physical construction details is in Smith (1966).

The number of elements is determined mainly by the design ratio τ. As τ increases, the number of elements also increases. Antenna size is determined primarily by the spacing factor σ. As σ increases, the boom length becomes greater.

Each of the geometrical parameters of a log periodic array is shown in Figure 15. The elements are spaced within a triangle according to the design ratio τ. The ratio of lengths l_m is

$$\tau = \frac{l_m}{l_{m+1}} \quad . \tag{139}$$

This is theoretically the ratio of dipole radii also, although this is not usually found in practice. The spacing factor is

$$\sigma = \frac{d_m}{4\, l_{m+1}} = .25\ (1-\tau)\ \cot\alpha \quad . \tag{140}$$

The distances from the apex are given by the x_m. The apex angle is α. The array is fed in a crossed dipole arrangement; i.e., adjacent dipoles are in a "phase-reversal" fashion via a transmission line of impedance Z_0.

Over a ground plane (Figure 16), the effect of the image of the antenna must be considered. The height of the first (lowest and shortest) dipole is H_1. The heights of the other dipoles are

$$H_m = H_1 + x_m \cot\beta . \tag{141}$$

The angle between the vertical and the array is β. The angle, ψ, between the antenna dipoles and the direction of the observation point $P(r,\theta,\ \phi)$ is given by

$$\cos\psi = \sin\theta\ \sin\beta \ . \tag{142}$$

The angle, ψ_a, between the antenna axis and the direction of the observation point is

$$\cos\psi_a = \sin\theta\ \sin\beta\ \cos\phi + \cos\theta\ \cos\beta \ . \tag{143}$$

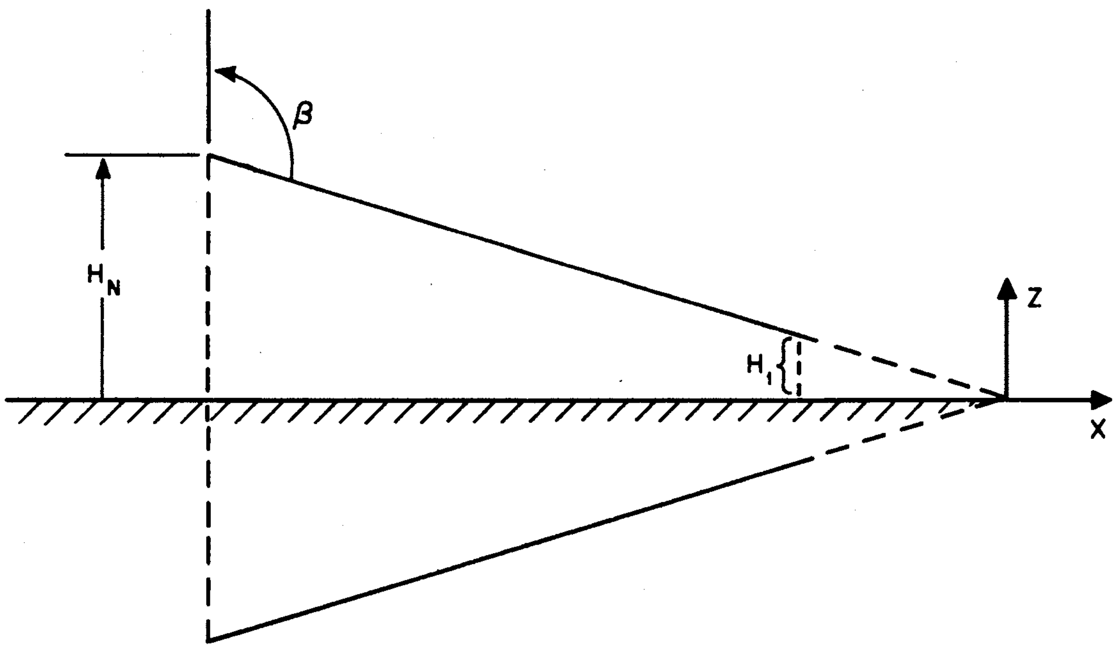

Figure 16. Array above ground.

The distance from the mth dipole to the observation point (far field approximation will be used) is:

$$r_m = r_1 - x_m \csc\beta \cos\psi_a \quad . \tag{144}$$

All of these geometric variables will be used in the calculation of the gain for this array.

Basic Theory

The log periodic array of horizontal dipoles is an approximation of a frequency independent antenna. The design is based upon two principles:

(1) The shape of the antenna is to be specified only by angles.

(2) The antenna is to be self similar; i.e., if the antenna is cut from a flat sheet, the remaining part looks like that cutaway.

The dipoles are an approximation to the "teeth" remaining when a triangular sheet is cut in a log periodic fashion. If the dipoles in Figure 15 were extended in both directions and fed at the apex, the antenna would be log periodic; i.e., whatever field is produced at a frequency, f, will be reproduced at frequency, τf, at location on the antenna also specified by τ. The rf energy at a given frequency travels along the feeder until it reaches a region (active region) where the electrical lengths and phase relations are such as to produce radiation towards the short end through elements shorter than $\lambda/2$. Due to the cross-fed connection, fields produced ahead of this active region (those in the transmission region) will cancel. The remaining region at the long end (the reflection region) has little effect since very little power travels past the active region.

Assuming a lossless structure, the behavior of the three regions can be described in terms of transmission line theory. The transmission region (short end) behaves like a feeder transmission line loaded by a capacitive reactance. This is why the truncation of the short end works in practical antennas.

The active region behaves like the loading is a capacitance in parallel with a resistance.

The reflection region behaves like a transmission line loaded with a shunt inductance. If the shunt inductance is greater than the capacitance of the line, then this is a series inductance and a shunt inductance. Since this is a network representation of a filter, a useful antenna must have most of the energy radiated before the reflection (or filter) region. If this occurs, the effect of the truncation at the long end will not be noticed.

Thus, the effect of truncating the structure is to create a practical antenna that behaves like an infinite structure between two frequencies. If the array is placed over a ground plane (Figure 16), the array must be sloped so that the antenna dipoles are at a constant electrical height above the ground. In the main beam (on azimuth), the pattern is similar to a halfwave dipole a quarterwave high within the frequency range of the antenna.

The analysis and approximations used here depend on the above observations and on separating the problem into two parts:

(1) the interior (circuit) problem which deals with the interaction of currents, voltage, etc., within the antenna system itself; and

(2) the exterior (radiation) problem which deals with the interaction of the antenna with the propagation medium.

The interior problem can be expressed as a matrix inversion problem. The dipole base currents are given by Ma (1974)

$$I_a = [U + Y\, Z_a]^{-1}\, [1\ 0 \ldots . 0]^t \ . \qquad (145)$$

I_a is a 1 by N matrix of base currents.

N is the number of dipoles and this is normalized such that $I_1 = 1$,

U is the identity matrix,

Y is an N by N matrix of admittances,

Z_a is an N by N matrix of impedances.

Instead of solving equation (145), a precalculated curve for an antenna in free space can be used. The radiation resistance, R_{in}, is the real part of Z_{in} given by

$$Z_{in} = \sum_{m=1}^{N} Z_{1m}\, I_m \qquad (146)$$

where the components Z_{1m} and I_m are from the matrices Z_a and I_a.

The gain, g, is

$$g = 120\, [\cos^2\theta\, \sin^2\phi\, |S_\theta|^2 + \cos^2\phi\, |S_\phi|^2] \qquad (147)$$

$$S_\theta = \sum_{m=1}^{N} I_m \exp\, (jkx_m \csc\beta \cos\psi_a)\, [1 - R_v \exp(-j2kH_m \cos\theta)]\, F_m \qquad (148)$$

$$S_\phi = \sum_{m=1}^{N} I_m \exp(jkx_m \csc\beta \cos\psi_a) [1 + R_H \exp(-2jH_m \cos\theta)] F_m \quad (149)$$

R_V and R_H are the Fresnel reflection coefficients.

The one term theory is used for the dipole factor F_m.

$$F_m = \frac{\cos(kl \cos\psi) - \cos(kl)}{\sin^2\psi} \quad (150)$$

where

$k = 2\pi/\lambda$; λ = wavelength.

The equations (148) and (149) will be summed only over the active region.

<u>Approximate solution of interior problem</u>

The relative current distribution has been both calculated and measured. A well-designed log periodic has a current relationship as in Figure 17. The usable bandwidth of the antenna depends on the relative bandwidth the antenna can move before it becomes distorted by the smallest or largest element. The high frequency limit is reached when the current of the smallest element reaches 10 dB of the maximum. This happens at a length of ℓ_-. (Lengths are used here, since the distance from the apex varies with the apex angle α.) The low frequency limit is reached when the current in the longest element is 3 dB less than the maximum. This is the length ℓ_c. The maximum occurs at a length ℓ_0 and the upper 10 dB at a length ℓ_+. The following empirical equations are used:

$$\ell_c = .5\ S(Z_0, \ell/a) \quad (151)$$

S is a shortening factor (Carrel, 1964). The curve, for a ratio of wire length to wire radius ℓ/a, for $\ell/a = 500$ developed using a calculated value from Ma (1974) (Figure 18).

Z_0 is the feeder impedance.

$$\ell_- = \ell_c/B_{ar} \quad (152)$$

$$B_{ar} = 1.1 + 30.7\ \sigma(1-\tau) \quad (153)$$

B_{ar} is the usable bandwidth of the antenna. Figure 19 shows the measured values of B_{ar} and equation (153).

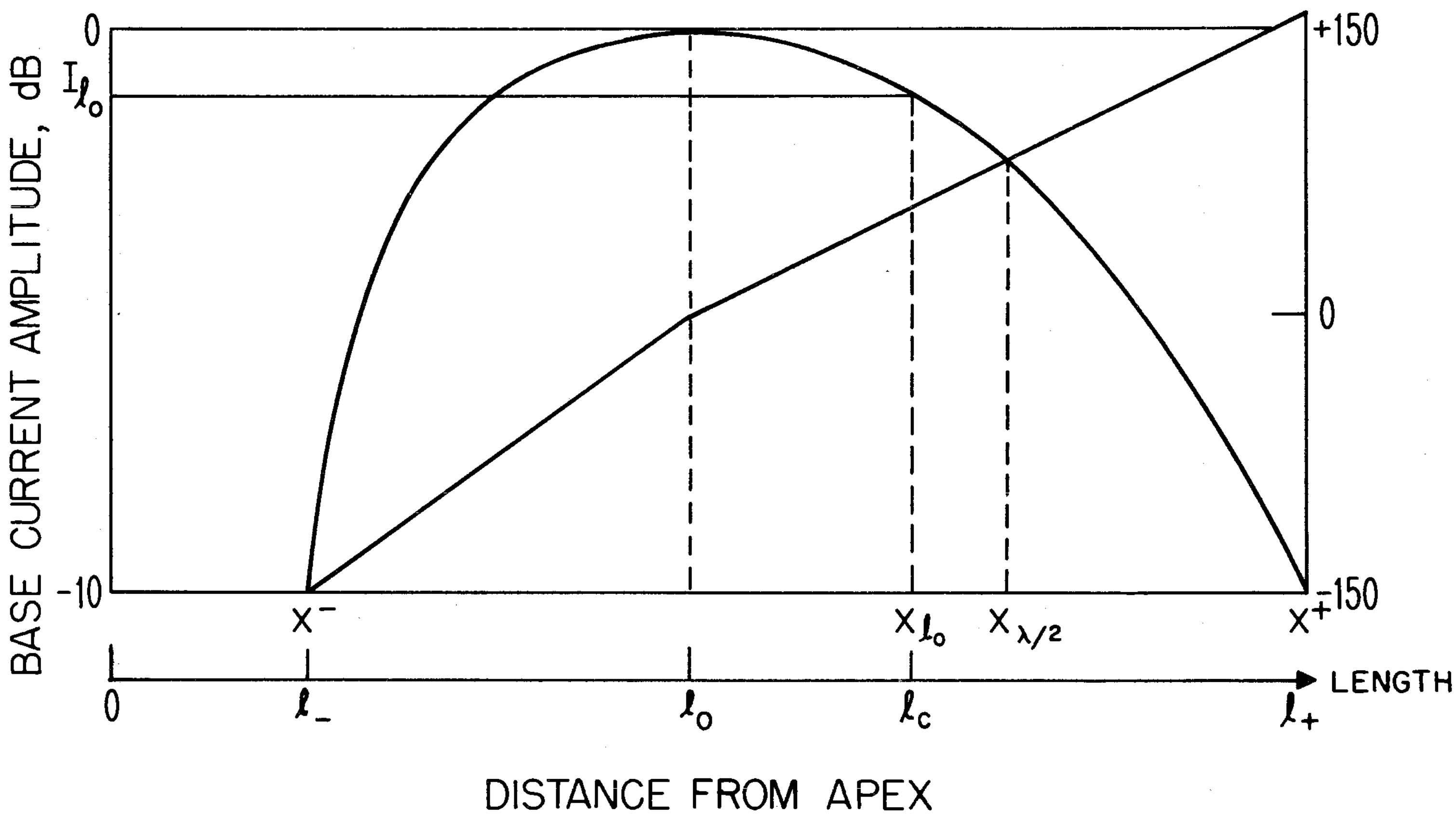

Figure 17. A typical curve of base current vs. distance from the apex or element length, showing the quantities used in the definition of the bandwidth and location of the active region.

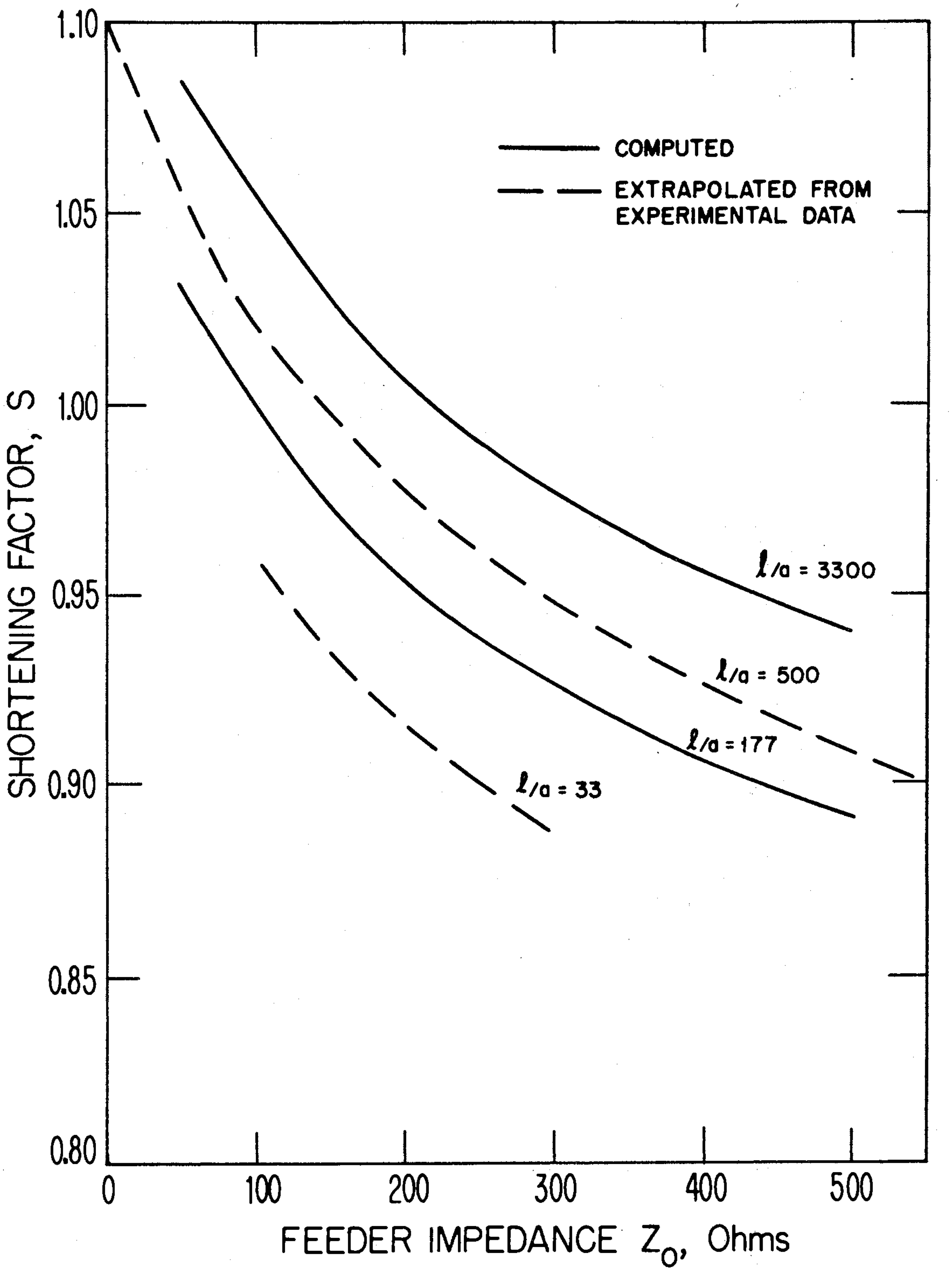

Figure 18. Shortening factor, S, vs. Z_0 and ℓ/a, the ratio of wire length to wire radius.

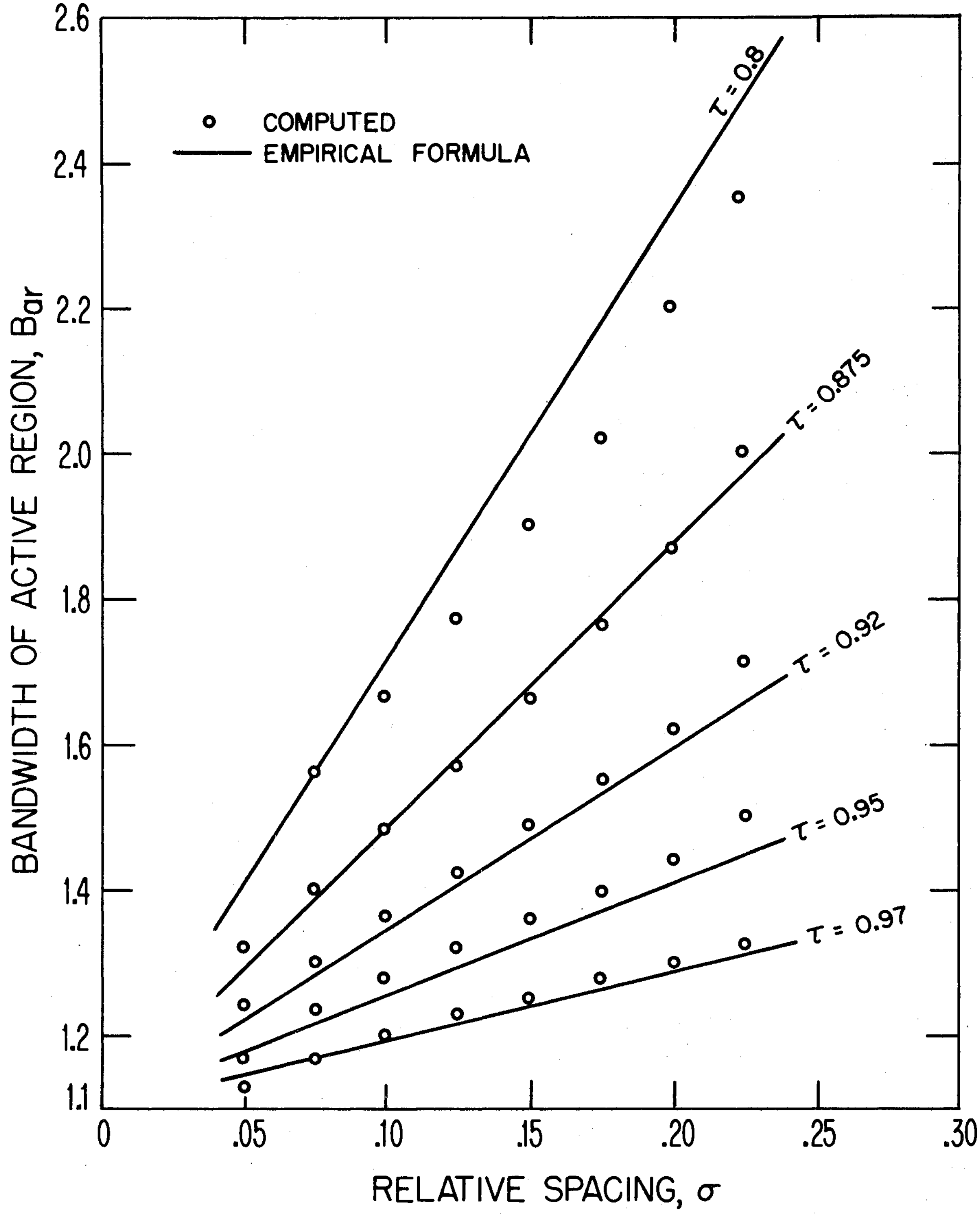

Figure 19. Bandwidth of the active region, B_{ar}, vs. σ and τ.

$$\ell_+ = 1.1\ \ell_c$$

$$= B_{ar}\ \ell_o \qquad (154)$$

and

$$\ell_o = \ell_- + .7166\ (\ell_c - \ell_-). \qquad (155)$$

Equations (154) and (155) are designed to reproduce the curves of both Carrel (1964) and Ma (1974). The coefficient (.7166) is for $\ell/a = 500$.

The procedure used is to evaluate only those dipoles that fall into the active region between ℓ_- and ℓ_+. For each antenna the curve of Figure 17 is reproduced. A current, I_m, is evaluated for each dipole within the active region. All the dipole currents are then renormalized so that the maximum current is 1. (A dipole will not usually fall exactly at ℓ_o.) Although these current curves are normally drawn as in Figure 17, the equations (146) through (149) assume the first dipole current, I_1, is equal to 1. Thus, to complete the calculations, the ratio I_1/R_{in} must be calculated.

The following formula for the average resistance level is used.

$$R_{in} = Z_o / \sqrt{1 + (Z_o/Z_a)\ (\sqrt{\tau}/(4\sigma))} \qquad (156)$$

where

Z_o = the impedance of the transmission line.

Z_a is the average characteristic of a dipole.

$$Z_a = 120 \log_e (\ell/a) - 2.25\ . \qquad (157)$$

The current levels, I_m, are then normalized by taking I_1 as 10 dB less than the maximum if the first dipole is outside the active region. The current value from the curve, Figure 17, is assigned to the first dipole when it is within the active region.

The resulting procedure is quite fast and is reasonably accurate within the designed frequency range of a log periodic antenna. This active region analysis is not limited by the number of dipoles as no matrix inversions are involved.

Log periodic array of vertical dipoles, number 22

The log periodic array of vertical dipoles can be constructed in two ways as indicated in Figure 20. If constructed at a constant height as on the left side, the array will have broadband characteristics, but the height factor resulting from the ground reflections will be frequency sensitive. In order to alleviate this problem, the array can be constructed with varying heights as on the right hand side. The geometry is somewhat more complicated in this

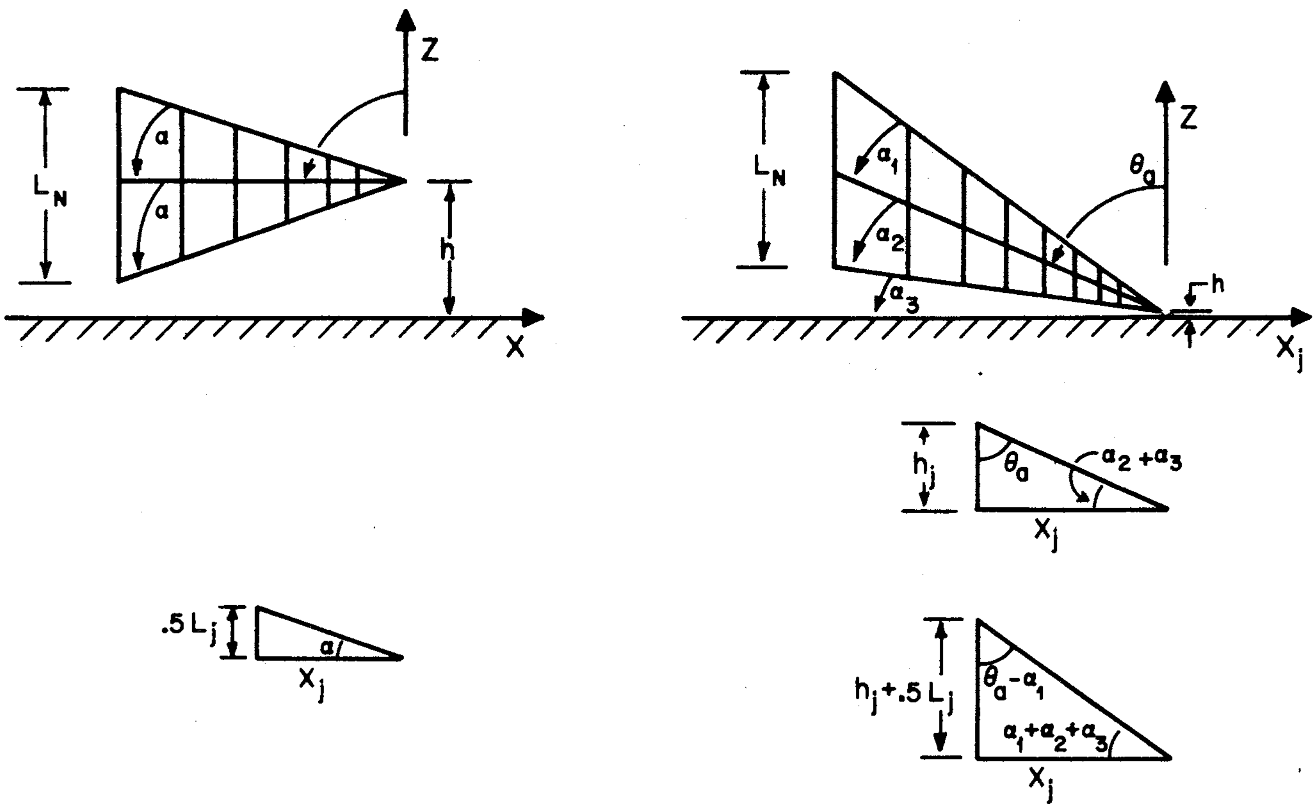

Figure 20. Geometry for log periodic arrays of vertical dipoles.

case. The necessary parameters can be obtained using the two input angles θ_a and α_1 (= α for the horizontal case). The angle between the array axis and the far field point is

$$\cos\psi_a = \cos\theta \cos\theta_a - \sin\theta \sin\theta_a \cos\phi \ . \tag{158}$$

As in any log periodic structure, the lengths are given by

$$L_m = L_N \tau^{(m-1)} . \tag{159}$$

The height of each dipole is obtained using a convenient identity and the auxiliary figures on the left side of Figure 20 (Ma, 1974).

$$h_m = (\frac{1}{2} L_m) \left[\frac{(h_m/x_m)}{\frac{h_m + \frac{1}{2} L_m}{x_m} - (h_m/x_m)} \right]$$

and

$$h_m/x_m = \cot\theta_a, \text{ (cot is cotangent)}$$

$$(h_m + \frac{1}{2} L_m)/x_m = \cot(\theta_a - \alpha_1)$$

so

$$h_m = (\frac{1}{2} L_m) \left[\frac{\cot \theta_a}{\cot(\theta_a - \alpha_1) - \cot\theta_a} \right] \tag{160}$$

(h_m = h for the horizontal case.)

The distance from the apex along the array axis is

$$d_m = h_m \sec\theta_a \ . \tag{161}$$

The gain is then (Ma, 1974)

$$g = (\frac{120}{R_{in}}) |S|^2$$

where

$$S = A_{17} + j\, B_{17}$$

$$= \sum_{1}^{N} I_m\, e^{jk(d_m - d_1)\cos\psi_a}\, F_m\, e^{jkh_m \cos\theta}$$

$$[1 + R_v\, e^{-j2kh_m \cos\theta}] \qquad (162)$$

$$S = e^{jkh\cos\theta}\, [1 + R_v\, e^{-j2kh\cos\theta}] \sum_{1}^{N} I_m\, e^{jk(x_m - x_1)\cos\psi a}\, F_m$$

(horizontal case) (163)

F_m is $\sin\theta\, C_1$ for each element

$$F_m = \frac{\cos(k \frac{L_m}{2} \cos\phi) - \cos(k\, L_m/2)}{\sin\theta} .$$

The solution of the interior problem for the relative current distribution, I_m, and the radiation resistance, R_{in}, is taken for free space conditions, i.e., identical to that described above for the horizontal LPA.

Stacked arrays of vertical log periodic dipole arrays, number 23

The log periodic array can itself be considered an element of a larger array. Identical units can then be arranged to form an array according to basic array theory. Direction for arranging the phase centers for optimum operation is given by Smith (1966). The only case considered here is an array of identical vertical log periodic dipole arrays. The intended use is the lower VHF range. The radiation pattern is taken as that of the single unit and an array factor. Parameters are

N_y, number of arrays in the y direction (width);
N_z, number of arrays in the z direction (height);
D_y, spacing in the y direction; and
D_z, spacing in the z direction.

The radiation pattern for the lowest unit VLPA is calculated using the method described in the previous section.

$$g_1 = (\frac{120}{R_a}) |E_t|^2 \tag{164}$$

R_a is the radiation resistance;

E_t = radiation pattern for single unit.

The total gain for the array is then

$$g = (\frac{120}{R_{in}}) |E_t|^2 |S_y|^2 |S_z|^2 \tag{165}$$

where

$$R_{in} = N_y N_z R_a$$

$$S_y = \sum_1^{N_y} e^{jky_m \sin\theta \sin\phi} \tag{166}$$

$$y_m = (m - 1) D_y$$

$$S_z = \sum_1^{N_z} e^{jky_m \cos\theta} \tag{167}$$

$$z_m = (m - 1) D_z$$

6. RHOMBICS AND TRAVELING WAVE ANTENNAS

The antennas discussed in the previous sections were designed such that the current on the wires was predominately a standing wave. This current distribution, approximately sinusoidal, can be considered as composed of two traveling waves. By appropriately terminating one end of the wire, in the direction desired for reception (or transmission), the current can be made to approximate a traveling wave. The basic idea (Kraus, 1950) is to terminate a wire so that only the traveling wave in the desired direction is present. This results in a unidirectional pattern. Typical patterns are shown in

Figure 21. The "back" lobes of the wire are reduced by the terminating resistance. By using two such wires to form a vee antenna, a pattern in the desired direction can be obtained. By bending the wires and terminating at a common juncture, a rhombic antenna is formed.

All of these antennas can be analyzed as the sum of the appropriate number of tilted wires each with a single outgoing traveling wave. In contrast to the dipole arrays, there is no complicated interior problem to be solved. The exterior (radiation) problem is solved using the appropriate geometry and the integral of the current [equation (45)]. The basic integral that will recur is

$$\int_0^L e^{-jks\,(1\,-\,\cos\psi_m)}\,ds = \left(\frac{1}{jk}\right)\left[\frac{1 - e^{-jkL\,(1\,-\,\cos\psi_m)}}{1 - \cos\psi_m}\right]$$

$$= \left(\frac{1}{jk}\right) F_m \ . \qquad (168)$$

As with the dipoles, the integration constant $(\frac{1}{jk})$ is merged with e_p for ease in writing the equations. F_m will then denote the bracketed expression for wire number m.

No new modeling or new computer code has been developed for this effort. Both the models and code are those included in various prediction programs used before, although some minor changes have been made in the code.

Terminated sloping long wire, number 20

This antenna has geometry identical to that of the standing wave wire antenna (Figure 9). The geometry (and notation) is

$$\cos\psi_a = \cos\psi_1 = \cos\theta\ \sin\alpha + \sin\theta\ \cos\alpha\ \cos\phi$$

$$\cos\psi_a' = \cos\psi_3 = -\cos\theta\ \sin\alpha + \sin\theta\ \cos\alpha\ \cos\phi$$

$$h_s = h + s\ \sin\alpha \ . \qquad (169)$$

The angle ψ_a' for the image of the wire is numbered here for convenience in comparing with the other antennas described below.

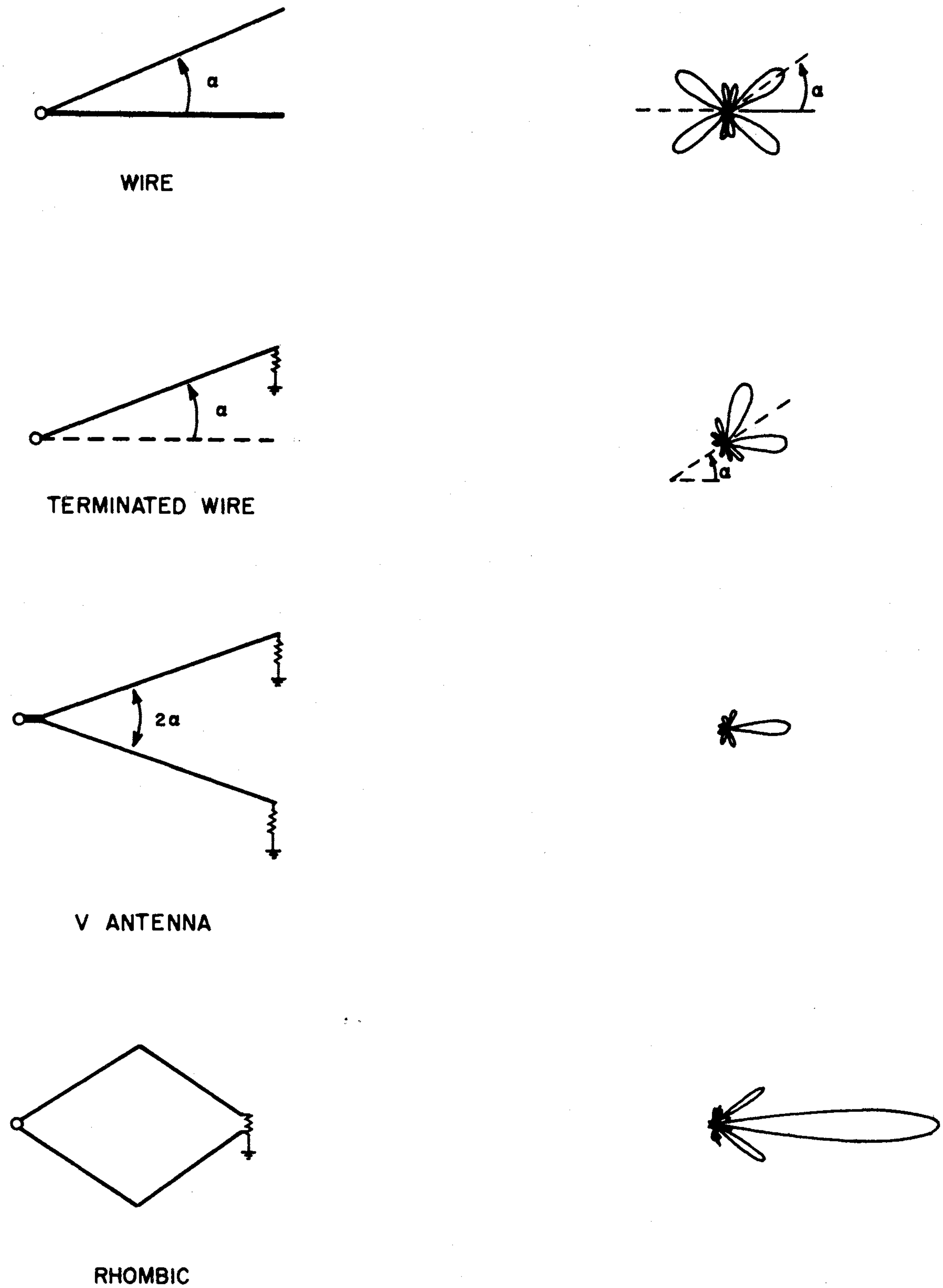

Figure 21. Wire antennas and typical patterns.

The current is

$$I(s) = I_m\, e^{-jks} \, . \tag{170}$$

The required integrals are similar to equations (73) and (74) with equation (73) substituted and equation (168) used for the integrations. The results are:

$$E_\theta = e_p\, I_m \Big\{ -\cos\alpha\, \cos\theta\, \cos\phi\, [F_1 - F_3\, R_V\, e^{-j2kh\, \cos\theta}] + \sin\alpha\, \sin\theta\, [F_1 + F_3\, R_V\, e^{-j2kh\, \cos\theta}] \Big\} \tag{171}$$

and

$$E_\phi = e_p\, I_m \cos\alpha\, \sin\phi\, [F_1 + F_3\, R_H\, e^{-j2kh\, \cos\theta}] \, . \tag{172}$$

The gain is

$$g = \left(\frac{30}{R_{in}}\right) \left(|E_\theta|^2 + |E_\phi|^2\right) . \tag{173}$$

The radiation resistance is taken as 300 ohms.

Terminated sloping vee, number 7

The terminated sloping vee antenna consists of two terminated wires separated by an angle of 2γ (Figure 22). The geometry is set so that the angle between horizontal projection of the wires and the x axis is γ. The geometry gives

$$\begin{aligned}
\cos\psi_1 &= \cos\theta\, \sin\alpha + \sin\theta\, \cos\alpha\, \cos(\phi - \gamma) \\
\cos\psi_3 &= -\cos\theta\, \sin\alpha + \sin\theta\, \cos\alpha\, \cos(\phi - \gamma) \\
\cos\psi_2 &= \cos\theta\, \sin\alpha + \sin\theta\, \cos\alpha\, \cos(\phi + \gamma) \\
\cos\psi_4 &= -\cos\theta\, \sin\alpha + \sin\theta\, \cos\alpha\, \cos(\phi + \gamma)
\end{aligned} \tag{174}$$

$$\sin\alpha = (H_t - H)/L \tag{175}$$

where ψ_3 and ψ_4 are for the images of wires 1 and 2. The current in wire 2 is out of phase with wire 1.

$$I_1(s) = -I_m\, e^{-jks} \tag{176}$$

$$I_2(s) = I_m\, e^{-jks} \tag{177}$$

$$h_s = H + s \sin\alpha\, . \tag{178}$$

The integral of the current yields

$$E_{\theta_1} = e_p\, I_m \Big\{-\cos\alpha \cos\theta \cos(\phi - \gamma)\, [F_1 - F_3\, R_v\, e^{-j2kh \cos\theta}]$$

$$+ \sin\alpha \sin\theta\, [F_1 + F_3\, R_v\, e^{-2jkh \cos\theta}]\Big\}$$

$$E_{\theta_2} = -e_p\, I_m \Big\{-\cos\alpha \cos\theta \cos(\phi + \gamma)\, [F_2 - F_4\, R_v\, e^{-j2kh \cos\theta}]$$

$$+ \sin\alpha \sin\theta\, [F_2 + F_4\, R_v\, e^{-2jkh \cos\theta}]\Big\}$$

$$E_{\phi_1} = e_p\, I_m \cos\alpha \sin(\phi - \gamma)\, [F_1 + F_3\, R_H\, e^{-j2kh \cos\theta}]$$

$$E_{\phi_2} = -\, e_p\, I_m \cos\alpha \sin(\phi + \gamma)\, [F_2 + F_4\, R_H\, e^{-j2kh \cos\theta}] \tag{179}$$

and

$$E_\theta = E_{\theta_1} + E_{\theta_2} = I_m\, e_p\, [F_5 + j\, G_5]$$

$$E_\phi = E_{\phi_1} + E_{\phi_2} = I_m\, e_p\, [F_6 + j\, G_6] \cos\alpha \tag{180}$$

where the notation is introduced to ease the comparison with the computer code. The gain is

$$g = \frac{30}{R_{in}}\, [F_5^2 + G_5^2 + \cos^2\alpha\, (F_6^2 + G_6^2)] \tag{181}$$

with R_{in} taken as 600 ohms.

The notation used in the code (and Ma and Walters, 1969) is

$$F_m = -\frac{Z_m}{U_m} - j\,\frac{V_m}{U_m}$$

$$Z_m = -1 + \cos(kLU_m)$$

$$U_m = 1 - \cos\psi_m$$

$$V_m = \sin(kLU_m)\ ,\ m = 1,\ 2,\ 3,\ 4. \qquad (182)$$

$$R_V\ e^{-2jk\,\cos\theta\ h} = C_V\ (W_3 + j\ W_4)\ , \qquad (183)$$

$$R_H\ e^{-2jk\,\cos\theta\ h} = C_H\ (W_1 + j\ W_2)\ . \qquad (184)$$

So the variable F_5 in equations (180) is

$$F_5 = \frac{-U_2\ Z_1\ \cos\psi_7 + U_1\ Z_2\ \cos\psi_8}{U_1\ U_2}$$

$$+ \frac{C_V}{U_3\ U_4}\,[(U_4\ Z_3\ W_3 + U_4\ V_3\ W_4)\ \cos\psi_5 - (U_3\ Z_4\ W_3 + U_3\ V_4\ W_6)\ \cos\psi_6], \qquad (185)$$

with the $\cos\psi_m$; m = 5, 6, 7, 8 being shorthand for sum and differences of the trigonometric terms.

$$\cos\psi_5 = \sin\theta\ \sin\alpha + \cos\theta\ \cos\alpha\ \cos(\phi - \gamma)$$

$$\cos\psi_6 = \sin\theta\ \sin\alpha + \cos\theta\ \cos\alpha\ \cos(\phi + \gamma)$$

$$\cos\psi_7 = -\sin\theta\ \sin\alpha + \cos\theta\ \cos\alpha\ \cos(\phi - \gamma)$$

$$\cos\psi_8 = -\sin\theta\ \sin\alpha + \cos\theta\ \cos\alpha\ \cos(\phi + \gamma)\ . \qquad (186)$$

The other variables, G_5, F_6, and G_6, also follow from the algebra (Ma and Walters, 1969).

Sloping rhombic, number 9

The sloping rhombic is an extension of the sloping vee with the wires bent to save space. The wires are numbered as in Figure 23. The geometry is the same as for the sloping vee. The length of the wire is input as L so equation (175) for the slope becomes

$$\sin\alpha = \frac{H_L - H}{2L} . \qquad (187)$$

The currents in wires 1 and 2 are the same. The currents in wires 3 and 4 are referenced to the center of the coordinate system and so are delayed in phase.

$$I_1(s) = -I_m e^{-jks}$$

$$I_2(s) = I_m e^{-jks}$$

$$I_3(s) = I_m e^{-jks} e^{-jkL}$$

$$I_4(s) = -I_m e^{-jks} e^{-jkL} . \qquad (188)$$

There is also a phase shift in the integrated fields due to the difference in distance to the far field point. Using the normal approximation, these are

$$r_3 = r - L \cos\psi_2$$
$$r_4 = r - L \cos\psi_1 . \qquad (189)$$

The off azimuth angles for wires 3 and 4 are the negative of those for 1 and 2. The integrated fields for wires 1 and 2 are again given by equations (179). For wires 3 and 4 the fields are

$$E_{\theta_3} = - e_p I_m e^{-jkL(1 - \cos\psi_2)} \Big\{ -\cos\alpha \cos\theta \cos(\phi - \gamma)$$

$$[F_1 - F_3 R_v e^{-2jkh \cos\theta} e^{-j2kLs \sin\alpha \cos\theta}]$$

$$+ \sin\alpha \sin\theta [F_1 + F_3 R_v e^{-2jkh \cos\theta} e^{-j2kLs \sin\alpha \cos\theta}] \Big\}$$

$$E_{\theta_4} = + e_p I_m e^{-jkL(1 - \cos\psi_1)} \Big\{ -\cos\alpha \cos\theta \cos(\phi + \gamma)$$

$$[F_2 - F_4 R_v e^{-j2kh \cos\theta} e^{-j2kLs \sin\alpha \cos\theta}]$$

$$+ \sin\alpha \sin\theta [F_2 + F_4 R_v e^{-2jkh \cos\theta} e^{-j2kLs \sin\alpha \cos\theta}] \Big\}$$

$$E_{\phi_3} = - e_p I_m e^{-jkL(1 - \cos\psi_1)} [\cos\alpha \sin(\phi - \gamma)$$

$$[F_1 + F_4 R_H e^{-j2kh \cos\theta} e^{-j2ks \sin\alpha \cos\theta}]]$$

$$E_{\phi_4} = + e_p I_m e^{-jkL(1 - \cos\psi_2)} [\cos\alpha \sin(\phi + \gamma)$$

$$[F_2 + F_4 R_H e^{-j2kh \cos\theta} e^{-j2ks \sin\alpha \cos\theta}]] . \qquad (190)$$

These equations are identical to those in Ma's text (1974) where here the height term for the start of the wires is written explicitly. The total fields and gain are

$$E_\theta = E_{\theta_1} + E_{\theta_2} + E_{\theta_3} + E_{\theta_4} = e_p I_m (F_1 + j G_7)$$
$$E_\phi = E_{\phi_1} + E_{\phi_2} + E_{\phi_3} + E_{\phi_4} = e_p I_m (F_8 + j G_8) \cos\alpha$$
$$g = \frac{30}{R_{in}} (F_7^2 + G_7^2 + \cos^2\alpha (F_8^2 + G_8^2)) . \qquad (191)$$

Again, the radiation resistance is taken as 600 ohms and the notation with F_7, G_7, F_8, and G_8 is to ease comparison with the computer code. The terms from wire 1 and 3 can be factored out as can those terms from wires 2 and 4. For the direct wave, the factors are (symbols as for the sloping vee)

$$A_6 + j B_6 = U_1 [F_1 - e^{-jkU_2} F_1] = U_2 [F_2 - e^{-jkU_1} F_2]$$

with

$$A_6 = 1 + \cos(kL(U_1 + U_2)) - \cos(kLU_1) - \cos(kLU_2),$$

$$B_6 = - \sin kL(U_1 + U_2) + \sin kLU_1 + \sin kLU_2 . \qquad (192)$$

For the ground reflected terms, the slope angle, α, was set to zero. This eliminates the extra height term and sets $U_1 = U_3$ and $U_2 = U_4$. Then the factors become

$$A_7 + j B_7 = U_4 [F_4 - e^{-jkU_1} F_4] = U_3 [F_3 - e^{-jkU_2} F_3]$$

$$= U_4 [F_4 - e^{-jkU_3} F_4] = U_3 [F_3 - e^{-jkU_4} F_3] \qquad (193)$$

with

$$A_7 = 1 + \cos kL(U_3 + U_4) - \cos kLU_3 - \cos kLU_4,$$

$$B_7 = - \sin kL(U_3 + U_4) + \sin kLU_3 + \sin kLU_4. \quad (194)$$

With these conventions, the variable F_7 in equation (191) is

$$F_7 = \left(\frac{\cos\psi_7}{U_1} - \frac{\cos\psi_8}{U_2} \right) A_6 - C_v \left(\frac{\cos\psi_5}{U_3} - \frac{\cos\psi_6}{U_4} \right) (A_7 W_3 - B_7 W_4). \quad (195)$$

The other variables, G_7, F_8, and G_8 then follow from similar algebra (Ma and Walters, 1969).

Horizontal rhombic, number 1

This antenna is a special case of the sloping rhombic. This was one of the earliest types analyzed. The equations derived above for the sloping rhombic can be used as is by setting the slope angle α to 0. These equations are here reduced to the special case. For $\alpha = 0$ the variables become

$$\cos\psi_1 = \cos\psi_3 = \sin\theta \cos(\phi - \gamma)$$

$$\cos\psi_2 = \cos\psi_4 = \sin\theta \cos(\phi + \gamma)$$

$$h_s = H$$

$$U_1 = U_3 = 1 - \sin\theta \cos(\phi - \gamma)$$

$$U_2 = U_4 = 1 - \sin\theta \cos(\phi + \gamma)$$

$$F_1 = F_3$$

$$F_2 = F_4$$

$$\cos\psi_5 = \cos\psi_7 = \cos\theta \cos(\phi - \gamma)$$

$$\cos\psi_8 = \cos\psi_6 = \cos\theta \cos(\phi + \gamma)$$

$$A_6 = A_7$$

$$B_6 = B_7.$$

The equality using A_6 and B_6 is evaluated as follows:

$$\frac{|A_6 + j\,B_6|^2}{U_1^2\,U_2^2} = \left|F_1 - e^{-jkLU_2}F_1\right|^2$$

$$= \left|F_2 - e^{-jkLU_1}F_2\right|^2$$

$$= \frac{\left|(1 - e^{-jkLU_1})\,(1 - e^{-jkLU_2})\right|^2}{U_1^2\,U_2^2}$$

$$= 16\,\frac{\sin^2\,(\tfrac{1}{2}kLU_1)\,\sin^2(\tfrac{1}{2}kLU_2)}{U_1^2\,U_1^2} \quad .$$

Then the E_θ and E_ϕ terms become

$$|F_7 + j\,G_7|^2 = 16\,\cos^2\theta\,[U_2\,\cos(\phi - \gamma) - U_1\,\cos(\phi + \gamma)]^2$$

$$\left(\frac{\sin^2\,(1/2\;LU_1)\,\sin^2\,(1/2\;kLU_2)}{U_1^2\,U_2^2}\right)(C_V^2\;|W_3 + j\,W_4|^2)$$

$$|F_8 + j\,G_8|^2 = 16\,[U_2^2\,\sin(\phi - \gamma) - U_1\,\sin(\phi + \gamma)]$$

$$\left(\frac{\sin^2\,(1/2\;kLU_1)\,\sin^2\,(1/2\;kLU_2)}{U_1^2\,U_2^2}\right)\,(C_H^2\;|W_1 + j\,W_2|^2) \quad .$$

The use of trignometric identities leads to

$$U_1\,\cos\psi_8 - U_2\,\cos\psi_7 = 2\,\cos\theta\,\sin\gamma\,\sin\phi$$

and

$$U_2\,\sin(\phi - \gamma) - U_1\,\sin(\phi + \gamma) = -2\,\sin\gamma\,(\cos\phi - \sin\theta\,\cos\gamma).$$

So the gain factors become

$$D_V^2 = \cos^2\theta \sin^2\phi \,[1 + C_V^2 + 2\, C_V \cos\psi_V']$$

$$D_H^2 = (\cos\phi - \sin\theta \cos\gamma)^2 \,[1 + C_H^2 - 2\, C_H \cos\psi_H']$$

$$g = 3.2\,(\sin^2\gamma)\,\left[\frac{\sin^2(1/2\; kLU_1)\,\sin^2(1/2\; kLU_2)}{U_1^2\, U_2^2}\right]\,[D_V^2 + D_H^2]\;. \qquad (196)$$

Interlaced rhombic, number 10

This array consists of two horizontal rhombics placed as in Figure 24. The notation used corresponds to that used in the computer code. The model is that for an end fire array as taken from Ma and Walters (1969). The geometric relations are

$$r_2 \sim r_1 - d\cos\psi_a$$

$$h_2 = h_1 + H_T$$

$$\cos\psi_a = \cos\theta \sin\alpha + \sin\theta \cos\alpha \sin\phi$$

$$d = \sqrt{\pi s^2 + H_T}$$

$$\tan\alpha = H_T/S.$$

The variable H_T is the difference in height here, not the total height. The angle ψ_a is the angle between the array axis and the vector to the far field point. The array is fed with an end fire phase difference of -kS. Since $S = d\alpha$, the total phase difference is

$$e^{-jk(S - d\cos\psi_a)} = e^{-jkd(\cos\alpha - \cos\psi_a)}$$

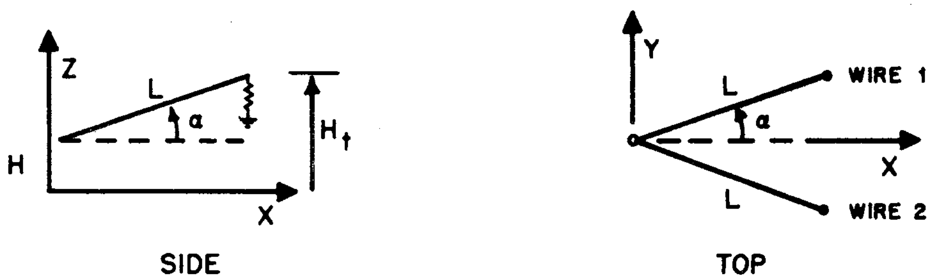

Figure 22. Terminated sloping vee antenna.

Figure 23. Sloping rhombic.

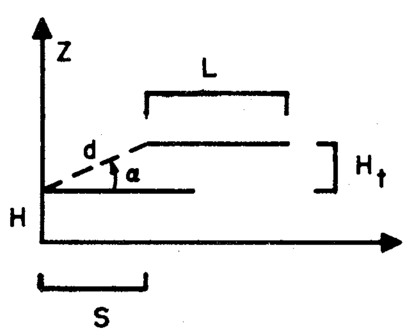

Figure 24. Interlaced rhombics.

which is the usual end fire condition in the α direction for an end fire array (Ma, 1974). The gain is given by equation (196) with D_V and D_H replaced by the following:

$$D_V = \cos\theta \sin\phi \, [1 + e^{-jY} - R_V e^{-2jkH \cos\theta} (1 + e^{-jZ})]$$

$$= \cos\theta \sin\phi \, [V_1 + j V_2]$$

$$D_H = (\cos\phi - \sin\theta \cos\gamma) \, [1 + e^{-jY} + R_H e^{-jZkH \cos\theta} (1 + e^{-jZ})]$$

$$= (\cos\phi - \sin\theta \cos\gamma) \, [H_1 + j H_2] \quad (197)$$

where

$$Y = k(S - d \cos\psi_a)$$

$$Z = Y + 2kH_T \cos\theta$$

$$V_1 = (1 + \cos Y) - C_V (\cos\psi_V' (1 + \cos Z) + \sin\psi_V' \sin Z)$$

$$V_2 = - \sin Y - C_V (- \sin Z \cos\psi_V' + \sin\psi_V' (1 + \cos Z))$$

$$H_1 = 1 + \cos Y + C_H (\cos\psi_H' (1 + \cos Z) + \sin\psi_H' \sin Z)$$

$$H_2 = - \sin Y + C_H (- \sin Z \cos\psi_H' + \sin\psi_H' (1 + \cos Z)) \quad (198)$$

$$C_V = |R_V|$$

$$\psi_V' = \psi_V - 2kH \cos\theta$$

$$C_H = |R_H|$$

$$\psi_H' = \psi_H - 2kH \cos\theta \; .$$

Horizontal double rhombic, number 16

This array consists of two identical rhombics offset from the desired direction by a small angle and fed at a common junction. The sides are numbered as in Figure 25. Sides 1, 3, 6, and 8 form one rhombic, while sides 2, 4, 5, and 7 form the second. The current in each wire is:

Rhombic 1:

$$I_1 = - I_m e^{-jks}$$

$$I_3 = I_m e^{-jks}$$

$$I_6 = I_3 e^{-jkL_1}$$

$$I_8 = I_3 e^{-jkL_2}$$

Rhombic 2:

$$I_2 = I_1$$

$$I_4 = I_3$$

$$I_5 = - I_8$$

$$I_7 = - I_6 .$$

The fields from each wire are evaluated ignoring the offset angle β. For the first rhombic, the fields are:

$$E_{\theta_1} = \cos\theta \, [(\frac{1 - e^{-jkL_1U_1}}{U_1}) (1 - e^{-jkL_2U_3}) \cos (\phi - \alpha_1)$$

$$- (\frac{1 - e^{-jkL_2U_3}}{U_3}) (1 - e^{-jkL_1U_1}) \cos (\phi + \alpha_2)] .$$

Ignoring the constant terms in the absolute value of E_{θ_1} (a factor of 4 is transferred to the constants), this becomes

$$E_{\theta_1} = \cos\theta \left[\frac{\sin(1/2\ kL_1U_1)\sin(1/2\ kL_2U_3)}{U_1\ U_3}\right] [U_3 \cos(\phi - \alpha_1) - U_1 \cos(\phi + \alpha_2)]$$

$$= \cos\theta \left[\frac{\sin(1/2\ kL_1U_1)\sin(1/2\ kL_2U_3)}{U_1\ U_3}\right] [\cos\phi\ (\cos\psi_1 - \cos\alpha_2)$$

$$+ \sin\phi\ (\sin\alpha_1 + \sin\alpha_2)] \qquad (199)$$

where, as before

$$U_1 = 1 - \sin\theta \cos(\phi - \alpha_1)$$

$$U_2 = 1 - \sin\theta \cos(\phi - \alpha_2)$$

$$U_3 = 1 - \sin\theta \cos(\phi + \alpha_2)$$

$$U_4 = 1 - \sin\theta \cos(\phi + \alpha_1) \qquad (200)$$

$$E_{\phi_1} = -\left(\frac{1 - e^{-jkL_1U_1}}{U_1}\right)(1 - e^{-jkL_2U_3}) \sin(\phi - \alpha_1)$$

$$+ \left(\frac{1 - e^{-jkL_2U_3}}{U_1}\right)(1 - e^{-jkL_1U_1}) \sin(\phi + \alpha_2)\ . \qquad (201)$$

Ignoring the constant terms in the absolute value of E_{ϕ_1}, this becomes

$$E_{\phi_1} = -\left[\frac{\sin(1/2\ kL_1U_1)\sin(1/2\ kL_2U_3)}{U_1\ U_3}\right] [U_3 \sin(\phi - \alpha_1)\ U_1 \sin(\phi + \alpha_2)]$$

$$= -\left[\frac{\sin(1/2\ kL_1U_1)\sin(1/2\ kL_2U_3)}{U_1\ U_3}\right] [\ \sin\phi\ (\cos\alpha_1 - \cos\alpha_2)$$

$$- \cos\phi\ (\sin\alpha_1 + \sin\alpha_2) + \sin\theta \sin(\alpha_1 + \alpha_2)]\ . \qquad (202)$$

For the second rhombic,

$$E_{\theta_2} = -\cos\theta \left[\frac{\sin(1/2\ kL_2U_2)\sin(1/2\ kL_1U_4)}{U_2\ U_4}\right]$$

$$* [\cos\phi\ (\cos\alpha_1 - \cos\alpha_2) - \sin\phi\ (\sin\alpha_1 + \sin\alpha_2)] \qquad (203)$$

$$E_{\phi_2} = \left[\frac{\sin(1/2\ kL_2U_2)\ \sin(1/2\ kL_1U_4)}{U_2\ U_4}\right]$$

$$* \left[\sin\phi\ (\cos\alpha_1 - \cos\alpha_2) + \cos\phi\ (\sin\alpha_1 + \sin\alpha_2) - \sin\theta\ \sin(\alpha_1 + \alpha_2)\right] \quad (204)$$

$$E_\theta = E_{\theta_1} + E_{\theta_2}$$

$$E_\phi = E_{\phi_1} + E_{\phi_2}$$

$$g = 1.6\ (E_\theta^2\ K_V^2 + E_\phi^2\ K_\phi^2) \quad (205)$$

where R_{in} is taken as 300 ohms corresponding to the doubled receiving area.

For the special case of equal leg lengths, $L_1 = L_2$, we have $\alpha = \alpha_1 = \alpha_2$, $U_1 = U_2$, $U_3 = U_4$.

$$E_\theta = 4\cos\theta\ \left[\frac{\sin(1/2\ kL_1U_1)\ \sin(1/2\ kL_2U_2)}{U_1\ U_2}\right] \sin\phi\ \sin\alpha$$

$$E_\phi = 4\sin\gamma\ \ (\cos\phi - \sin\theta\ \cos\gamma)\ \left[\frac{\sin(1/2\ kL_1U_1)\ \sin(1/2\ kL_2U_2)}{U_1\ U_2}\right]$$

which agrees with the single rhombic equation (196).

Side loaded vertical half-rhombic, number 15

This antenna consists of two wires arranged so that the antenna would be a vertical rhombic over perfectly conducting earth (Figure 26). The geometric relationships for this antenna are

$\theta_a = 90° - \alpha = 90° - \gamma$ for wire number 1.

$\theta_a = 90° - \alpha = 90° + \gamma$ for wire number 2.

$\cos\psi_a = \cos\psi_1 = \cos\theta\ \sin\gamma + \sin\theta\ \cos\gamma\ \cos\phi$; wire 1

$\cos\psi_a' = \cos\psi_2 = -\cos\theta\ \sin\gamma + \sin\theta\ \cos\gamma\ \cos\phi$

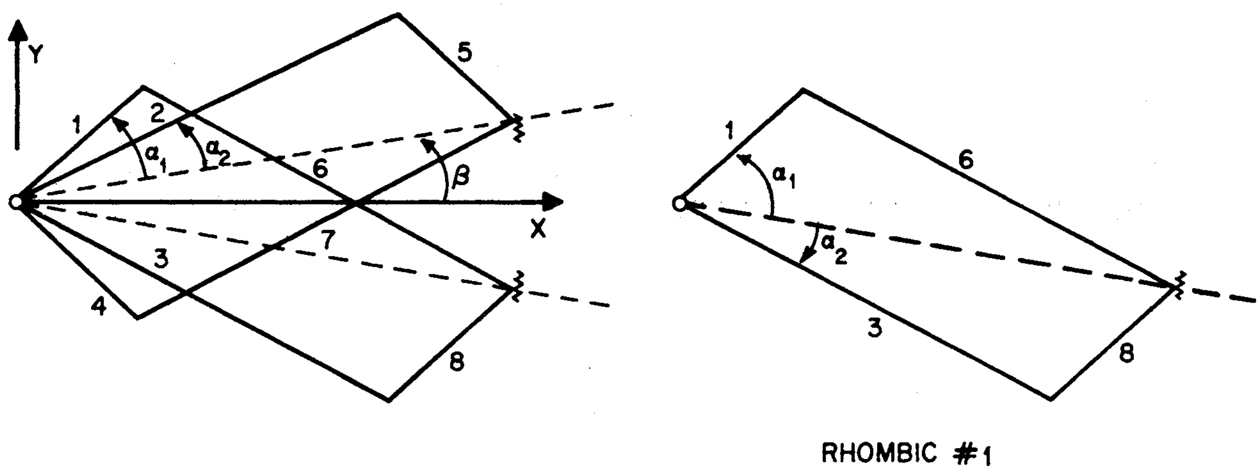

Figure 25. Horizontal double rhombic.

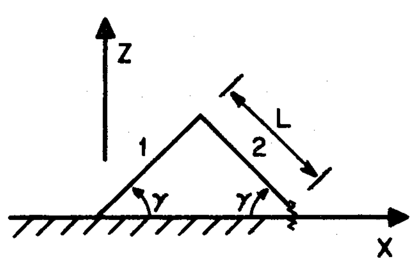

Figure 26. Vertical half rhombic.

for the image of wire 1 and the angle for wire 2. Also

$$\cos\psi_a = \cos\psi_2$$

$$\cos\psi_a' = \cos\psi_1 \text{ , for wire 2.}$$

$$h_s = s \sin\gamma, \qquad \text{for wire 1}$$

$$h_s = (L - s) \sin\gamma, \text{ for wire 2.}$$

The currents are

$$I_1 = I_m e^{-jks}, \text{ for wire 1;}$$

$$I_2 = I_m e^{-jks} e^{-jkL}.$$

The usual approximation for the distance to the far field point is used

$$r_2 \sim r_1 - L \cos\psi_1 \quad \text{for wire 2.}$$

This gives for wire 2 a total phase lag

$$e^{-jkLU_1} \text{ where as before}$$

$$U_1 = 1 - \cos\psi_1$$

$$U_2 = 1 - \cos\psi_2.$$

The field integrals for wire 2 will contain the factor

$$a = e^{-2jkL \sin\gamma \cos\theta}.$$

When combined with the phase lag,

$$a\, e^{-jkLU_1} = e^{-jkLU_2}.$$

Combining equations (50) and (51) with the integral equation (168) and the geometry above, the field equations are

$$E_{\theta_1} = \cos\gamma \cos\theta \cos\phi \,(F_1 - R_V F_2) - \sin\gamma \sin\theta \,[F_1 + R_V F_2]$$

$$E_{\theta_2} = e^{-jkLU_1} [\cos\gamma \cos\theta \cos\phi \,(F_2 - R_V F_1 e^{-jkL \sin\gamma \cos\theta})$$

$$+ \sin\gamma \sin\theta \,[F_2 + R_V F_1 e^{-2jkL \sin\gamma \cos\theta}]$$

$$E_{\phi_1} = \cos\gamma \sin\phi \; (F_1 + R_H F_2)$$

$$E_{\phi_2} = e^{-jkU_1} \cos\gamma \sin\phi \; [F_2 + R_H \; F_1 e^{-2jkL \sin\gamma \cos\theta}] \; . \qquad (206)$$

The gain is then

$$g = \frac{30}{R_{in}} \; (|E_\theta|^2 + |E_\phi|^2) \qquad (207)$$

where

$$R_{in} = 300 \text{ ohms}$$

$$E_\theta = E_{\theta_1} + E_{\theta_2}$$

$$E_\phi = E_{\phi_1} + E_{\phi_2} \; .$$

The computer code uses the notation (Ma and Walters, 1969)

$$E_\theta = F_9 + j \; G_9$$

$$E_\phi = \cos\gamma \sin\phi \; (F_{10} + j \; G_{10})$$

$$A_8 = \cos\gamma \cos\theta \cos\phi - \sin\gamma \sin\theta$$

$$B_8 = \cos\gamma \cos\theta \cos\phi + \sin\gamma \sin\theta \; .$$

Separating equations (206) into the real and imaginary parts

$$F_9 = A_8 \left(\frac{1 - \cos kLU_1}{U_1}\right) + B_8 \left[\frac{\cos (kLU_1 - \cos [kL (U_1 + U_2)]}{U_2}\right]$$

$$- C_V \left[B_8 \left(\frac{\cos\psi_V - \cos (\psi_V - kLU_2)}{U2}\right)\right.$$

$$\left. + A_8 \left(\frac{\cos (\psi_V - kLU_2) - \cos (\psi_V - kL (U_1 + U_2))}{U_1}\right)\right]$$

$$G_9 = A_8 \frac{\sin (kLU_1)}{U_1} - B_8 \left[\frac{(\sin kLU_1 - \sin [kL (U_1 + U_2)])}{U_2}\right]$$

$$- C_V \left[B_8 \left(\frac{\sin\psi_V - \sin(\psi_V - kLU_2)}{U_2}\right)\right.$$

$$\left. + A_8 \left(\frac{\sin (\psi_V - kLU_2) - \sin (\psi_V - kL (U_1 + U_2))}{U_1}\right)\right]$$

$$F_{10} = \left(\frac{1 - \cos (kLU_1)}{U_1}\right) + \frac{\cos (kLU_1) - \cos [kL (U_1 + U_2)]}{U_2}$$

$$+ R_H \left[\left(\frac{\cos\psi_H - \cos (\psi_H - kLU_2)}{U_2}\right)\right.$$

$$\left. + \left(\frac{\cos (\psi_H - kLU_2) - \cos (\psi_V - kL (U_1 + U_2))}{U_1}\right)\right]$$

$$G_{10} = \frac{\sin (kLU_1)}{U_1} - \frac{\sin (kLU_1) - \sin [kL (U_1 + U_2)]}{U_2}$$

$$+ R_H \left[\frac{\sin\psi_H - \sin (\psi_H - kLU_2)}{U_2}\right.$$

$$\left. + \frac{\sin (\psi_H - kLU_2) - \sin (\psi_H - kL (U_1 + U_2))}{U_1}\right] . \qquad (208)$$

So the gain becomes

$$g = .1 (F_9^2 + G_9^2 + \cos^2\gamma \sin^2\phi (F_{10}^2 + G_{10}^2)) . \qquad (209)$$

7. MISCELLANEA

A description of remaining antenna models is presented in this section.

7.1 Isotropic, Number 12

The reference antenna is an isotropic antenna as described in Section 2.1. For this antenna, the gain is 0 dBI with an efficiency of 1. (0 dB loss). For use with the prediction program, the user can input added gain and efficiency. This procedure will, howeve, not include ground effect or polarization effects. The option to use the ground reflection factors has been added to the subroutine; vertical, horizontal, or circular polarization may be specified. The equations are

Horizontal:

$$g = (C_H^2 + 1 + 2\ C_H \cos\psi_H'$$

$$+ C_V^2 + 1. - 2\ C_V \cos\psi_V')/2. \qquad (210)$$

Vertical:

$$g = C_V^2 + 1 + 2\ C_V \cos\psi_V'. \qquad (211)$$

Circular:

$$g = (C_H^2 + 1. + 2\ C_H \cos\psi_H' + C_V^2 + 1. - 2\ C_V \cos\psi_V'$$

$$+ C_V^2 + 1 + 2\ C_V \cos\psi_V')/3. \qquad (212)$$

7.2 Measured Pattern Adjustment, Number 25

This model makes use of measured patterns in free space and adds the effect of the ground. If the antenna (array) is at a constant height, the ground effect can be factored from the general antenna equations (as for the Yagi). Then the ground reflection factors can be used to evaluate the ground effect. The measured gain is obtained by table look-up.

7.3 Smoothing the Nulls in the Antennna Patterns

While the prediction program uses a ray to describe the propagation path, the actual propagation is by a wave that may arise from a larger part of the antenna pattern than that indicated by the ray alone. The standard practice was to take the minimum gain as -10 dBI corresponding to long distance (i.e., low radiation angles) propagation. For short distances (high radiation angles), this procedure can result in gains being unrealistically high. A simple procedure based on the variation with radiation angle of the area illuminated at the ionosphere by the antenna is used. This area is proportional to the square of the sine of the radiation angle (Δ). The minimum gain is set to -10 dBI at 3 degrees.

$$
\begin{aligned}
g_M &= -35.624 \quad \text{for } \Delta \geq 70° \\
&= -35.624 - 20 \log_{10} (\sin\Delta); \; 3° \leq \Delta < 70° \\
&= -10. \quad \text{for } \Delta \leq 3°. \qquad (213)
\end{aligned}
$$

This procedure allows the nulls of the antenna pattern to vary smoothly from -10 dBI at long distances to -35 dBI at short distances.

8. REFERENCES

Barghausen, A. F., J. W. Finney, L. L. Proctor, and L. D. Schultz (1969), Predicting long-term operational parameters of high-frequency skywave telecommunication systems, ESSA Technical Report ERL 110-ITS 78, May, (NTIA Access. No. N70-24144, Springfield, VA 22161).

Beckmann, B. (1965), Bemerkungen zur Abhangigkeit der Empfangsfeldstarke von den Grenzen des Ubertragungsfrequenzbereiches, NTZ, Vol. 19, 643-653.

Bremmer, H. (1949), Terrestrial Radio Waves, (Elsevier Publishing Co., New York, New York).

Carrel, R. L. (1961), Analysis and design of the log-periodic dipole antenna, University of Illinois Tech. Report No. 52, Urbana, Illinois.

CCIR (1970), Report 252-2, CCIR Interim method for estimating skywave field strength and transmission loss at frequencies between the approximate limits of 2 and 30 MHz, ITU, Geneva, Switzerland.

CCIR (1978), Antenna Diagrams, ISBN 92-61-00531-4, ITU, Geneva, Switzerland.

Central Radio Propagation Laboratory (CRPL), (1948), Ionospheric radio propagation, NBS Circular 462 (NTIS Access. No. PB257342/6ST).

Feldman, C. B. (1933), Optical behavior of the ground for short radio waves, Proc. IRE 21 764.

Haydon, G. W., and D. L. Lucas (1968), Predicting ionosphere electron density profiles, Radio Sci. 3, No. 13, pp. 111-119.

Haydon, G. W., D. L. Lucas, and R. A. Hanson (1969), Technical considerations in the selection of optimum frequencies for high frequency skywave communication services, ESSA Tech. Report ERL 113-ITS 81, U.S. Dept. of Commerce, Boulder, Colorado. This report is a reprint of NBS Report 7249, originally issued November 1962.

Haydon, G. W., M. Leftin, and R. K. Rosich (1976), Predicting the performance of high frequency skywave telecommunications systems, OT Report 76-102, (NTIA Access. No. PB258556/AS).

IEEE (1965), Test Procedures for Antennas, No. 149 (revision of 48 IRE 252), Trans. Ant. Prop. AP-13, No. 6, pp 896-903, November.

Isbell, D. E. (1959), A log-periodic reflector feed, Proc. IRE 47, No. 6, pp. 1152-1153, June.

Jordan, E. C. (1950), Electromagnetic Waves and Radiating Systems, (Prentice-Hall, Englewood Cliffs, N.J).

King, R. W. (1967), The linear antenna - Eighty years of progress, Proc. IEEE 55, pp. 2-10.

Kraus, J. (1950), Antennas, (McGraw-Hill Co., Inc., New York, NY).

Laitinen, P. O., and G. W. Haydon (1950), Analysis and prediction of skywave field intensities in the high frequency band, U.S. Army Signal Radio Propagation Agency Tech. Report No. 9, Rev. (RPN 203).

Laitinen, P. O. (1957), Linear communication antennas, U.S. Army Signal RPA, Technical Report No. 7, Fort Monmouth, N.J.

Lucas, D. L., and G. W. Haydon (1961), MUF-FOT predictions by electronic computers, NBS Report 6789. U.S. Department of Commerce, Boulder, CO.

Lucas, D. L., and G. W. Haydon (1966), Predicting statistical performance indexes for high frequency telecommunications systems, ESSA Tech. Report IER 1-ITSA 1, (NTIS Access. No. AD644827).

Ma, M. T., and L. C. Walters (1969), Power gains for antennas over lossy plane ground, ESSA Tech. Report ERL 104-ITS 74, U.S. Dept. of Commerce, Boulder, CO 80303. See also Ma (1974).

Ma, M. T. (1974), Theory and Application of Antenna Arrays, (John Wiley & Sons, New York).

Mailloux, R. (1966), The long Yagi-Uda array, IEEE Trans. Ant. Prop. 14, No. 2, pp. 128-137.

Norton, K. A. (1937), The propagation of radio waves over the surface of the earth and in the upper atmosphere, Part II, Proc. IRE 25, pp. 1192-1202, Sept.

Norton, K. A. (1941), The calculation of ground-wave field intensity over a finitely conducting spherical earth, Proc. IRE 29, pp. 623-639, Dec.

Norton, K. A. (1959), Transmission loss in radio propagation - II, NBSA Tech. Note No. 12.

Okumura, Y., E. Ohmori, T. Kawano, and K. Fukuda (1968), Field strength and its variability in VHF and UHF land-mobile radio service, Review of Electrical Communication Lab.

Ramo, S., and J. R. Whinnery (1960), Fields and Waves in Modern Radio, (John Wiley and Sons, New York).

Rice, P. L., A. G. Longley, K. A. Norton, and A. P. Barsis (1965), Transmission loss predictions for tropospheric communication circuits, NBS Tech. Note 101, (NTIS Access. Nos. AD687820 and AD687821).

Schelkunoff, S. A. (1939), A general radiation formula, Proc. IRE 27, Oct.

Schelkunoff, S. A., and H. T. Friis (1952), Antennas - Theory and Practice, (John Wiley and Sons, New York).

Smith, C. E. (1966) Log periodic antenna design handbook, 1st ed., Smith Electronics, Inc., Cleveland.

Sommerfeld, A. (1964), Theoretical Physics, Vol. 6, (Academic Press).

Stewart, A. C., M. E. Chrisman, C. O. Stearns (1964), Computed antenna pattern for Voice of America curtain arrays, NBS Report 8220, Boulder, CO.

Strait, B. J. (1980), Applications of the Method of Moments to Electromagnetic Fields, (The SCEEE Press, St. Cloud, Florida).

Thiele, G. A. (1969), Analysis of Yagi-Uda type antennas, IEEE Trans. Ant. Prop. 17, pp. 24-31.

Uda, S., and Y. Mushiake (1954), Yagi-Uda Antenna, (Sasaki Printing and Publishing Co., LTD, Sendai, Japan).

Wolfe, E. (1967), Antenna Analysis, (John Wiley and Sons, Inc., New York, NY).

SECTION 2. USER'S INFORMATION

1. INTRODUCTION

This section is arranged in accordance with the more complete manual describing the use of the general systems performance prediction program. Only information relating to the antenna submodule is included here.

2. PRIMARY PROGRAM RELATED REQUIREMENTS

The computer requirements for use of the antenna submodule are presented here. The computer code is as close to ANS FORTRAN as was possible for implementation on the available computer. No external data base is necessary for the antenna submodule. No complex arithmetic, numeric integration method, or matrix inversion routines are required. Computer systems using 16 bit integer words and 32 floating point words are adequate for this submodule (and for the full IONCAP program as well). The antenna submodule can be used as part of the full prediction program or as part of a separate program using the ANTCAP program as a driver. The computer requirements for the prediction program are found in the user's manual for that program. For use as a stand-alone program with ANTCAP, the computer requirements follow. The load module requires 17000 (decimal) floating point words. Of this, 5586 are the output arrays and 3914 are the operating system. Three files are used:

TAPE 5: An input file, 80 characters per record are used (card images).

TAPE 6: An output file, 135 characters per record (print file).

OUTPUT: System output file, used for system messages.

3. INPUT DATA REQUIREMENTS

The input for the antennas submodule consists of a description of the antenna site, of the antenna configuration, and of the run options desired. Each antenna is described by a single card (Table 4) with the exception of the stacked arrays which require an additional card. Only those input cards that are relevant to the antenna submodule are described here. Figures 38 to 57 describe the antenna configurations and the corresponding input cards.

Each card format consists of an alphanumeric name up to 10 columns, followed by up to 14 data fields of 5 columns each. Each floating point variable may have a decimal inserted, while the integer variables must be right justified.

Floating variables are read in an F5.1 format. Thus "12345" in the field is the number 1234.5 for all variables.

Each input card diagram for an antenna contains three columns; the first is the card column number of the field; the second is the format used to decode the field; and the third is the description of the variable.

The ANTENNA input card defines whether the antenna is transmitting or receiving, specifies the type of the antenna, the ground conductivity, and dielectric constants in addition to the other parameters necessary to compute the necessary antenna patterns. Typical values for selected ground types are given in Table 5 where typical good ground is low hills with unforested rich soil or flat wet coastal regions; fair ground is medium hills or forested heavy soil; and typical poor ground includes rocky steep hills, sandy dry coastal regions, and city industrial areas. The ground constants are optional on each antenna card for the IONCAP program but are required for the ANTCAP program. If not specified by the user, they will be calculated with the land mass map from the ionospheric long-term data base file. The ground constants will be set to poor ground as a default if they are not specified by the user and the land mass map is not available. The user may specify up to three transmitter antennas and three receiver antennas to cover the frequency range considered for each system configuration. It is also possible, with the IONCAP program, to indicate that the antenna is to be read from an external antenna file (LU25) instead of being calculated by the program. The input parameters required vary with antenna type. The basic ANTENNA card parameters are described below and the geometric description of each available antenna type is given in Figures 38 through 57.

(a) IAT indicates whether the antenna is transmitting or receiving,

IAT = 1 for transmitting, IAT = 2 for receiving.

(b) IANTR indicates the number that corresponds to the antenna type desired.

(c) AETA indicates the antenna bearing in degrees from east of north. Negative denotes off-azimuth from along the desired path. Positive denotes the main beam direction.

(d) ASIG indicates the ground conductivity (σ) in mhos per meter.

(e) AEPS indicates the relative dielectric constant (ε).

The following parameters describe various characteristics dependent on the antenna type specified. The user should refer to Tables 6 through 46 for the description of the following antenna parameters and the antenna characteristics required for each antenna type.

(f) AND - usually an angle.

(g) ANH - usually a height term; negative being in wavelengths.

(h) ANL - usually antenna length (height); negative being in wavelengths.

(i) AEX(4) - four variables used to describe the more complicated antennas. If not needed, AEX(1) is gain, dB, above computed gain by the model.

(j) AFQB - ending frequency when more than one antenna is used for a pattern. Starting frequency is 1 MHz; each antenna card then indicates the last frequency for that one. The starting frequency for each antenna is 1 MHz more than the last ending frequency. Thirty frequencies are used for each antenna pattern.

(k) IAIN - indicates antenna number 1, 2, or 3 for multiantenna patterns.

The placement of the input parameters on the output formats is given in Table 3.

In order to specify the arrangement of a stacked array, an additional antenna card is required. The system used is to add 100 to the antenna number; e.g., for a stacked array of vertical log periodic dipoles, antenna number 23, the auxiliary card uses 123 as the antenna type. The number 100 was used to indicate a change of starting frequency for the pattern, AETA becoming the new start frequency (1. MHz is default).

Other input cards relevant to the antenna submodule include the METHOD card, the EXECUTE card, the COMMENT card, and the QUIT card. The METHOD card, if used for antenna patterns, has 13, 14, or 15 in columns 11-15 (I5 format). The EXECUTE card needs no additional information. The COMMENT card allows description of the input in columns 11-80. The QUIT card is required at the end of the input card record. The ANTCAP program ignores all cards except the ANTENNA card and the QUIT card. The ANTENNA card will execute and print a pattern. The QUIT card will end program execution.

Table 3. Output of input parameters

OUTPUT:

Field	INPUT	PRINT OUT
0	"ANTENNA"	
1	IAT	---
2	IANTR	Alpha
3	AETA	Azimuth
4	ASIG	Conductivity
5	AEPS	Dielectric Constant
6	AND	Angle
7	ANH	Height
8	ANL	Length
9	AEX(1)	EX(1)
10	AEX(2)	EX(2)
11	AEX(3)	EX(3)
12	AEX(4)	EX(4)
13	AFQB	"Frequency Range"
14	IAIN	

4. OUTPUT OPTIONS

The only output of the antenna module is antenna gain (dBI) and efficiency (dB). A set of sample patterns is given in Tables 27 to 50. Table 26 is the input data used to generate these tables. Where available these correspond to published patterns (Ma, 1974). The ANTCAP program includes the radiation resistance output line.

5. APPLICATIONS

The output of the antenna submodule consists of the antenna gain in dBI as a function of elevation angle, azimuth, and frequency, and the efficiency in dB as a function of frequency. The antenna models were based upon the assumption that the antenna was well designed and that the operating frequencies used are within the design limits of the antenna. Operation outside the designed frequency range of the antenna or constructing a hypothetical antenna that does not correspond to a reasonable configuration may result in misleading and erroneous results from these models.

The antenna gain consists of three components: the space pattern corresponding to the $(|E_\theta|^2 + |E_\phi|^2)$ term, the radiation resistance, and the efficiency.

The radiation resistance and efficiency terms will set the maximum gain at each frequency but will not affect the variation with elevation angle and azimuth. Thus a knowledgeable user can adjust the power/gain input to overcome suspected deficiencies in the radiation resistance or efficiency calculations.

The subroutines in the antenna module are listed in Tables 47 and 48. General subroutines are listed along with their function in Table 47. The subroutine for each antenna type is listed in Table 48 along with a cross-reference to the input table and to the theoretical equations used.

As was described in Section 2, the antennas modeled are for skywave patterns, are referred to an isotropic radiator, and are to be used in the system loss calculation. Most of the variation in the system loss calculation is due to those variables which depend upon the state of the ionosphere. The effect on the use of the antenna models is the change of usable frequency with the resultant changes in elevation angle. The problem to be solved by the user of the antenna models is then to select or design an antenna system that will, with some acceptable probability, provide the necessary power/gain pattern over the required period of time and area of coverage. There are basically two methods that have been used with the prediction programs. The first is a brute-force method of running all possible antenna models with complete system performance predictions and then selecting the optimum antenna from the output. An alternate approach is to first run the prediction with a standard reference antenna, e.g., isotropic radiator, or a short vertical or horizontal dipole. The prediction run could be based only on MUFs for each layer saving the elevation angles. Then from a collection of antenna patterns, select an adequate antenna system(s). Finally, check the selection using a full systems performance. The alternate approach tends to much shorter labor time and computer cost.

The collection of antenna patterns could come from measured patterns or be precalculated from other models or from those included here. Within limits, the models used here can be used to design antenna systems to operate at specified elevation angles at specified frequencies. The known limitations in the models used here are discussed in the same order as they were presented in Section 1.

Vertical Monopole, No. 2: This model uses the traditional equations (64 ff.) with the efficiency factor modeled assuming a properly designed ground screen. The radition resistance is the perfect ground approximation.

Sloping Long Wire (Standing Wave), No. 11: This model uses the usual equations (71 ff.) with a perfect ground assumption for the radiation resistance. The base of the antenna may be raised above the ground. The radiation resistance has an elevation angle limitation of 10 degrees. When the antenna is horizontal and low to the ground, this approximation will not cancel the field as is appropriate for perfect ground (Sommerfeld, 1964).

Inverted L, No. 8: This model uses the usual equations (96 ff.). The radiation resistance assumes the perfect ground approximation. The efficiency factor assumes an appropriate ground screen. Problems with the radiation resistance model at low frequencies for some configurations have been corrected. The base of the antenna may be raised above ground.

Tilted Dipole, No. 14; Horizontal Dipole, No. 3; and Vertical Dipole, No. 5: These antennas are based on the same basic equations for the radiated field (113 ff.). The radiation resistance is the free-space approximation. With this approximation, the tilted dipole model will yield the horizontal dipole or the vertical dipole with the appropriate input.

Yagi Array, No. 4: This model uses the usual equations (129, 130) for the radiated field with the currents for each element taken from a table appropriate for the HF and low VHF frequency bands. The radiation resistance is a free-space approximation. The number of elements may be two or more. Appropriate curves have been devised to design this type of antenna (Uda and Mushiake, 1954). The model implemented here will give valid results for antennas designed this way.

Curtain Array, No. 6: This model uses the standard array equations (135 ff.). The radiation resistance is the constant 480. A reflecting curtain is always included. See the discussion of the model in Section 4 for the use of the CCIR notation HR N/M/H, for the possible inclusion of beam steering, and for the quick method of estimating maximum gain.

Horizontal LPD Array, No. 13; Vertical LPD Array, No. 22: These models employ the usual equations for the radiated field (138 ff.) with the currents given by a preconstructed curve. The radiation resistance is given by an empirical formula. The model is intended to be correct only within the design range of the antenna. Outside the design range, the model returns a dipole pattern. Only the halfwave active region is considered. Higher order, e.g., 3/2 wave, active regions are not considered. Design methods for these types of antennas is given in Smith (1966). This design method corresponds to the measured criteria given by Carrel (1961) as do the antenna models used here.

The rhombic and other traveling wave antennas assume proper termination and use radiation resistances of 600 or 300 ohms. The efficiency of these antennas was taken as -1.7 dB (67 percent) which corresponds to that used in previous antenna programs. This value should vary in accordance with the radiation resistance used. The -1.7 corresponds to a radiation resistance of 600 ohms. For a value of 1000 ohms, the efficiency is -3 dB; for 300 ohms, -0.5 dB (Schelkunoff and Friis, 1952). Design criteria for rhombic antennas is given by Harper (1941). Some criteria for arrays of rhombics are given by De Carvalho (1959).

Terminated Sloping Long Wire, No. 20: This model is based on the equations for a traveling wave when a terminator used (Eq. 169 ff.). The radiation resistance is taken as 300 ohms. The base of the antenna may be elevated from the ground, in which case it corresponds to a wave or Beverage antenna. This antenna is intended for use as a receiving antenna. For use as a receiver, the low powers involved allow an easy method of termination. For use as a transmitter, the terminating resistance must be capable of dissipating a significant proportion of the power supplied while the terminating resistance has no inductance or capacity (Thourel, 1960).

Terminated Sloping Vee, No. 7: This model uses the usual equations (174 ff.) with a radiation resistance of 600 ohms.

Sloping Rhombic, No. 9: This model uses the usual equations (187 ff.) with a radiation resistance of 600 ohms. The ground reflected wave is taken as if the image is horizontal. This was implicit in some of the older gain programs.

Horizontal Rhombic, No. 1: This is a special case of the sloping rhombic. However, the equations have been rearranged into the traditional form (Eq. 196) used in design (Harper, 1941). That is a term depending on the angle between the wires, a term depending largely upon the length of the wires, and a term depending on polarization and ground reflections. The mistake in the sign of the vertical ground reflection factor has been corrected.

Interlaced Rhombic, No. 10: This array consists of two horizontal rhombics offset in the horizontal direction and possibly in the vertical direction. The rhombics are assumed to be fed as an end fire antenna. The signs on the reflected wave terms (Eq. 197, 198) are corrected to agree with the reflection coefficient normalization and the phase difference in currents between the rhombics. The radiation resistance is taken as 600 ohms.

Horizontal Double Rhombic, No. 16: This array consists of two rhombics offset from the desired direction by a small angle (Eq. 199 ff.). The rhombics are fed at a common junction. The radiation resistance is taken as 300 ohms.

Side Loaded Vertical Half Rhombic, No. 15: This antenna is constructed so that it would be a vertical rhombic when over perfectly conducting earth (Eq. 206 ff.). The radiation resistance is 300 ohms.

Isotropic Antenna, No. 12: This antenna is included as a reference antenna. A common practice has been to use this option and to use the minimum angle option with the prediction program. This procedure is intended to eliminate those lower angles at which the antenna is not expected to operate effectively. For long distance circuits this procedure can be misleading, since the MUFs may be artificially reduced due to lower order modes not being present. A more effective method is to use a standard reference antenna that will include the effect of the ground cutback factors. The vertical polarization or the circular polarization options included with this model is a possible choice of a reference.

6. CONCLUSIONS

The work presented here is intended to be documentation of antenna models intended for use with the HF skywave systems performance program (IONCAP). This report is not intended to be a general antenna design guide or user's handbook. The general antenna equations are included here and all radiation equations are derived here. Thus, the work could be used as a reference to derive equations for other wire antennas. The radiation resistance equations are not derived here but are selected from the literature. Most of the equations used are found and derived in the monograph by Schelkunoff and Friis (1952).The major benefits of this work are:

(1) direct correlation between the equations and the computer code

(2) all radiation pattern equations are derived and compared with published equations if available

(3) the use of the radiation resistance equations is clarified and referred to their source

(4) the normalization of the reflection coefficients and their use with the ground reflection factors is clarified. (This problem has been recurring for 50 years)

(5) the models for use with the prediction program are simplified and computational stability of the computer code enhanced.

The chief limitations of the work are:

(1) Possibly invalid results when the antenna is placed close to the ground. This problem arises for smooth ground sites because of the approximation of free space or of perfect ground that is used for the radiation resistance. For realistic antenna sites, local variations in the site parameters are important and cannot be included in general routines as provided here. A table of this effect for horizontal dipoles over perfect ground is included in this report.

(2) The use of the models outside the design limits of the antenna may not be valid. This is not always apparent when a frequency complement covering a large band is used. Some attempt has been made to assure that the antenna will appear to perform poorly outside its intended region when compared to performance within the designed range. But no claim to absolute accuracy of the pattern outside its design range is made.

Possible areas of improvement to this work are:

(1) incorporation of antenna types not included here

(2) improvements to the solution of the interior problem, mainly radiation resistances, as used here.

Methods such as those using numeric integration and matrix inversion techniques such as the three-term theory (Ma, 1974) or the many method-of-moment programs (Strait, 1980) are not really improvements to the work here but rather are alternative and sometimes more accurate approaches. Patterns generated by these methods or from measurements can, of course, be used by the prediction program with the precalculated antenna file option.

7. REFERENCES

Carrel, R. L. (1961), Analysis and design of the log-periodic dipole antenna, University of Illinois Technical Report No. 52, Urbana, Illinois.

DeCarvalho, F. (1959), On the design of some rhombic antenna arrays, IEEE Trans. Ant. Prep. AP-7, No. 1, January.

Harper, A. E. (1941), Rhombic Antenna Design, (D. Van Nordstrand Co., New York).

Ma, M. T. (1974), Theory and Application of Antenna Arrays, (John Wiley & Sons, New York).

Schelkunoff, S. A., and H. T. Friis (1952), Antennas - Theory and Practice, (John Wiley and Sons, New York).

Smith, C. E. (1966) Log periodic antenna design handbook, 1st ed., Smith Electronics, Inc., Cleveland.

Sommerfeld, A. (1964), Theoretical Physics, Vol. 6, (Academic Press).

Strait, B. J. (1980), Applications of the Method of Moments to Electromagnetic Fields, (The SCEEE Press, St. Cloud, Florida).

Thourel, L. (1960), The Antenna, (John Wiley & Sons, NY).

Uda, S., and Y. Mushiake (1954), Yagi-Uda Antenna, (Sasaki Printing and Publishing Co., LTD, Sendai, Japan).

Table 4. Antenna Input Card Formats

```
IONOSPHERIC COMMUNICATIONS ANALYSIS AND PREDICTION PROGRAM - IONCAP   VERSION 78.03

      . 1         2         3         4         5         6         7         8
12345678901234567890123456789012345678901234567890123456789012345678901234567890

COMMENT           THESE CARDS ARE FOR LOSSY GROUND
COMMENT
COMMENT   RUN TEST CASES       THEORY AND APPLICATION OF ANTENNA
COMMENT   ARRAYS. M.T.MA.  J.WILEY AND SONS, 1974
METHOD       13
COMMENT   HORIZONTAL RHOMBIC,  NO TEST CASE, SO DO OT-76-102
ANTENNA       1    1      .001   4.67.5 88.3916.76
EXECUTE
COMMENT   VERTICAL MONOPOLE,  NO TEST CASE, DO OT-76-102
ANTENNA       1    2      .001   4.     -.25
EXECUTE
COMMENT   HORIZONTAL DIPOLE, PAGE 249, THIS IS ALSO OT-76-102
ANTENNA       1    3      .001   4.      -.5  -.25
EXECUTE
COMMENT   HORIZONTAL YAGI, PAGE 264
ANTENNA       1    4      .001   4.15.6 15.0 -.25 14.    3. 6.    7.5
EXECUTE
COMMENT   VERTICAL DIPOLE, NO TEST CASE, USE OT-76-102
ANTENNA       1    5      .001   4.      -.5  -.25
EXECUTE
COMMENT   CURTAIN, PAGE 277.
ANTENNA       1    6      .001   4. 1.    15.  7.5  4.    15.  7.5  15.
EXECUTE
COMMENT   SLOPING VEE, PAGE 379
ANTENNA       1    7      .001   4. 15. 150.  15. 33.75
EXECUTE
COMMENT   INVERTED L,  NO TEST CASE, DO OT-76-102
ANTENNA       1    8      .001   4.     21.34  10.
EXECUTE
COMMENT   TERMINATED SLOPING RHOMBIC, PAGE 392
ANTENNA       1    9      .001   4. 30. 120.  10. 20.
EXECUTE
COMMENT   INTERLACED RHOMBIC, NO TEST CASE, THIS IS A ITSA-1
ANTENNA       1   10      .001   4.  70.114.  20.  4.   33.
EXECUTE
COMMENT   SLOPING LONG WIRE, NO TEST CASE, DO OT-76-102
ANTENNA       1   11      .001   4. 10. 91.44
EXECUTE
COMMENT   ISOTROPIC ANTENNA IN FREE SPACE, GAIN IS 5 DB
ANTENNA       1   12      .001   4.                5.
EXECUTE
COMMENT   LOG PERIODIC ARRAY OF HORIZONTAL DIPOLES, MA PAGE 361
ANTENNA       1   13      .001   4. 46. 33.47 2.96      18.  .87  12.
EXECUTE
COMMENT   ARBITRARY TILTED DIPOLE, OT-76-102
ANTENNA       1   14      .001   4. 45.  -.5  -.25
EXECUTE
COMMENT   VERTICAL HALF RHOMBIC, MA PAGE 400
ANTENNA       1   15      .001   4. 27.5 120.
EXECUTE
COMMENT   HORIZONTAL DOUBLE RHOMBOID
ANTENNA       1   16      .001   4.     150.  62. 25.5 17.5 214.8 62.
EXECUTE
COMMENT   LOG PERIODIC ARRAY OF VERTICAL DIPOLES
COMMENT    LPA V.D., POOR GROUND.  MA PAGE 344
ANTENNA       1   22      .001   4.  90. 15.  8.        12.5 .87  12.
EXECUTE
QUIT
```

Table 5. Typical Values of Ground Electrical Characteristics

GROUND TYPE	CONDUCTIVITY	DIELECTRIC CONSTANT
Sea Water	5.0 mhos/m	80.
Good Ground	0.01	10.
Poor Ground and Sea Ice	0.001	4.
Polar Ice Cap	0.0001	1.
Fresh Water	0.002	80.
From Maps	blank	blank
Perfect Ground	blank	- 2.
Free Space	blank	- 1.
Variable	ASIG	AEPS
Columns	26-30	31-35

Table 6. Horizontal Rhombic, Input Card

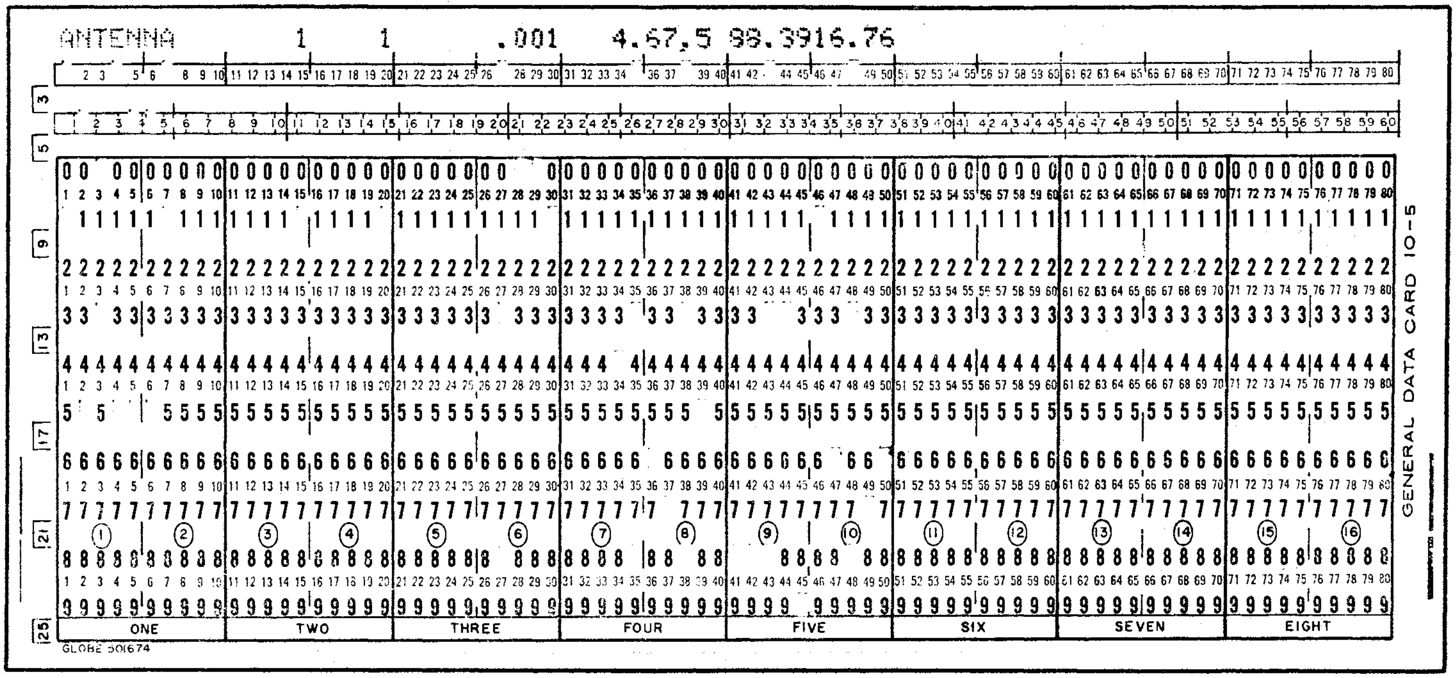

ANTENNA CARD, HORIZONTAL RHOMBIC

Column	Name	Format	Description of Input Data
1-10		A10	"ANTENNA" 1
11-15	IAT	I5	1 for transmitter, 2 for receiver
16-20	IANTR	I5	Antenna type = 1
21-25	AETA	F5.1	Bearing of antenna, degrees, E of N, negative; off azimuth if positive?
26-30	ASIG	F5.1	Ground conductivity
31-35	AEPS	F5.1	Relative dielectric constant
36-40	AND	F5.1	Tilt angle, degrees (1/2 the interior angle (at feed end))
41-45	ANL	F5.1	Antenna leg length, meters, or wavelength if negative
46-50	ANH	F5.1	Antenna height, meters
51-55	AEX (1)	F5.1	Additional gain, dB
56-60			
61-65			
66-70			
71-75	AFQB	F5.1	Ending frequency when more than one antenna is used
76-80	IAIN	I5	Antenna number indicator (each transmitter or receiver antenna can be defined by up to three different antennas
			over the frequency range; default is one, if IAIN is left blank.

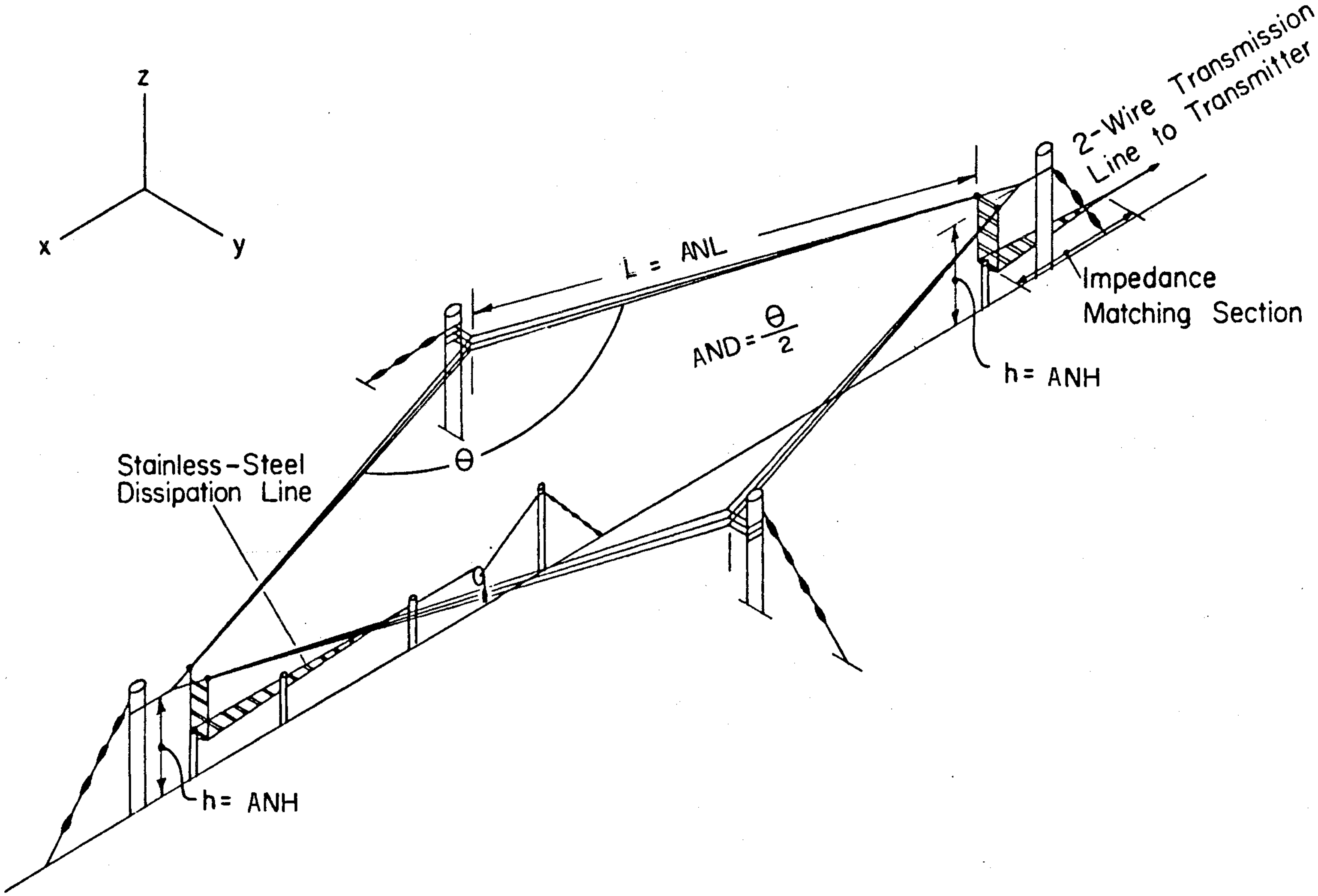

Figure 27. Horizontal rhombic structure (1).

Table 7. Vertical Monopole, Input Card

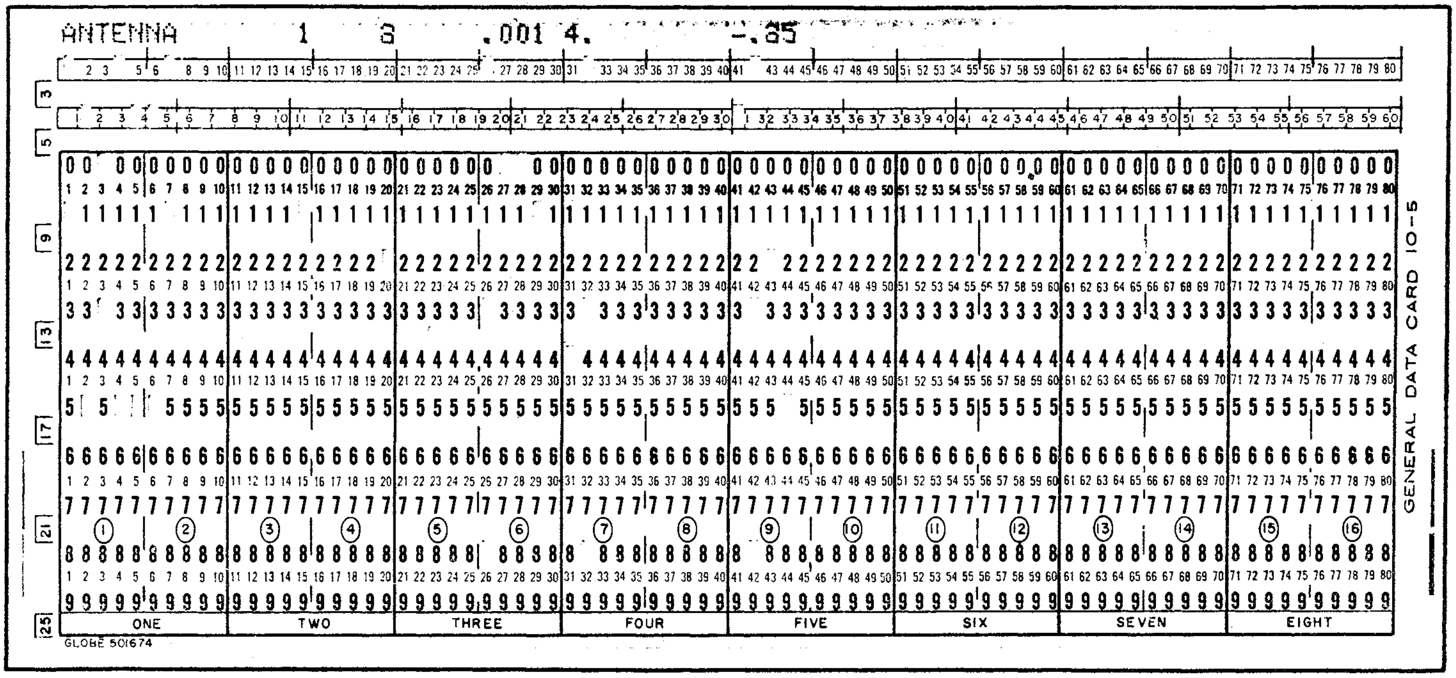

ANTENNA CARD, VERTICAL MONOPOLE

Columns	Name	Format	Description of Input Data
1-10		A10	"ANTENNA" 2
11-15	IAT	I5	1 for transmitter, 2 for receiver
16-20	IANTR	I5	antenna type = 2
21-25			
26-30	ASIG	F5.1	ground conductivity
31-35	AEPS	F5.1	relative dielectric constant
36-40			
41-45	ANL	F5.1	antenna height, meters
46-50	ANH	F5.1	gain above a dipole, dB
51-55	AEX(1)	F5.1	additional gain
56-60			
61-65			
66-70			
71-75	AFQB	F5.1	ending frequency when more than one antenna is used
76-80	IAIN	I5	antenna number indicator (each transmitter or receiver antenna can be defined by up to three different antennas
			over the frequency range; default is one, if IAIN is left blank

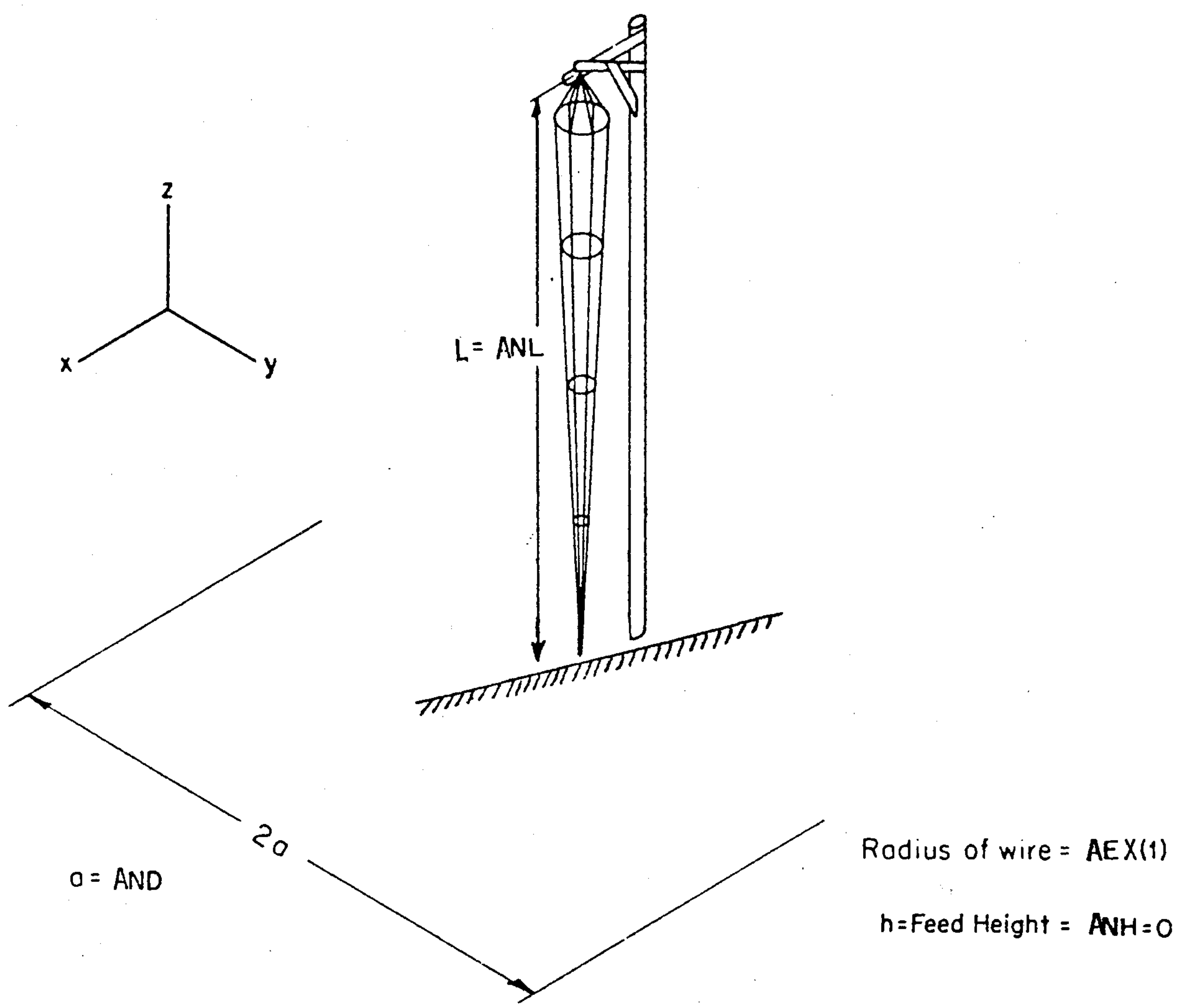

Figure 28. Vertical monopole structure (2).

Table 8. Horizontal Dipole, Input Card

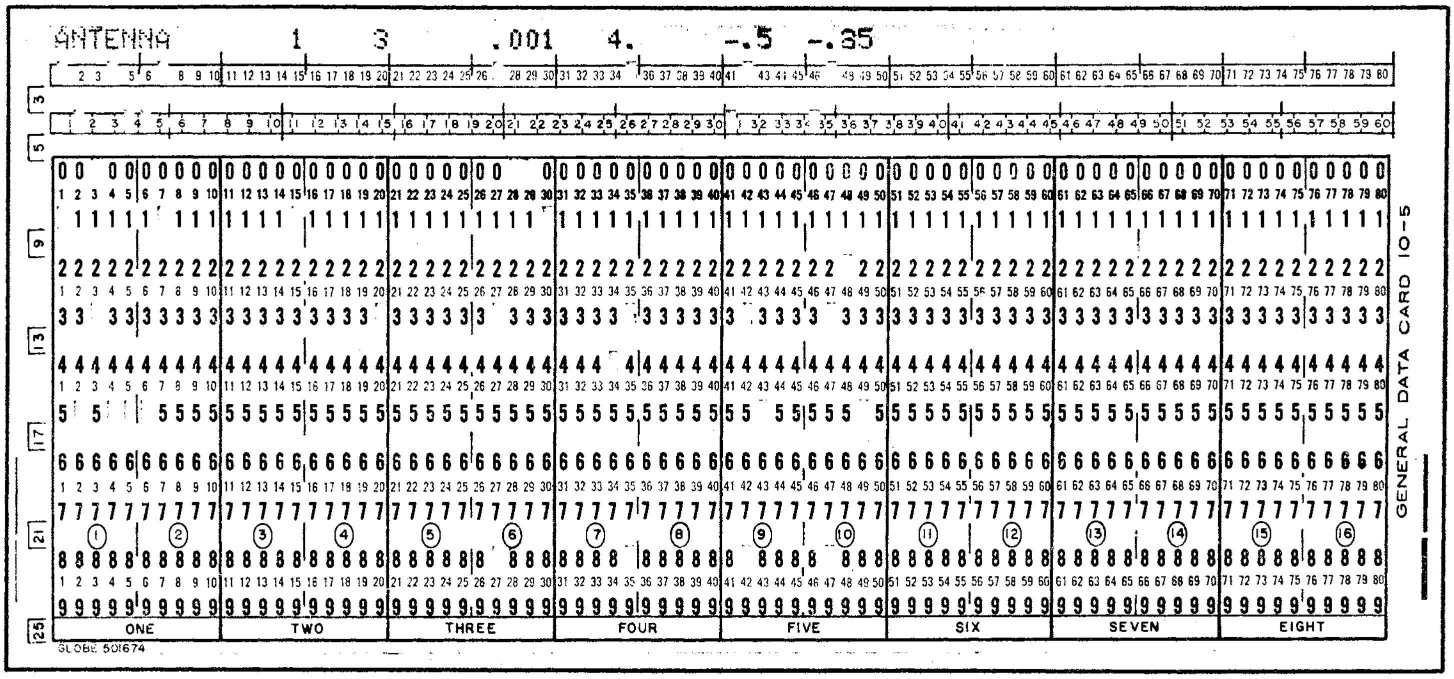

ANTENNA CARD, HORIZONTAL DIPOLE

Columns	Name	Format	Description of Input Data
1-10		A10	"ANTENNA" 3
11-15	IAT	I5	1 for transmitter, 2 for receiver
16-20	IANTR	I5	antenna type = 3
21-25	AETA	F5.1	bearing, degrees E of N
26-30	ASIG	F5.1	σ
31-35	AEPS	F5.1	ε
36-40			
41-45	ANL	F5.1	antenna length, meters
46-50	ANH	F5.1	antenna height, meters
51-55	AEX(1)	F5.1	additional gain, dB
56-60			
61-65			
66-70			
71-75	AFQB	F5.1	ending frequency when more than one antenna is used
76-80	IAIN	I5	antenna number indicator (each transmitter or receiver antenna can be defined by up to three different antennas over the frequency range; default is one, if IAIN is left blank

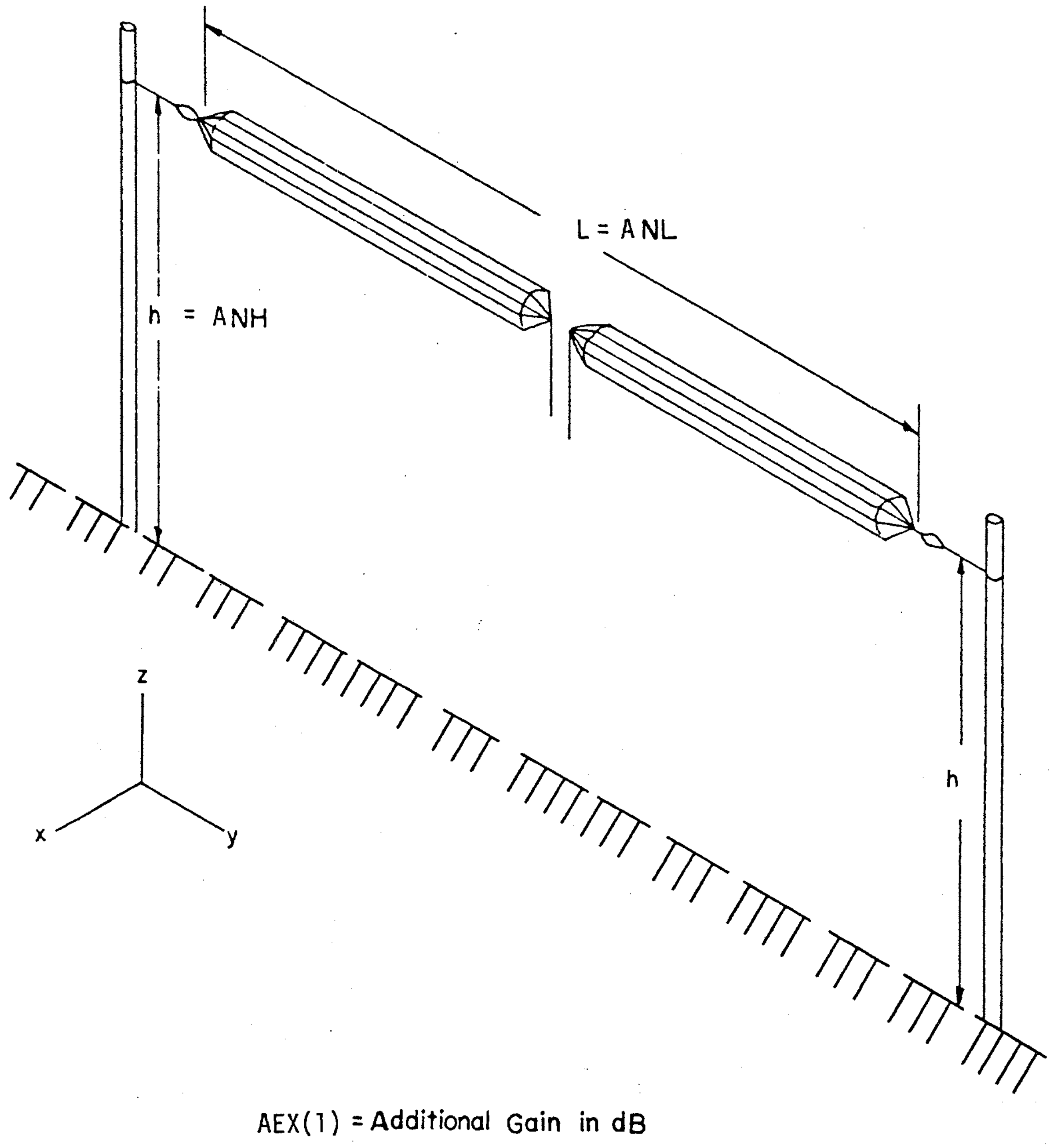

Figure 29. Horizontal dipole structure (3).

Table 9. Horizontal Yagi, Input Card

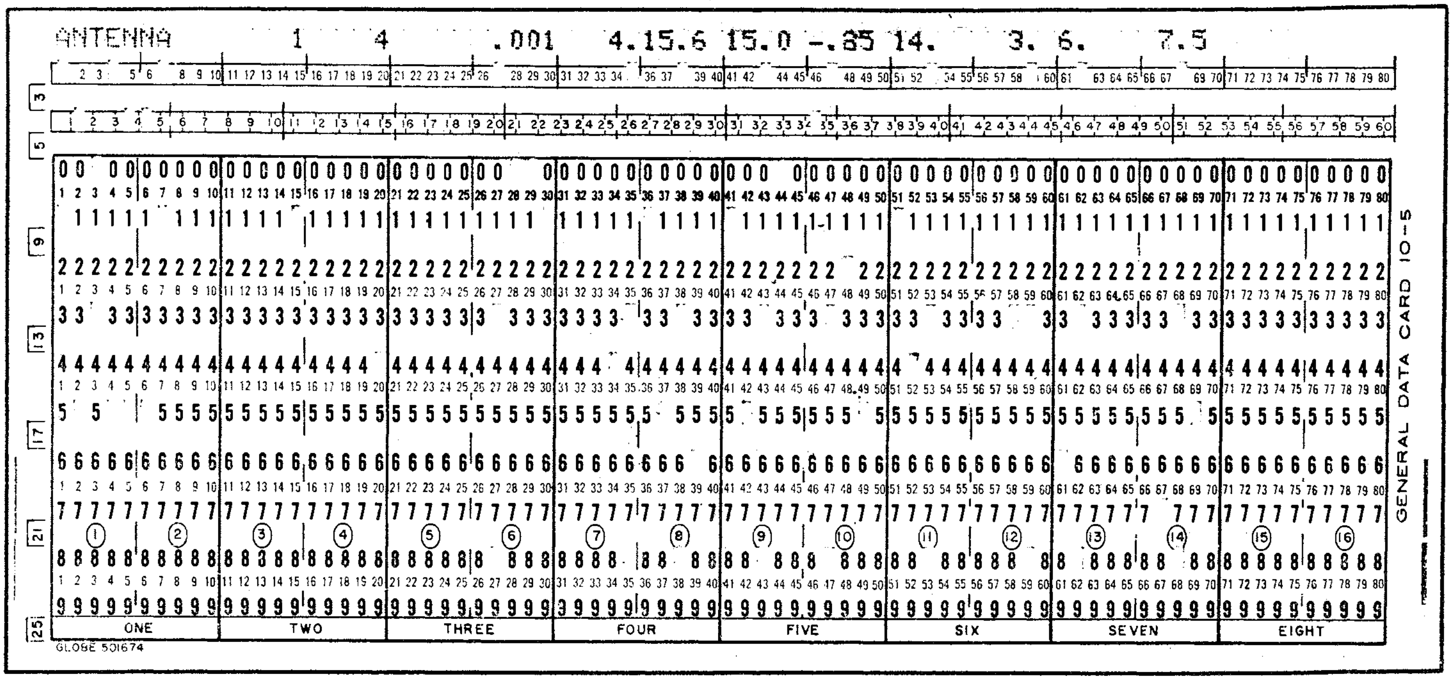

ANTENNA CARD, HORIZONTAL YAGI

Columns	Name	Format	Description of Input Data
1-10		A10	"ANTENNA" 4
11-15	IAT	I5	1 for transmitter, 2 for receiver
16-20	IANTR	I5	antenna type = 4
21-25	AETA	F5.1	bearing of antenna, E of N
26-30	ASIG	F5.1	σ
31-35	AEPS	F5.1	ε
36-40	AND	F5.1	length of reflector - wavelength
41-45	ANL	F5.1	driven element length, meters - wavelength
46-50	ANH	F5.1	antenna height, meters - wavelength
51-55	AEX(1)	F5.1	director length
56-60	AEX(2)	F5.1	number of elements, 1, 2, 3, ...
61-65	AEX(3)	F5.1	director spacing
66-70	AEX(4)	F5.1	reflector spacing
71-75	AFQB	F5.1	ending frequency when more than one antenna is used
76-80	IAIN	I5	antenna number indicator (each transmitter or receiver antenna can be defined by up to three different antennas over the frequency range; default is one; if IAIN is left blank

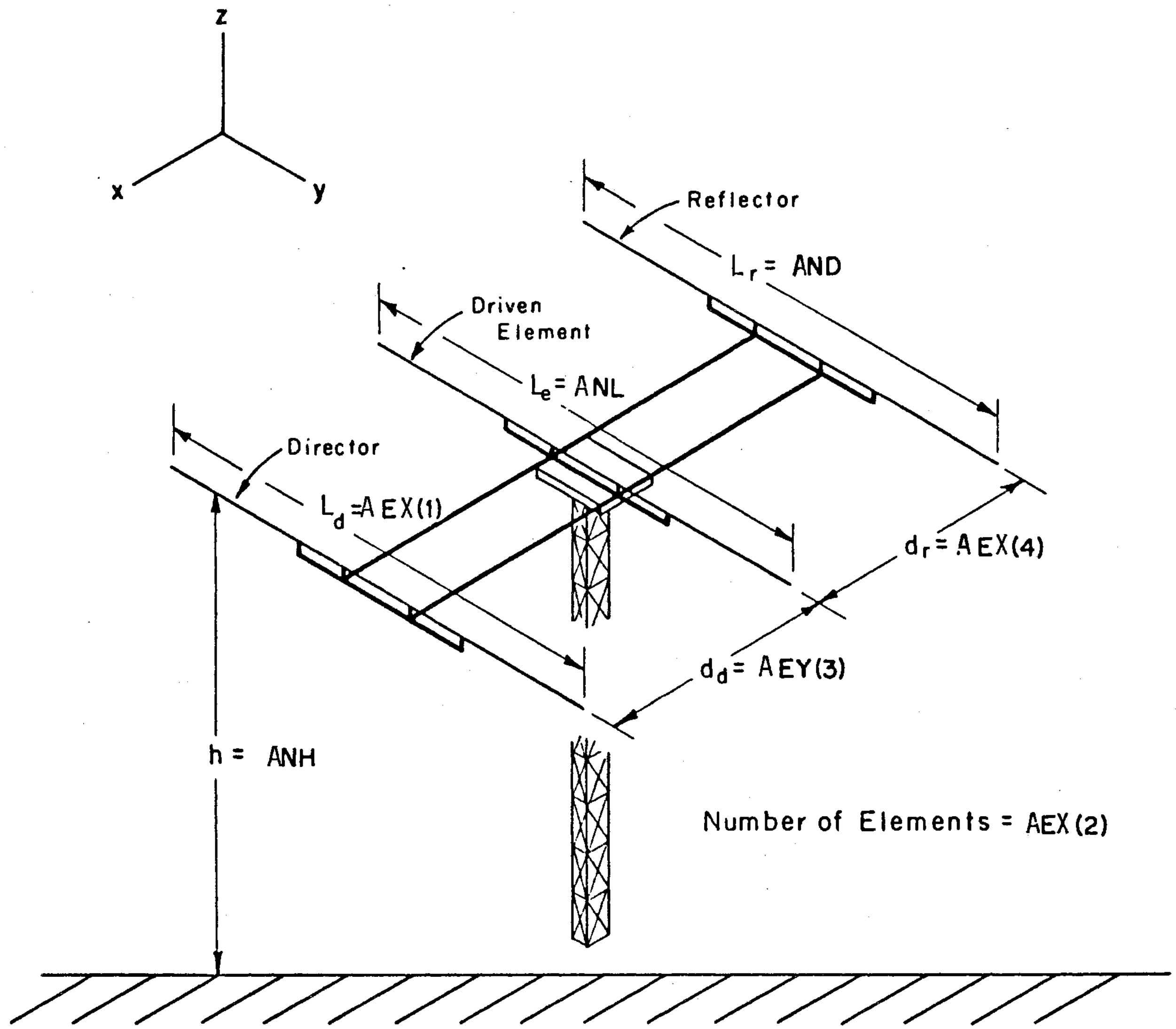

Figure 30. Horizontal Yagi structure (4).

Table 10. Vertical Dipole, Input Card

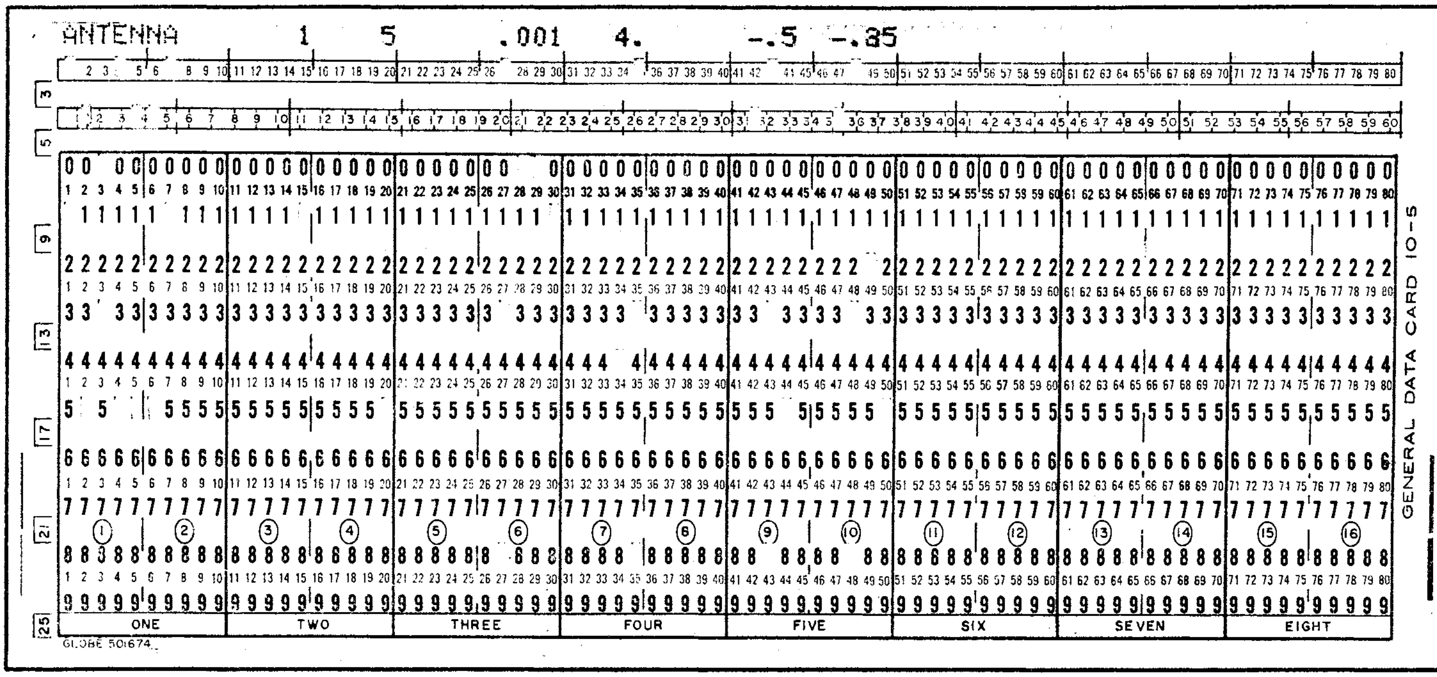

ANTENNA CARD, VERTICAL DIPOLE

Columns	Name	Format	Description of Input Data
1-10		A10	"ANTENNA" 5
11-15	IAT	I5	1 for transmitter, 2 for receiver
16-20	IANTR	I5	antenna type = 5
21-25	AETA	F5.1	bearing or off azimuth (-)
26-30	ASIG	F5.1	
31-35	AEPS	F5.1	note: -1 is free space -2 is perfect ground
36-40			
41-45	ANL	F5.1	element length
46-50	ANH	F5.1	feed height
51-55	AEX(1)	F5.1	additional gain, dB

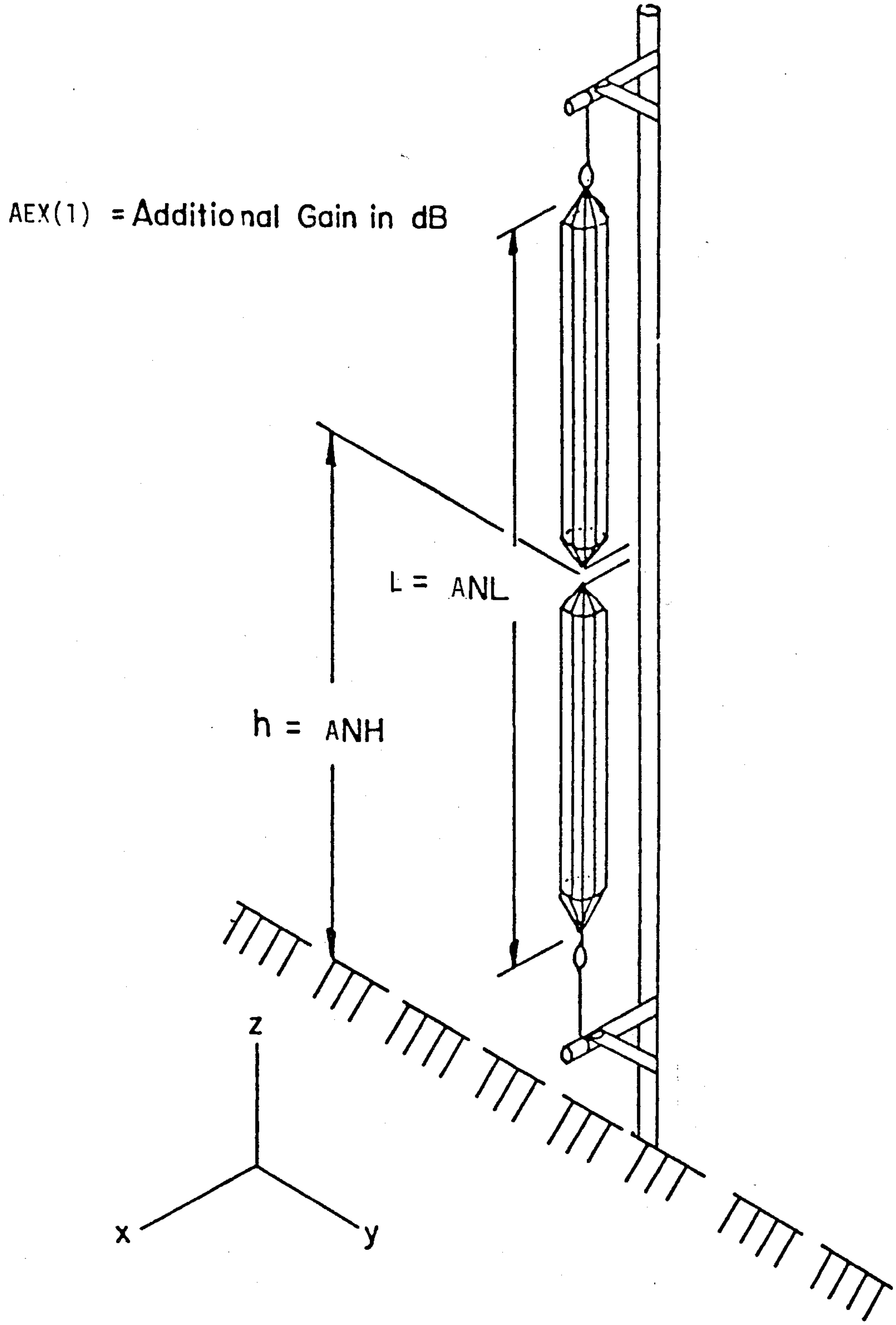

Figure 31. Vertical dipole antenna structure (type 5).

Table 11. Curtain, Input Card

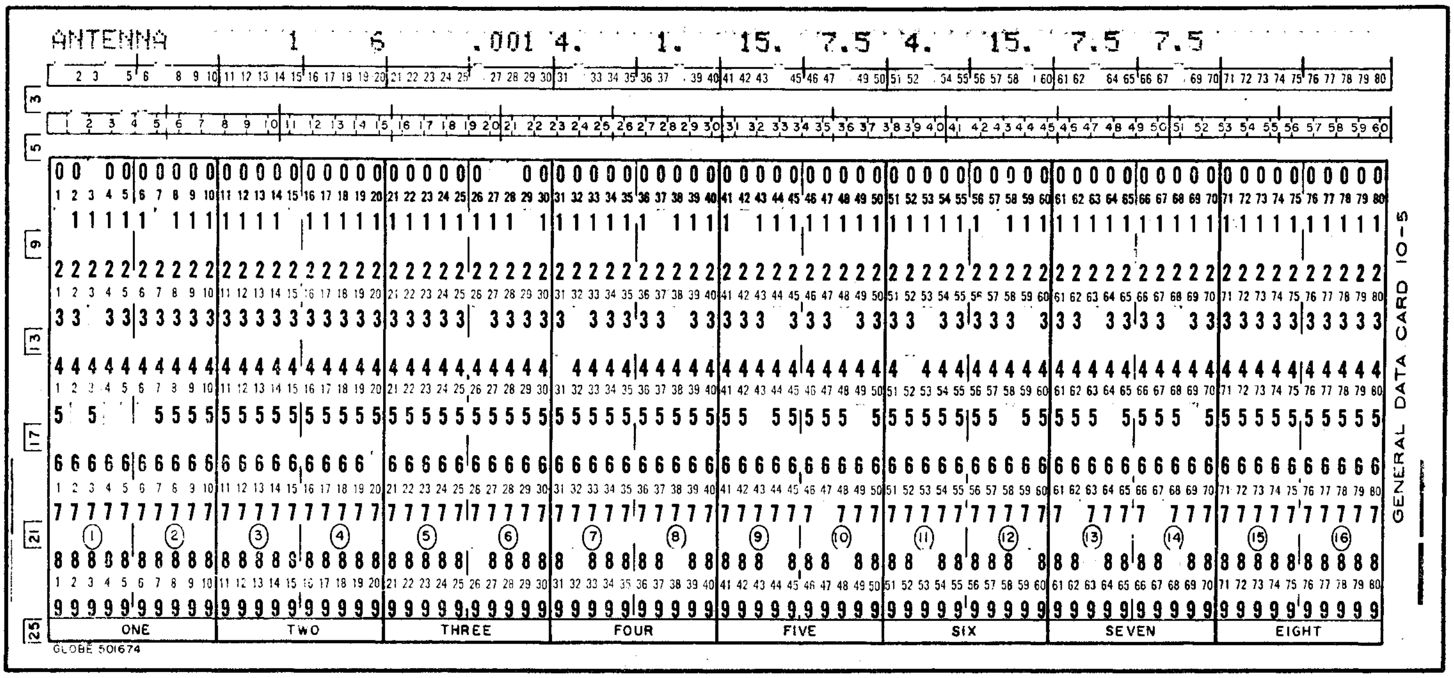

ANTENNA CARD, CURTAIN ANTENNA

Columns	Name	Format	Description of Input Data
1-10		A10	"ANTENNA" 6
11-15	IAT	I5	1 for transmitter, 2 for receiver
16-20	IANTR	I5	antenna type = 6
21-25	AETA	I5	antenna bearing
26-30	ASIG	F5.1	σ
31-35	AEPS	F5.1	ε
36-40	AND	F5.1	number of bays
41-45	ANL	F5.1	antenna element length, meters
46-50	ANH	F5.1	antenna height to first element, meters
51-55	AEX (1)	F5.1	number of elements per bay
56-60	AEX (2)	F5.1	distance between elements centers
61-65	AEX (3)	F5.1	vertical spacing of elements
66-70	AEX (4)	F5.1	distance from screen
71-75	AFQB	F5.1	ending frequency when more than one antenna is used
76-80	IAIN	I5	antenna number indicator (each transmitter or receiver antenna can be defined by up to three different antennas
			over the frequency range; default is one, if IAIN is left blank

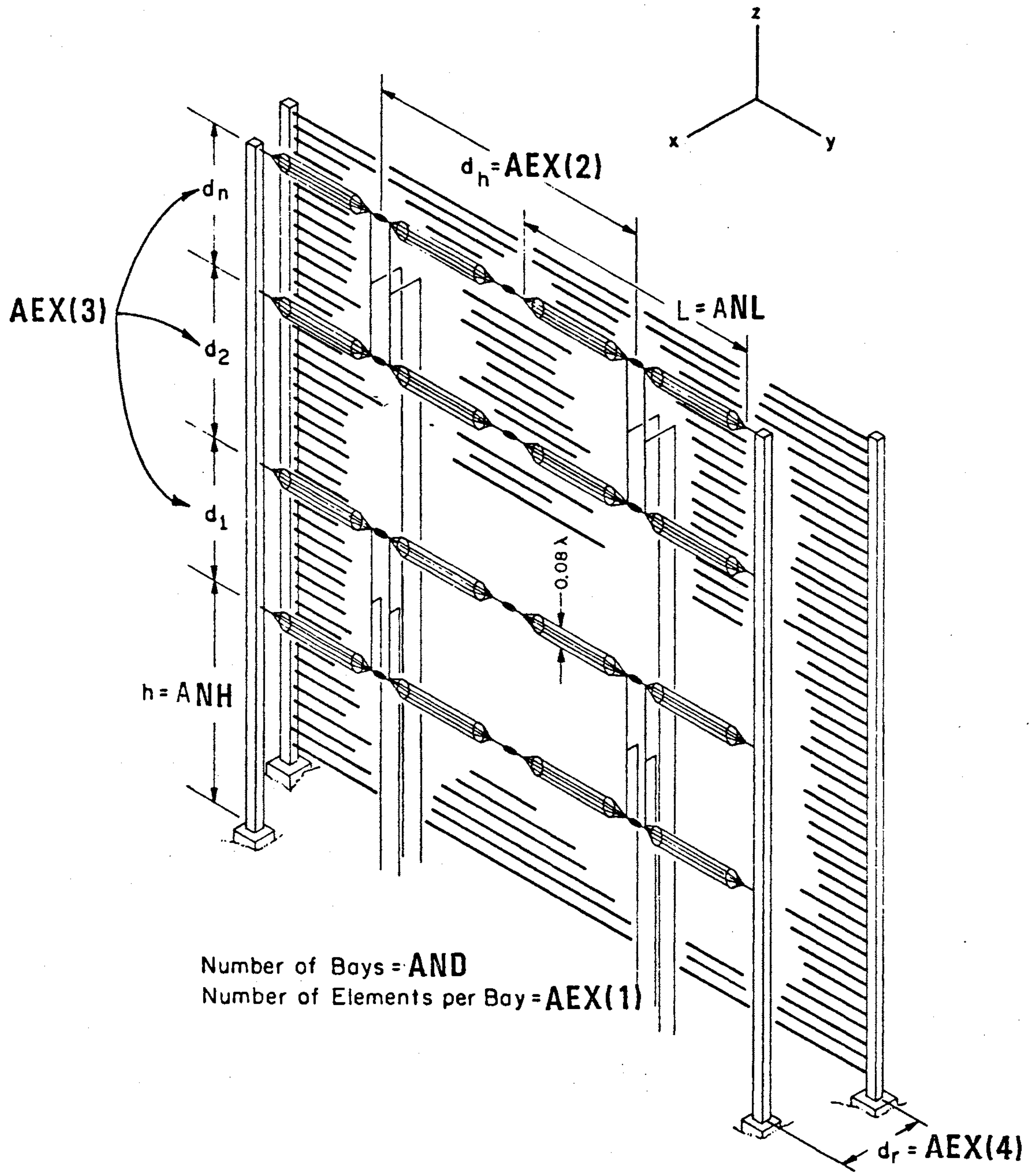

Figure 32. Curtain structure (6).

Table 12. Sloping Vee, Input Card

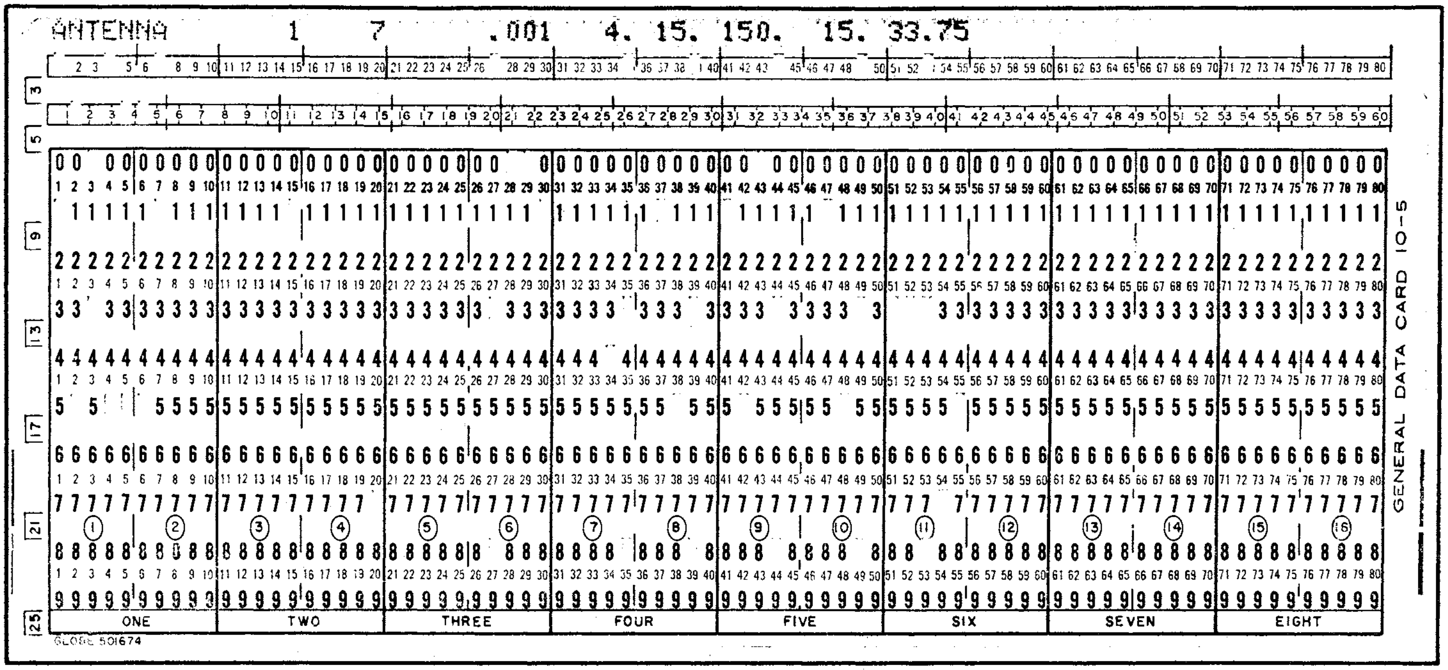

ANTENNA CARD, SLOPING VEE

Columns	Name	Format	Description of Input Data
1-10		A10	"ANTENNA" 7
11-15	IAT	I5	
16-20	IANTR	I5	antenna type = 7
21-25	AETA	F5.1	bearing of antenna
26-30	ASIG	F5.1	σ
31-35	AEPS	F5.1	ε
36-40	AND	F5.1	1/2 apex angle in plane of wires
41-45	ANL	F5.1	antenna leg length, meters
46-50	ANH	F5.1	antenna height, meters
51-55	AEX (1)	F5.1	terminated height
56-60			
61-65			
66-70			
71-75	AFQB	F5.1	ending frequency when more than one antenna is used
76-80	IAIN	I5	Antenna number indicator--each transmitter or receiver antenna can be defined by up to three different antennas over the frequency range; default is one; if IAIN is left blank.

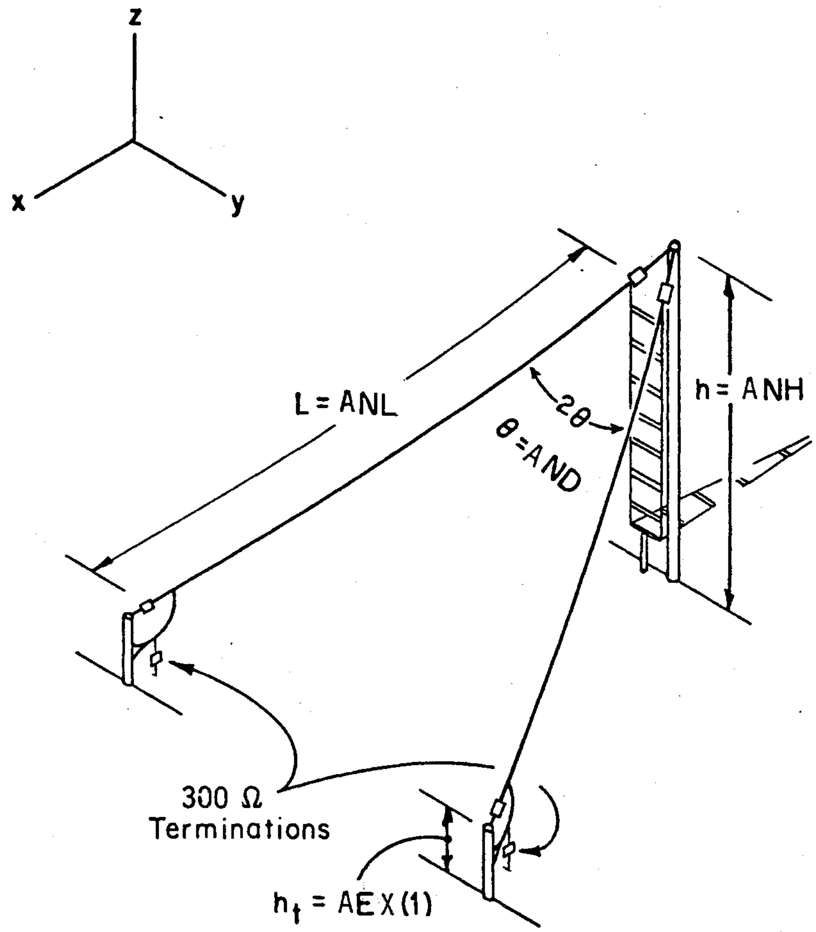

Figure 33. Sloping vee structure (7).

Table 13. Inverted L, Input Card

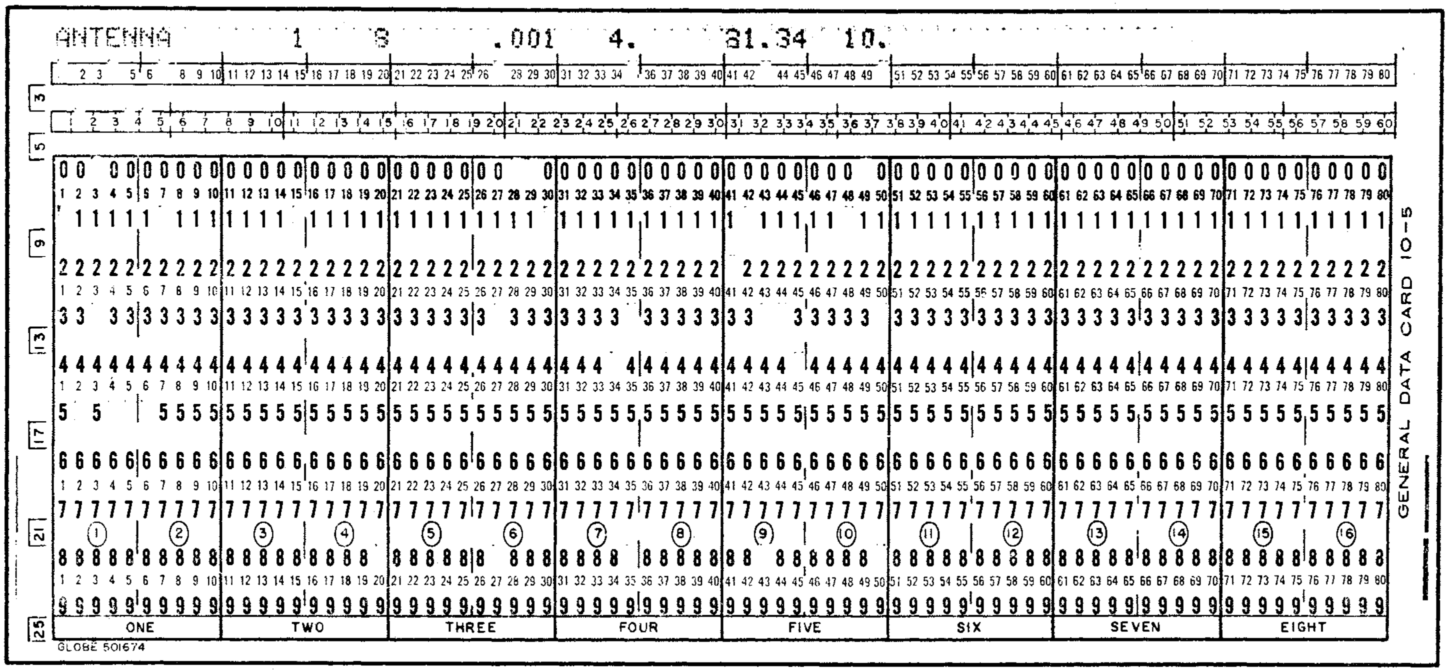

ANTENNA CARD, INVERTED L

Columns	Name	Format	Description of Input Data
1-10		A10	"ANTENNA" 8
11-15	IAT	I5	
16-20	IANTR	I5	antenna type = 8
21-25	AETA	F5.1	bearing
26-30	ASIG	F5.1	σ
31-35	AEPS	F5.1	ε
36-40		F5.1	
41-45	ANL	F5.1	antenna length, meters
46-50	ANH	F5.1	antenna height, meters
51-55	AEX(1)	F5.1	additional gain
56-60	AEX(2)	F5.1	feed height above ground, meters
61-65			
66-70			
71-75	AFQB	F5.1	ending frequency when more than one antenna is used
76-80	IAIN	I5	Antenna number indicator--each transmitter or receiver antenna can be defined by up to three different antennas over the frequency range; default is one, if IAIN is left blank.

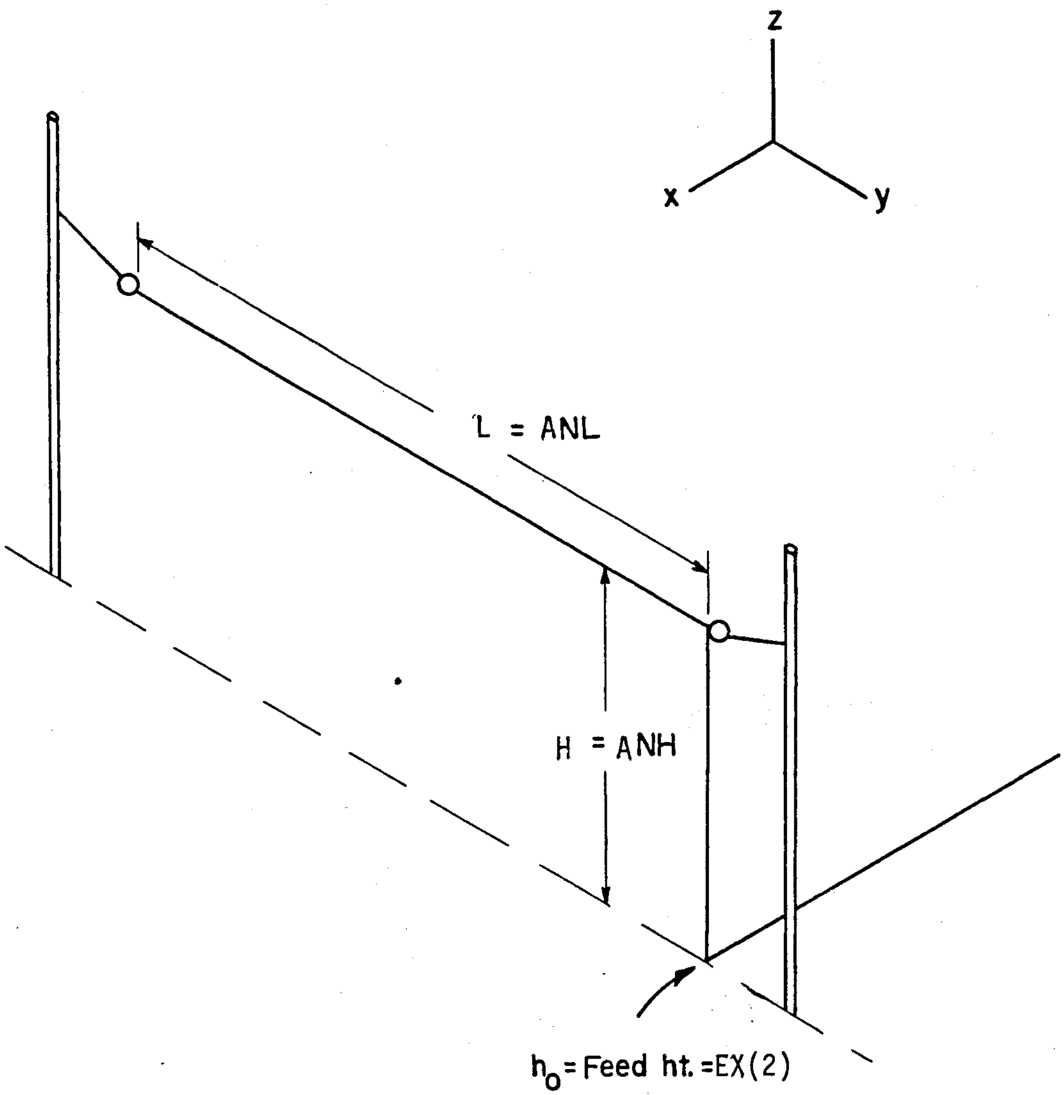

Figure 34. Inverted L structure (8).

Table 14. Sloping Rhombic, Input Card

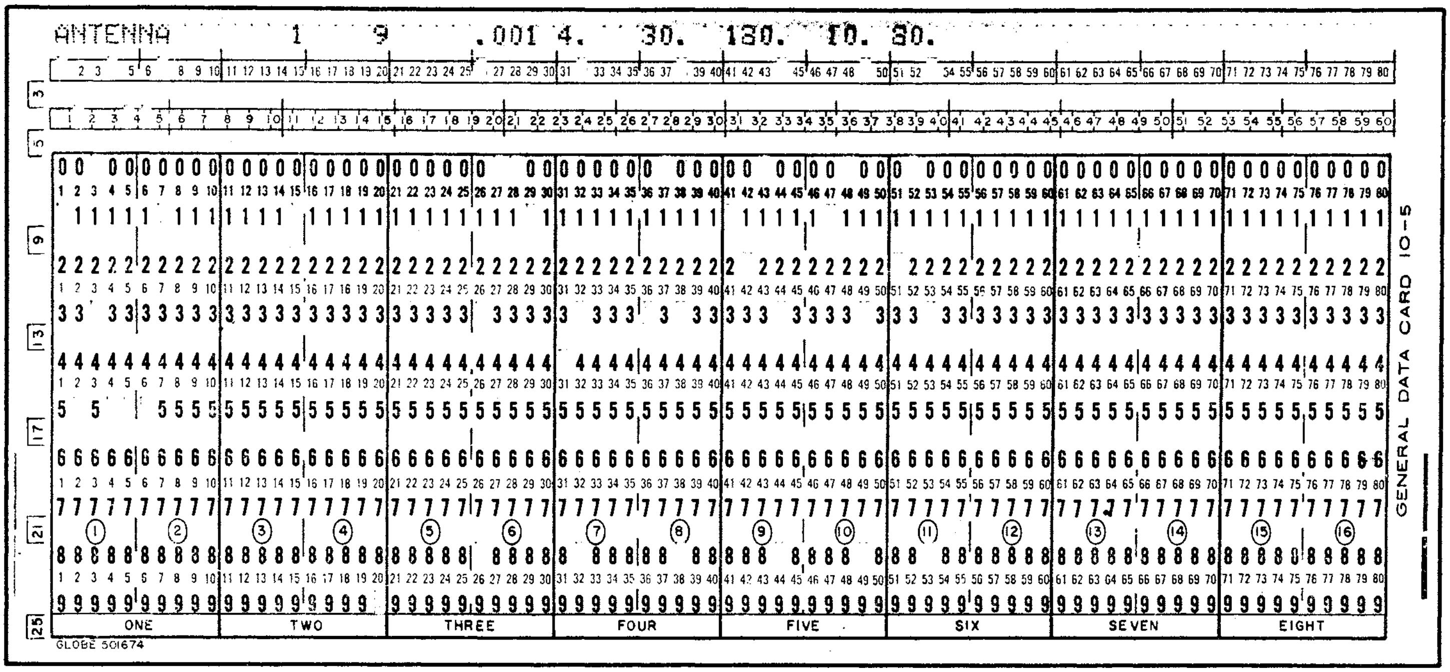

ANTENNA CARD, SLOPING RHOMBIC

Columns	Name	Format	Description of Input Data
1-10		A10	"ANTENNA" 9
11-15	IAT	I5	
16-20	IANTR	I5	antenna type = 9
21-25	AETA	F5.1	bearing
26-30	ASIG	F5.1	σ
31-35	AEPS	F5.1	ε
36-40	AND	F5.1	1/2 large interior angle at feed end in plane of wire
41-45	ANL	F5.1	leg length, meters
46-50	ANH	F5.1	antenna height, meters
51-55	AEX(1)	F5.1	terminate height
56-60			
61-65			
66-70			
71-75	AFQB	F5.1	ending frequency when more than one antenna is used
76-80	IAIN	I5	Antenna number indicator--each transmitter or receiver antenna can be defined by up to three different antennas over the frequency range; default is one; if IAIN is left blank.

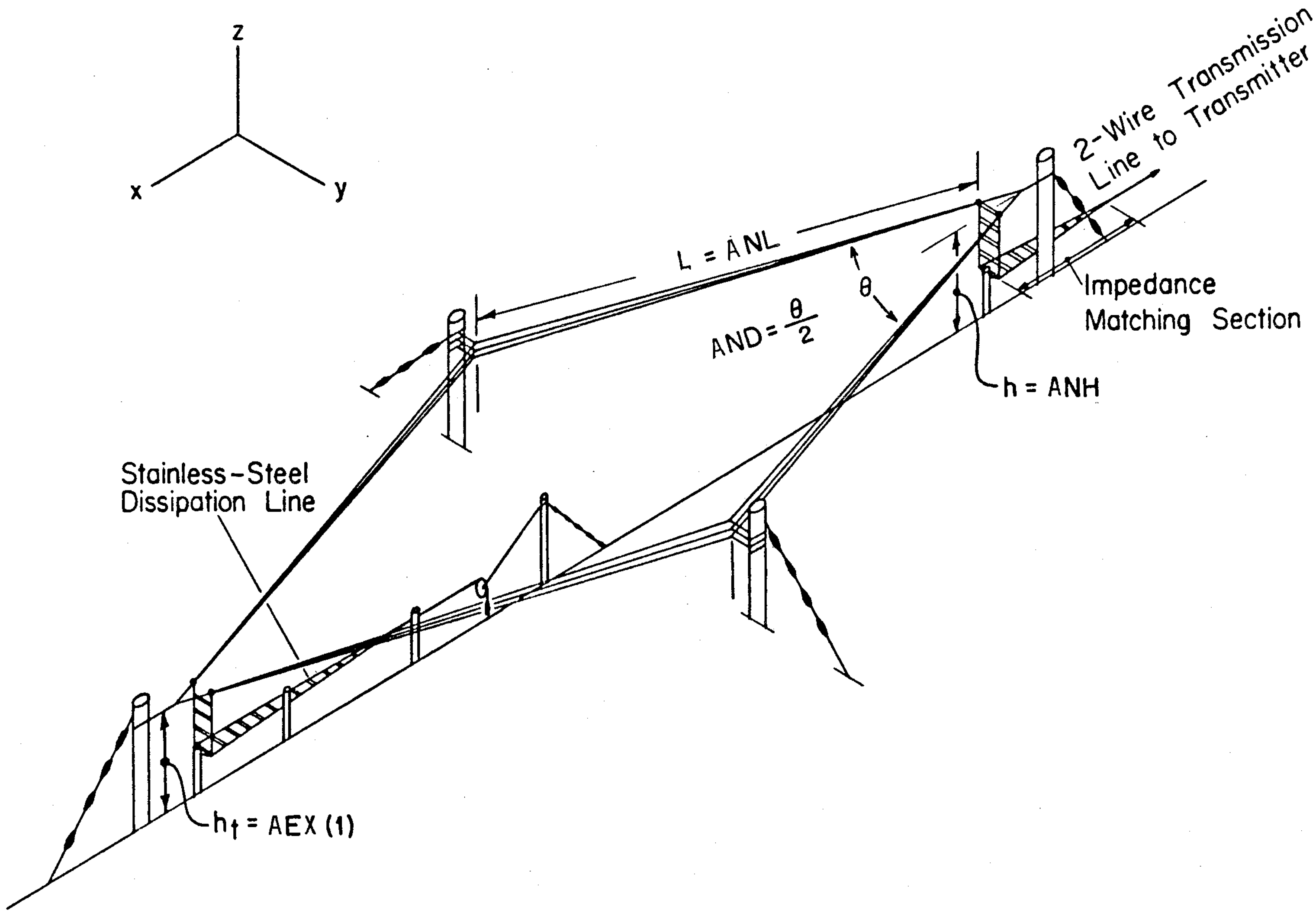

Figure 35. Sloping rhombic structure (9).

Table 15. Interlaced Rhombic, Input Card

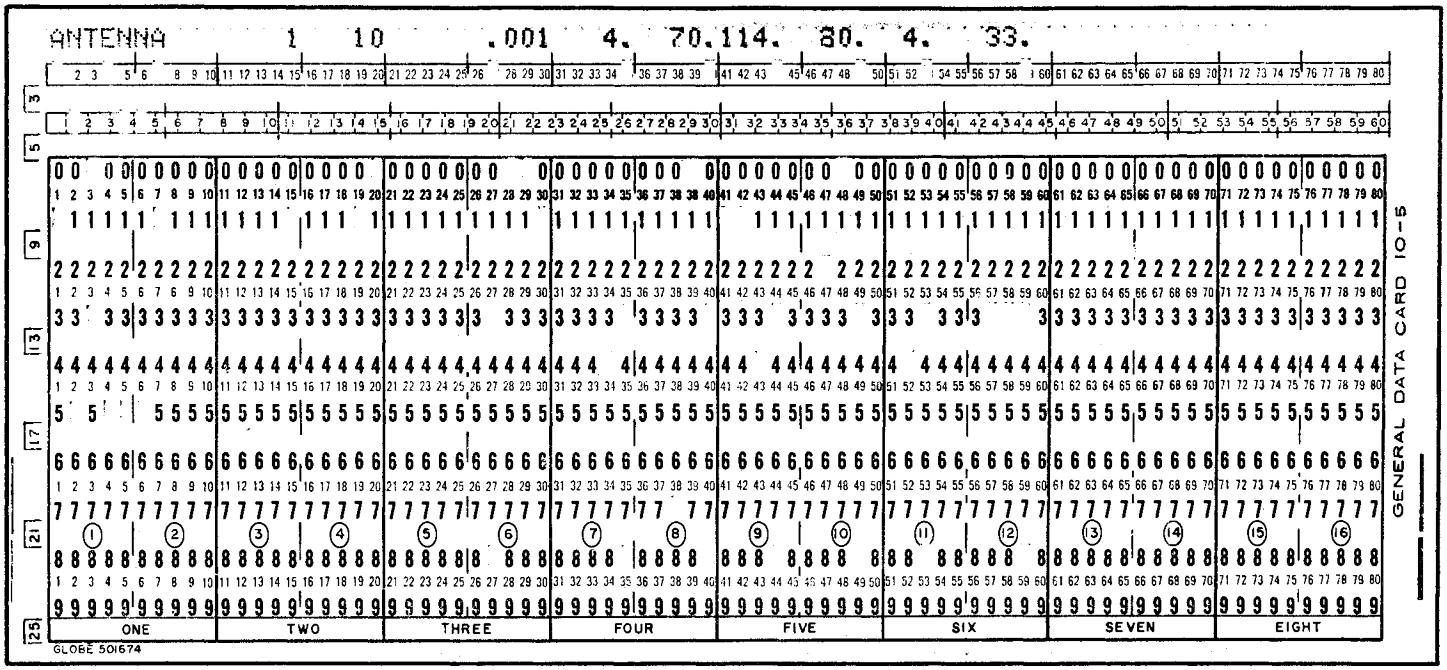

ANTENNA CARD, INTERLACED RHOMBIC

Columns	Name	Format	Description of Input Data
1-10		A10	"ANTENNA" 10
11-15	IAT	I5	
16-20	IANTR	I5	antenna type = 10
21-25	AETA	F5.1	bearing
26-30	ASIG	F5.1	σ
31-35	AEPS	F5.1	ε
36-40	AND	F5.1	1/2 large interior angle in plane of wire
41-45	ANL	F5.1	leg length
46-50	ANH	F5.1	lower antenna height
51-55	AEX(1)	F5.1	vertical displacement
56-60	AEX(2)	F5.1	horizontal feed point displacement, meters
61-65			
66-70			
71-75	AFQB	F5.1	ending frequency when more than one antenna is used
76-80	IAIN	I5	Antenna number indicator--each transmitter or receiver antenna can be defined by up to three different antennas over the frequency range; default is one, if IAIN is left blank.

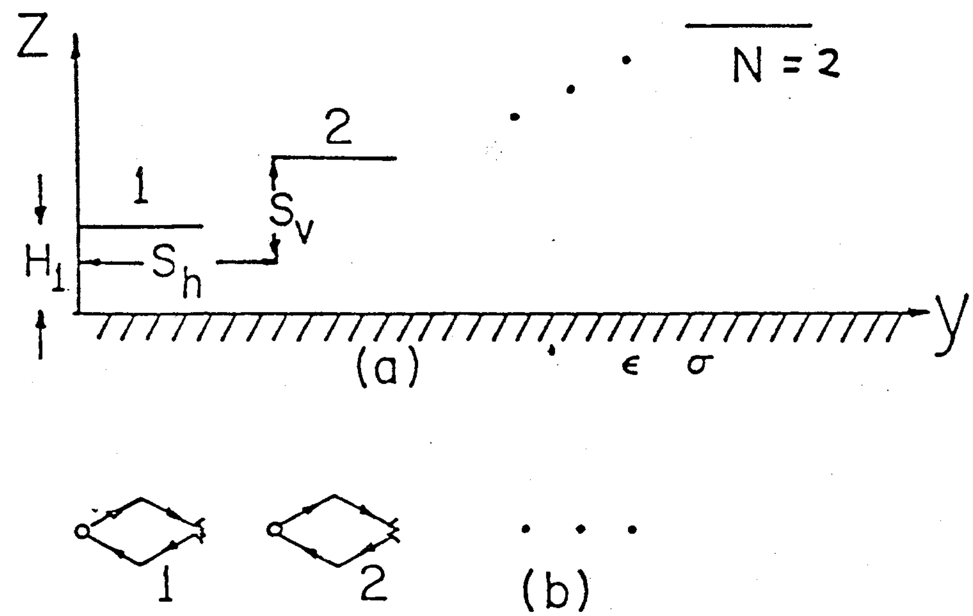

Figure 36. Interlaced rhombic structure (10)
(only two rhombics are coded).

Table 16. Sloping Long Wire, Input Card

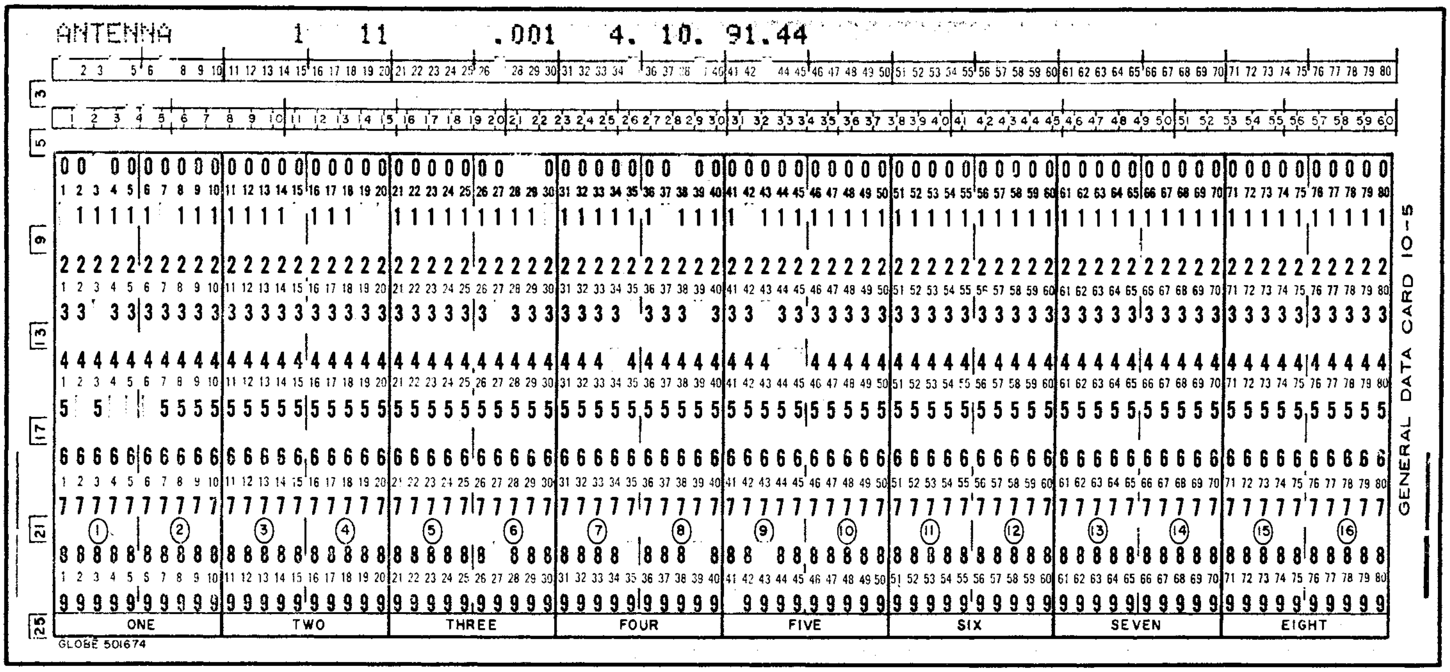

ANTENNA CARD, SLOPING LONG WIRE

Columns	Name	Format	Description of Input Data
1-10		A10	"ANTENNA" 11
11-15	IAT	I5	1 for transmitter, 2 for receiver
16-20	IANTR	I5	antenna type = 11
21-25	AETA	F5.1	
26-30	ASIG	F5.1	σ
31-35	AEPS	F5.1	ε
36-40	AND	F5.1	α, slope from horizontal, degrees
41-45	ANL	F5.1	element length
46-50	ANH	F5.1	feed height
51-55	AEX(1)	F5.1	additional gain

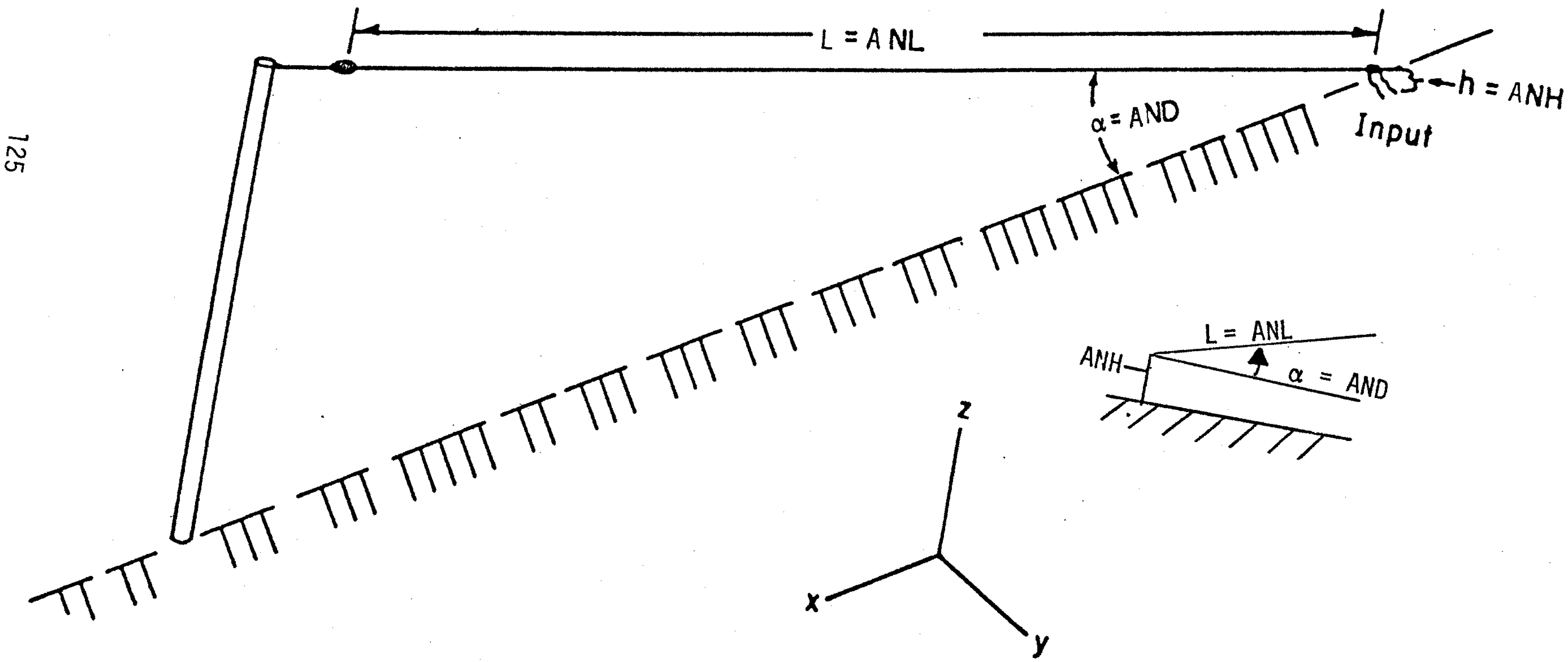

Figure 37. Sloping long-wire antenna structure (type 11).

Table 17. Isotropic Antenna, Input Card

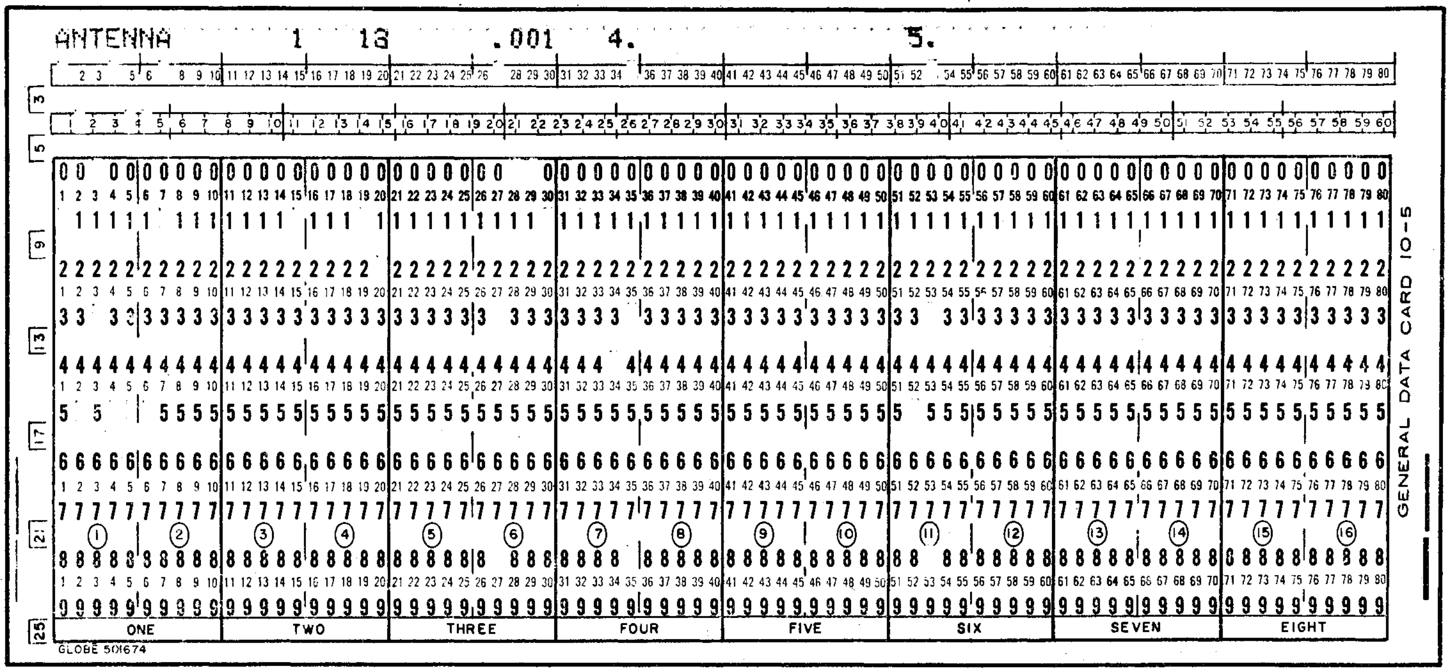

ANTENNA CARD, ISOTROPIC

Columns	Name	Format	Description of Input Data
1-10		A10	"ANTENNA" 12
11-15	IAT	I5	1 for transmitter, 2 for receiver
16-20	IANTR	I5	antenna type = 12
21-25	AETA	F5.1	
26-30	ASIG	F5.1	σ
31-35	AEPS	F5.1	ε
36-40			
41-45	ANL	F5.1	
46-50	ANH	F5.1	
51-55	AEX(1)	F5.1	gain above isotropic, dB
56-60	AEX(2)	F5.1	receiver antenna efficiency, dB
61-65	AEX(3)	F5.1	1. is horiz. isotrope over ground, 2. is vert. isotrope 3. is circ. isotrope over ground, 4. is old constant gain
66-70			
71-75	AFOB	F5.1	ending frequency when more than one antenna is used
76-80	IAIN	I5	Antenna number indicator--each transmitter or receiver antenna can be defined by up to three different antennas over the frequency range; default is one, if IAIN is left blank.

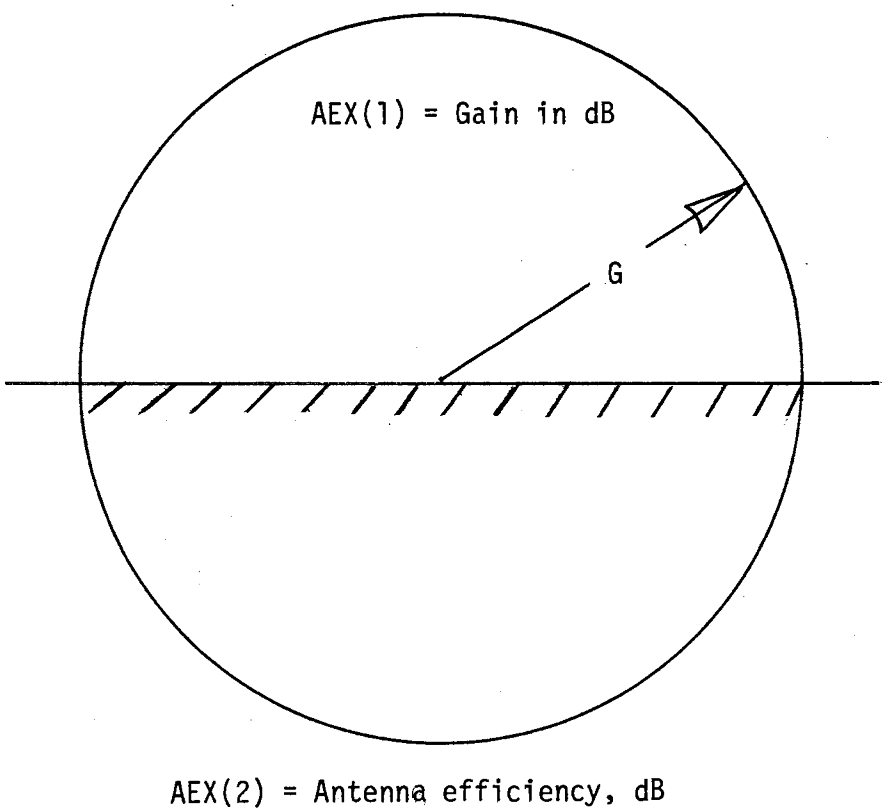

Figure 38. Constant gain pictorial pattern (12) (isotropic in free space is 0 dBI).

Table 18. Horizontal LPD, Input Card

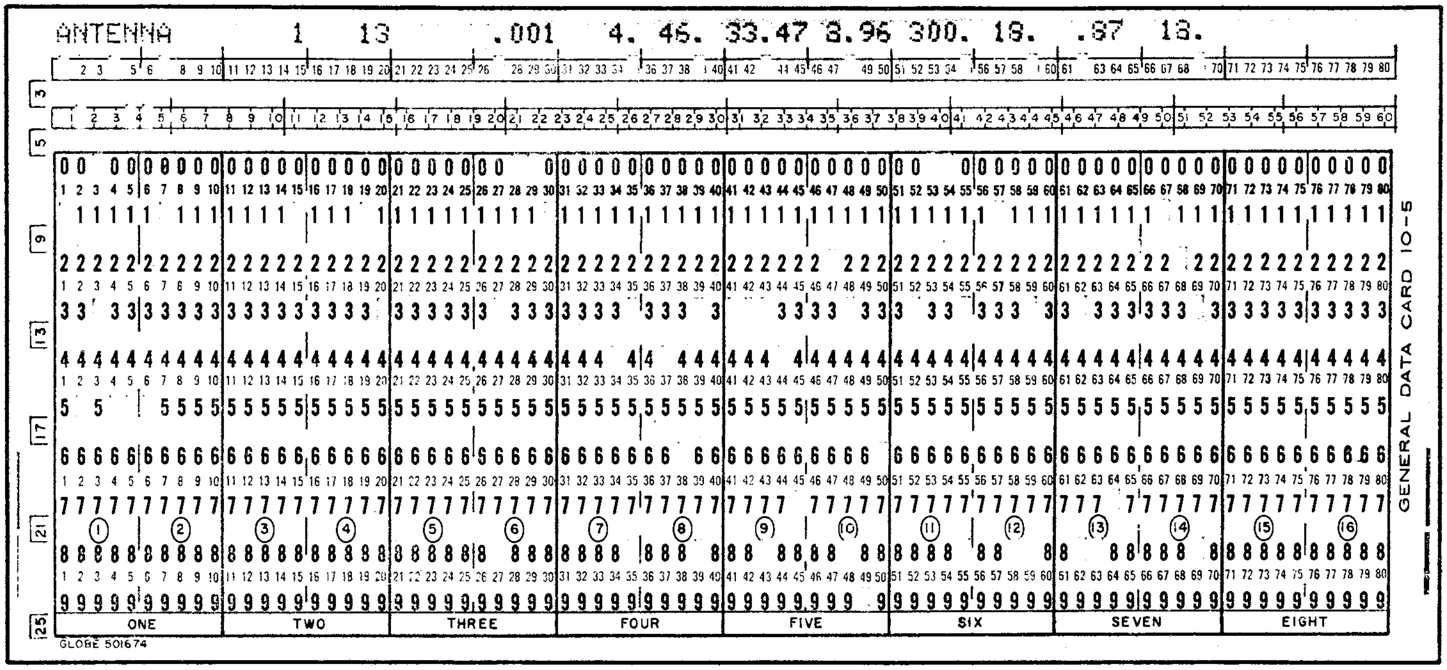

ANTENNA CARDS, LOG PERIODIC ARRAY OF HORIZONTAL DIPOLES

Columns	Name	Format	Description of Input Data
1-10		A10	"ANTENNA" 13
11-15	IAT	I5	1 for transmitter, 2 for receiver
16-20	IANTR	I5	antenna type = 13
21-25	AETA	F5.1	
26-30	ASIG	F5.1	σ
31-35	AEPS	F5.1	ε
36-40	AND	F5.1	array slope from vertical, degrees
41-45	ANL	F5.1	rear element length (-)
46-50	ANH	F5.1	feed height, meters or wavelengths (-)
51-55	AEX(1)	F5.1	transmission line impedance, ohms
56-60	AEX(2)	F5.1	angle between array axis and element tips, degrees
61-65	AEX(3)	F5.1	τ, geometric ratio of element lengths, < 1
66-70	AEX(4)	F5.1	number of elements
71-75	AFQB	F5.1	
76-80	IAIN	I5	

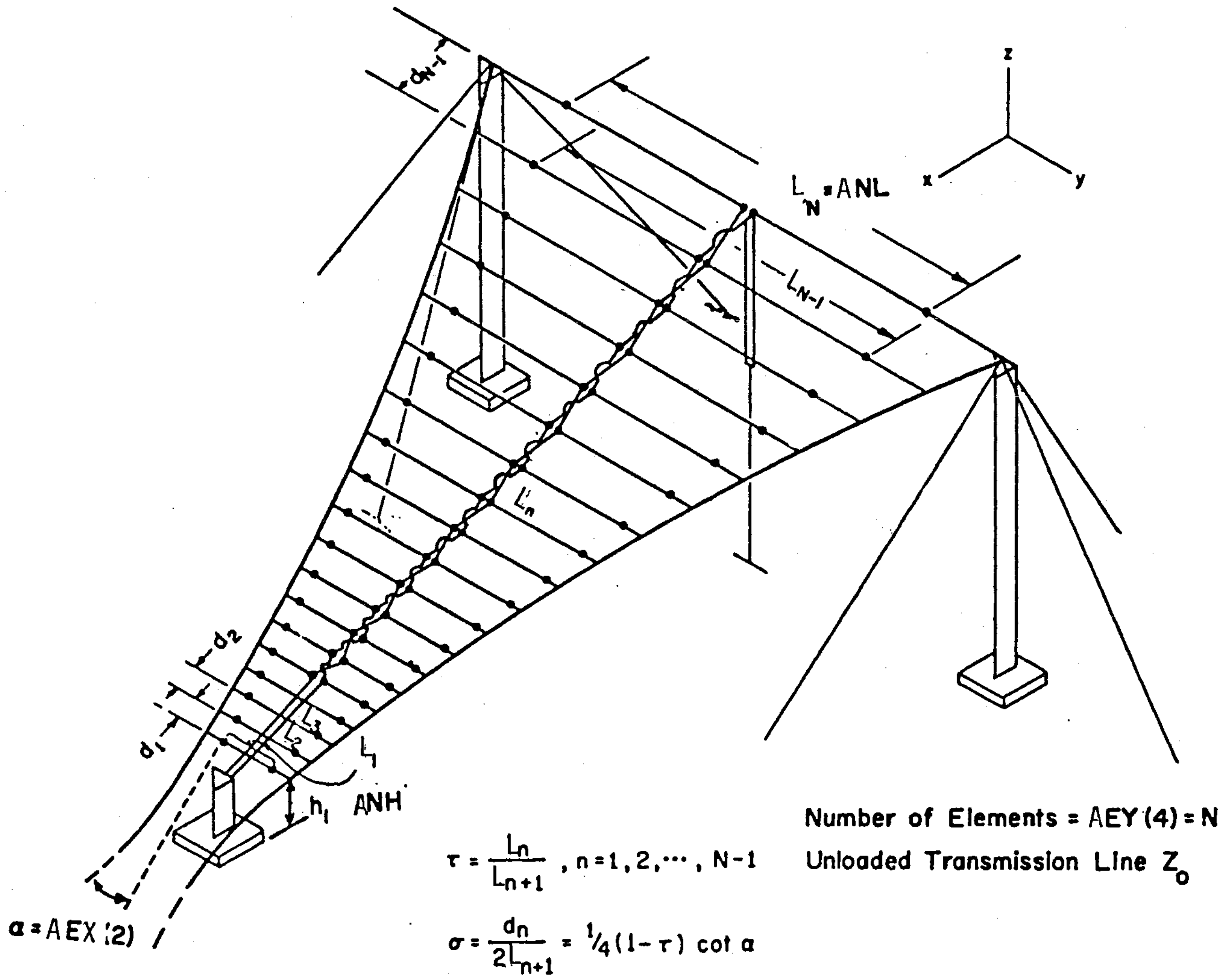

Figure 39. Horizontally polarized crossed-dipole log periodic antenna structure (type 13).

Table 19. Tilted Dipole, Input Card

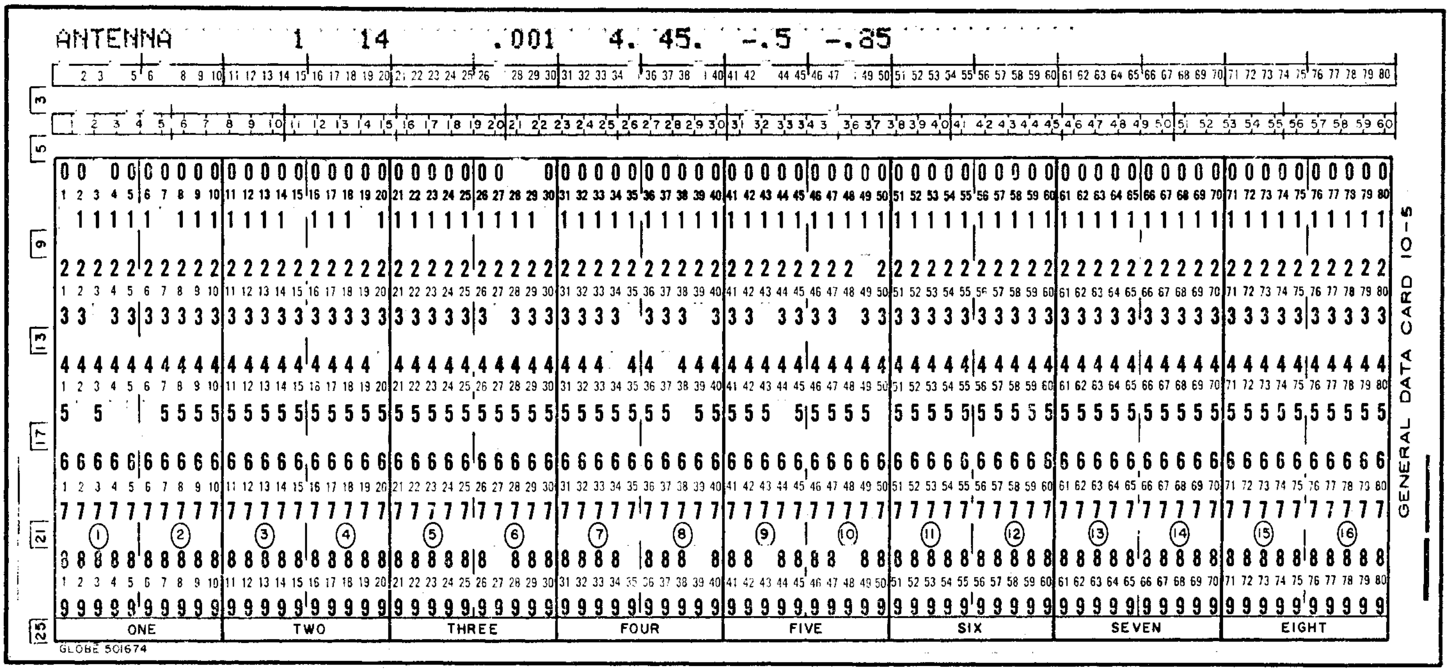

ANTENNA CARD, TILTED DIPOLE

Columns	Name	Format	Description of Input Data
1-10		A10	14
11-15	IAT	I5	
16-20	IANTR	I5	antenna type = 14
21-25	AETA	F5.1	
26-30	ASIG	F5.1	σ
31-35	AEPS	F5.1	ε
36-40	AND	F5.1	tilt of element from horizontal, degrees
41-45	ANH	F5.1	feed height
46-50	ANL	F5.1	element length
51-55	AEX(1)	F5.1	additional gain

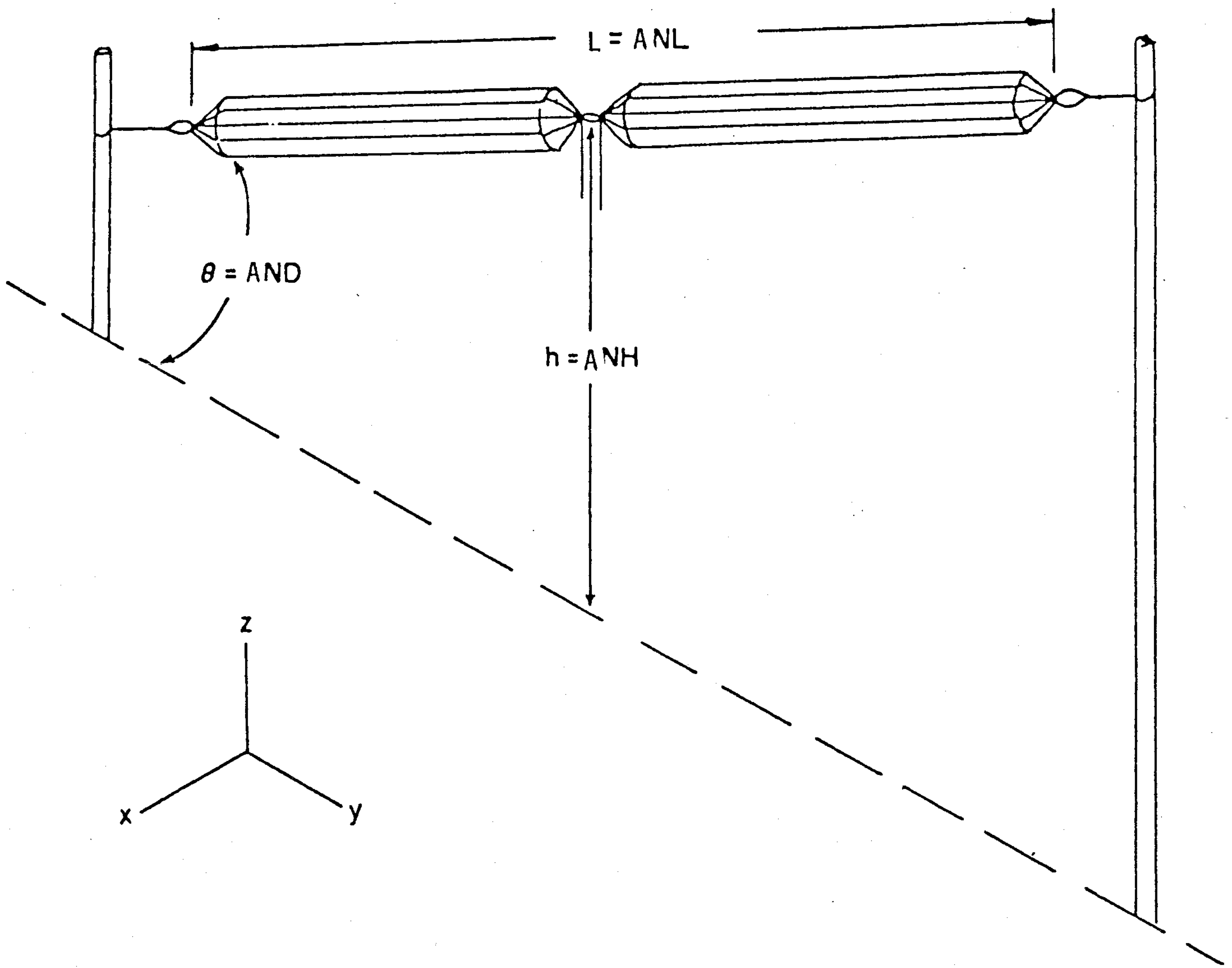

Figure 40. Arbitrarily tilted dipole antenna (type 14).

Table 20. Vertical Half Rhombic, Input Card

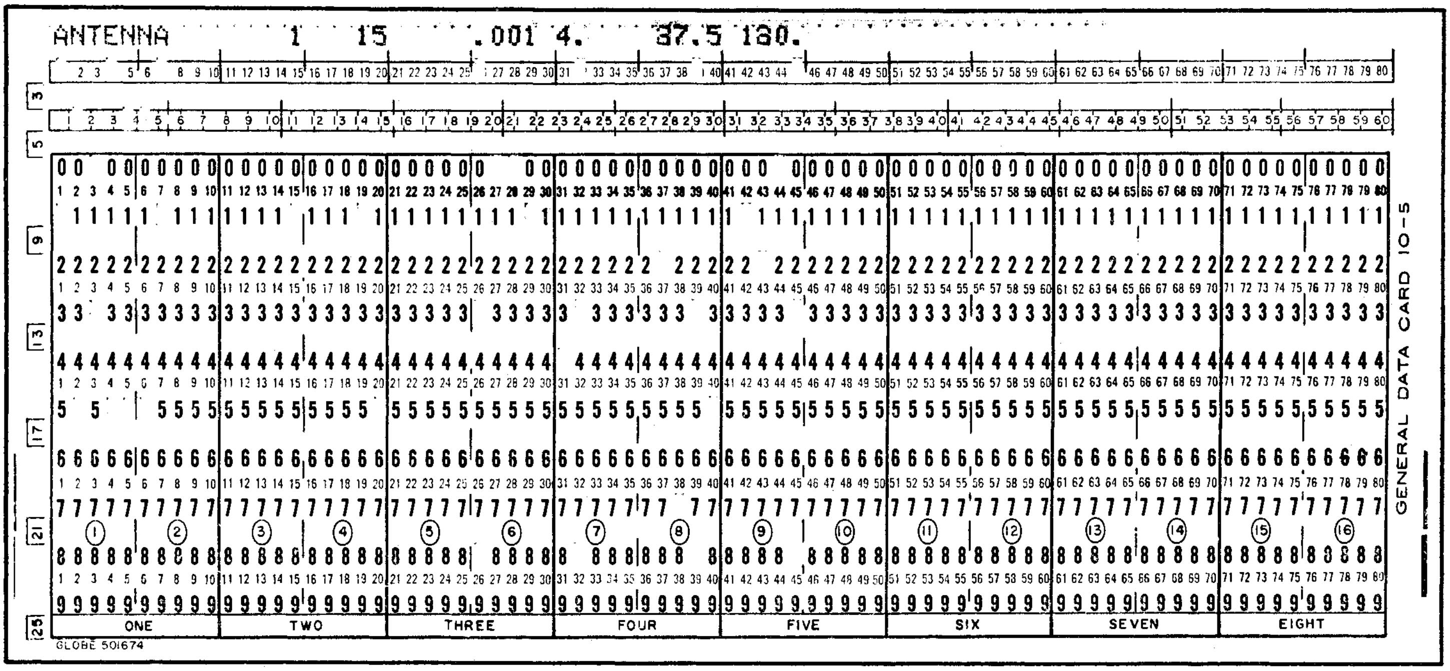

ANTENNA CARD, VERTICAL HALF-RHOMBIC

Columns	Name	Format	Description of Input Data
1-10			15
11-15	IAT	I5	
16-20	IANTR	I5	antenna type = 15
21-25	AETA	F5.1	
26-30	ASIG	F5.1	σ
31-35	AEPS	F5.1	ε
36-40	AND	F5.1	interior angle between leg and ground, degrees
41-45	ANL	F5.1	leg length

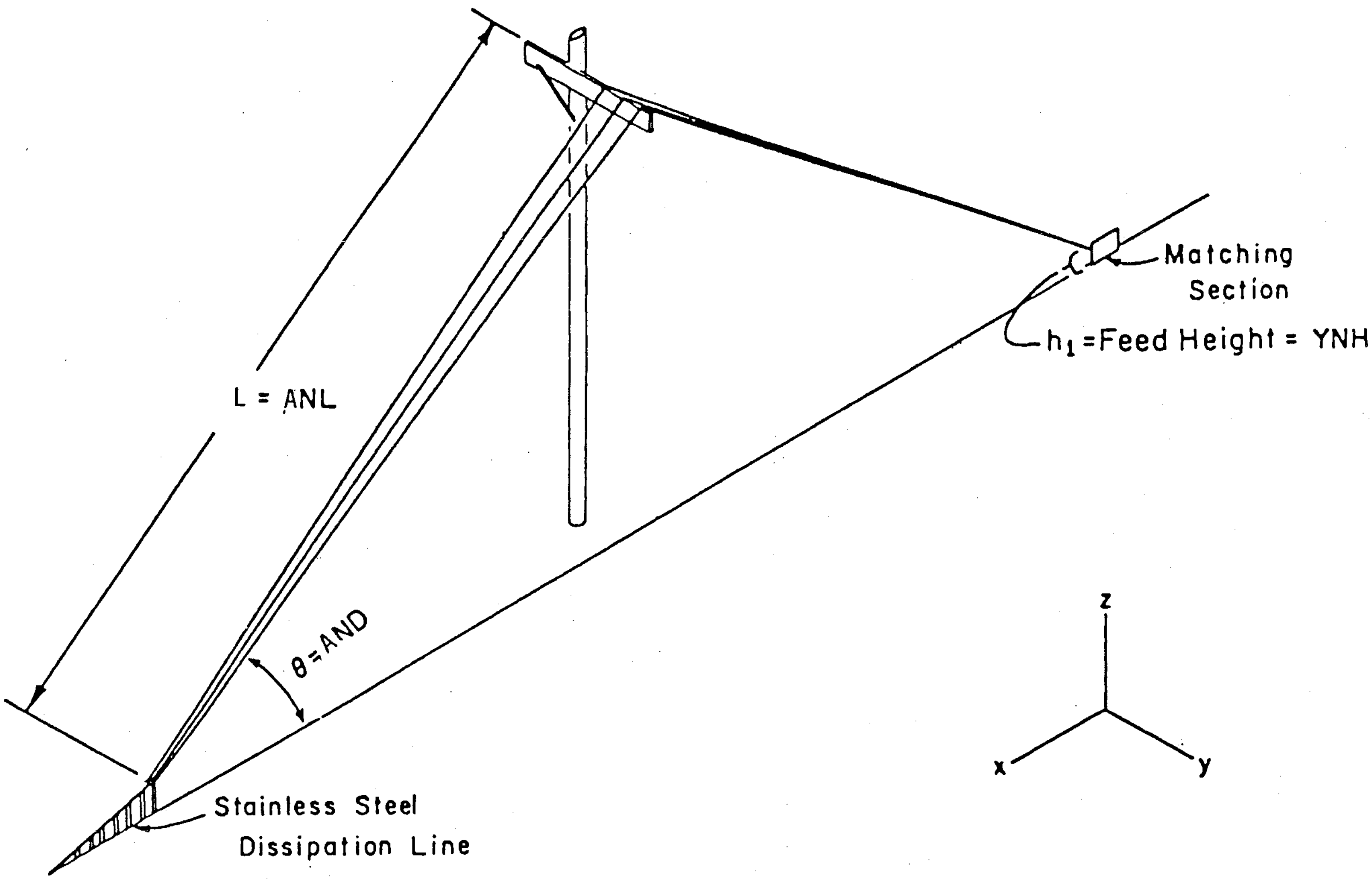

Figure 41. Vertical half-rhombic antenna (type 15).

Table 21. Horizontal Double Rhombic, Input Card

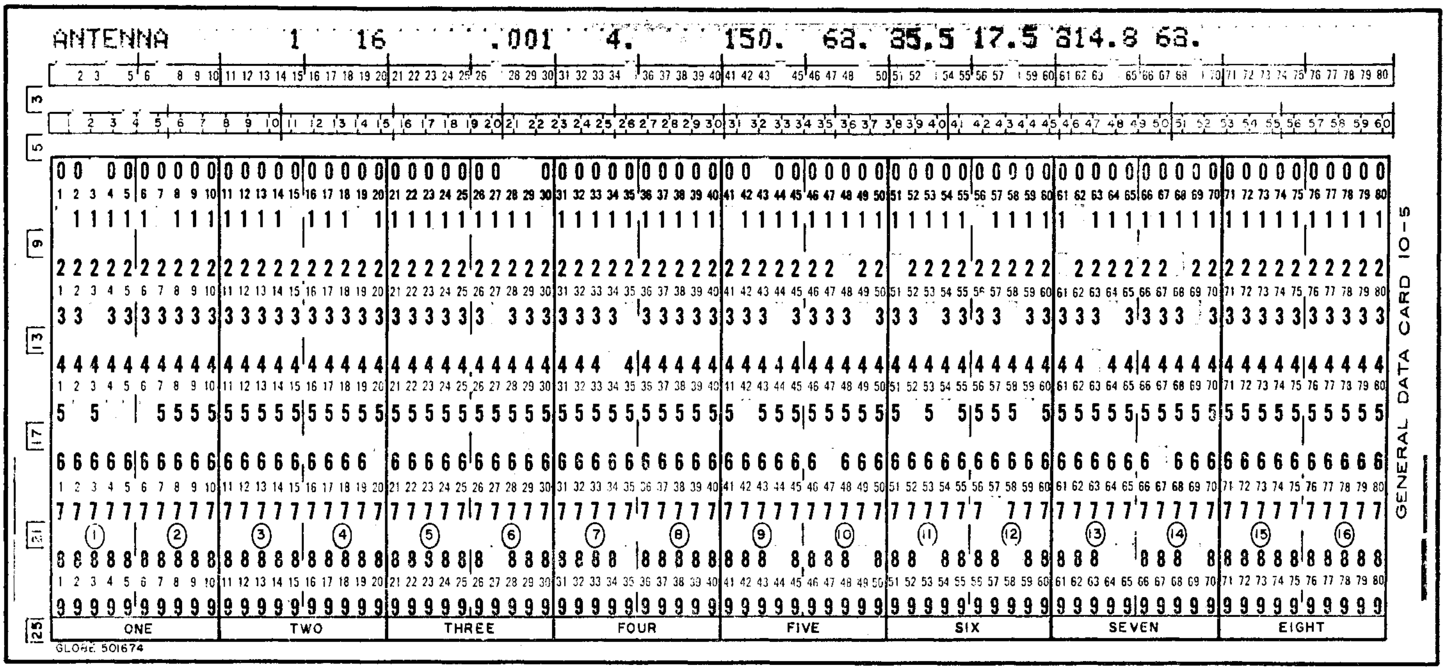

ANTENNA CARD, HORIZONTAL DOUBLE RHOMBIC

Columns	Name	Format	Description of Input Data
1-10		A10	16
11-15	IAT	I5	
16-20	IANTR	F5.1	antenna type = 16
21-25	AETA	F5.1	off azimuth
26-30	ASIG	F5.1	σ
31-35	AEPS	F5.1	ε
36-40	AND	F5.1	angle between principal antenna axis and rhomboid major at 15
41-45	ANH	F5.1	feed height
46-50	ANL	F5.1	short leg length
51-55	AEX(1)	F5.1	angle between major rhomboid axis and short leg (°)
56-60	AEX(2)	F5.1	angle between major rhomboid axis and long leg (°)
61-65	AEX(3)	F5.1	long leg length in meters or wavelengths (-)
66-70	AEX(4)	F5.1	termination height in meters or wavelengths (-)

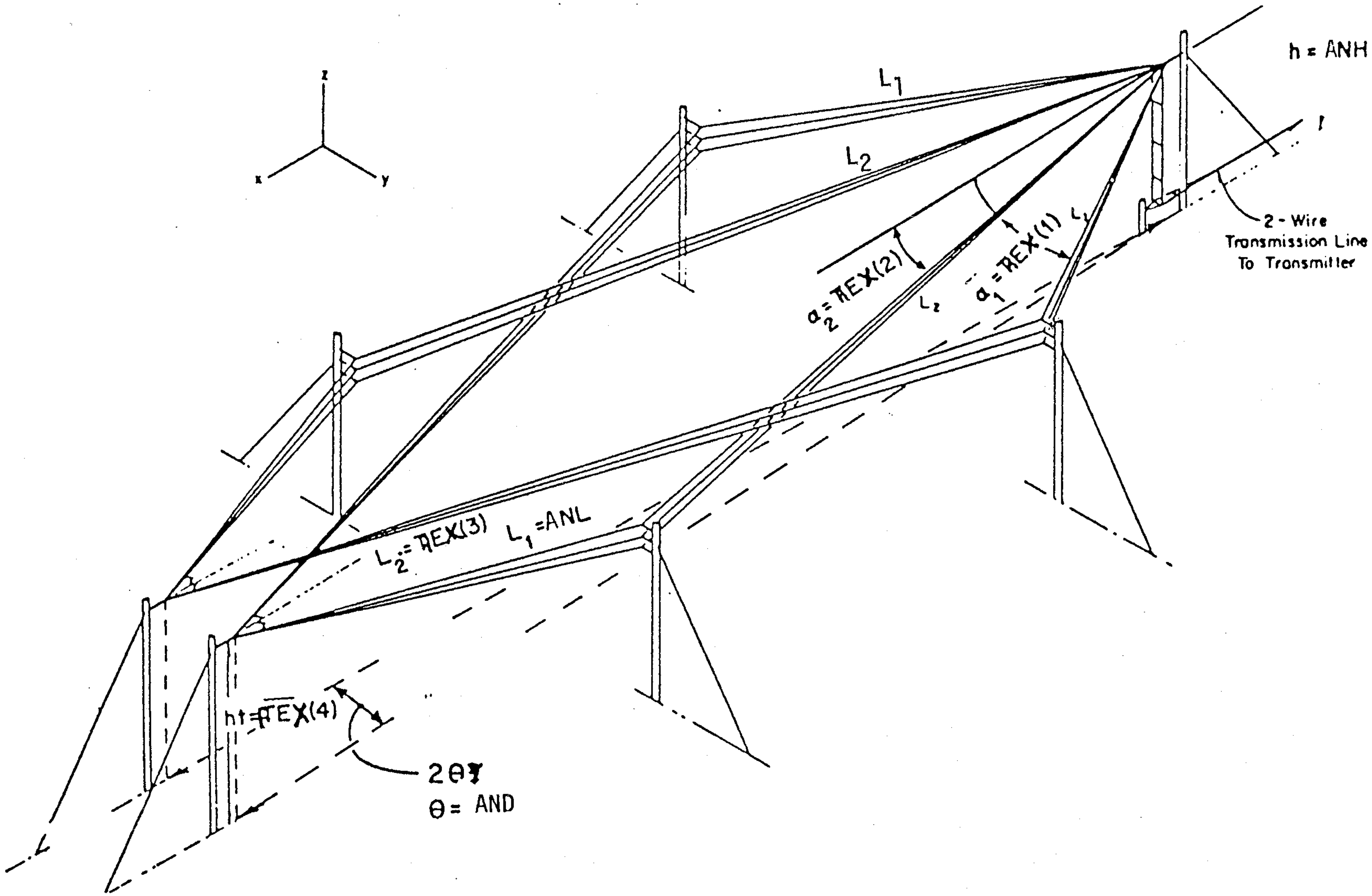

Figure 42. Double rhomboid antenna (type 16).

Table 22. Vertical Monopole with Ground Screen, Input Card

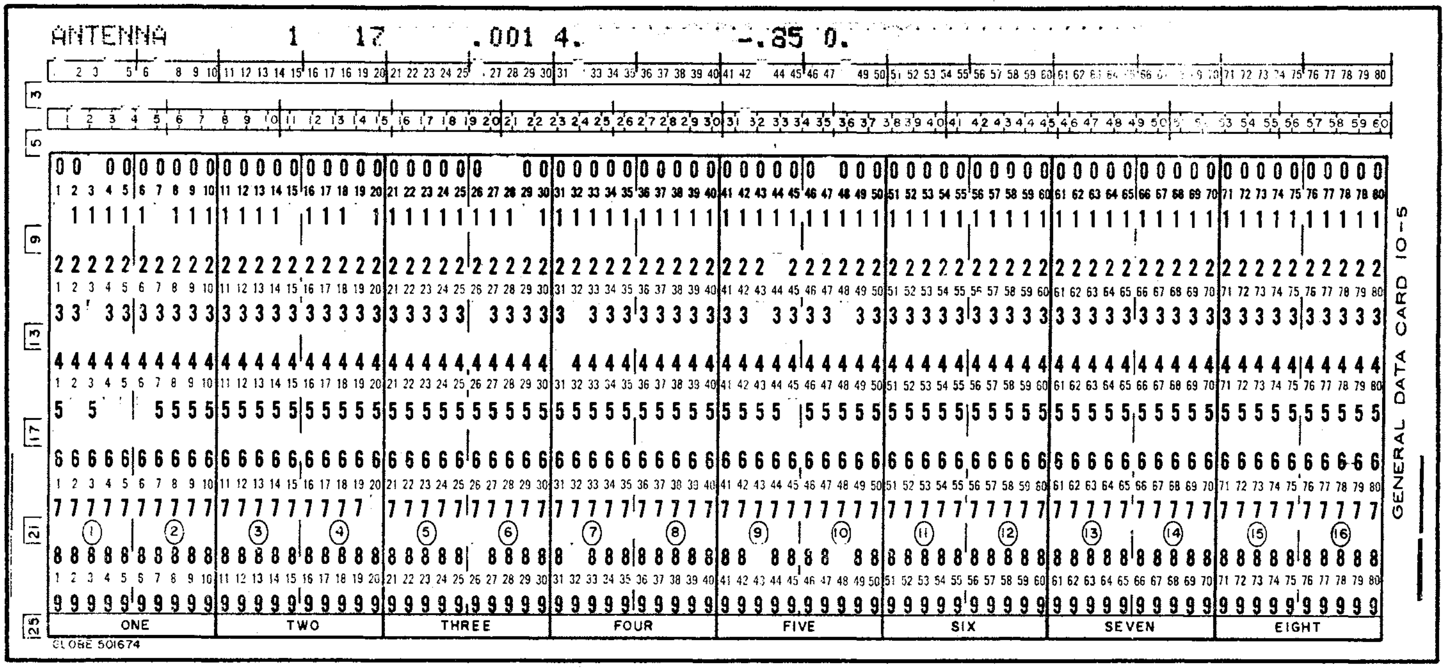

ANTENNA CARD, VERTICAL MONOPOLE WITH GROUND SCREEN*

Columns	Name	Format	Description of Input Data
1-10		A10	17
11-15	IAT	I5	
16-20	IANTR	I5	antenna type = 17
21-25	AETA	F5.1	
26-30	ASIG	F5.1	
31-35	AEPS	F5.1	
36-40	AND	F5.1	length of radials
41-45	ANH	F5.1	gain above monopole over ground specified
46-50	ANL	F5.1	length of element
51-55	AEX(1)	F5.1	additional gain
56-60	AEX(2)	F5.1	
			*No valid computer code for this was available; this is
			now a call to Antenna No. 2.

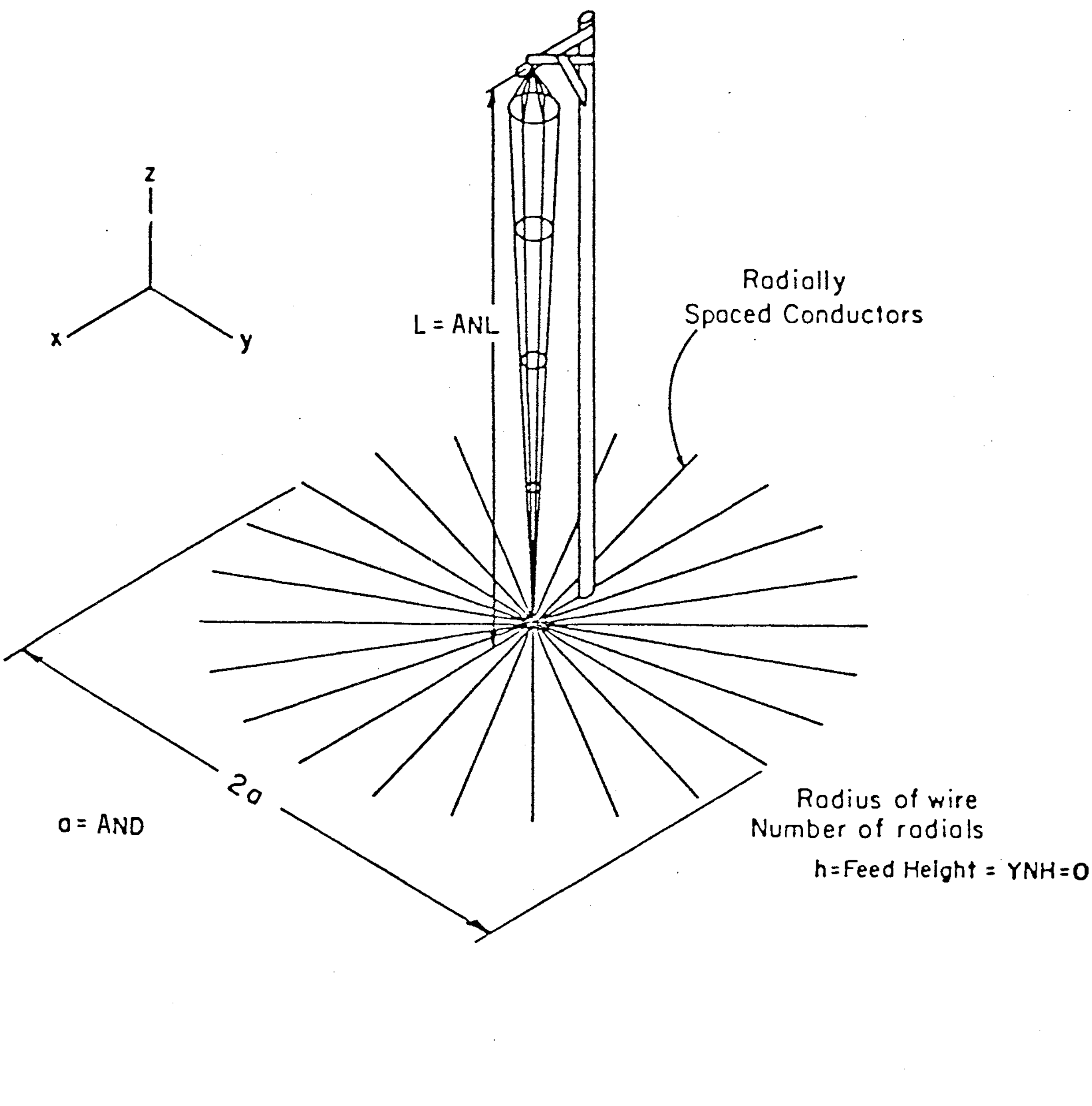

Figure 43. Vertical antenna with a radial-conductor earth system (type 17).

Table 23. Input Pattern from Data File

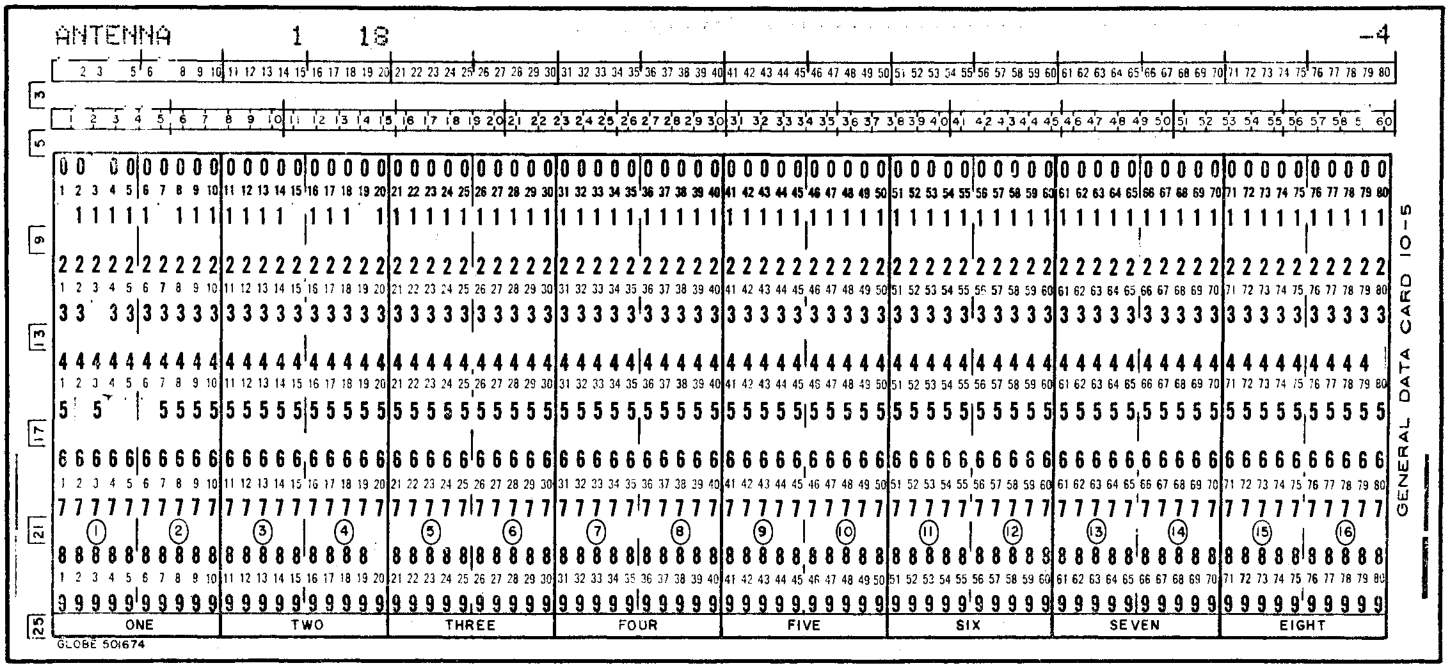

Columns	Name	Format	Description of Input Data
1-10		A10	"ANTENNA" 18
11-15	IAT	I5	1 for transmitter, 2 for receiver
16-20	IANTR	I5	antenna type = 18
21-25			
26-30			
31-35			
36-40			
41-45			
46-50			
51-55			
56-60			Antenna type 18 (a). If IAIN $\geq$ 0, then IAIN indicates
61-65			the number of antennas to skip forward from present
66-70			position on the antenna file (LU26) before reading the
71-75			desired pattern. (b) If IAIN < 0, then the antenna file
76-80	IAIN	I5	is rewound before searching for the antenna pattern.
			The pattern that is used is |IAIN| on the antenna file.

Table 24. Vertical Log Periodic Monopole Array, Input Card

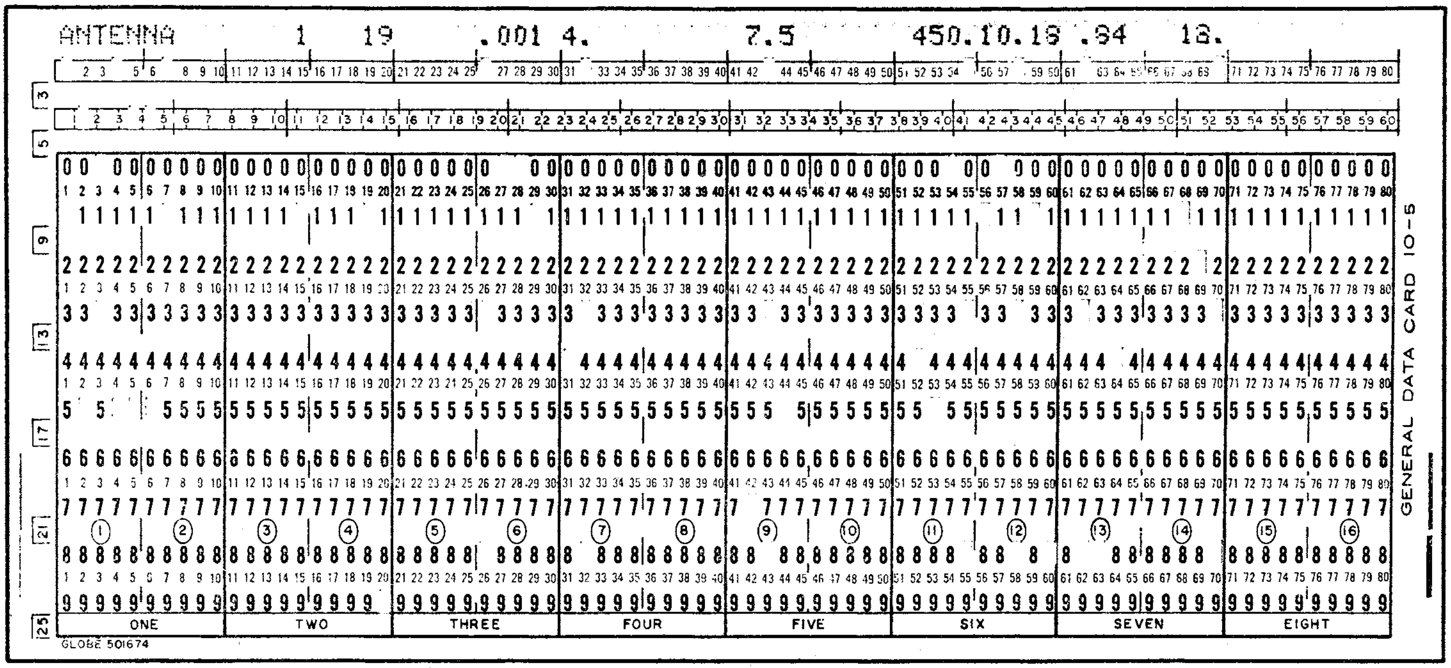

ANTENNA CARD, VERTICAL LOG PERIODIC MONOPOLE ARRAY

Columns	Name	Format	Description of Input Data
1-10		A10	"ANTENNA" 19
11-15	IAT	I5	1 for transmitter, 2 for receiver
16-20	IANTR	I5	antenna type = 19
21-25	AETA	F5.1	bearing degrees E of N. (-) is off azimuth
26-30	ASIG	F5.1	
31-35	AEPS	F5.1	
36-40			
41-45	ANL	F5.1	rear element length (height), meters or wavelengths (-)
46-50	ANH	F5.1	
51-55	AEX(1)	F5.1	
56-60			
61-65	AEX(3)	F5.1	ratio of element length, γ, e.g., 0.86
66-70	AEX(4)	F5.1	number of elements
71-75	AFOB	F5.1	ending frequency when more than one antenna is used
76-80	IAIN	I5	Antenna number indicator--each transmitter or receiver antenna can be defined by up to three different antennas over the frequency range; default is one, if IAIN is left blank.

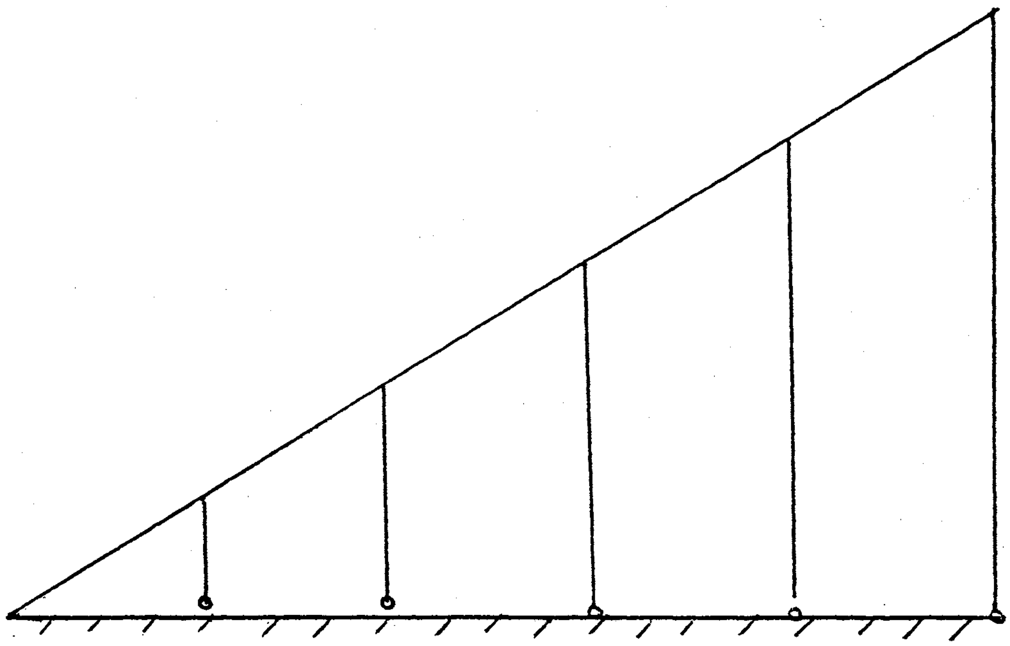

Figure 44. Vertical log periodic array of monopoles (type 19) (estimated by 1/4 wave monopole plus additional gain).

Table 25. Terminated Long Wire

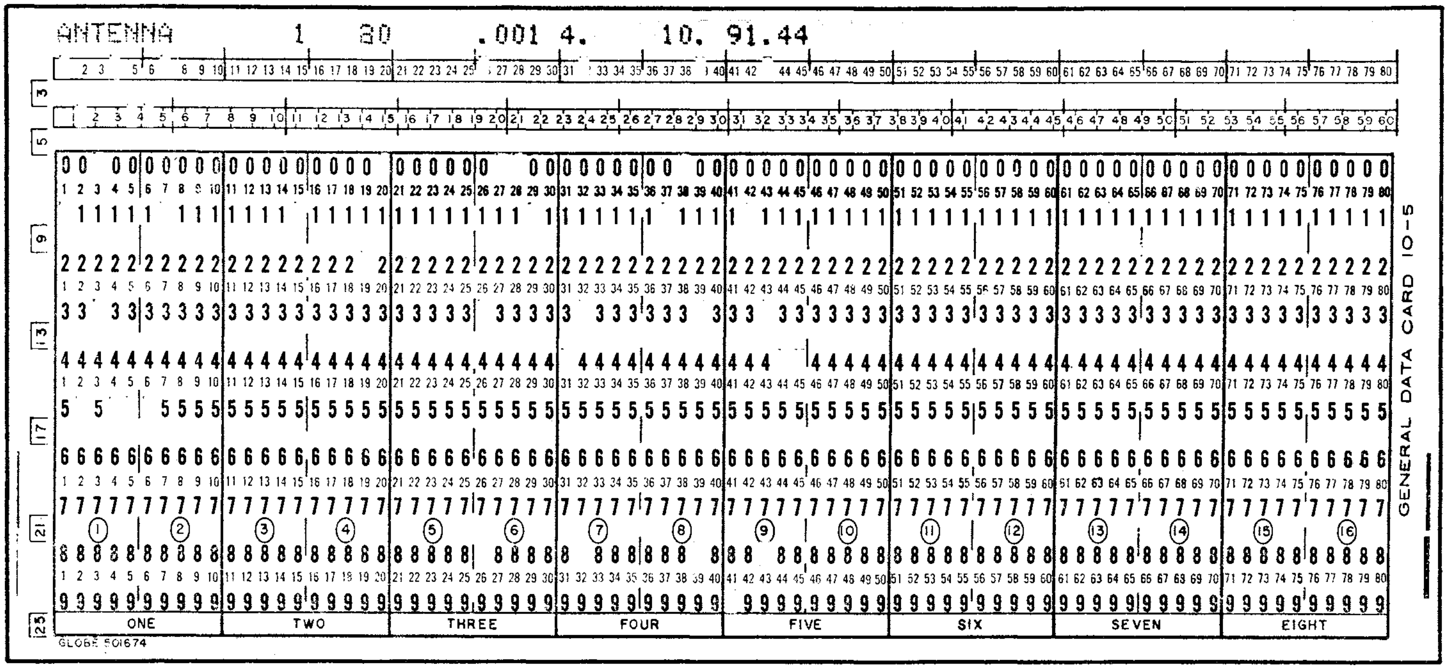

ANTENNA CARD, SLOPING LONG WIRE, TERMINATED

Columns	Name	Format	Description of Input Data
1-10		A10	"ANTENNA" 20
11-15	IAT	I5	1 for transmitter, 2 for receiver
16-20	IANTR	I5	antenna type = 20
21-25	AETA	F5.1	
26-30	ASIG	F5.1	σ
31-35	AEPS	F5.1	ε
36-40	AND	F5.1	α, slope from horizontal, degrees
41-45	ANL	F5.1	element length
46-50	ANH	F5.1	feed height
51-55	AEX(1)	F5.1	additional gain

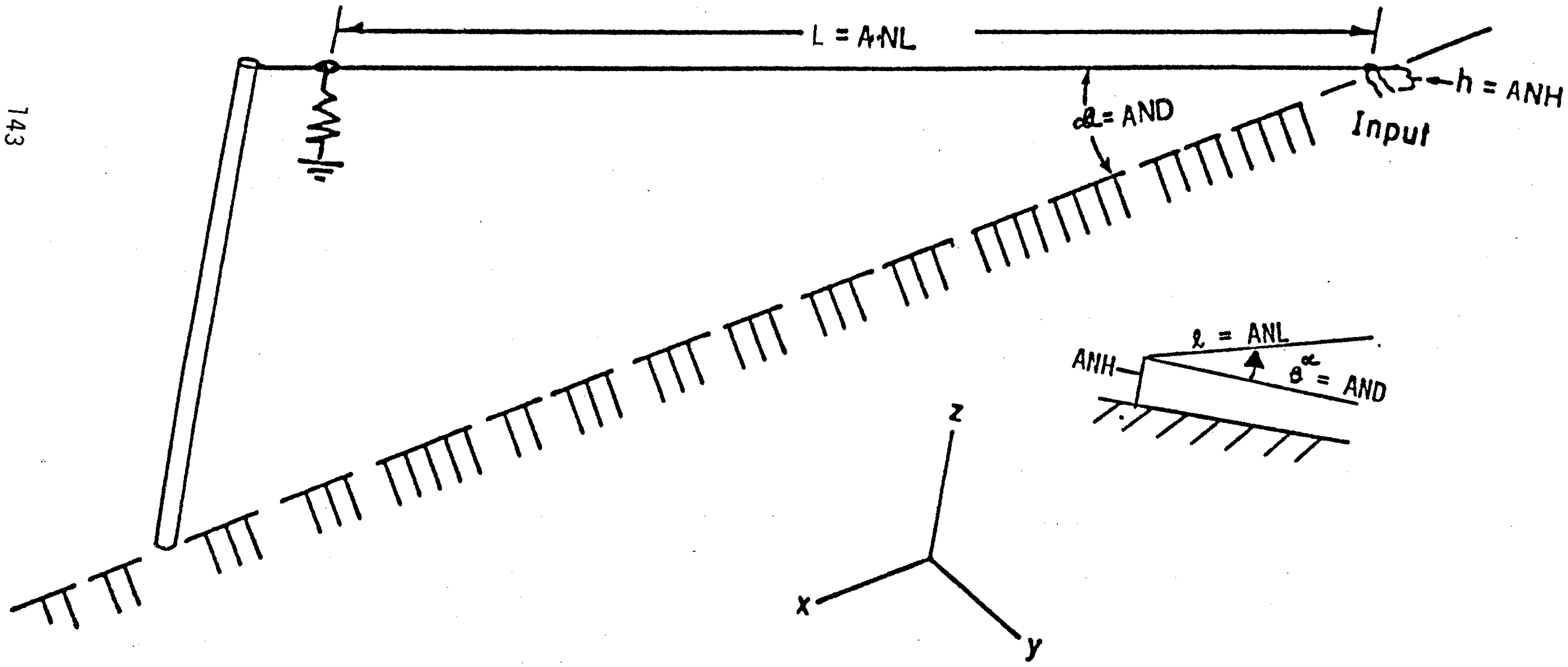

Figure 45. Sloping long-wire terminated antenna (type 20).

Table 26. Log Periodic Array of Vertical Dipoles

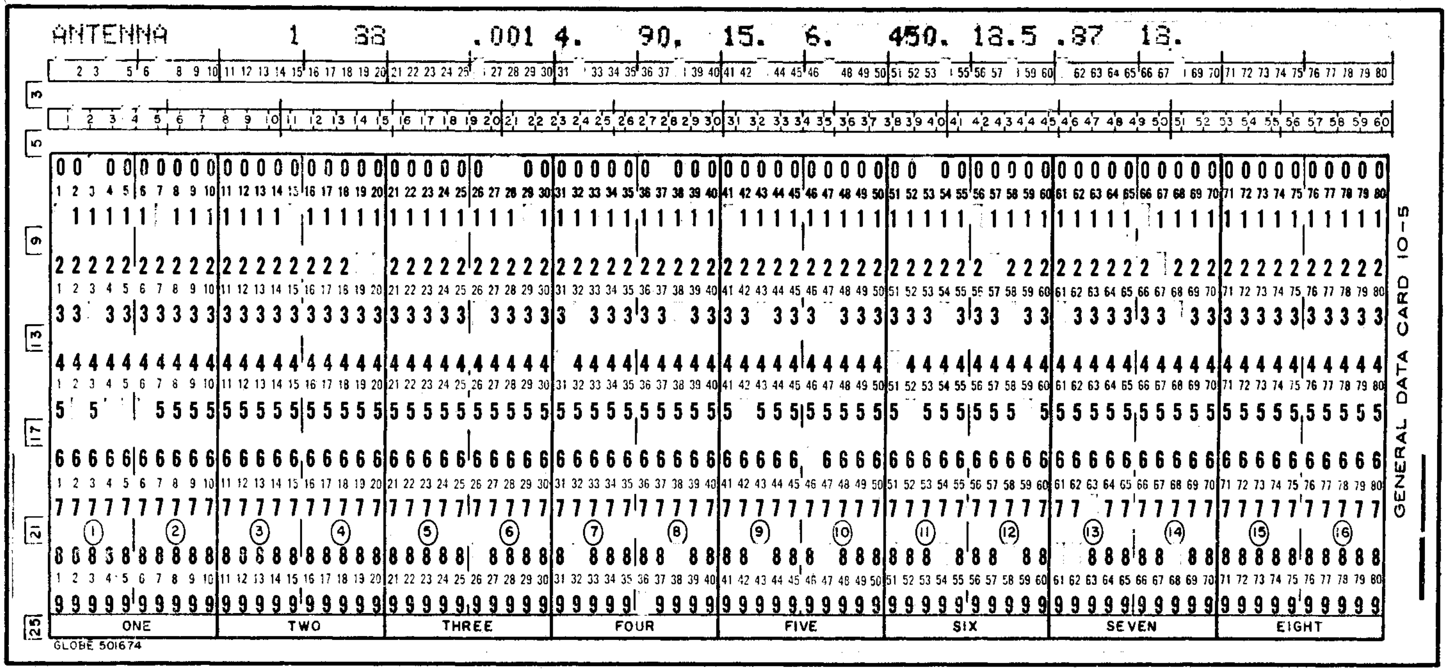

ANTENNA CARD, LOG PERIODIC ARRAY OF VERTICAL DIPOLES

Columns	Name	Format	Description of Input Data
1-10		A10	22
11-15	IAT	I5	
16-20	IANTR	I5	antenna type = 22
21-25	AETA	F5.1	bearing
26-30	ASIG	F5.1	σ
31-35	AEPS	F5.1	ε
36-40	AND	F5.1	array slope from vertical
41-45	ANL	F5.1	rear element length
46-50	ANH	F5.1	feed height
51-55	AEX(1)	F5.1	transmission line impedance, ohms
56-60	AEX(2)	F5.1	angle between array axis and element tip*, α_1
61-65	AEX(3)	F5.1	γ, geometric ratio of element lengths, < 1.
66-70	AEX(4)	F5.1	number of elements
71-75			
76-80			
			*Upper angle if array is sloped AND is not 90°.

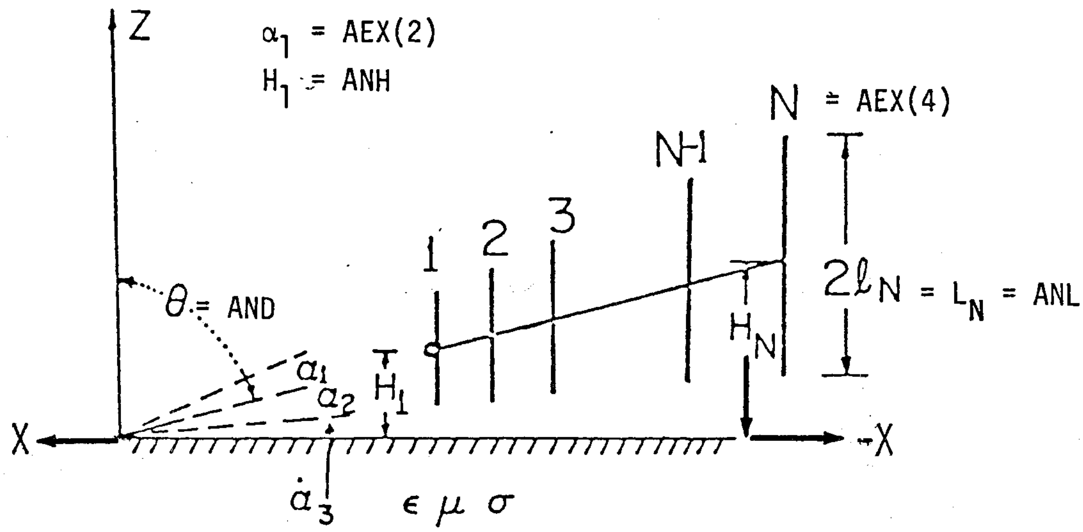

Figure 46. Vertical log-periodic antenna above flat earth.

Table 27. Stacked Array of Vertical Log Periodic Dipole Arrays

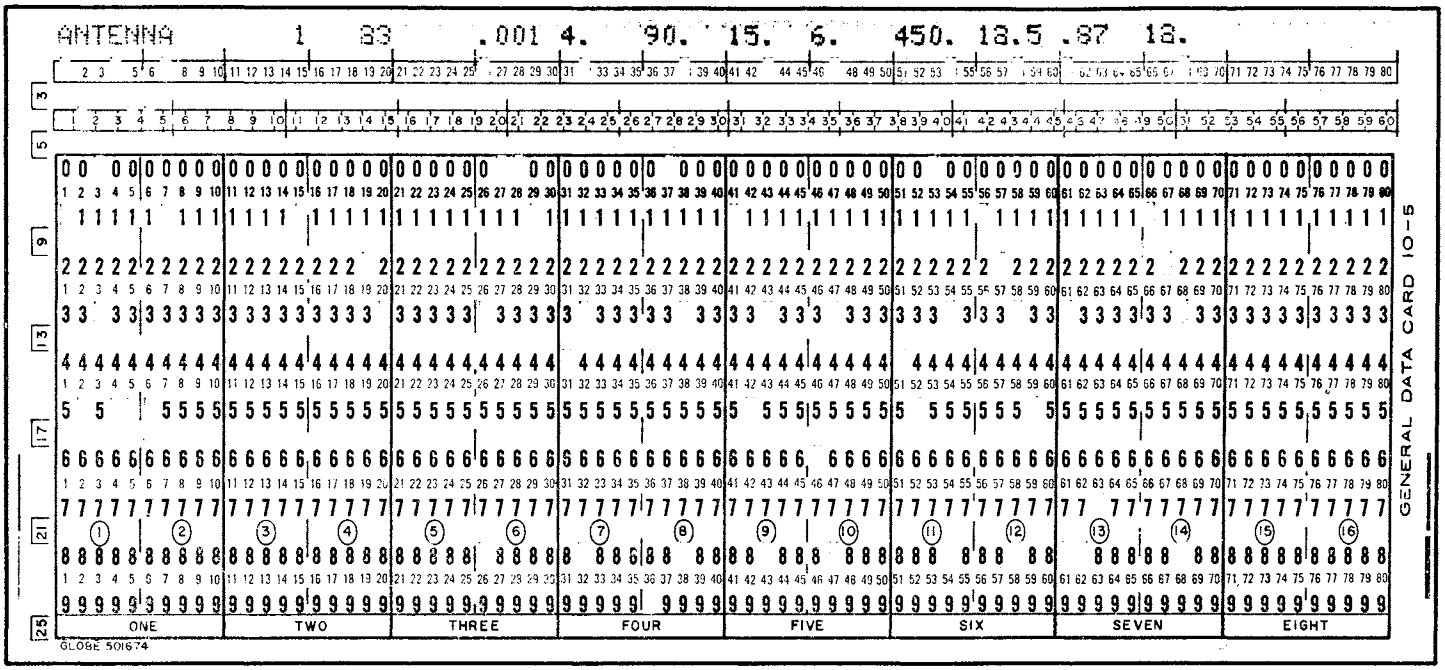

ANTENNA CARD, STACKED ARRAYS OF LOG PERIODIC ARRAY OF VERTICAL DIPOLES (Card 1)

Columns	Name	Format	Description of Input Data
1-10		A10	"ANTENNA" 23
11-15	IAT	I5	1 or 2 for T or R
16-20	IANTR	I5	antenna type = 23
21-25	AETA	F5.1	bearing
26-30	ASIG	F5.1	σ
31-35	AEPS	F5.1	ε
36-40	AND	F5.1	array slope from vertical
41-45	ANH	F5.1	feed height
46-50	ANL	F5.1	rear element length
51-55	AEX(1)	F5.1	transmission line impedance, ohms
56-60	AEX(2)	F5.1	angle between array axis and element tip*, α_1
61-65	AEX(3)	F5.1	γ, geometric ratio of element lengths, < 1
66-70	AEX(4)	F5.1	number of elements
71-75			
76-80			
			*Upper angle if array is sloped, AND is not 90°.

Table 28. Auxiliary Card for Stacked Arrays

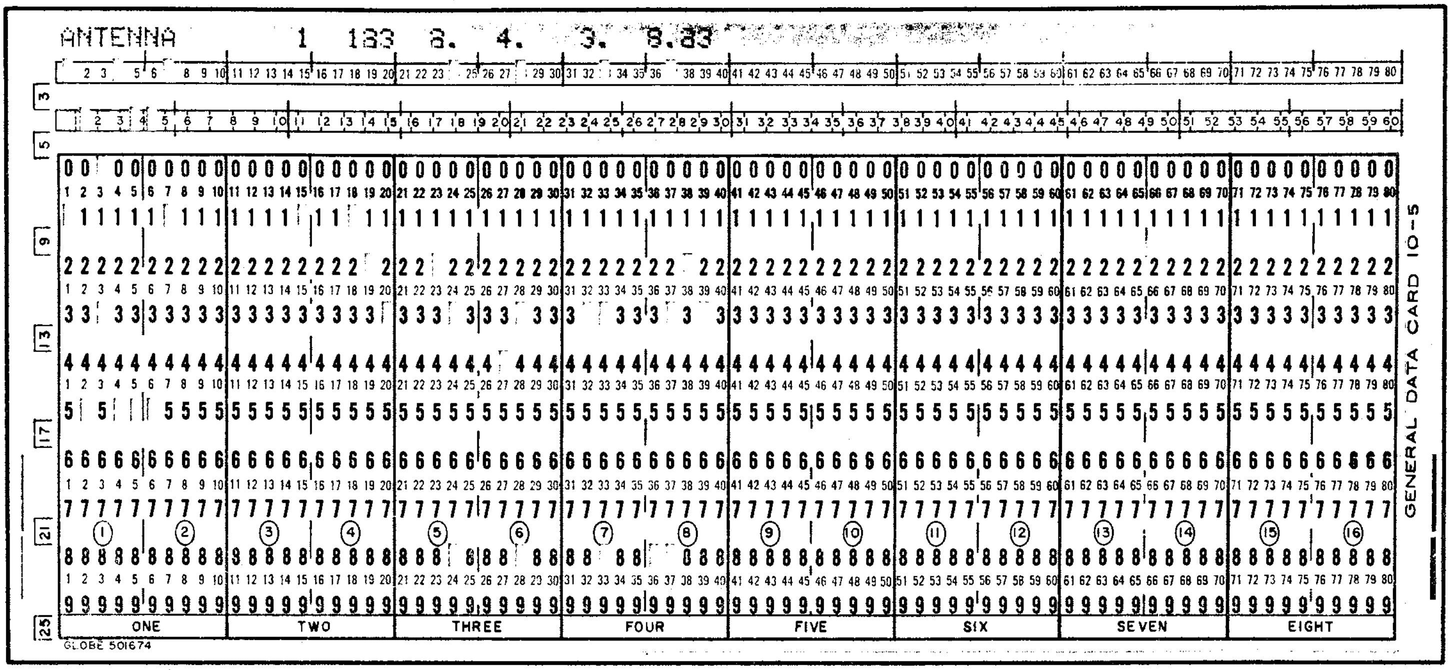

ANTENNA CARD, STACKED ARRAY OF VERTICAL LPD (card 2)

Columns	Name	Format	Description of Input Data
1-10		A10	"ANTENNA" 23
11-15	IAT	I5	1 or 2
16-20	IANTR	I5	"123"
21-25	F(1,IAT)	F5.1	number of arrays in horizontal (X) direction
26-30	F(2,IAT)	F5.1	distance between arrays, meters, (-) is wavelengths
31-36	F(3,IAT)	F5.1	number of arrays in vertical
37-40	F(4,IAT)	F5.1	height between arrays

Table 29. End Fire Array of Vertical Loops

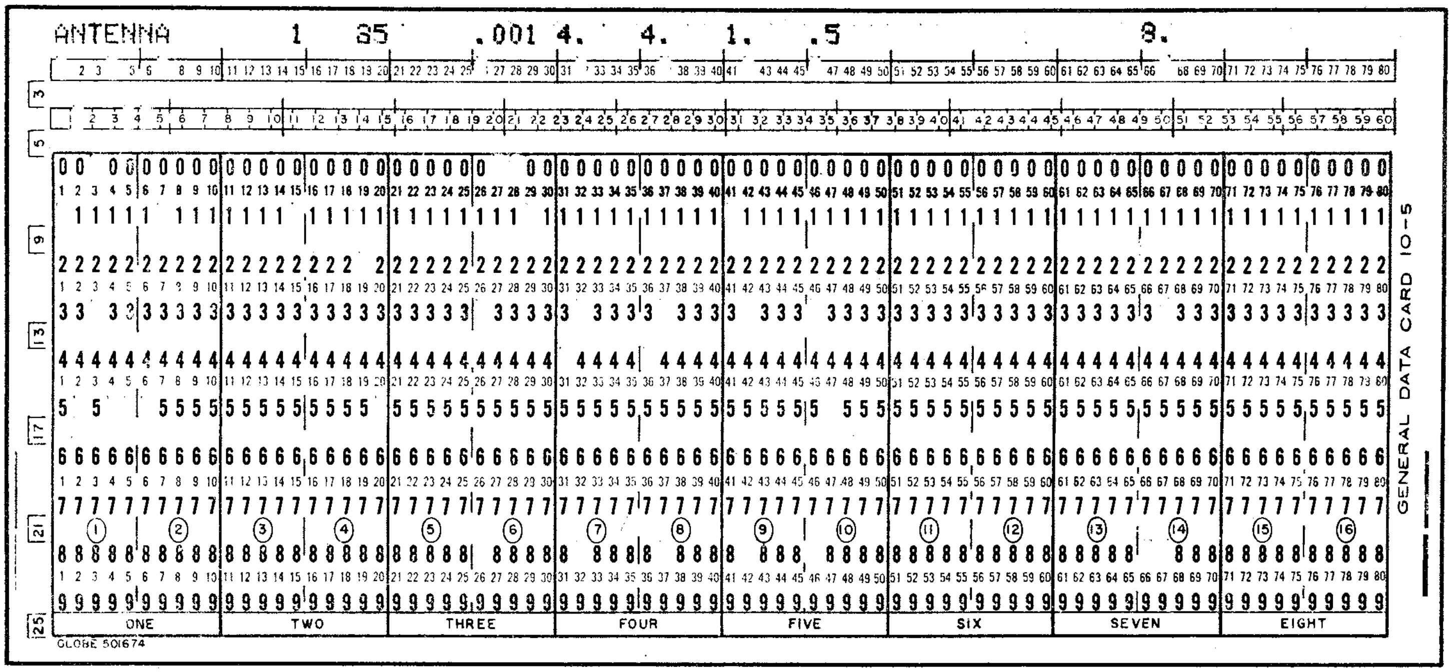

ANTENNA CARD, END FIRE ARRAY OF VERTICAL LOOPS

Columns	Name	Format	Description of Input Data
1-10		A10	25
11-15	IAT	I5	
16-20	IANTR	I5	antenna type = 25
21-25	AETA		
26-30	ASIG		
31-35	AEPS		
36-40	AND		distance between elements
41-45	ANH		height of loop
46-50	ANL		radius of loop
51-55	AEX(1)		
56-60	AEX(2)		
61-65	AEX(3)		
66-70	AEX(4)	F5.1	number of elements

Table 30. Horizontal Rhombic, Output Antenna Pattern

METHOD 13   IONCAP 78.03   PAGE 1

IONCAP 80.01 ANTENNA PACKAGE   ANTENNA PATTERN

FREQUENCY RANGE	ANTENNA TYPE	HEIGHT	LENGTH	ANGLE	AZIMUTH	EX(1)	EX(2)	EX(3)	EX(4)	CONDUCT.	DIELECT.
1.0 TO 30.0	HOR RHOM	16.760	88.390	67.500	0.000	0.000	0.000	0.000	0.000	.001	4.000

		2	3	4	5	6	7	8	9	10	11	12	13	14	16	18	20	22	24	26	28	30		
	90	-3.7	-19.8	-12.5	-2.4	-11.0	-34.2	-10.4	-10.8	-37.3	-10.6	-3.0	-14.4	-19.0	-10.2	-11.9	-24.2	-2.5	-28.8	-10.4	-12.2	-16.2	90	
	88	-3.1	-15.9	-16.0	-2.5	-7.7	-37.3	-12.8	-8.8	-20.1	-18.9	-3.1	-6.1	-37.3	-5.8	-23.5	-8.0	-6.8	-17.0	-8.2	-37.3	-3.1	88	
	86	-2.7	-12.7	-20.9	-3.0	-5.4	-32.2	-16.8	-8.2	-12.3	-37.3	-5.6	-2.4	-17.1	-5.7	-37.3	-3.9	-28.7	-4.4	-18.8	-10.8	-7.3	86	
	84	-2.2	-10.1	-28.3	-4.0	-3.7	-20.6	-23.6	-8.8	-8.0	-29.8	-11.5	-1.6	-6.7	-10.1	-16.5	-6.4	-16.4	-3.7	-32.1	-6.1	-37.3	84	
	82	-1.9	-7.8	-37.3	-5.4	-2.7	-13.9	-37.3	-10.9	-5.8	-14.5	-25.3	-3.4	-2.2	-22.9	-8.8	-18.5	-3.4	-14.3	-9.2	-15.6	-6.1	82	
	80	-1.5	-5.9	-37.3	-7.4	-2.1	-9.5	-37.3	-14.8	-5.3	-7.6	-37.3	-8.8	-1.1	-37.3	-7.4	-35.9	-1.2	-31.1	-5.9	-32.7	-2.5	80	
	78	-1.3	-4.2	-33.0	-10.3	-2.1	-6.4	-27.9	-21.6	-6.3	-4.0	-15.9	-21.5	-3.0	-13.2	-11.1	-10.2	-7.3	-5.6	-14.6	-8.7	-16.1	78	
	76	-1.1	-2.8	-22.7	-14.2	-2.7	-4.3	-17.9	-35.9	-9.1	-2.6	-6.9	-37.3	-9.0	-4.9	-23.8	-3.9	-37.3	-.7	-37.1	-6.8	-17.8	76	
	74	-.9	-1.6	-16.2	-20.1	-3.8	-3.0	-11.9	-37.3	-14.3	-3.1	-2.4	-14.3	-24.7	-1.9	-37.3	-4.4	-12.4	-4.9	-7.4	-19.5	-2.9	74	
	72	-.8	-.5	-11.6	-30.2	-5.6	-2.3	-8.0	-26.2	-24.1	-5.4	-.6	-5.0	-31.3	-2.6	-14.1	-11.9	-1.7	-29.9	-2.2	-26.0	-5.3	72	
E	70	-.8	.5	-8.0	-36.8	-8.3	-2.4	-5.4	-16.5	-36.8	-10.2	-.9	-.6	-10.1	-7.8	-6.2	-36.8	-.3	-11.8	-7.5	-7.2	-35.0	70	E
L	68	-.8	1.2	-5.1	-36.1	-12.3	-3.1	-3.7	-10.9	-30.7	-19.5	-3.4	1.0	-2.2	-22.9	-3.8	-18.5	-6.5	-.0	-36.7	-5.2	-11.5	68	L
E	66	-.8	1.9	-2.7	-21.9	-18.4	-4.6	-2.9	-7.3	-17.5	-36.5	-8.7	.2	1.4	-29.5	-5.9	-7.3	-32.6	1.2	-7.4	-16.4	-4.1	66	E
V	64	-.9	2.5	-.7	-14.2	-29.5	-7.0	-2.9	-5.1	-10.9	-28.7	-19.6	-3.1	2.1	-8.0	-14.5	-4.5	-15.0	-6.4	1.4	-24.1	-9.8	64	V
A	62	-1.1	2.9	.9	-8.9	-36.2	-10.9	-3.7	-3.8	-7.1	-14.8	-36.2	-10.1	.2	-.2	-36.2	-6.6	-3.4	-36.2	.2	-2.8	-36.2	62	A
T	60	-1.3	3.2	2.3	-4.9	-29.8	-17.0	-5.4	-3.4	-5.0	-8.4	-21.2	-26.7	-4.9	3.0	-13.6	-15.1	-1.2	-7.4	-13.5	1.1	-9.4	60	T
I	58	-1.6	3.5	3.4	-1.8	-17.2	-28.6	-8.4	-3.9	-3.9	-5.0	-10.0	-32.8	-16.2	3.0	-2.2	-35.9	-5.2	1.1	-19.0	-5.5	-1.0	58	I
O	56	-1.9	3.6	4.4	.7	-9.9	-35.7	-13.4	-5.4	-3.8	-3.4	-4.6	-12.3	-35.7	-.2	2.6	-14.7	-18.0	1.3	.2	-35.7	-3.7	56	O
N	54	-2.2	3.7	5.1	2.7	-4.9	-26.0	-22.3	-8.2	-4.5	-3.0	-2.1	-4.6	-14.9	-8.3	3.5	-2.7	-35.5	-5.8	4.2	-2.6	-32.4	54	N
	52	-2.6	3.7	5.7	4.3	-1.1	-14.0	-35.3	-13.1	-6.3	-3.7	-1.3	-.8	-4.6	-33.5	.8	2.2	-11.1	-31.7	.5	5.0	-5.9	52	
A	50	-3.1	3.6	6.2	5.6	1.8	-7.0	-30.9	-22.3	-9.5	-5.3	-2.0	.6	.2	-17.8	-7.3	3.0	-1.9	-17.6	-14.9	3.7	4.9	50	A
N	48	-3.6	3.4	6.5	6.7	4.1	-2.0	-15.3	-34.7	-15.4	-8.0	-3.8	.2	2.2	-3.5	-34.7	-.6	1.8	-5.4	-23.3	-7.9	5.2	48	N
G	46	-4.2	3.1	6.7	7.5	6.0	1.7	-7.0	-27.7	-27.6	-12.4	-6.7	-1.8	2.1	2.5	-13.4	-11.9	1.1	-.7	-5.0	-29.9	-4.9	46	G
L	44	-4.8	2.8	6.7	8.2	7.5	4.5	-1.5	-12.9	-34.2	-21.0	-11.0	-5.1	.3	5.1	-.2	-34.2	-5.4	.4	-1.1	-3.3	-32.5	44	L
E	42	-5.5	2.3	6.6	8.6	8.6	6.8	2.6	-4.9	-19.6	-33.8	-18.2	-10.0	-3.4	5.2	5.4	-5.0	-31.9	-3.4	-.9	1.2	-1.2	42	E
	40	-6.2	1.8	6.5	8.9	9.5	8.5	5.7	.6	-8.2	-26.5	-33.5	-17.2	-8.9	3.2	7.6	4.4	-10.9	-20.0	-3.7	-.6	3.8	40	
I	38	-7.0	1.3	6.2	9.0	10.1	9.9	8.1	4.6	-1.2	-11.0	-32.6	-33.1	-16.9	-1.0	7.2	8.5	3.0	-16.4	-17.2	-4.9	1.1	38	I
N	36	-7.8	.6	5.8	8.9	10.5	10.9	9.9	7.6	3.7	-2.6	-12.9	-32.7	-32.7	-7.9	4.4	9.4	8.9	2.0	-19.4	-18.0	-6.2	36	N
	34	-8.7	-.1	5.3	8.7	10.8	11.6	11.3	9.9	7.3	3.1	-3.3	-13.5	-32.3	-18.8	-1.0	7.8	10.8	9.2	1.8	-18.6	-21.9	34	
D	32	-9.7	-.9	4.7	8.4	10.8	12.1	12.4	11.7	10.0	7.2	3.0	-3.2	-12.8	-31.8	-10.3	3.4	9.9	11.9	9.7	2.6	-14.6	32	D
E	30	-10.7	-1.8	4.0	7.9	10.6	12.3	13.1	13.0	12.1	10.3	7.5	3.4	-2.4	-25.4	-27.1	-4.6	6.2	11.4	12.8	10.7	4.4	30	E
G	28	-11.8	-2.8	3.2	7.3	10.3	12.3	13.5	13.9	13.6	12.6	10.9	8.2	4.4	-8.3	-30.8	-19.1	-1.1	7.9	12.4	13.7	12.0	28	G
R	26	-13.0	-3.8	2.3	5.6	9.8	12.1	13.6	14.5	14.7	14.3	13.3	11.6	9.2	1.3	-13.9	-30.2	-14.7	.7	8.9	13.1	14.5	26	R
E	24	-14.2	-5.0	1.3	5.8	9.2	11.7	13.5	14.7	15.4	15.5	15.1	14.2	12.7	7.6	-1.4	-18.4	-29.5	-12.9	1.3	9.1	13.4	24	E
E	22	-15.5	-6.2	.2	4.9	8.4	11.1	13.2	14.7	15.7	16.2	16.3	16.0	15.2	12.1	6.4	-3.1	-20.8	-28.8	-13.2	.8	8.7	22	E
S	20	-16.9	-7.5	-1.0	3.8	7.5	10.4	12.7	14.4	15.7	16.6	17.1	17.2	16.9	15.2	11.7	6.0	-3.4	-20.6	-28.0	-15.7	-1.1	20	S
	18	-18.4	-8.9	-2.3	2.6	6.4	9.5	11.9	13.9	15.4	16.6	17.4	17.9	18.0	17.4	15.4	11.9	6.3	-2.5	-17.9	-27.1	-21.0	18	
	16	-19.9	-10.4	-3.8	1.3	5.2	8.4	11.0	13.1	14.9	16.3	17.3	18.1	18.6	18.8	17.9	15.9	12.5	7.4	-.5	-13.6	-26.1	16	
	14	-21.6	-12.0	-5.3	-.2	3.8	7.1	9.9	12.2	14.0	15.6	16.9	17.9	18.7	19.5	19.4	18.5	16.5	13.4	8.9	2.1	-8.8	14	
	12	-23.5	-13.8	-7.0	-1.9	2.3	5.7	8.5	10.9	12.9	14.7	16.1	17.3	18.3	19.6	20.2	20.0	19.0	17.2	14.5	10.5	4.6	12	
	10	-22.1	-15.8	-9.0	-3.7	.5	3.9	6.9	9.4	11.5	13.4	14.9	16.3	17.4	19.1	20.2	20.5	20.3	19.4	17.8	15.3	11.8	10	
	8	-20.2	-18.1	-11.2	-5.9	-1.7	1.9	4.9	7.4	9.7	11.6	13.3	14.8	16.0	18.1	19.4	20.2	20.5	20.2	19.3	17.8	15.6	8	
	6	-17.7	-17.7	-13.9	-8.6	-4.3	-.7	2.3	5.0	7.3	9.3	11.1	12.6	14.0	16.2	17.8	18.9	19.5	19.7	19.3	18.4	16.9	6	
	4	-14.2	-14.2	-14.2	-12.2	-7.9	-4.3	-1.2	1.5	3.8	5.9	7.7	9.3	10.8	13.1	15.0	16.3	17.1	17.5	17.5	17.0	16.0	4	
	2	-11.7	-11.7	-11.7	-11.7	-11.7	-10.3	-7.2	-4.4	-2.1	.0	1.9	3.5	5.0	7.5	9.4	10.8	11.8	12.3	12.5	12.2	11.5	2	
	0	-11.7	-11.7	-11.7	-11.7	-11.7	-11.7	-11.7	-11.7	-11.7	-11.7	-11.7	-11.7	-11.7	-11.7	-11.7	-11.7	-11.7	-11.7	-11.7	-11.7	-11.7	0	
		2	3	4	5	6	7	8	9	10	11	12	13	14	16	18	20	22	24	26	28	30		

FREQUENCY IN MEGAHERTZ

ANTENNA EFFICIENCY

-1.7	-1.7	-1.7	-1.7	-1.7	-1.7	-1.7	-1.7	-1.7	-1.7	-1.7	-1.7	-1.7	-1.7	-1.7	-1.7	-1.7	-1.7	-1.7	-1.7	-1.7
2	3	4	5	6	7	8	9	10	11	12	13	14	16	18	20	22	24	26	28	30

FREQUENCY IN MEGAHERTZ

Table 31. Vertical Monopole, Output Antenna Pattern

METHOD 13 IONCAP 78.03 PAGE 2

IONCAP 80.01 ANTENNA PACKAGE ANTENNA PATTERN

FREQUENCY RANGE	ANTENNA TYPE	HEIGHT	LENGTH	ANGLE	AZIMUTH	EX(1)	EX(2)	EX(3)	EX(4)	CONDUCT.	DIELECT.
1.0 TO 30.0	VER MONO	0.000	-.250	0.000	0.000	0.000	0.000	0.000	0.000	.001	4.000

		2	3	4	5	6	7	8	9	10	11	12	13	14	16	18	20	22	24	26	28	30		
	90	-36.2	-36.2	-36.2	-36.2	-36.2	-36.2	-36.2	-36.2	-36.2	-36.2	-36.2	-36.2	-36.2	-36.2	-36.2	-36.2	-36.2	-36.2	-36.2	-36.2	-36.2	90	
	88	-29.7	-30.0	-30.1	-30.2	-30.2	-30.2	-30.2	-30.2	-30.2	-30.1	-30.1	-30.1	-30.1	-30.0	-30.0	-30.0	-30.0	-30.0	-30.0	-29.9	-29.9	88	
	86	-23.6	-24.0	-24.1	-24.2	-24.2	-24.2	-24.2	-24.2	-24.1	-24.1	-24.1	-24.1	-24.1	-24.0	-24.0	-24.0	-24.0	-23.9	-23.9	-23.9	-23.9	86	
	84	-20.1	-20.4	-20.6	-20.7	-20.7	-20.7	-20.7	-20.6	-20.6	-20.6	-20.6	-20.6	-20.5	-20.5	-20.5	-20.5	-20.4	-20.4	-20.4	-20.4	-20.4	84	
	82	-17.6	-18.0	-18.1	-18.2	-18.2	-18.2	-18.2	-18.1	-18.1	-18.1	-18.1	-18.1	-18.0	-18.0	-18.0	-18.0	-17.9	-17.9	-17.9	-17.9	-17.9	82	
	80	-15.7	-16.0	-16.2	-16.2	-16.2	-16.2	-16.2	-16.2	-16.2	-16.2	-16.1	-16.1	-16.1	-16.1	-16.1	-16.0	-16.0	-16.0	-16.0	-16.0	-16.0	80	
	78	-14.1	-14.4	-14.6	-14.7	-14.7	-14.7	-14.6	-14.6	-14.6	-14.6	-14.6	-14.6	-14.5	-14.5	-14.5	-14.5	-14.4	-14.4	-14.4	-14.4	-14.4	78	
	76	-12.8	-13.1	-13.3	-13.3	-13.3	-13.3	-13.3	-13.3	-13.3	-13.3	-13.2	-13.2	-13.2	-13.2	-13.2	-13.1	-13.1	-13.1	-13.1	-13.1	-13.1	76	
	74	-11.6	-11.9	-12.1	-12.2	-12.2	-12.2	-12.2	-12.1	-12.1	-12.1	-12.1	-12.1	-12.1	-12.0	-12.0	-12.0	-12.0	-11.9	-11.9	-11.9	-11.9	74	
	72	-10.6	-10.9	-11.1	-11.2	-11.2	-11.2	-11.2	-11.1	-11.1	-11.1	-11.1	-11.1	-11.0	-11.0	-11.0	-11.0	-11.0	-10.9	-10.9	-10.9	-10.9	72	
E	70	-9.7	-10.0	-10.2	-10.3	-10.3	-10.3	-10.3	-10.2	-10.2	-10.2	-10.2	-10.2	-10.1	-10.1	-10.1	-10.1	-10.1	-10.0	-10.0	-10.0	-10.0	70	E
L	68	-8.9	-9.2	-9.4	-9.4	-9.5	-9.5	-9.4	-9.4	-9.4	-9.4	-9.4	-9.4	-9.3	-9.3	-9.3	-9.3	-9.2	-9.2	-9.2	-9.2	-9.2	68	L
E	66	-8.1	-8.5	-8.6	-8.7	-8.7	-8.7	-8.7	-8.7	-8.7	-8.7	-8.6	-8.6	-8.6	-8.6	-8.6	-8.5	-8.5	-8.5	-8.5	-8.5	-8.5	66	E
V	64	-7.4	-7.8	-8.0	-8.0	-8.0	-8.0	-8.0	-8.0	-8.0	-8.0	-8.0	-7.9	-7.9	-7.9	-7.9	-7.9	-7.8	-7.8	-7.8	-7.8	-7.8	64	V
A	62	-6.8	-7.2	-7.3	-7.4	-7.4	-7.4	-7.4	-7.4	-7.4	-7.4	-7.4	-7.3	-7.3	-7.3	-7.3	-7.3	-7.2	-7.2	-7.2	-7.2	-7.2	62	A
T	60	-6.2	-6.6	-6.8	-6.8	-6.9	-6.9	-6.9	-6.8	-6.8	-6.8	-6.8	-6.8	-6.8	-6.7	-6.7	-6.7	-6.7	-6.7	-6.6	-6.6	-6.6	60	T
I	58	-5.7	-6.1	-6.3	-6.3	-6.3	-6.3	-6.3	-6.3	-6.3	-6.3	-6.3	-6.3	-6.2	-6.2	-6.2	-6.2	-6.2	-6.1	-6.1	-6.1	-6.1	58	I
O	56	-5.2	-5.6	-5.8	-5.8	-5.9	-5.9	-5.9	-5.8	-5.8	-5.8	-5.8	-5.8	-5.8	-5.7	-5.7	-5.7	-5.7	-5.7	-5.7	-5.6	-5.6	56	O
N	54	-4.8	-5.2	-5.3	-5.4	-5.4	-5.4	-5.4	-5.4	-5.4	-5.4	-5.4	-5.3	-5.3	-5.3	-5.3	-5.3	-5.2	-5.2	-5.2	-5.2	-5.2	54	N
	52	-4.4	-4.7	-4.9	-5.0	-5.0	-5.0	-5.0	-5.0	-5.0	-5.0	-5.0	-4.9	-4.9	-4.9	-4.9	-4.9	-4.8	-4.8	-4.8	-4.8	-4.8	52	
A	50	-4.0	-4.4	-4.5	-4.6	-4.6	-4.6	-4.6	-4.6	-4.6	-4.6	-4.6	-4.6	-4.5	-4.5	-4.5	-4.5	-4.5	-4.5	-4.5	-4.4	-4.4	50	A
N	48	-3.6	-4.0	-4.2	-4.3	-4.3	-4.3	-4.3	-4.3	-4.3	-4.3	-4.2	-4.2	-4.2	-4.2	-4.2	-4.2	-4.1	-4.1	-4.1	-4.1	-4.1	48	N
G	46	-3.3	-3.7	-3.9	-4.0	-4.0	-4.0	-4.0	-4.0	-4.0	-4.0	-3.9	-3.9	-3.9	-3.9	-3.9	-3.9	-3.8	-3.8	-3.8	-3.8	-3.8	46	G
L	44	-3.0	-3.4	-3.6	-3.7	-3.7	-3.7	-3.7	-3.7	-3.7	-3.7	-3.7	-3.7	-3.6	-3.6	-3.6	-3.6	-3.6	-3.6	-3.6	-3.5	-3.5	44	L
E	42	-2.7	-3.2	-3.4	-3.4	-3.5	-3.5	-3.5	-3.5	-3.5	-3.4	-3.4	-3.4	-3.4	-3.4	-3.4	-3.3	-3.3	-3.3	-3.3	-3.3	-3.3	42	E
	40	-2.5	-2.9	-3.1	-3.2	-3.3	-3.3	-3.3	-3.3	-3.2	-3.2	-3.2	-3.2	-3.2	-3.2	-3.2	-3.1	-3.1	-3.1	-3.1	-3.1	-3.1	40	
I	38	-2.3	-2.8	-3.0	-3.0	-3.1	-3.1	-3.1	-3.1	-3.1	-3.1	-3.0	-3.0	-3.0	-3.0	-3.0	-3.0	-3.0	-2.9	-2.9	-2.9	-2.9	38	I
N	36	-2.1	-2.6	-2.8	-2.9	-2.9	-2.9	-2.9	-2.9	-2.9	-2.9	-2.9	-2.9	-2.9	-2.9	-2.8	-2.8	-2.8	-2.8	-2.8	-2.8	-2.8	36	N
	34	-2.0	-2.5	-2.7	-2.8	-2.8	-2.8	-2.8	-2.8	-2.8	-2.8	-2.8	-2.8	-2.8	-2.7	-2.7	-2.7	-2.7	-2.7	-2.7	-2.7	-2.7	34	
D	32	-1.9	-2.4	-2.6	-2.7	-2.7	-2.8	-2.8	-2.8	-2.7	-2.7	-2.7	-2.7	-2.7	-2.7	-2.7	-2.6	-2.6	-2.6	-2.6	-2.6	-2.6	32	D
E	30	-1.8	-2.3	-2.6	-2.7	-2.7	-2.7	-2.7	-2.7	-2.7	-2.7	-2.7	-2.7	-2.7	-2.6	-2.6	-2.6	-2.6	-2.6	-2.6	-2.6	-2.6	30	E
G	28	-1.8	-2.3	-2.6	-2.7	-2.7	-2.7	-2.7	-2.7	-2.7	-2.7	-2.7	-2.7	-2.7	-2.7	-2.6	-2.6	-2.6	-2.6	-2.6	-2.6	-2.6	28	G
R	26	-1.8	-2.4	-2.6	-2.7	-2.8	-2.8	-2.8	-2.8	-2.8	-2.8	-2.8	-2.8	-2.7	-2.7	-2.7	-2.7	-2.7	-2.7	-2.7	-2.7	-2.7	26	R
E	24	-1.9	-2.5	-2.7	-2.9	-2.9	-2.9	-2.9	-2.9	-2.9	-2.9	-2.9	-2.9	-2.9	-2.8	-2.8	-2.8	-2.8	-2.8	-2.8	-2.8	-2.8	24	E
E	22	-2.0	-2.6	-2.9	-3.0	-3.1	-3.1	-3.1	-3.1	-3.1	-3.1	-3.1	-3.1	-3.0	-3.0	-3.0	-3.0	-3.0	-3.0	-3.0	-3.0	-3.0	22	E
S	20	-2.2	-2.9	-3.1	-3.3	-3.3	-3.3	-3.4	-3.3	-3.3	-3.3	-3.3	-3.3	-3.3	-3.3	-3.3	-3.3	-3.2	-3.2	-3.2	-3.2	-3.2	20	S
	18	-2.5	-3.2	-3.5	-3.6	-3.7	-3.7	-3.7	-3.7	-3.7	-3.7	-3.7	-3.7	-3.6	-3.6	-3.6	-3.6	-3.6	-3.6	-3.6	-3.6	-3.6	18	
	16	-2.9	-3.6	-3.9	-4.0	-4.1	-4.1	-4.1	-4.1	-4.1	-4.1	-4.1	-4.1	-4.1	-4.1	-4.1	-4.0	-4.0	-4.0	-4.0	-4.0	-4.0	16	
	14	-3.4	-4.1	-4.5	-4.6	-4.7	-4.7	-4.7	-4.7	-4.7	-4.7	-4.7	-4.7	-4.7	-4.7	-4.6	-4.6	-4.6	-4.6	-4.6	-4.6	-4.6	14	
	12	-4.1	-4.8	-5.2	-5.3	-5.4	-5.5	-5.5	-5.5	-5.5	-5.5	-5.4	-5.4	-5.4	-5.4	-5.4	-5.4	-5.4	-5.4	-5.4	-5.4	-5.3	12	
	10	-5.0	-5.8	-6.1	-6.3	-6.4	-6.4	-6.4	-6.5	-6.4	-6.4	-6.4	-6.4	-6.4	-6.4	-6.4	-6.4	-6.4	-6.4	-6.3	-6.3	-6.3	10	
	8	-6.2	-7.1	-7.5	-7.6	-7.7	-7.8	-7.8	-7.8	-7.8	-7.8	-7.8	-7.8	-7.7	-7.7	-7.7	-7.7	-7.7	-7.7	-7.7	-7.7	-7.7	8	
	6	-8.0	-8.9	-9.3	-9.5	-9.6	-9.6	-9.7	-9.7	-9.7	-9.7	-9.6	-9.6	-9.6	-9.6	-9.6	-9.6	-9.6	-9.6	-9.6	-9.6	-9.6	6	
	4	-10.7	-11.7	-12.2	-12.4	-12.5	-12.5	-12.5	-12.5	-12.5	-12.5	-12.5	-12.5	-12.5	-12.5	-12.5	-12.5	-12.5	-12.5	-12.5	-12.4	-12.4	4	
	2	-10.6	-10.6	-10.6	-10.6	-10.6	-10.6	-10.6	-10.6	-10.6	-10.6	-10.6	-10.6	-10.6	-10.6	-10.6	-10.6	-10.6	-10.6	-10.6	-10.6	-10.6	2	
	0	-10.6	-10.6	-10.6	-10.6	-10.6	-10.6	-10.6	-10.6	-10.6	-10.6	-10.6	-10.6	-10.6	-10.6	-10.6	-10.6	-10.6	-10.6	-10.6	-10.6	-10.6	0	
		2	3	4	5	6	7	8	9	10	11	12	13	14	16	18	20	22	24	26	28	30		

FREQUENCY IN MEGAHERTZ

ANTENNA EFFICIENCY

-.6	-.6	-.6	-.6	-.6	-.6	-.6	-.6	-.6	-.6	-.6	-.6	-.6	-.6	-.6	-.6	-.6	-.6	-.6	-.6	-.6
2	3	4	5	6	7	8	9	10	11	12	13	14	16	18	20	22	24	26	28	30

FREQUENCY IN MEGAHERTZ

Table 32. Horizontal Dipole, Output Antenna Pattern

METHOD 13 IONCAP 78.03 PAGE 3

IONCAP 80.01 ANTENNA PACKAGE

FREQUENCY RANGE	ANTENNA TYPE	HEIGHT	LENGTH	ANTENNA PATTERN ANGLE	AZIMUTH	EX(1)	EX(2)	EX(3)	EX(4)	CONDUCT.	DIELECT.
1.0 TO 30.0	HOR DPOL	-.250	-.500	0.000	0.000	0.000	0.000	0.000	0.000	.001	4.000

ELEVATION ANGLE IN DEGREES	2	3	4	5	6	7	8	9	10	11	12	13	14	16	18	20	22	24	26	28	30	
90	6.0	5.6	5.4	5.2	5.1	5.0	4.9	4.9	4.8	4.8	4.8	4.8	4.7	4.7	4.7	4.7	4.7	4.7	4.7	4.7	4.7	90
88	6.0	5.6	5.4	5.2	5.1	5.0	4.9	4.9	4.8	4.8	4.8	4.8	4.7	4.7	4.7	4.7	4.7	4.7	4.7	4.7	4.7	88
86	6.0	5.6	5.4	5.2	5.1	5.0	4.9	4.9	4.8	4.8	4.8	4.8	4.8	4.7	4.7	4.7	4.7	4.7	4.7	4.7	4.7	86
84	6.1	5.7	5.4	5.2	5.1	5.0	4.9	4.9	4.8	4.8	4.8	4.8	4.8	4.7	4.7	4.7	4.7	4.7	4.7	4.7	4.7	84
82	6.1	5.7	5.4	5.2	5.1	5.0	4.9	4.9	4.9	4.8	4.8	4.8	4.8	4.8	4.7	4.7	4.7	4.7	4.7	4.7	4.7	82
80	6.1	5.7	5.4	5.2	5.1	5.0	5.0	4.9	4.9	4.8	4.8	4.8	4.8	4.8	4.8	4.7	4.7	4.7	4.7	4.7	4.7	80
78	6.1	5.7	5.5	5.3	5.1	5.1	5.0	4.9	4.9	4.9	4.8	4.8	4.8	4.8	4.8	4.8	4.7	4.7	4.7	4.7	4.7	78
76	6.2	5.8	5.5	5.3	5.2	5.1	5.0	5.0	4.9	4.9	4.9	4.8	4.8	4.8	4.8	4.8	4.8	4.8	4.8	4.7	4.7	76
74	6.2	5.8	5.5	5.3	5.2	5.1	5.0	5.0	5.0	4.9	4.9	4.9	4.9	4.8	4.8	4.8	4.8	4.8	4.8	4.8	4.8	74
72	6.2	5.8	5.6	5.4	5.2	5.1	5.1	5.0	5.0	4.9	4.9	4.9	4.9	4.9	4.8	4.8	4.8	4.8	4.8	4.8	4.8	72
E 70	6.3	5.9	5.6	5.4	5.3	5.2	5.1	5.1	5.0	5.0	5.0	4.9	4.9	4.9	4.9	4.8	4.8	4.8	4.8	4.8	4.8	70 E
L 68	6.3	5.9	5.6	5.4	5.3	5.2	5.1	5.1	5.0	5.0	5.0	5.0	4.9	4.9	4.9	4.9	4.9	4.8	4.8	4.8	4.8	68 L
E 66	6.3	5.9	5.7	5.5	5.4	5.3	5.2	5.1	5.1	5.0	5.0	5.0	5.0	4.9	4.9	4.9	4.9	4.9	4.9	4.9	4.8	66 E
V 64	6.3	6.0	5.7	5.5	5.4	5.3	5.2	5.2	5.1	5.1	5.0	5.0	5.0	5.0	4.9	4.9	4.9	4.9	4.9	4.9	4.9	64 V
A 62	6.4	6.0	5.7	5.6	5.4	5.3	5.2	5.2	5.1	5.1	5.1	5.0	5.0	5.0	5.0	4.9	4.9	4.9	4.9	4.9	4.9	62 A
T 60	6.4	6.0	5.8	5.6	5.5	5.3	5.3	5.2	5.2	5.1	5.1	5.1	5.0	5.0	5.0	4.9	4.9	4.9	4.9	4.9	4.9	60 T
I 58	6.4	6.1	5.8	5.6	5.5	5.4	5.3	5.2	5.2	5.1	5.1	5.1	5.0	5.0	5.0	5.0	4.9	4.9	4.9	4.9	4.9	58 I
O 56	6.4	6.1	5.8	5.6	5.5	5.4	5.3	5.2	5.2	5.1	5.1	5.1	5.1	5.0	5.0	5.0	4.9	4.9	4.9	4.9	4.9	56 O
N 54	6.4	6.1	5.8	5.6	5.5	5.4	5.3	5.2	5.2	5.2	5.1	5.1	5.1	5.0	5.0	5.0	4.9	4.9	4.9	4.9	4.9	54 N
52	6.4	6.1	5.8	5.6	5.5	5.4	5.3	5.2	5.2	5.1	5.1	5.1	5.1	5.0	5.0	5.0	4.9	4.9	4.9	4.9	4.9	52
A 50	6.4	6.1	5.8	5.6	5.5	5.4	5.3	5.2	5.2	5.1	5.1	5.1	5.0	5.0	5.0	4.9	4.9	4.9	4.9	4.9	4.9	50 A
N 48	6.3	6.0	5.8	5.6	5.5	5.4	5.3	5.2	5.2	5.1	5.1	5.0	5.0	5.0	4.9	4.9	4.9	4.9	4.8	4.8	4.8	48 N
G 46	6.3	6.0	5.8	5.6	5.4	5.3	5.2	5.2	5.1	5.1	5.0	5.0	5.0	4.9	4.9	4.8	4.8	4.8	4.8	4.8	4.8	46 G
L 44	6.2	5.9	5.7	5.5	5.4	5.3	5.2	5.1	5.1	5.0	5.0	4.9	4.9	4.9	4.8	4.8	4.8	4.7	4.7	4.7	4.7	44 L
E 42	6.1	5.8	5.6	5.4	5.3	5.2	5.1	5.0	5.0	4.9	4.9	4.9	4.8	4.8	4.7	4.7	4.7	4.7	4.6	4.6	4.6	42 E
40	6.0	5.7	5.5	5.4	5.2	5.1	5.0	4.9	4.9	4.8	4.8	4.8	4.7	4.7	4.6	4.6	4.6	4.6	4.5	4.5	4.5	40
I 38	5.8	5.6	5.4	5.2	5.1	5.0	4.9	4.8	4.8	4.7	4.7	4.6	4.6	4.6	4.5	4.5	4.5	4.4	4.4	4.4	4.4	38 I
N 36	5.6	5.4	5.2	5.1	4.9	4.8	4.8	4.7	4.6	4.6	4.5	4.5	4.5	4.4	4.4	4.3	4.3	4.3	4.3	4.2	4.2	36 N
34	5.4	5.2	5.0	4.9	4.8	4.7	4.6	4.5	4.4	4.4	4.4	4.3	4.3	4.2	4.2	4.1	4.1	4.1	4.1	4.1	4.0	34
D 32	5.2	5.0	4.8	4.7	4.6	4.5	4.4	4.3	4.2	4.2	4.1	4.1	4.1	4.0	4.0	3.9	3.9	3.9	3.9	3.8	3.8	32 D
E 30	4.9	4.7	4.6	4.4	4.3	4.2	4.1	4.0	4.0	3.9	3.9	3.8	3.8	3.8	3.7	3.7	3.7	3.6	3.6	3.6	3.6	30 E
G 28	4.5	4.4	4.2	4.1	4.0	3.9	3.8	3.7	3.7	3.6	3.6	3.6	3.5	3.5	3.4	3.4	3.4	3.3	3.3	3.3	3.3	28 G
R 26	4.2	4.0	3.9	3.8	3.6	3.6	3.5	3.4	3.3	3.3	3.2	3.2	3.2	3.1	3.1	3.0	3.0	3.0	3.0	2.9	2.9	26 R
E 24	3.7	3.6	3.5	3.3	3.2	3.1	3.1	3.0	2.9	2.9	2.8	2.8	2.8	2.7	2.7	2.6	2.6	2.6	2.6	2.5	2.5	24 E
E 22	3.2	3.1	3.0	2.8	2.8	2.7	2.6	2.5	2.5	2.4	2.4	2.3	2.3	2.2	2.2	2.2	2.1	2.1	2.1	2.1	2.0	22 E
S 20	2.6	2.5	2.4	2.3	2.2	2.1	2.0	2.0	1.9	1.9	1.8	1.8	1.8	1.7	1.7	1.6	1.6	1.6	1.5	1.5	1.5	20 S
18	1.8	1.8	1.7	1.6	1.5	1.4	1.4	1.3	1.3	1.2	1.2	1.1	1.1	1.1	1.0	1.0	.9	.9	.9	.9	.9	18
16	1.0	1.0	.9	.8	.7	.7	.6	.6	.5	.5	.4	.4	.3	.3	.2	.2	.2	.1	.1	.1	.1	16
14	.0	.0	-.0	-.1	-.2	-.2	-.3	-.4	-.4	-.5	-.5	-.5	-.6	-.6	-.7	-.7	-.7	-.8	-.8	-.8	-.8	14
12	-1.1	-1.1	-1.2	-1.2	-1.3	-1.4	-1.4	-1.5	-1.5	-1.6	-1.6	-1.6	-1.7	-1.7	-1.8	-1.8	-1.8	-1.9	-1.9	-1.9	-1.9	12
10	-2.6	-2.5	-2.6	-2.6	-2.7	-2.7	-2.8	-2.8	-2.9	-2.9	-3.0	-3.0	-3.0	-3.1	-3.1	-3.2	-3.2	-3.2	-3.2	-3.2	-3.3	10
8	-4.4	-4.3	-4.3	-4.4	-4.4	-4.5	-4.5	-4.6	-4.6	-4.6	-4.7	-4.7	-4.7	-4.8	-4.8	-4.9	-4.9	-4.9	-4.9	-5.0	-5.0	8
6	-6.7	-6.7	-6.7	-6.7	-6.7	-6.8	-6.8	-6.9	-6.9	-6.9	-7.0	-7.0	-7.0	-7.1	-7.1	-7.2	-7.2	-7.2	-7.2	-7.3	-7.3	6
4	-10.1	-10.1	-10.0	-10.1	-10.1	-10.1	-10.2	-10.2	-10.2	-10.3	-10.3	-10.3	-10.4	-10.4	-10.4	-10.5	-10.5	-10.5	-10.6	-10.6	-10.6	4
2	-10.0	-10.0	-10.0	-10.0	-10.0	-10.0	-10.0	-10.0	-10.0	-10.0	-10.0	-10.0	-10.0	-10.0	-10.0	-10.0	-10.0	-10.0	-10.0	-10.0	-10.0	2
0	-10.0	-10.0	-10.0	-10.0	-10.0	-10.0	-10.0	-10.0	-10.0	-10.0	-10.0	-10.0	-10.0	-10.0	-10.0	-10.0	-10.0	-10.0	-10.0	-10.0	-10.0	0
	2	3	4	5	6	7	8	9	10	11	12	13	14	16	18	20	22	24	26	28	30	

FREQUENCY IN MEGAHERTZ

ANTENNA EFFICIENCY

2	3	4	5	6	7	8	9	10	11	12	13	14	16	18	20	22	24	26	28	30
0.0	0.0	0.0	0.0	0.0	0.0	0.0	0.0	0.0	0.0	0.0	0.0	0.0	0.0	0.0	0.0	0.0	0.0	0.0	0.0	0.0

FREQUENCY IN MEGAHERTZ

Table 33. Horizontal Yagi, Output Antenna Pattern

METHOD 13 IONCAP 78.03 PAGE 4

IONCAP 80.01 ANTENNA PACKAGE — ANTENNA PATTERN

FREQUENCY RANGE	ANTENNA TYPE	HEIGHT	LENGTH	ANGLE	AZIMUTH	EX(1)	EX(2)	EX(3)	EX(4)	CONDUCT.	DIELECT.
1.0 TO 30.0	HOR YAGI	-.250	15.000	15.600	0.000	14.000	3.000	6.000	7.500	.001	4.000

	2	3	4	5	6	7	8	9	10	11	12	13	14	16	18	20	22	24	26	28	30	
90	6.1	8.4	10.0	11.2	11.3	10.4	8.3	2.6	-.1	.3	5.0	7.2	8.3	9.1	8.5	7.5	7.1	7.9	8.4	7.7	5.0	90
88	6.1	8.4	10.0	11.2	11.2	10.4	8.2	2.6	.4	.6	5.0	7.2	8.2	8.9	8.4	7.5	7.5	8.2	8.4	7.3	4.7	88
86	6.1	8.4	10.0	11.1	11.1	10.3	8.1	2.5	.9	.9	5.0	7.1	8.1	8.7	8.2	7.6	7.9	8.5	8.3	6.9	4.3	86
84	6.1	8.4	10.0	11.1	11.1	10.2	8.0	2.5	1.4	1.2	5.1	7.1	8.0	8.4	8.0	7.7	8.2	8.8	8.2	6.5	4.0	84
82	6.1	8.4	10.0	11.1	11.0	10.1	7.9	2.5	1.9	1.6	5.1	7.1	7.8	8.2	7.8	7.8	8.6	9.1	8.2	6.1	3.6	82
80	6.1	8.4	10.0	11.0	11.0	10.0	7.8	2.5	2.3	1.9	5.2	7.0	7.7	8.0	7.6	8.0	8.9	9.3	8.2	5.8	3.3	80
78	6.1	8.4	10.0	11.0	10.9	10.0	7.7	2.6	2.8	2.3	5.2	7.0	7.6	7.7	7.5	8.1	9.3	9.6	8.2	5.5	3.0	78
76	6.1	8.4	10.0	11.0	10.9	9.9	7.6	2.7	3.2	2.6	5.3	7.0	7.5	7.5	7.3	8.3	9.6	9.9	8.3	5.2	2.7	76
74	6.2	8.4	10.0	11.0	10.8	9.8	7.4	2.8	3.7	3.0	5.4	6.9	7.3	7.2	7.2	8.5	9.9	10.1	8.3	4.9	2.5	74
72	6.2	8.4	10.0	10.9	10.8	9.7	7.3	2.9	4.1	3.4	5.5	6.9	7.2	6.9	7.1	8.6	10.2	10.3	8.4	4.7	2.3	72
E 70	6.2	8.5	10.0	10.9	10.7	9.6	7.2	3.1	4.5	3.8	5.6	6.9	7.1	6.7	7.0	8.8	10.4	10.5	8.4	4.6	2.2	70 E
L 68	6.2	8.5	10.0	10.9	10.6	9.5	7.0	3.3	4.9	4.1	5.7	6.9	7.0	6.4	6.9	9.0	10.6	10.7	8.5	4.5	2.0	68 L
E 66	6.3	8.5	10.0	10.8	10.5	9.3	6.9	3.5	5.3	4.5	5.8	6.8	6.8	6.1	6.8	9.2	10.8	10.8	8.5	4.5	2.0	66 E
V 64	6.3	8.5	10.0	10.8	10.5	9.2	6.7	3.7	5.6	4.8	6.0	6.8	6.7	5.8	6.8	9.3	11.0	10.9	8.6	4.6	1.9	64 V
A 62	6.3	8.5	10.0	10.8	10.4	9.1	6.6	4.0	6.0	5.2	6.1	6.8	6.6	5.5	6.7	9.5	11.1	11.0	8.6	4.7	2.0	62 A
T 60	6.3	8.5	9.9	10.7	10.3	9.0	6.5	4.3	6.3	5.5	6.2	6.8	6.4	5.2	6.7	9.6	11.2	11.0	8.7	4.8	2.0	60 T
I 58	6.3	8.5	9.9	10.7	10.2	8.8	6.3	4.5	6.6	5.8	6.3	6.8	6.3	5.0	6.7	9.7	11.3	11.1	8.7	5.0	2.1	58 I
O 56	6.3	8.5	9.9	10.6	10.1	8.7	6.2	4.8	6.9	6.0	6.4	6.8	6.2	4.7	6.7	9.8	11.4	11.1	8.8	5.2	2.3	56 O
N 54	6.3	8.5	9.9	10.5	10.0	8.5	6.1	5.0	7.2	6.3	6.5	6.8	6.0	4.4	6.7	9.9	11.4	11.1	8.8	5.5	2.4	54 N
52	6.3	8.5	9.8	10.5	9.9	8.4	5.9	5.3	7.4	6.5	6.6	6.7	5.9	4.1	6.6	10.0	11.4	11.0	8.8	5.7	2.6	52
A 50	6.2	8.4	9.7	10.4	9.7	8.2	5.8	5.5	7.6	6.8	6.7	6.7	5.8	3.8	6.6	10.0	11.4	10.9	8.8	6.0	2.8	50 A
N 48	6.2	8.4	9.7	10.2	9.6	8.0	5.7	5.7	7.8	7.0	6.8	6.6	5.6	3.6	6.6	10.0	11.3	10.9	8.9	6.2	3.0	48 N
G 46	6.1	8.3	9.6	10.1	9.4	7.8	5.5	5.9	8.0	7.1	6.9	6.5	5.5	3.3	6.6	10.0	11.3	10.7	8.9	6.5	3.1	46 G
L 44	6.0	8.2	9.5	10.0	9.2	7.6	5.4	6.1	8.1	7.3	6.9	6.5	5.3	3.0	6.6	9.9	11.1	10.6	8.9	6.7	3.3	44 L
E 42	5.9	8.1	9.4	9.8	9.0	7.4	5.2	6.3	8.2	7.4	6.9	6.4	5.1	2.8	6.5	9.8	11.0	10.4	8.8	6.9	3.5	42 E
40	5.8	7.9	9.2	9.6	8.8	7.2	5.1	6.4	8.3	7.4	6.9	6.3	4.9	2.5	6.4	9.7	10.8	10.2	8.8	7.0	3.6	40
I 38	5.6	7.8	9.0	9.4	8.6	6.9	4.9	6.5	8.4	7.5	6.9	6.2	4.7	2.2	6.3	9.6	10.6	10.0	8.8	7.2	3.7	38 I
N 36	5.4	7.6	8.8	9.2	8.3	6.7	4.8	6.5	8.4	7.5	6.8	6.1	4.5	2.0	6.2	9.4	10.4	9.8	8.7	7.2	3.7	36 N
34	5.2	7.4	8.6	9.0	8.0	6.4	4.6	6.5	8.3	7.4	6.7	5.9	4.3	1.7	6.0	9.2	10.1	9.5	8.6	7.3	3.7	34
D 32	5.0	7.1	8.3	8.7	7.7	6.0	4.4	6.5	8.2	7.3	6.5	5.7	4.0	1.4	5.8	9.0	9.8	9.2	8.5	7.3	3.7	32 D
E 30	4.7	6.8	8.0	8.3	7.3	5.7	4.1	6.4	8.1	7.2	6.3	5.4	3.7	1.0	5.6	8.7	9.5	8.9	8.3	7.2	3.6	30 E
G 28	4.3	6.5	7.7	8.0	6.9	5.3	3.8	6.3	7.9	7.0	6.1	5.1	3.3	.7	5.3	8.3	9.1	8.5	8.1	7.1	3.4	28 G
R 26	3.9	6.1	7.3	7.5	6.5	4.9	3.5	6.1	7.7	6.8	5.8	4.8	2.9	.3	5.0	8.0	8.6	8.1	7.8	6.9	3.2	26 R
E 24	3.4	5.6	6.8	7.0	6.0	4.4	3.1	5.8	7.4	6.4	5.5	4.3	2.5	-.2	4.6	7.5	8.1	7.6	7.5	6.6	2.9	24 E
E 22	2.9	5.1	6.3	6.5	5.4	3.8	2.7	5.4	7.0	6.1	5.0	3.9	2.0	-.7	4.1	7.0	7.6	7.0	7.1	6.3	2.6	22 E
S 20	2.3	4.5	5.7	5.9	4.8	3.2	2.2	5.0	6.5	5.6	4.5	3.3	1.4	-1.2	3.6	6.4	6.9	6.4	6.6	5.8	2.1	20 S
18	1.6	3.8	5.0	5.2	4.0	2.5	1.6	4.4	5.9	5.0	3.9	2.7	.7	-1.9	2.9	5.7	6.2	5.7	6.0	5.3	1.6	18
16	.7	2.9	4.1	4.3	3.2	1.6	.8	3.7	5.2	4.3	3.2	1.9	-.1	-2.7	2.2	4.9	5.3	4.9	5.3	4.6	.9	16
14	-.3	2.0	3.2	3.4	2.2	.7	-.1	2.9	4.3	3.4	2.3	1.0	-1.0	-3.6	1.3	4.0	4.4	4.0	4.4	3.8	.0	14
12	-1.4	.8	2.0	2.2	1.1	-.5	-1.1	1.9	3.3	2.4	1.2	-.1	-2.2	-4.7	.2	2.8	3.2	2.8	3.4	2.7	-1.0	12
10	-2.9	-.6	.6	.8	-.4	-1.9	-2.5	.5	1.9	1.0	-.1	-1.5	-3.5	-6.0	-1.2	1.5	1.8	1.5	2.1	1.4	-2.3	10
8	-4.7	-2.4	-1.2	-1.0	-2.1	-3.6	-4.2	-1.1	.3	-.7	-1.8	-3.2	-5.3	-7.7	-2.9	-.3	.0	-.3	.4	-.3	-4.0	8
6	-7.0	-4.7	-3.5	-3.3	-4.5	-6.0	-6.5	-3.4	-2.0	-2.9	-4.1	-5.5	-7.6	-10.0	-5.2	-2.6	-2.3	-2.6	-1.9	-2.5	-6.3	6
4	-10.4	-8.1	-6.9	-6.7	-7.9	-9.3	-9.8	-6.7	-5.3	-6.3	-7.4	-8.8	-10.9	-12.5	-8.5	-5.9	-5.6	-5.9	-5.2	-5.8	-9.6	4
2	-10.0	-10.0	-10.0	-10.0	-10.0	-10.0	-10.0	-10.0	-10.0	-10.0	-10.0	-10.0	-10.0	-10.0	-10.0	-10.0	-10.0	-10.0	-10.0	-10.0	-10.0	2
0	-10.0	-10.0	-10.0	-10.0	-10.0	-10.0	-10.0	-10.0	-10.0	-10.0	-10.0	-10.0	-10.0	-10.0	-10.0	-10.0	-10.0	-10.0	-10.0	-10.0	-10.0	0
	2	3	4	5	6	7	8	9	10	11	12	13	14	16	18	20	22	24	26	28	30	

FREQUENCY IN MEGAHERTZ

ANTENNA EFFICIENCY

2	3	4	5	6	7	8	9	10	11	12	13	14	16	18	20	22	24	26	28	30
0.0	0.0	0.0	0.0	0.0	0.0	0.0	0.0	0.0	0.0	0.0	0.0	0.0	0.0	0.0	0.0	0.0	0.0	0.0	0.0	0.0

FREQUENCY IN MEGAHERTZ

Table 34. Vertical Dipole, Output Antenna Pattern

METHOD 13 IONCAP 78.03 PAGE 5

IONCAP 80.01 ANTENNA PACKAGE ANTENNA PATTERN

FREQUENCY RANGE	ANTENNA TYPE	HEIGHT	LENGTH	ANGLE	AZIMUTH	EX(1)	EX(2)	EX(3)	EX(4)	CONDUCT.	DIELECT.
1.0 TO 30.0	VER DPOL	-.250	-.500	0.000	0.000	0.000	0.000	0.000	0.000	.001	4.000

		2	3	4	5	6	7	8	9	10	11	12	13	14	16	18	20	22	24	26	28	30		
	90	-35.6	-35.6	-35.6	-35.6	-35.6	-35.6	-35.6	-35.5	-35.6	-35.6	-35.6	-35.5	-35.6	-35.6	-35.6	-35.6	-35.6	-35.6	-35.6	-35.6	-35.6	90	
	88	-35.1	-34.2	-33.6	-33.3	-33.1	-33.0	-32.9	-32.8	-32.8	-32.8	-32.7	-32.7	-32.7	-32.7	-32.6	-32.6	-32.5	-32.6	-32.6	-32.6	-32.6	88	
	86	-29.1	-28.2	-27.6	-27.3	-27.1	-27.0	-26.9	-26.8	-26.8	-26.7	-26.7	-26.7	-26.7	-26.6	-26.6	-26.6	-26.5	-26.6	-26.6	-26.6	-26.6	86	
	84	-25.7	-24.7	-24.1	-23.8	-23.6	-23.5	-23.4	-23.3	-23.3	-23.2	-23.2	-23.2	-23.1	-23.1	-23.1	-23.1	-23.1	-23.0	-23.0	-23.0	-23.0	84	
	82	-23.2	-22.2	-21.7	-21.3	-21.1	-21.0	-20.9	-20.8	-20.8	-20.7	-20.7	-20.7	-20.6	-20.6	-20.6	-20.6	-20.5	-20.5	-20.5	-20.5	-20.5	82	
	80	-21.4	-20.3	-19.8	-19.4	-19.2	-19.1	-18.9	-18.9	-18.8	-18.8	-18.7	-18.7	-18.7	-18.7	-18.6	-18.6	-18.6	-18.6	-18.6	-18.6	-18.6	80	
	78	-19.9	-18.8	-18.2	-17.9	-17.6	-17.5	-17.4	-17.3	-17.2	-17.2	-17.1	-17.1	-17.1	-17.0	-17.0	-17.0	-17.0	-17.0	-17.0	-17.0	-17.0	78	
	76	-18.6	-17.5	-16.9	-16.5	-16.3	-16.1	-16.0	-15.9	-15.9	-15.8	-15.8	-15.8	-15.7	-15.7	-15.7	-15.6	-15.6	-15.6	-15.6	-15.6	-15.6	76	
	74	-17.6	-16.4	-15.8	-15.4	-15.1	-15.0	-14.9	-14.8	-14.7	-14.6	-14.6	-14.6	-14.5	-14.5	-14.5	-14.4	-14.4	-14.4	-14.4	-14.4	-14.4	74	
	72	-16.6	-15.4	-14.8	-14.4	-14.1	-13.9	-13.8	-13.7	-13.6	-13.6	-13.5	-13.5	-13.5	-13.4	-13.4	-13.4	-13.3	-13.3	-13.3	-13.3	-13.3	72	
E	70	-15.8	-14.6	-13.9	-13.5	-13.2	-13.0	-12.9	-12.8	-12.7	-12.6	-12.6	-12.5	-12.5	-12.5	-12.4	-12.4	-12.4	-12.3	-12.3	-12.3	-12.3	70	E
L	68	-15.0	-13.8	-13.1	-12.6	-12.3	-12.1	-12.0	-11.9	-11.8	-11.7	-11.7	-11.6	-11.6	-11.6	-11.5	-11.5	-11.5	-11.4	-11.4	-11.4	-11.4	68	L
E	66	-14.3	-13.0	-12.3	-11.8	-11.5	-11.3	-11.2	-11.1	-11.0	-10.9	-10.8	-10.8	-10.8	-10.7	-10.7	-10.6	-10.6	-10.6	-10.6	-10.6	-10.6	66	E
V	64	-13.6	-12.3	-11.5	-11.1	-10.8	-10.6	-10.4	-10.3	-10.2	-10.1	-10.1	-10.0	-10.0	-9.9	-9.9	-9.8	-9.8	-9.8	-9.8	-9.8	-9.7	64	V
A	62	-12.9	-11.6	-10.8	-10.4	-10.0	-9.8	-9.7	-9.5	-9.4	-9.4	-9.3	-9.2	-9.2	-9.1	-9.1	-9.1	-9.0	-9.0	-9.0	-9.0	-9.0	62	A
T	60	-12.2	-10.9	-10.1	-9.7	-9.3	-9.1	-8.9	-8.8	-8.7	-8.6	-8.6	-8.5	-8.5	-8.4	-8.3	-8.3	-8.3	-8.3	-8.2	-8.2	-8.2	60	T
I	58	-11.5	-10.2	-9.5	-9.0	-8.6	-8.4	-8.2	-8.1	-8.0	-7.9	-7.9	-7.8	-7.8	-7.7	-7.6	-7.6	-7.6	-7.5	-7.5	-7.5	-7.5	58	I
O	56	-10.8	-9.5	-8.8	-8.3	-8.0	-7.7	-7.5	-7.4	-7.3	-7.2	-7.2	-7.1	-7.1	-7.0	-6.9	-6.9	-6.9	-6.8	-6.8	-6.8	-6.8	56	O
N	54	-10.0	-8.8	-8.1	-7.6	-7.3	-7.1	-6.9	-6.7	-6.6	-6.6	-6.5	-6.4	-6.4	-6.3	-6.2	-6.2	-6.2	-6.1	-6.1	-6.1	-6.1	54	N
	52	-9.2	-8.1	-7.4	-7.0	-6.6	-6.4	-6.2	-6.1	-6.0	-5.9	-5.8	-5.8	-5.7	-5.6	-5.6	-5.5	-5.5	-5.5	-5.5	-5.4	-5.4	52	
A	50	-8.4	-7.4	-6.8	-6.3	-6.0	-5.7	-5.6	-5.4	-5.3	-5.2	-5.2	-5.1	-5.1	-5.0	-4.9	-4.9	-4.9	-4.8	-4.8	-4.8	-4.8	50	A
N	48	-7.6	-6.7	-6.1	-5.6	-5.3	-5.1	-4.9	-4.8	-4.7	-4.6	-4.6	-4.5	-4.4	-4.4	-4.3	-4.3	-4.2	-4.2	-4.2	-4.2	-4.1	48	N
G	46	-6.9	-6.0	-5.4	-5.0	-4.7	-4.5	-4.3	-4.2	-4.1	-4.0	-3.9	-3.9	-3.8	-3.8	-3.7	-3.7	-3.6	-3.6	-3.6	-3.6	-3.5	46	G
L	44	-6.1	-5.4	-4.8	-4.4	-4.1	-3.9	-3.7	-3.6	-3.5	-3.4	-3.4	-3.3	-3.3	-3.2	-3.1	-3.1	-3.0	-3.0	-3.0	-3.0	-3.0	44	L
E	42	-5.4	-4.7	-4.2	-3.8	-3.5	-3.3	-3.2	-3.1	-3.0	-2.9	-2.8	-2.7	-2.7	-2.6	-2.6	-2.5	-2.5	-2.5	-2.4	-2.4	-2.4	42	E
	40	-4.7	-4.1	-3.6	-3.3	-3.0	-2.8	-2.6	-2.5	-2.4	-2.3	-2.3	-2.2	-2.2	-2.1	-2.0	-2.0	-2.0	-1.9	-1.9	-1.9	-1.9	40	
I	38	-4.0	-3.5	-3.1	-2.7	-2.5	-2.3	-2.1	-2.0	-1.9	-1.9	-1.8	-1.7	-1.7	-1.6	-1.6	-1.5	-1.5	-1.5	-1.4	-1.4	-1.4	38	I
N	36	-3.4	-3.0	-2.6	-2.2	-2.0	-1.8	-1.7	-1.6	-1.5	-1.4	-1.3	-1.3	-1.2	-1.2	-1.1	-1.1	-1.0	-1.0	-1.0	-1.0	-.9	36	N
	34	-2.8	-2.4	-2.1	-1.8	-1.6	-1.4	-1.2	-1.1	-1.1	-1.0	-.9	-.9	-.8	-.8	-.7	-.7	-.6	-.6	-.6	-.6	-.5	34	
D	32	-2.3	-2.0	-1.7	-1.4	-1.2	-1.0	-.9	-.8	-.7	-.6	-.6	-.5	-.5	-.4	-.3	-.3	-.3	-.2	-.2	-.2	-.2	32	D
E	30	-1.8	-1.6	-1.3	-1.0	-.8	-.7	-.5	-.4	-.4	-.3	-.2	-.2	-.2	-.1	-.0	.0	.0	.1	.1	.1	.1	30	E
G	28	-1.4	-1.2	-1.0	-.7	-.6	-.4	-.3	-.2	-.1	-.0	.0	.1	.1	.2	.2	.3	.3	.3	.3	.4	.4	28	G
R	26	-1.1	-1.0	-.7	-.5	-.3	-.2	-.1	.0	.1	.2	.2	.3	.3	.4	.4	.5	.5	.5	.5	.6	.6	26	R
E	24	-.8	-.8	-.6	-.4	-.2	-.1	.1	.1	.2	.3	.3	.4	.4	.5	.5	.6	.6	.6	.7	.7	.7	24	E
E	22	-.6	-.6	-.5	-.3	-.1	.0	.1	.2	.3	.3	.4	.4	.5	.5	.6	.6	.6	.7	.7	.7	.7	22	E
S	20	-.6	-.6	-.5	-.3	-.1	-.0	.1	.2	.2	.3	.3	.4	.4	.5	.5	.6	.6	.6	.7	.7	.7	20	S
	18	-.6	-.7	-.6	-.4	-.3	-.2	-.1	.0	.1	.1	.2	.2	.3	.3	.4	.4	.4	.5	.5	.5	.5	18	
	16	-.7	-.9	-.8	-.7	-.5	-.4	-.3	-.2	-.2	-.1	-.1	-.0	-.0	.1	.1	.1	.2	.2	.2	.2	.3	16	
	14	-1.0	-1.3	-1.2	-1.1	-.9	-.8	-.7	-.7	-.6	-.6	-.5	-.5	-.4	-.4	-.3	-.3	-.3	-.2	-.2	-.2	-.2	14	
	12	-1.5	-1.8	-1.8	-1.7	-1.5	-1.4	-1.4	-1.3	-1.2	-1.2	-1.1	-1.1	-1.1	-1.0	-.9	-.9	-.9	-.9	-.8	-.8	-.8	12	
	10	-2.3	-2.6	-2.6	-2.5	-2.4	-2.3	-2.2	-2.2	-2.1	-2.0	-2.0	-2.0	-1.9	-1.9	-1.8	-1.8	-1.8	-1.7	-1.7	-1.7	-1.7	10	
	8	-3.4	-3.8	-3.8	-3.7	-3.6	-3.5	-3.5	-3.4	-3.3	-3.3	-3.2	-3.2	-3.2	-3.1	-3.1	-3.0	-3.0	-3.0	-3.0	-2.9	-2.9	8	
	6	-5.1	-5.5	-5.6	-5.5	-5.4	-5.3	-5.3	-5.2	-5.1	-5.1	-5.0	-5.0	-5.0	-4.9	-4.9	-4.8	-4.8	-4.8	-4.8	-4.7	-4.7	6	
	4	-7.8	-8.3	-8.4	-8.3	-8.2	-8.2	-8.1	-8.0	-8.0	-7.9	-7.9	-7.8	-7.8	-7.8	-7.7	-7.7	-7.6	-7.6	-7.6	-7.6	-7.6	4	
	2	-10.0	-10.0	-10.0	-10.0	-10.0	-10.0	-10.0	-10.0	-10.0	-10.0	-10.0	-10.0	-10.0	-10.0	-10.0	-10.0	-10.0	-10.0	-10.0	-10.0	-10.0	2	
	0	-10.0	-10.0	-10.0	-10.0	-10.0	-10.0	-10.0	-10.0	-10.0	-10.0	-10.0	-10.0	-10.0	-10.0	-10.0	-10.0	-10.0	-10.0	-10.0	-10.0	-10.0	0	
		2	3	4	5	6	7	8	9	10	11	12	13	14	16	18	20	22	24	26	28	30		

FREQUENCY IN MEGAHERTZ

ANTENNA EFFICIENCY

0.0	0.0	0.0	0.0	0.0	0.0	0.0	0.0	0.0	0.0	0.0	0.0	0.0	0.0	0.0	0.0	0.0	0.0	0.0	0.0	0.0
2	3	4	5	6	7	8	9	10	11	12	13	14	16	18	20	22	24	26	28	30

FREQUENCY IN MEGAHERTZ

Table 35. Curtain, Output Antenna Pattern

METHOD 13 IONCAP 78.03 PAGE 6

IONCAP 80.01 ANTENNA PACKAGE — ANTENNA PATTERN

FREQUENCY RANGE	ANTENNA TYPE	HEIGHT	LENGTH	ANGLE	AZIMUTH	EX(1)	EX(2)	EX(3)	EX(4)	CONDUCT.	DIELECT.
1.0 TO 30.0	HOR CURT	7.500	15.000	1.000	0.000	4.000	15.000	7.500	15.000	.001	4.000

		2	3	4	5	6	7	8	9	10	11	12	13	14	16	18	20	22	24	26	28	30		
	90	-35.6	-35.6	-35.6	-35.6	-35.6	-35.6	-35.6	-35.6	-35.6	-35.6	-35.6	-35.6	-35.6	-35.6	-35.6	-35.6	-35.6	-35.6	-35.6	-35.6	-35.6	90	
	88	-35.6	-35.6	-29.5	-26.6	-26.4	-28.2	-29.2	-30.1	-35.6	-23.5	-16.4	-13.3	-12.7	-14.6	-12.9	-35.6	-12.0	-11.1	-6.6	-9.3	-35.6	88	
	86	-35.6	-29.6	-23.5	-20.6	-20.3	-22.1	-23.2	-24.1	-35.6	-17.7	-10.5	-7.4	-6.8	-8.7	-7.0	-35.6	-6.3	-5.5	-1.1	-3.5	-35.6	86	
	84	-35.6	-26.1	-20.0	-17.0	-16.7	-18.6	-19.7	-20.5	-35.6	-14.6	-7.2	-4.0	-3.4	-5.4	-3.7	-27.1	-3.3	-2.6	1.7	-.4	-26.1	84	
	82	-34.4	-23.6	-17.5	-14.5	-14.1	-16.0	-17.2	-17.9	-35.2	-12.7	-5.1	-1.8	-1.0	-3.2	-1.5	-19.6	-1.7	-1.0	3.1	1.3	-19.1	82	
	80	-32.5	-21.7	-15.5	-12.5	-12.1	-13.9	-15.2	-15.8	-29.4	-11.5	-3.6	-.1	.7	-1.7	.0	-14.2	-.8	-.2	3.6	2.2	-14.5	80	
	78	-30.9	-20.1	-13.9	-10.8	-10.4	-12.2	-13.7	-14.1	-24.9	-11.0	-2.6	1.0	2.0	-.5	1.0	-10.2	-.8	.0	3.2	2.3	-11.7	78	
	76	-29.7	-18.8	-12.6	-9.4	-8.9	-10.6	-12.3	-12.7	-21.1	-11.0	-2.0	1.9	3.0	.3	1.6	-7.2	-1.4	-.3	2.0	1.5	-10.5	76	
	74	-28.6	-17.7	-11.4	-8.2	-7.6	-9.2	-11.1	-11.5	-18.1	-11.6	-1.7	2.4	3.8	1.0	1.8	-5.1	-2.9	-1.1	-.1	-.5	-11.4	74	
	72	-27.6	-16.7	-10.4	-7.1	-6.4	-8.0	-10.1	-10.4	-15.5	-12.8	-1.8	2.7	4.3	1.5	1.6	-3.7	-5.3	-2.6	-3.5	-4.5	-16.6	72	
E	70	-26.8	-15.8	-9.4	-6.1	-5.3	-6.7	-9.1	-9.5	-13.3	-15.1	-2.2	2.7	4.5	1.9	1.0	-3.0	-9.3	-5.2	-9.1	-14.6	-23.4	70	E
L	68	-26.0	-15.0	-8.6	-5.2	-4.2	-5.6	-8.1	-8.7	-11.5	-19.3	-2.9	2.5	4.5	2.2	.0	-3.2	-16.0	-10.0	-22.6	-13.5	-8.9	68	L
E	66	-25.4	-14.3	-7.9	-4.4	-3.3	-4.5	-7.1	-8.1	-10.0	-30.6	-4.1	1.9	4.3	2.2	-1.5	-4.4	-31.4	-23.0	-16.0	-5.5	-3.5	66	E
V	64	-24.8	-13.7	-7.2	-3.6	-2.4	-3.4	-6.1	-7.5	-8.9	-25.1	-5.9	1.0	3.8	2.1	-3.4	-7.0	-34.7	-16.7	-8.7	-2.8	-.6	64	V
A	62	-24.3	-13.2	-6.5	-2.8	-1.5	-2.4	-5.1	-7.0	-7.9	-17.0	-8.5	-.2	2.9	1.5	-5.9	-12.6	-27.1	-10.8	-5.0	-2.2	.6	62	A
T	60	-23.8	-12.6	-6.0	-2.2	-.7	-1.4	-4.0	-6.4	-7.2	-13.0	-12.4	-1.9	1.7	.5	-9.3	-34.4	-13.5	-10.1	-2.7	-2.7	.4	60	T
I	58	-23.4	-12.2	-5.4	-1.5	.1	-.4	-2.9	-5.8	-6.8	-10.6	-19.7	-4.2	.0	-1.2	-15.2	-12.8	-6.8	-14.3	-1.7	-3.3	-1.1	58	I
O	56	-23.1	-11.8	-4.9	-1.0	.8	.5	-1.7	-5.1	-6.5	-9.0	-32.8	-7.4	-2.2	-3.9	-30.0	-7.6	-2.8	-25.0	-2.2	-3.3	-4.1	56	O
N	54	-22.8	-11.4	-4.5	-.4	1.5	1.4	-.6	-4.1	-6.3	-8.1	-17.7	-12.0	-5.2	-8.7	-10.6	-5.1	-.4	-8.2	-4.5	-3.6	-8.3	54	N
	52	-22.5	-11.1	-4.1	.1	2.2	2.3	.5	-3.1	-6.2	-7.7	-13.5	-19.8	-9.2	-21.2	-4.2	-3.0	.8	-2.9	-10.6	-5.0	-12.7	52	
A	50	-22.3	-10.8	-3.7	.6	2.8	3.1	1.5	-1.9	-5.8	-7.7	-11.7	-33.3	-15.0	-15.5	-.3	-.6	.8	-.3	-28.5	-8.6	-18.5	50	A
N	48	-22.1	-10.6	-3.4	1.0	3.3	3.8	2.5	-.6	-5.1	-8.0	-11.1	-21.7	-24.1	-8.8	2.3	2.1	.1	.4	-10.4	-16.1	-33.0	48	N
G	46	-22.0	-10.4	-3.1	1.4	3.8	4.5	3.5	.6	-4.0	-8.3	-11.4	-19.2	-32.8	-6.5	3.9	4.5	-.3	-.4	-7.5	-32.8	-17.3	46	G
L	44	-21.9	-10.2	-2.9	1.7	4.3	5.2	4.4	1.8	-2.7	-8.2	-12.5	-20.1	-32.5	-6.4	4.6	6.2	.9	-2.6	-8.6	-32.5	-16.1	44	L
E	42	-21.8	-10.1	-2.7	2.0	4.7	5.7	5.1	2.8	-1.5	-7.6	-14.1	-24.5	-25.9	-8.7	4.5	7.1	2.8	-5.5	-13.8	-16.2	-32.1	42	E
	40	-21.8	-10.0	-2.5	2.2	5.1	6.3	5.9	3.8	-.3	-6.7	-15.6	-31.8	-18.2	-15.5	3.3	7.2	4.0	-6.6	-31.8	-9.1	-12.8	40	
I	38	-21.8	-9.9	-2.4	2.4	5.4	6.7	6.5	4.6	.8	-5.7	-17.1	-26.0	-14.0	-21.4	.6	6.4	4.3	-6.9	-19.1	-6.4	-6.2	38	I
N	36	-21.9	-10.0	-2.4	2.6	5.6	7.1	7.0	5.3	1.6	-5.1	-20.0	-18.3	-11.6	-9.4	-4.7	4.5	3.3	-9.8	-10.8	-6.7	-4.3	36	N
	34	-22.0	-10.0	-2.4	2.7	5.8	7.4	7.4	5.9	2.2	-4.9	-30.6	-12.2	-9.4	-5.5	-23.4	.9	1.0	-24.5	-3.8	-6.0	-5.6	34	
D	32	-22.1	-10.1	-2.4	2.7	6.0	7.6	7.8	6.3	2.6	-5.3	-18.5	-6.6	-5.6	-4.3	-8.7	-5.8	-3.2	-12.1	.6	-1.0	-8.0	32	D
E	30	-22.4	-10.3	-2.5	2.7	6.0	7.8	8.0	6.6	2.7	-6.7	-9.5	-1.9	-1.0	-3.8	-4.1	-29.6	-10.3	-6.7	2.8	2.7	-4.0	30	E
G	28	-22.6	-10.5	-2.6	2.6	6.0	7.9	8.2	6.7	2.6	-9.7	-4.0	2.1	3.3	-.9	-3.5	-10.0	-24.6	-6.7	3.0	4.2	-.6	28	G
R	26	-23.0	-10.8	-2.9	2.5	5.9	7.8	8.2	6.7	2.3	-16.9	.0	5.4	6.9	4.0	-3.7	-7.9	-28.5	-12.4	.6	3.5	.1	26	R
E	24	-23.4	-11.1	-3.1	2.3	5.8	7.7	8.1	6.6	1.6	-21.5	3.1	8.1	9.9	8.4	.8	-9.6	-27.8	-19.3	-6.8	-.0	-1.7	24	E
E	22	-23.8	-11.5	-3.5	1.9	5.5	7.5	7.9	6.3	.6	-9.4	5.6	10.3	12.3	11.9	6.1	-7.2	-22.2	-8.5	-15.2	-9.6	-7.1	22	E
S	20	-24.4	-12.1	-4.0	1.5	5.2	7.2	7.6	5.9	-.7	-4.4	7.4	12.0	14.2	14.6	10.0	-1.9	-14.3	-8.5	-6.0	-13.5	-22.6	20	S
	18	-25.1	-12.7	-4.6	1.0	4.7	6.8	7.2	5.3	-2.3	-1.4	8.9	13.4	15.7	16.6	12.9	1.4	-3.6	-2.5	-7.6	-8.9	-18.6	18	
	16	-24.4	-13.4	-5.3	.3	4.1	6.2	6.6	4.5	-4.4	.6	9.9	14.3	16.8	18.0	14.8	3.0	3.6	6.4	1.6	-9.3	-20.8	16	
	14	-23.3	-14.4	-6.2	-.5	3.3	5.4	5.8	3.6	-7.1	1.8	10.4	14.8	17.4	18.9	16.0	3.2	8.6	12.2	9.5	1.8	-14.9	14	
	12	-22.0	-15.5	-7.2	-1.5	2.3	4.4	4.8	2.4	-10.4	2.4	10.6	14.9	17.6	19.3	16.6	2.1	12.0	15.9	14.2	7.9	-8.1	12	
	10	-20.4	-16.8	-8.6	-2.8	1.0	3.2	3.5	1.0	-14.6	2.4	10.2	14.6	17.3	19.2	16.6	-.4	14.1	18.1	17.0	11.3	-6.2	10	
	8	-18.5	-18.5	-10.3	-4.5	-.7	1.5	1.8	-.8	-18.5	1.7	9.3	13.7	16.4	18.4	15.9	-4.5	15.0	19.1	18.3	12.9	-7.5	8	
	6	-16.0	-16.0	-12.6	-6.8	-2.9	-.7	-.4	-3.2	-16.0	.2	7.7	12.0	14.7	16.9	14.3	-11.0	14.6	18.8	18.1	12.8	-12.2	6	
	4	-12.5	-12.5	-12.5	-10.1	-6.2	-4.0	-3.7	-6.6	-12.5	-2.6	4.8	9.1	11.9	14.1	11.5	-12.5	12.6	16.8	16.3	11.0	-12.5	4	
	2	-10.0	-10.0	-10.0	-10.0	-10.0	-9.9	-9.6	-10.0	-10.0	-8.1	-.8	3.5	6.3	8.5	6.0	-10.0	7.6	11.8	11.3	6.0	-10.0	2	
	0	-10.0	-10.0	-10.0	-10.0	-10.0	-10.0	-10.0	-10.0	-10.0	-10.0	-10.0	-10.0	-10.0	-10.0	-10.0	-10.0	-10.0	-10.0	-10.0	-10.0	-10.0	0	
		2	3	4	5	6	7	8	9	10	11	12	13	14	16	18	20	22	24	26	28	30		

FREQUENCY IN MEGAHERTZ

ANTENNA EFFICIENCY

0.0	0.0	0.0	0.0	0.0	0.0	0.0	0.0	0.0	0.0	0.0	0.0	0.0	0.0	0.0	0.0	0.0	0.0	0.0	0.0	0.0
2	3	4	5	6	7	8	9	10	11	12	13	14	16	18	20	22	24	26	28	30

FREQUENCY IN MEGAHERTZ

Table 36. Sloping Vee, Output Antenna Pattern

METHOD 13   IONCAP 78.03   PAGE 7

IONCAP 80.01 ANTENNA PACKAGE   ANTENNA PATTERN

FREQUENCY RANGE	ANTENNA TYPE	HEIGHT	LENGTH	ANGLE	AZIMUTH	EX(1)	EX(2)	EX(3)	EX(4)	CONDUCT.	DIELECT.
1.0 TO 30.0	SLP VEE	15.000	150.000	15.000	0.000	33.750	0.000	0.000	0.000	.001	4.000

ELEVATION ANGLE DEGREES

	2	3	4	5	6	7	8	9	10	11	12	13	14	16	18	20	22	24	26	28	30	
90	-24.5	-12.1	-16.6	-20.2	-11.6	-27.8	-14.6	-25.5	-15.0	-19.4	-14.1	-16.3	-21.9	-37.3	-19.9	-16.5	-15.1	-11.5	-13.6	-18.2	-19.6	90
88	-21.2	-12.3	-14.8	-25.4	-11.1	-24.3	-15.0	-18.4	-18.5	-13.8	-20.1	-13.4	-19.6	-14.1	-14.5	-13.1	-15.7	-20.8	-26.3	-14.9	-15.6	88
86	-18.5	-12.7	-13.5	-24.4	-11.5	-16.5	-17.2	-15.6	-26.9	-12.1	-26.6	-14.7	-12.8	-11.0	-18.1	-20.7	-28.1	-12.8	-12.4	-15.4	-18.9	86
84	-16.4	-13.4	-12.5	-18.8	-12.9	-12.8	-23.2	-15.0	-19.5	-13.4	-14.7	-21.5	-12.1	-15.0	-25.6	-15.4	-13.9	-12.2	-20.7	-16.2	-14.6	84
82	-14.6	-14.5	-11.9	-15.1	-15.8	-11.0	-34.7	-16.3	-14.3	-18.8	-11.6	-20.5	-16.5	-25.2	-14.2	-12.1	-16.3	-21.9	-12.8	-13.2	-17.6	82
80	-13.1	-16.2	-11.5	-12.7	-22.4	-10.3	-19.0	-20.5	-12.6	-22.3	-12.1	-13.4	-24.1	-11.2	-13.9	-19.7	-22.1	-10.1	-13.1	-19.7	-13.5	80
78	-11.8	-18.7	-11.4	-11.1	-32.1	-10.7	-14.0	-37.3	-13.1	-13.9	-17.3	-11.5	-13.5	-9.5	-24.1	-14.4	-12.3	-17.4	-16.9	-11.6	-15.8	78
76	-10.7	-22.9	-11.6	-10.1	-17.7	-12.6	-11.6	-21.9	-16.5	-10.7	-25.7	-13.1	-10.7	-14.8	-16.3	-11.0	-16.3	-13.0	-9.4	-30.1	-12.4	76
74	-9.7	-32.4	-12.0	-9.7	-12.7	-16.8	-10.7	-15.6	-26.7	-10.5	-13.1	-21.5	-11.9	-19.7	-11.2	-18.4	-18.0	-10.4	-27.9	-11.0	-13.8	74
72	-8.8	-27.8	-12.8	-9.6	-9.8	-28.8	-11.1	-12.8	-19.8	-13.3	-9.5	-18.9	-17.8	-9.1	-12.9	-14.5	-10.3	-27.6	-8.7	-16.2	-11.9	72
70	-8.0	-20.0	-14.1	-10.0	-8.2	-18.5	-13.2	-11.6	-13.7	-21.0	-9.3	-10.9	-19.3	-7.8	-30.1	-10.1	-15.3	-11.2	-11.1	-12.8	-11.7	70
68	-7.3	-15.6	-15.8	-10.8	-7.3	-11.8	-18.9	-11.8	-11.3	-16.7	-12.7	-8.6	-11.6	-12.7	-11.1	-15.3	-14.0	-11.1	-13.1	-9.3	-13.5	68
66	-6.7	-12.6	-18.1	-12.0	-7.2	-8.4	-28.0	-13.7	-10.9	-10.9	-21.6	-9.7	-8.8	-21.0	-7.5	-19.0	-8.4	-27.5	-7.0	-25.0	-9.4	66
64	-6.1	-10.3	-20.0	-13.6	-7.7	-6.5	-14.4	-19.1	-12.3	-8.9	-13.0	-16.2	-9.1	-8.7	-10.6	-9.9	-14.2	-10.6	-19.7	-6.6	-22.1	64
62	-5.6	-8.4	-18.8	-15.4	-9.0	-5.6	-9.1	-32.5	-16.0	-9.3	-8.2	-18.2	-13.6	-6.5	-23.3	-9.5	-11.9	-9.0	-9.2	-11.0	-8.0	62
60	-5.2	-6.8	-15.3	-16.5	-11.2	-5.5	-6.3	-14.6	-27.2	-12.2	-7.0	-8.8	-28.1	-8.5	-6.9	-16.3	-7.3	-22.6	-8.1	-9.0	-10.7	60
58	-4.8	-5.5	-12.0	-15.8	-14.7	-6.4	-4.8	-9.0	-19.9	-20.6	-8.4	-5.9	-9.9	-15.5	-4.3	-13.9	-12.6	-7.6	-19.2	-5.1	-10.5	58
56	-4.5	-4.4	-9.3	-13.7	-18.8	-8.4	-4.4	-5.9	-11.8	-21.9	-13.6	-6.1	-5.5	-15.0	-7.7	-5.5	-16.6	-6.8	-10.2	-22.0	-4.0	56
54	-4.3	-3.4	-7.1	-11.2	-16.2	-12.5	-5.0	-4.3	-7.7	-12.3	-21.8	-9.6	-4.8	-8.1	-26.7	-4.5	-7.3	-17.8	-5.8	-7.3	-20.2	54
52	-4.0	-2.6	-5.2	-8.9	-11.8	-22.1	-7.1	-3.9	-5.2	-8.3	-11.5	-18.0	-7.5	-4.8	-7.1	-11.8	-5.5	-6.3	-13.2	-5.9	-4.2	52
50	-3.9	-1.9	-3.6	-6.8	-8.6	-16.7	-11.7	-4.7	-3.9	-5.9	-7.4	-10.6	-15.5	-4.1	-3.7	-9.5	-8.9	-5.4	-6.4	-13.6	-4.9	50
48	-3.8	-1.2	-2.2	-4.9	-6.3	-9.6	-31.6	-7.4	-3.9	-4.4	-5.5	-6.0	-9.6	-6.9	-3.6	-2.0	-15.3	-11.5	-3.5	-7.4	-19.6	48
46	-3.7	-.7	-1.0	-3.2	-4.5	-5.8	-12.7	-14.4	-5.5	-4.0	-4.6	-4.3	-4.5	-17.7	-5.4	-1.3	-2.0	-14.4	-12.7	-2.4	-6.3	46
44	-3.6	-.3	.0	-1.6	-3.0	-3.4	-6.1	-17.9	-10.3	-5.0	-4.4	-4.2	-2.9	-6.6	-11.8	-4.8	.4	-2.6	-9.3	-10.0	-2.1	44
42	-3.6	.1	.9	-.2	-1.6	-1.8	-2.7	-6.8	-22.3	-8.9	-5.3	-4.8	-3.4	-1.5	-12.5	-11.7	-3.0	.8	-2.4	-5.5	-9.8	42
40	-3.7	.3	1.6	1.1	-.2	-.5	-.5	-2.1	-7.4	-22.0	-9.1	-6.2	-5.1	-.3	-2.0	-10.9	-16.1	-2.0	.4	-1.3	-2.6	40
38	-3.8	.5	2.2	2.2	1.2	.6	.9	.6	-1.6	-7.2	-23.5	-10.7	-7.7	-1.9	1.3	-2.4	-5.4	-21.9	-2.6	-.6	-.2	38
36	-3.9	.6	2.7	3.1	2.5	1.8	2.0	2.3	1.7	-.8	-6.1	-21.2	-14.6	-6.5	1.2	2.0	-.8	-1.4	-12.0	-5.3	-2.6	36
34	-4.1	.7	3.1	3.9	3.7	3.0	2.9	3.4	3.6	2.8	.4	-4.2	-13.4	-16.2	-2.6	2.9	2.6	1.7	1.7	-4.7	-13.0	34
32	-4.4	.7	3.4	4.6	4.7	4.2	3.8	4.2	4.8	4.9	4.0	1.9	-1.9	-14.7	-14.4	.1	3.9	3.5	3.8	4.3	.5	32
30	-4.7	.6	3.6	5.1	5.6	5.4	4.9	4.9	5.5	6.1	6.1	5.4	3.6	-3.3	-10.2	-9.2	1.5	4.4	4.3	5.4	6.4	30
28	-5.0	.4	3.6	5.5	6.4	6.5	6.1	5.8	6.0	6.7	7.3	7.4	6.8	3.2	-2.4	-6.0	-7.0	1.8	4.6	4.8	6.2	28
26	-5.4	.2	3.6	5.7	6.9	7.4	7.3	7.0	6.8	7.2	7.9	8.5	8.7	7.3	3.5	-.2	-2.4	-6.0	1.0	4.3	4.9	26
24	-5.9	-.2	3.5	5.8	7.3	8.1	8.3	8.2	7.9	7.8	8.2	8.9	9.5	9.7	8.0	4.6	2.2	.8	-3.6	-1.3	3.3	24
22	-6.4	-.6	3.2	5.8	7.5	8.6	9.2	9.3	9.1	8.8	8.8	9.1	9.8	10.9	10.8	9.0	6.1	4.4	3.7	.7	-4.0	22
20	-7.1	-1.1	2.8	5.6	7.6	8.9	9.8	10.2	10.3	10.1	9.9	9.8	10.0	11.2	12.1	11.9	10.4	7.9	6.3	6.0	4.6	20
18	-7.8	-1.7	2.3	5.3	7.5	9.0	10.2	10.9	11.3	11.3	11.2	11.0	10.8	11.2	12.3	13.2	13.1	12.0	9.9	8.0	7.6	18
16	-8.7	-2.5	1.7	4.8	7.1	8.9	10.3	11.2	11.9	12.3	12.4	12.4	12.2	11.8	12.2	13.3	14.2	14.4	13.7	12.2	10.2	16
14	-9.7	-3.4	.9	4.1	6.6	8.5	10.1	11.3	12.2	12.9	13.3	13.5	13.5	13.2	12.9	13.1	13.9	14.9	15.4	15.3	14.4	14
12	-10.9	-4.6	-.2	3.2	5.8	7.9	9.6	11.0	12.1	13.0	13.7	14.2	14.5	14.7	14.4	14.0	13.8	14.3	15.2	15.9	16.3	12
10	-12.3	-5.9	-1.5	1.9	4.6	6.9	8.7	10.3	11.6	12.6	13.5	14.3	14.8	15.5	15.8	15.6	15.2	14.7	14.6	15.0	15.7	10
8	-14.1	-7.7	-3.2	.3	3.1	5.4	7.4	9.0	10.5	11.7	12.8	13.7	14.4	15.6	16.3	16.7	16.7	16.4	15.9	15.3	14.9	8
6	-16.5	-10.0	-5.5	-1.9	.9	3.3	5.4	7.1	8.7	10.0	11.2	12.2	13.1	14.7	15.8	16.6	17.0	17.2	17.1	16.8	16.2	6
4	-14.2	-13.4	-8.8	-5.2	-2.3	.1	2.2	4.1	5.7	7.1	8.4	9.5	10.5	12.2	13.6	14.7	15.5	16.1	16.5	16.6	16.5	4
2	-11.7	-11.7	-11.7	-11.0	-8.1	-5.6	-3.5	-1.6	.0	1.5	2.8	4.0	5.1	7.0	8.5	9.8	10.8	11.6	12.2	12.6	12.8	2
0	-11.7	-11.7	-11.7	-11.7	-11.7	-11.7	-11.7	-11.7	-11.7	-11.7	-11.7	-11.7	-11.7	-11.7	-11.7	-11.7	-11.7	-11.7	-11.7	-11.7	-11.7	0
	2	3	4	5	6	7	8	9	10	11	12	13	14	16	18	20	22	24	26	28	30	

FREQUENCY IN MEGAHERTZ

ANTENNA EFFICIENCY

2	3	4	5	6	7	8	9	10	11	12	13	14	16	18	20	22	24	26	28	30
-1.7	-1.7	-1.7	-1.7	-1.7	-1.7	-1.7	-1.7	-1.7	-1.7	-1.7	-1.7	-1.7	-1.7	-1.7	-1.7	-1.7	-1.7	-1.7	-1.7	-1.7

FREQUENCY IN MEGAHERTZ

Table 37. Inverted "L", Output Antenna Pattern

METHOD 13 IONCAP 78.03 PAGE 8

IONCAP 80.01 ANTENNA PACKAGE — ANTENNA PATTERN

FREQUENCY RANGE	ANTENNA TYPE	HEIGHT	LENGTH	ANGLE	AZIMUTH	EX(1)	EX(2)	EX(3)	EX(4)	CONDUCT.	DIELECT.
1.0 TO 30.0	INVT L	10.000	21.340	0.000	0.000	0.000	0.000	0.000	0.000	.001	4.000

		2	3	4	5	6	7	8	9	10	11	12	13	14	16	18	20	22	24	26	28	30		
	90	-8.2	-5.0	-1.6	.8	3.7	4.1	1.5	-1.8	-4.6	-6.3	-16.6	-26.2	-35.5	-17.4	-11.1	-2.9	-6.3	-6.1	-15.5	-35.6	-16.1	90	
	88	-13.6	-7.8	-3.7	-.7	-3.4	-2.5	-5.2	-7.8	-9.7	-11.1	-15.2	-26.6	-35.6	-14.3	-5.3	-.6	-.4	-5.6	-14.7	-31.4	-19.2	88	
	86	-13.6	-7.8	-3.7	-.7	-3.4	-2.5	-5.2	-7.8	-9.7	-11.0	-14.9	-24.9	-31.8	-13.9	-5.3	-.5	-.4	-5.6	-14.0	-25.3	-17.5	86	
	84	-13.5	-7.7	-3.7	-.8	-3.4	-2.5	-5.2	-7.8	-9.7	-10.9	-14.6	-23.1	-28.2	-13.3	-5.2	-.5	-.3	-5.6	-13.1	-21.8	-15.6	84	
	82	-13.4	-7.7	-3.8	-.8	-3.4	-2.4	-5.1	-7.8	-9.7	-10.8	-14.1	-21.3	-25.7	-12.6	-5.1	-.5	-.3	-5.6	-12.1	-19.2	-13.9	82	
	80	-13.3	-7.7	-3.8	-.8	-3.4	-2.4	-5.1	-7.7	-9.6	-10.7	-13.6	-19.8	-23.7	-11.9	-4.9	-.5	-.2	-5.6	-11.1	-17.1	-12.5	80	
	78	-13.2	-7.7	-3.8	-.8	-3.4	-2.3	-5.0	-7.7	-9.6	-10.5	-13.1	-18.4	-22.1	-11.1	-4.8	-.4	-.2	-5.6	-10.1	-15.4	-11.3	78	
	76	-13.1	-7.6	-3.8	-.8	-3.3	-2.2	-4.9	-7.6	-9.5	-10.3	-12.5	-17.2	-20.5	-10.4	-4.6	-.4	-.1	-5.5	-9.3	-13.9	-10.3	76	
	74	-12.9	-7.6	-3.8	-.9	-3.3	-2.1	-4.8	-7.5	-9.5	-10.1	-11.9	-16.1	-19.4	-9.8	-4.4	-.4	-.0	-5.5	-8.5	-12.6	-9.4	74	
	72	-12.8	-7.6	-3.8	-.9	-3.2	-2.0	-4.6	-7.3	-9.4	-9.9	-11.4	-15.1	-18.3	-9.2	-4.2	-.3	.0	-5.5	-7.8	-11.4	-8.7	72	
E	70	-12.6	-7.5	-3.8	-.9	-3.1	-1.9	-4.5	-7.2	-9.2	-9.6	-10.9	-14.2	-17.2	-8.6	-4.0	-.3	.1	-5.5	-7.2	-10.3	-8.1	70	E
L	68	-12.4	-7.5	-3.8	-1.0	-3.1	-1.7	-4.3	-7.0	-9.1	-9.4	-10.4	-13.4	-16.3	-8.1	-3.8	-.3	.2	-5.4	-6.6	-9.3	-7.7	68	L
E	66	-12.3	-7.4	-3.9	-1.0	-2.9	-1.5	-4.1	-6.8	-9.0	-9.2	-9.9	-12.6	-15.4	-7.7	-3.5	-.3	.2	-5.4	-6.2	-8.3	-7.3	66	E
V	64	-12.1	-7.4	-3.9	-1.1	-2.8	-1.4	-3.9	-6.6	-8.8	-9.0	-9.5	-11.9	-14.5	-7.3	-3.3	-.3	.3	-5.3	-5.8	-7.4	-7.0	64	V
A	62	-11.9	-7.4	-3.9	-1.2	-2.7	-1.2	-3.7	-6.4	-8.6	-8.7	-9.1	-11.3	-13.7	-6.9	-3.1	-.4	.3	-5.3	-5.4	-6.6	-6.8	62	A
T	60	-11.8	-7.3	-4.0	-1.2	-2.5	-.9	-3.4	-6.1	-8.3	-8.5	-8.7	-10.7	-13.0	-6.6	-2.9	-.4	.3	-5.2	-5.2	-5.8	-6.6	60	T
I	58	-11.6	-7.3	-4.0	-1.3	-2.3	-.7	-3.1	-5.8	-8.0	-8.3	-8.4	-10.1	-12.2	-6.4	-2.8	-.5	.3	-5.1	-5.0	-5.1	-6.5	58	I
O	56	-11.5	-7.3	-4.1	-1.4	-2.0	-.4	-2.8	-5.5	-7.7	-8.0	-8.1	-9.6	-11.5	-6.2	-2.6	-.7	.2	-5.0	-4.8	-4.5	-6.3	56	O
N	54	-11.3	-7.2	-4.1	-1.5	-1.7	-.2	-2.5	-5.2	-7.4	-7.8	-7.8	-9.1	-10.8	-6.1	-2.5	-.8	.1	-4.9	-4.7	-3.9	-6.2	54	N
	52	-11.2	-7.2	-4.2	-1.6	-1.5	.1	-2.2	-4.8	-7.1	-7.6	-7.6	-8.7	-10.2	-5.9	-2.4	-1.0	.0	-4.7	-4.7	-3.4	-5.9	52	
A	50	-11.1	-7.2	-4.3	-1.8	-1.1	.4	-1.9	-4.4	-6.7	-7.3	-7.4	-8.2	-9.6	-5.9	-2.3	-1.3	-.1	-4.5	-4.7	-2.9	-5.7	50	A
N	48	-11.0	-7.2	-4.4	-1.9	-.8	.7	-1.6	-4.1	-6.3	-7.1	-7.2	-7.8	-9.0	-5.8	-2.3	-1.6	-.3	-4.4	-4.8	-2.5	-5.3	48	N
G	46	-10.9	-7.2	-4.5	-2.0	-.4	1.0	-1.2	-3.7	-5.9	-6.8	-7.0	-7.5	-8.4	-5.8	-2.4	-1.9	-.5	-4.2	-4.9	-2.2	-5.0	46	G
L	44	-10.8	-7.2	-4.6	-2.2	-.1	1.4	-.9	-3.3	-5.5	-6.6	-6.9	-7.2	-7.9	-5.8	-2.4	-2.3	-.8	-4.0	-5.0	-1.9	-4.6	44	L
E	42	-10.7	-7.3	-4.7	-2.4	.3	1.7	-.5	-2.9	-5.1	-6.3	-6.8	-6.9	-7.4	-5.8	-2.6	-2.7	-1.0	-3.8	-5.1	-1.8	-4.2	42	E
	40	-10.7	-7.3	-4.8	-2.6	.7	2.0	-.2	-2.5	-4.7	-6.1	-6.8	-6.6	-6.9	-5.8	-2.8	-3.1	-1.2	-3.6	-5.1	-1.7	-3.8	40	
I	38	-10.7	-7.4	-5.0	-2.8	1.1	2.4	.2	-2.2	-4.3	-5.8	-6.8	-6.4	-6.5	-5.7	-3.0	-3.6	-1.4	-3.4	-5.2	-1.7	-3.5	38	I
N	36	-10.7	-7.5	-5.2	-3.1	1.5	2.7	.5	-1.8	-3.9	-5.5	-6.8	-6.2	-6.1	-5.7	-3.4	-4.0	-1.6	-3.3	-5.3	-1.8	-3.3	36	N
	34	-10.7	-7.6	-5.4	-3.4	1.9	3.0	.9	-1.4	-3.5	-5.3	-6.8	-6.1	-5.8	-5.6	-3.8	-4.3	-1.6	-3.1	-5.3	-2.0	-3.2	34	
D	32	-10.8	-7.7	-5.6	-3.7	2.3	3.4	1.2	-1.1	-3.1	-5.0	-6.9	-5.9	-5.5	-5.5	-4.3	-4.5	-1.4	-2.9	-5.2	-2.2	-3.3	32	D
E	30	-10.8	-7.9	-5.9	-4.0	2.7	3.7	1.5	-.8	-2.8	-4.8	-7.0	-5.9	-5.2	-5.4	-4.9	-4.5	-1.2	-2.8	-5.2	-2.6	-3.5	30	E
G	28	-10.9	-8.1	-6.2	-4.4	3.1	4.0	1.8	-.4	-2.4	-4.5	-7.2	-5.9	-5.0	-5.3	-5.5	-4.2	-.8	-2.6	-5.2	-3.0	-3.9	28	G
R	26	-11.1	-8.3	-6.5	-4.8	3.5	4.3	2.1	-.1	-2.1	-4.3	-7.4	-5.9	-4.9	-5.1	-6.2	-3.8	-.3	-2.4	-5.1	-3.5	-4.5	26	R
E	24	-11.3	-8.6	-6.9	-5.3	3.9	4.6	2.4	.1	-1.8	-4.1	-7.6	-6.0	-4.8	-5.0	-6.8	-3.2	.3	-2.3	-5.1	-4.0	-5.2	24	E
E	22	-11.5	-8.9	-7.3	-5.8	4.2	4.9	2.7	.4	-1.6	-3.9	-8.0	-6.1	-4.8	-5.0	-7.3	-2.5	.8	-2.1	-5.2	-4.4	-6.0	22	E
S	20	-11.8	-9.3	-7.8	-6.4	4.6	5.2	2.9	.6	-1.3	-3.7	-8.4	-6.4	-4.9	-5.0	-7.5	-1.7	1.3	-2.0	-5.3	-4.9	-7.0	20	S
	18	-12.2	-9.8	-8.4	-7.1	4.9	5.4	3.2	.9	-1.1	-3.5	-8.9	-6.7	-5.1	-5.1	-7.4	-1.0	1.8	-2.0	-5.6	-5.3	-8.0	18	
	16	-12.7	-10.4	-9.1	-8.0	5.2	5.7	3.4	1.1	-.9	-3.4	-9.5	-7.1	-5.4	-5.3	-6.8	-.3	2.2	-2.1	-5.9	-5.7	-8.9	16	
	14	-13.3	-11.0	-9.9	-8.9	5.5	5.9	3.6	1.3	-.7	-3.2	-10.3	-7.7	-5.9	-5.6	-6.1	.3	2.5	-2.3	-6.4	-6.1	-9.6	14	
	12	-14.0	-11.9	-10.9	-10.0	5.8	6.1	3.8	1.4	-.5	-3.1	-11.2	-8.4	-6.6	-6.2	-5.1	.9	2.8	-2.7	-7.1	-6.6	-10.1	12	
	10	-15.0	-12.9	-12.0	-11.4	6.0	6.3	4.0	1.6	-.4	-3.0	-12.4	-9.4	-7.5	-7.0	-4.2	1.4	2.9	-3.3	-8.1	-7.3	-10.6	10	
	8	-16.2	-14.3	-13.6	-13.1	6.2	6.5	4.1	1.7	-.3	-2.9	-13.9	-10.7	-8.7	-8.2	-3.4	1.8	3.0	-4.4	-9.4	-8.4	-11.3	8	
	6	-18.1	-16.3	-15.6	-15.4	6.5	6.7	4.3	1.8	-.2	-2.8	-15.9	-12.6	-10.6	-9.9	-2.7	2.2	3.1	-6.0	-11.3	-10.0	-12.3	6	
	4	-17.7	-14.6	-13.3	-12.8	6.6	6.9	4.4	1.9	-.1	-2.7	-12.5	-12.5	-12.5	-12.5	-2.1	2.5	3.1	-8.9	-12.5	-12.5	-12.5	4	
	2	-15.2	-12.2	-10.8	-10.3	6.8	7.0	4.6	2.1	.0	-2.5	-10.0	-10.0	-10.0	-10.0	-1.7	2.7	3.2	-10.0	-10.0	-10.0	-10.0	2	
	0	-15.2	-12.2	-10.8	-10.3	7.0	7.2	4.7	2.2	.2	-2.4	-10.0	-10.0	-10.0	-10.0	-1.5	2.9	3.3	-10.0	-10.0	-10.0	-10.0	0	
		2	3	4	5	6	7	8	9	10	11	12	13	14	16	18	20	22	24	26	28	30		

FREQUENCY IN MEGAHERTZ

ANTENNA EFFICIENCY

-5.2	-2.2	-.8	-.3	0.0	0.0	0.0	0.0	0.0	0.0	0.0	0.0	0.0	0.0	0.0	0.0	0.0	0.0	0.0	0.0	0.0
2	3	4	5	6	7	8	9	10	11	12	13	14	16	18	20	22	24	26	28	30

FREQUENCY IN MEGAHERTZ

Table 38. Sloping Rhombic, Output Antenna Pattern

METHOD 13 IONCAP 78.03 PAGE 9

IONCAP 80.01 ANTENNA PACKAGE — ANTENNA PATTERN

FREQUENCY RANGE	ANTENNA TYPE	HEIGHT	LENGTH	ANGLE	AZIMUTH	EX(1)	EX(2)	EX(3)	EX(4)	CONDUCT.	DIELECT.
1.0 TO 30.0	SLP RHOM	10.000	120.000	30.000	0.000	20.000	0.000	0.000	0.000	.001	4.000

ELEVATION ANGLE IN DEGREES	2	3	4	5	6	7	8	9	10	11	12	13	14	16	18	20	22	24	26	28	30	
90	-8.8	-10.1	.0	-23.1	-2.9	-5.4	-14.5	-4.0	-18.2	-12.4	-3.2	-12.5	-3.1	-10.7	-13.1	-8.4	-2.7	-11.1	-24.6	-8.7	-5.5	90
88	-7.1	-13.0	.7	-16.5	-5.1	-2.9	-17.9	-7.6	-6.5	-12.9	-2.2	-10.4	-6.8	-11.4	-5.1	-2.7	-13.6	-14.1	-1.9	-3.5	-19.4	88
86	-5.6	-16.7	1.0	-10.7	-8.2	-1.6	-20.1	-16.5	-2.7	-14.7	-4.8	-4.2	-11.3	-5.5	-1.9	-13.6	-13.7	-.8	-2.9	-29.4	-13.1	86
84	-4.2	-21.4	.9	-6.3	-12.6	-1.4	-9.3	-15.7	-2.5	-14.4	-9.8	-1.4	-9.5	-1.6	-7.6	-13.4	-3.5	-3.3	-29.1	-6.9	-5.1	84
82	-3.0	-27.0	.4	-3.0	-17.9	-2.3	-4.3	-13.5	-5.9	-4.6	-11.3	-2.2	-3.9	-2.4	-12.9	-10.2	-2.5	-21.9	-2.7	-2.4	-30.7	82
80	-2.0	-31.8	-.5	-.7	-21.5	-4.2	-1.9	-23.8	-17.5	-1.3	-14.4	-6.2	-.9	-7.5	-10.3	-1.3	-18.6	-4.0	-.1	-28.9	-8.4	80
78	-1.1	-27.7	-1.9	1.0	-16.2	-7.0	-1.1	-11.2	-14.6	-1.8	-6.4	-9.9	-1.3	-10.3	-1.9	-7.8	-12.0	.5	-18.8	-5.1	-5.1	78
76	-.2	-20.7	-3.8	2.1	-9.5	-10.6	-1.8	-4.0	-12.2	-6.4	-1.1	-11.3	-5.0	-5.4	-1.0	-12.2	-2.2	-8.9	-5.1	-.5	-37.3	76
74	.5	-15.2	-6.3	2.6	-4.7	-14.7	-3.8	-1.0	-37.3	-14.3	-.2	-5.7	-9.1	-.6	-8.7	-15.2	-1.8	-12.5	2.1	-22.8	-4.8	74
72	1.1	-10.9	-9.7	2.6	-1.3	-19.3	-6.7	-.5	-7.5	-10.3	-3.0	-.5	-8.8	.3	-9.6	-.5	-22.0	-.2	-7.8	-4.0	-3.8	72
E 70	1.6	-7.5	-14.2	2.1	1.1	-13.9	-9.4	-2.0	-1.5	-15.5	-9.1	.8	-3.2	-2.5	-5.1	-2.1	-13.8	-.1	-11.6	2.0	-34.8	70 E
L 68	2.0	-4.7	-19.8	1.0	2.7	-7.0	-11.8	-5.4	.4	-10.3	-9.0	-1.7	.8	-7.2	.7	-15.7	-1.9	-15.3	2.3	-13.4	-1.2	68 L
E 66	2.4	-2.4	-25.1	-.7	3.6	-2.3	-16.6	-9.1	-.4	-1.5	-12.7	-6.7	1.3	-6.7	.7	-9.5	.1	-8.4	.1	-5.3	-1.0	66 E
V 64	2.7	-.4	-23.4	-3.2	3.9	.8	-13.6	-9.6	-4.2	1.3	-9.0	-7.8	-1.7	-1.4	-4.3	-1.3	-23.7	.3	-17.6	4.1	-28.5	64 V
A 62	2.9	1.2	-15.6	-6.6	3.5	2.9	-5.7	-11.1	-11.1	.8	-.4	-12.0	-5.9	2.1	-7.0	2.2	-9.8	.3	-2.5	-3.8	1.4	62 A
T 60	3.0	2.6	-10.8	-11.3	2.4	4.2	-.9	-17.5	-9.7	-3.5	2.3	-4.7	-7.4	2.5	-2.8	-2.9	-2.9	-20.3	3.1	-12.3	2.8	60 T
I 58	3.0	3.7	-6.2	-17.1	.7	4.8	2.2	-8.1	-8.8	-16.0	1.3	1.7	-8.5	-.2	2.1	-6.9	2.9	-11.4	-1.9	3.4	-19.2	58 I
O 56	3.0	4.7	-2.7	-21.3	-2.0	4.6	4.1	-1.6	-15.5	-9.1	-4.3	3.2	-.1	-4.2	3.6	-3.3	-3.6	-.4	-10.5	3.2	.6	56 O
N 54	2.9	5.5	.2	-17.9	-5.8	3.7	5.2	2.1	-8.5	-7.6	-25.2	.9	3.7	-5.6	2.1	2.7	-6.2	3.1	-5.9	-11.2	5.9	54 N
52	2.8	6.1	2.5	-11.4	-10.9	2.0	5.5	4.3	-.9	-16.5	-6.6	-7.9	3.4	-2.4	-1.7	4.5	-2.8	-10.3	3.4	-4.9	-3.5	52
A 50	2.5	6.6	4.3	-5.9	-16.6	-.7	5.1	5.6	2.9	-5.9	-7.6	-9.0	-1.5	3.3	-3.7	2.7	4.0	-4.2	.7	2.6	-7.3	50 A
N 48	2.3	6.9	5.9	-1.6	-17.6	-4.5	3.9	6.1	5.1	1.1	-16.8	-4.8	-10.2	5.4	-1.1	-1.0	5.1	-.5	-8.0	3.9	3.3	48 N
G 46	1.9	7.1	7.1	1.7	-12.0	-9.7	1.8	5.9	6.2	4.4	-1.6	-12.5	-3.9	3.5	3.9	-2.1	2.1	5.8	-5.7	-19.9	5.2	46 G
L 44	1.5	7.2	8.0	4.3	-5.9	-14.9	-1.4	4.9	6.6	6.1	3.7	-5.3	-6.7	-3.0	6.5	1.4	-1.0	4.6	4.4	-3.8	-5.1	44 L
E 42	1.1	7.2	8.8	6.4	-1.0	-14.3	-6.0	3.0	6.4	6.9	6.0	2.8	-10.6	-2.8	5.4	5.5	.2	.4	6.5	1.1	-2.7	42 E
40	.6	7.1	9.3	8.0	2.7	-8.4	-11.4	-.1	5.4	7.1	7.1	6.0	1.9	-2.5	.3	7.6	4.3	-.0	1.8	7.4	-3.7	40
I 38	-.0	6.9	9.7	9.3	5.6	-2.6	-13.5	-4.4	3.4	6.7	7.6	7.4	6.1	-33.1	-.8	6.0	7.5	3.6	.4	3.6	7.6	38 I
N 36	-.7	6.5	9.9	10.3	7.9	1.9	-8.7	-9.8	.2	5.5	7.6	8.0	7.7	1.2	-.9	1.3	8.3	7.1	3.2	.8	5.1	36 N
34	-1.3	6.2	10.0	11.0	9.6	5.4	-2.7	-11.9	-4.3	3.3	6.9	8.2	8.4	6.6	-23.6	1.3	5.5	9.1	7.0	3.1	1.0	34
D 32	-2.1	5.7	9.9	11.5	11.0	8.1	2.2	-7.3	-9.5	-.4	5.3	8.0	8.8	8.6	2.5	-.8	2.0	8.2	9.4	7.1	3.5	32 D
E 30	-2.9	5.2	9.7	11.8	11.9	10.1	5.9	-1.4	-10.0	-5.4	2.4	6.9	8.8	9.4	7.8	-9.7	2.7	4.0	9.6	9.7	7.3	30 E
G 28	-3.7	4.5	9.3	11.9	12.6	11.6	8.7	3.4	-4.8	-9.6	-1.9	4.5	8.1	10.0	9.7	5.3	-4.7	3.8	6.2	10.5	10.0	28 G
R 26	-4.7	3.8	8.9	11.8	13.0	12.7	10.9	7.1	.8	-7.5	-7.2	.7	5.2	10.5	10.6	9.3	.3	1.8	4.2	7.8	11.2	26 R
E 24	-5.6	3.0	8.3	11.5	13.2	13.5	12.4	9.8	5.2	-1.9	-8.8	-4.5	2.8	10.3	11.7	10.9	8.1	-12.9	4.4	4.4	8.8	24 E
E 22	-6.7	2.1	7.6	11.1	13.2	13.9	13.5	11.8	8.5	3.2	-4.3	-8.6	-2.2	8.8	12.5	12.3	10.8	5.9	-5.9	5.8	4.1	22 E
S 20	-7.8	1.1	6.8	10.6	12.9	14.1	14.2	13.1	10.9	7.0	1.1	-6.5	-7.4	6.0	12.4	13.8	12.7	10.2	2.6	.9	6.4	20 S
18	-9.0	.0	5.9	9.9	12.5	14.0	14.5	14.0	12.5	9.7	5.4	-1.2	-8.3	1.6	11.0	14.6	14.7	12.6	9.0	-1.9	4.1	18
16	-10.3	-1.2	4.9	9.0	11.8	13.6	14.5	14.5	13.5	11.6	8.4	3.5	-3.7	-4.0	8.5	14.4	16.2	15.2	12.1	7.0	-3.7	16
14	-11.7	-2.5	3.7	8.0	11.0	13.0	14.1	14.5	14.1	12.7	10.4	6.7	1.1	-9.8	4.8	13.0	16.6	17.1	15.1	10.9	4.2	14
12	-13.3	-4.0	2.3	6.7	9.9	12.1	13.5	14.1	14.1	13.2	11.5	8.7	4.5	-10.9	-.0	10.7	16.0	18.0	17.5	14.4	8.8	12
10	-15.0	-5.7	.7	5.2	8.5	10.9	12.5	13.3	13.5	13.1	11.8	9.7	6.4	-6.2	-5.8	7.6	14.5	17.8	18.6	16.9	12.6	10
8	-17.1	-7.7	-1.3	3.3	6.7	9.2	11.0	12.0	12.5	12.2	11.4	9.7	7.1	-2.8	-13.2	3.8	12.2	16.7	18.5	18.0	15.1	8
6	-17.7	-10.2	-3.8	.9	4.4	7.0	8.8	10.0	10.6	10.6	10.0	8.6	6.5	-1.7	-17.7	-.6	9.2	14.6	17.2	17.6	15.8	6
4	-14.2	-13.8	-7.3	-2.5	1.0	3.7	5.6	6.9	7.6	7.7	7.3	6.2	4.3	-2.8	-14.2	-5.7	5.1	11.2	14.4	15.4	14.4	4
2	-11.7	-11.7	-11.7	-8.5	-4.9	-2.2	-.2	1.2	1.9	2.2	1.8	.8	-.9	-7.4	-11.7	-11.7	-1.2	5.3	8.8	10.2	9.6	2
0	-11.7	-11.7	-11.7	-11.7	-11.7	-11.7	-11.7	-11.7	-11.7	-11.7	-11.7	-11.7	-11.7	-11.7	-11.7	-11.7	-11.7	-11.7	-11.7	-11.7	-11.7	0
	2	3	4	5	6	7	8	9	10	11	12	13	14	16	18	20	22	24	26	28	30	

FREQUENCY IN MEGAHERTZ

ANTENNA EFFICIENCY

-1.7	-1.7	-1.7	-1.7	-1.7	-1.7	-1.7	-1.7	-1.7	-1.7	-1.7	-1.7	-1.7	-1.7	-1.7	-1.7	-1.7	-1.7	-1.7	-1.7	-1.7
2	3	4	5	6	7	8	9	10	11	12	13	14	16	18	20	22	24	26	28	30

FREQUENCY IN MEGAHERTZ

Table 39. Interlaced Rhombic, Output Antenna Pattern

METHOD 13 IONCAP 78.03 PAGE 10

IONCAP 80.01 ANTENNA PACKAGE

ANTENNA PATTERN

FREQUENCY RANGE	ANTENNA TYPE	HEIGHT	LENGTH	ANGLE	AZIMUTH	EX(1)	EX(2)	EX(3)	EX(4)	CONDUCT.	DIELECT.
1.0 TO 30.0	INT RHOM	20.000	114.000	70.000	0.000	4.000	33.000	0.000	0.000	.001	4.000

		2	3	4	5	6	7	8	9	10	11	12	13	14	16	18	20	22	24	26	28	30		
	90	-11.6	-22.5	-15.0	-37.3	-29.3	-19.7	-37.3	-5.0	-13.3	-15.9	-7.5	-37.3	-12.5	-35.9	-20.5	-7.4	-8.1	-35.5	-36.4	-12.7	-8.8	90	
	88	-9.8	-26.8	-13.4	-32.5	-32.7	-19.4	-37.3	-7.8	-6.4	-37.3	-7.1	-15.0	-22.0	-34.0	-9.8	-9.5	-27.6	-24.0	-12.0	-22.2	-37.3	88	
	86	-8.2	-33.7	-12.4	-26.0	-37.3	-20.7	-22.0	-14.0	-3.6	-26.1	-11.1	-7.7	-37.3	-21.4	-11.2	-29.2	-16.0	-9.1	-14.4	-37.3	-13.0	86	
	84	-6.8	-37.3	-12.0	-21.1	-37.3	-23.2	-15.4	-27.8	-3.6	-11.0	-23.4	-6.2	-15.4	-15.2	-24.1	-28.2	-5.9	-14.2	-28.8	-10.1	-19.3	84	
	82	-5.5	-37.3	-12.2	-17.2	-37.3	-25.9	-12.5	-37.3	-6.7	-5.0	-37.3	-9.6	-7.0	-15.4	-37.3	-20.7	-11.8	-32.9	-5.1	-11.1	-37.3	82	
	80	-4.4	-37.3	-13.1	-14.3	-37.3	-28.5	-12.0	-21.1	-14.0	-3.2	-15.3	-20.9	-5.4	-30.2	-21.6	-19.7	-37.3	-6.8	-8.8	-25.3	-12.6	80	
	78	-3.4	-27.2	-14.7	-12.2	-27.0	-33.4	-13.4	-12.7	-32.7	-4.7	-7.0	-37.3	-9.5	-25.8	-13.8	-29.6	-17.6	-7.5	-37.3	-2.5	-18.3	78	
	76	-2.5	-20.4	-17.4	-10.8	-20.1	-37.3	-16.6	-9.3	-32.6	-10.1	-4.2	-16.5	-23.6	-8.3	-14.3	-25.4	-15.2	-37.3	-6.7	-9.5	-14.9	76	
	74	-1.8	-15.4	-21.6	-10.2	-15.4	-37.3	-21.4	-8.8	-15.2	-23.7	-5.2	-8.2	-36.2	-3.5	-33.2	-7.9	-20.2	-15.0	-8.8	-21.9	-3.2	74	
	72	-1.1	-11.5	-28.5	-10.2	-12.1	-31.3	-28.3	-10.6	-9.1	-37.3	-10.6	-5.9	-14.1	-5.9	-19.5	-5.7	-34.8	-11.5	-37.3	-5.8	-24.1	72	
E	70	-.5	-8.3	-36.8	-11.1	-10.0	-20.9	-36.8	-14.8	-7.1	-16.6	-25.0	-7.8	-8.5	-18.9	-5.0	-16.3	-6.7	-22.3	-13.8	-17.2	-9.7	70	E
L	68	-.1	-5.7	-36.7	-12.9	-8.7	-14.6	-36.7	-21.5	-8.2	-9.0	-36.7	-14.8	-8.5	-32.8	-2.2	-28.9	-2.6	-31.0	-15.0	-34.4	-9.0	68	L
E	66	.3	-3.5	-30.5	-16.0	-8.3	-10.6	-27.9	-32.1	-12.2	-6.6	-15.4	-36.5	-13.1	-10.3	-8.2	-5.7	-13.0	-5.9	-36.5	-12.1	-36.5	66	E
V	64	.6	-1.7	-20.1	-21.2	-8.8	-8.1	-17.4	-36.4	-19.4	-7.8	-8.4	-27.4	-25.0	-5.8	-36.4	-1.3	-24.8	-3.2	-22.7	-14.3	-15.6	64	V
A	62	.8	-.1	-13.5	-30.8	-10.2	-6.8	-11.3	-33.0	-31.0	-12.5	-6.8	-12.7	-36.2	-8.6	-11.7	-6.4	-3.4	-20.6	-5.7	-36.2	-6.1	62	A
T	60	.9	1.2	-8.7	-36.1	-12.8	-6.6	-7.6	-18.6	-36.1	-21.8	-9.1	-7.9	-19.1	-19.8	-2.4	-36.1	-1.0	-12.2	-8.5	-8.6	-35.0	60	T
I	58	.9	2.3	-5.0	-34.2	-17.3	-7.4	-5.5	-11.0	-32.1	-35.9	-15.9	-7.9	-10.4	-35.9	-2.5	-9.9	-9.7	-.5	-35.9	-6.2	-6.1	58	I
O	56	.9	3.2	-2.0	-20.0	-25.5	-9.4	-4.9	-6.4	-16.9	-35.7	-31.0	-12.4	-8.0	-35.7	-10.4	-.3	-35.7	-3.3	-2.6	-32.7	-2.0	56	O
N	54	.8	3.9	.4	-12.1	-35.5	-12.9	-5.5	-4.0	-9.0	-25.4	-35.5	-23.4	-10.1	-15.3	-35.3	-.7	-5.0	-24.6	-.3	-6.4	-20.2	54	N
	52	.6	4.5	2.4	-6.6	-35.3	-19.0	-7.5	-3.3	-4.5	-12.5	-35.3	-35.3	-17.4	-7.7	-27.6	-10.2	.9	-14.7	-13.6	1.0	-9.4	52	
A	50	.3	4.9	4.0	-2.4	-19.3	-31.6	-11.2	-4.2	-2.3	-5.6	-16.3	-35.0	-32.5	-6.4	-11.4	-35.0	-2.6	-1.6	-27.3	-8.3	1.5	50	A
N	48	-.1	5.2	5.3	.8	-10.4	-34.7	-17.5	-6.6	-2.0	-1.9	-6.8	-19.0	-34.7	-10.7	-4.3	-16.2	-20.2	-.9	-6.8	-34.7	-5.7	48	N
G	46	-.5	5.3	6.3	3.4	-4.5	-23.2	-30.4	-11.2	-3.5	-.6	-1.7	-7.4	-19.7	-23.5	-3.4	-5.3	-24.0	-12.0	-2.4	-15.3	-34.5	46	G
L	44	-1.0	5.3	7.1	5.4	-.1	-11.8	-34.2	-19.3	-7.2	-1.3	.5	-1.3	-7.1	-34.2	-8.9	-1.0	-7.5	-34.2	-9.8	-6.3	-13.9	44	L
E	42	-1.5	5.2	7.7	7.1	3.2	-4.7	-21.1	-33.8	-13.7	-4.3	.3	1.5	-.5	-14.7	-28.2	-2.8	-.8	-10.1	-33.8	-10.3	-9.3	42	E
	40	-2.2	4.9	8.1	8.3	5.9	.4	-9.8	-33.5	-26.7	-10.1	-2.3	1.6	2.5	-3.6	-23.7	-13.8	-.2	-2.0	-12.5	-33.5	-11.2	40	
I	38	-2.9	4.6	8.2	9.3	7.9	4.2	-2.7	-15.0	-33.1	-21.4	-7.8	-.8	2.7	2.3	-6.3	-33.1	-7.9	.6	-4.2	-13.2	-33.1	38	I
N	36	-3.6	4.1	8.3	9.9	9.5	7.1	2.4	-5.5	-19.3	-32.7	-18.7	-6.5	.1	4.8	1.6	-8.1	-32.7	-5.5	.4	-8.1	-9.9	36	N
	34	-4.5	3.6	8.1	10.3	10.7	9.4	6.2	.8	-7.6	-21.9	-32.3	-17.9	-6.0	4.2	5.7	1.5	-8.7	-32.3	-5.1	-.3	-13.0	34	
D	32	-5.4	2.9	7.8	10.5	11.5	11.1	9.1	5.5	-.2	-8.7	-22.2	-31.8	-19.0	.3	6.5	6.4	2.1	-7.7	-31.8	-6.4	-1.0	32	D
E	30	-6.5	2.1	7.3	10.5	12.1	12.3	11.3	9.0	5.1	-.5	-8.5	-20.4	-31.3	-8.4	4.0	8.0	7.3	3.3	-5.3	-31.3	-9.9	30	E
G	28	-7.6	1.2	6.7	10.2	12.3	13.2	12.9	11.6	9.1	5.3	-.1	-7.4	-17.2	-30.8	-2.9	6.3	9.3	8.4	5.0	-1.8	-21.1	28	G
R	26	-8.7	.2	5.9	9.8	12.3	13.7	14.1	13.6	12.1	9.7	6.0	1.1	-5.4	-25.3	-19.3	.1	7.7	10.4	9.7	6.9	1.9	26	R
E	24	-10.0	-.9	5.1	9.2	12.0	13.8	14.8	14.9	14.3	12.9	10.6	7.3	2.9	-9.5	-29.5	-14.5	1.7	8.7	11.3	11.1	9.0	24	E
E	22	-11.4	-2.1	4.0	8.4	11.5	13.7	15.1	15.8	15.8	15.2	13.9	11.9	9.0	.3	-11.8	-28.8	-13.1	2.1	9.1	12.1	12.6	22	E
S	20	-12.8	-3.5	2.9	7.4	10.8	13.3	15.1	16.2	16.8	16.8	16.3	15.2	13.5	7.9	-1.1	-12.6	-28.0	-14.5	1.3	8.8	12.6	20	S
	18	-14.4	-4.9	1.6	6.3	9.9	12.7	14.7	16.3	17.2	17.8	17.8	17.4	16.6	13.4	7.7	-1.2	-12.4	-27.1	-19.1	-1.0	7.6	18	
	16	-16.1	-6.5	.1	5.0	8.8	11.8	14.1	15.9	17.2	18.2	18.7	18.9	18.7	17.1	13.9	8.6	.3	-11.2	-26.1	-26.1	-5.2	16	
	14	-17.9	-8.2	-1.5	3.5	7.5	10.6	13.2	15.2	16.8	18.1	19.0	19.6	19.8	19.5	17.9	15.0	10.4	3.4	-7.2	-22.6	-25.0	14	
	12	-19.8	-10.1	-3.3	1.9	5.9	9.2	11.9	14.2	16.0	17.5	18.7	19.6	20.3	20.8	20.4	19.0	16.5	12.7	7.1	-1.2	-14.5	12	
	10	-22.0	-12.1	-5.3	-.1	4.1	7.5	10.4	12.8	14.8	16.5	17.9	19.1	20.0	21.2	21.6	21.3	20.1	18.1	15.0	10.6	4.3	10	
	8	-20.2	-14.5	-7.6	-2.3	2.0	5.5	8.4	11.0	13.1	15.0	16.6	17.9	19.0	20.7	21.7	22.1	21.8	20.9	19.2	16.7	13.1	8	
	6	-17.7	-17.4	-10.4	-5.0	-.7	2.9	5.9	8.5	10.8	12.8	14.5	16.0	17.2	19.3	20.7	21.6	21.9	21.6	20.8	19.4	17.2	6	
	4	-14.2	-14.2	-14.1	-8.7	-4.3	-.7	2.4	5.1	7.4	9.5	11.3	12.8	14.2	16.5	18.2	19.4	20.0	20.2	20.0	19.2	17.8	4	
	2	-11.7	-11.7	-11.7	-11.7	-10.4	-6.7	-3.6	-.9	1.5	3.6	5.5	7.1	8.6	11.0	12.8	14.2	15.1	15.5	15.5	15.1	14.1	2	
	0	-11.7	-11.7	-11.7	-11.7	-11.7	-11.7	-11.7	-11.7	-11.7	-11.7	-11.7	-11.7	-11.7	-11.7	-11.7	-11.7	-11.7	-11.7	-11.7	-11.7	-11.7	0	
		2	3	4	5	6	7	8	9	10	11	12	13	14	16	18	20	22	24	26	28	30		

FREQUENCY IN MEGAHERTZ

ANTENNA EFFICIENCY

-1.7	-1.7	-1.7	-1.7	-1.7	-1.7	-1.7	-1.7	-1.7	-1.7	-1.7	-1.7	-1.7	-1.7	-1.7	-1.7	-1.7	-1.7	-1.7	-1.7	-1.7
2	3	4	5	6	7	8	9	10	11	12	13	14	16	18	20	22	24	26	28	30

FREQUENCY IN MEGAHERTZ

Table 40. Sloping Long Wire, Output Antenna Pattern

METHOD 13   IONCAP 78.03   PAGE 11

IONCAP 80.01 ANTENNA PACKAGE

ANTENNA PATTERN

FREQUENCY RANGE	ANTENNA TYPE	HEIGHT	LENGTH	ANGLE	AZIMUTH	EX(1)	EX(2)	EX(3)	EX(4)	CONDUCT.	DIELECT.
1.0 TO 30.0	SLP WIRE	0.000	91.440	10.000	0.000	0.000	0.000	0.000	0.000	.001	4.000

ELEVATION ANGLE IN DEGREES	2	3	4	5	6	7	8	9	10	11	12	13	14	16	18	20	22	24	26	28	30	
90	8.6	3.2	.3	2.3	-.1	-3.5	-8.9	-7.2	-1.1	-4.6	-5.4	.0	-.4	-5.0	-2.5	-13.5	-1.3	-3.9	-2.2	-19.3	-2.7	90
88	8.6	3.8	.5	1.5	.5	-1.8	-15.9	-9.0	-1.8	-2.2	-2.7	-3.3	-.3	-8.8	-2.5	-4.3	-3.1	-4.5	-1.6	-6.1	-8.5	88
86	8.5	4.5	.8	.4	.8	-.7	-16.5	-11.6	-3.6	-1.0	-.6	-7.5	-1.3	-4.5	-6.0	-1.8	-5.8	-1.0	-8.5	-2.7	-6.8	86
84	8.4	5.0	1.2	-1.0	.9	.1	-8.9	-12.9	-7.0	-.8	.4	-4.6	-3.0	-1.0	-21.7	-3.0	-3.2	-.8	-6.2	-7.6	-2.3	84
82	8.4	5.5	1.8	-2.6	.8	.4	-4.9	-10.6	-14.7	-1.7	.4	-.6	-3.8	-.0	-8.2	-9.1	-.9	-4.2	-.7	-13.2	-5.8	82
80	8.2	6.0	2.4	-4.1	.3	.5	-2.4	-7.5	-18.9	-3.8	-.5	1.5	-2.3	-1.1	-2.5	-14.2	-1.5	-4.2	-1.8	-2.8	-11.6	80
78	8.1	6.4	3.0	-4.8	-.4	.1	-.9	-5.1	-8.3	-7.5	-2.7	2.1	-.2	-4.6	-.9	-4.3	-5.3	-.3	-10.4	-2.5	-3.1	78
76	8.0	6.7	3.6	-4.1	-1.4	-.6	-.0	-3.4	-4.0	-11.2	-6.3	1.3	.9	-8.1	-2.1	-1.6	-6.4	-.0	-3.1	-11.9	-3.3	76
74	7.8	7.0	4.2	-2.4	-2.7	-1.7	.3	-2.3	-1.6	-7.7	-8.4	-1.1	.9	-3.4	-7.3	-2.0	-2.0	-3.7	.7	-6.6	-13.5	74
72	7.6	7.2	4.7	-.6	-3.9	-3.5	.1	-1.7	-.3	-3.7	-5.0	-5.7	-.4	.2	-17.2	-6.0	-.6	-5.1	-1.1	-.6	-6.9	72
E 70	7.4	7.4	5.1	1.0	-4.5	-5.8	-.6	-1.7	.3	-1.3	-1.7	-9.2	-3.0	1.6	-4.1	-22.8	-2.3	-.3	-9.1	-1.5	-2.1	70 E
L 68	7.2	7.5	5.5	2.4	-3.8	-8.3	-1.9	-2.1	.3	-.0	.3	-3.6	-5.2	1.1	.2	-7.5	-8.3	.9	-1.5	-12.2	-3.7	68 L
E 66	6.9	7.5	5.8	3.5	-2.3	-8.5	-4.2	-3.2	-.3	.5	1.3	.2	-3.3	-1.4	1.5	-1.8	-8.8	-1.9	2.0	-3.0	-16.7	66 E
V 64	6.7	7.5	6.1	4.5	-.5	-5.7	-8.0	-5.1	-1.6	.2	1.4	2.1	-.3	-6.1	.5	.2	-2.6	-8.5	.5	1.7	-4.2	64 V
A 62	6.4	7.5	6.3	5.2	1.1	-2.7	-13.3	-8.3	-3.8	-.8	.7	2.8	1.7	-5.1	-3.6	-.2	-.4	-3.0	-7.3	.6	.4	62 A
T 60	6.1	7.4	6.4	5.8	2.5	-.2	-10.1	-12.2	-7.9	-2.7	-.9	2.5	2.4	-.1	-11.5	-3.3	-.8	.7	-2.9	-7.9	-.8	60 T
I 58	5.8	7.3	6.5	6.2	3.6	1.6	-4.6	-10.3	-18.3	-6.1	-3.7	1.1	2.1	2.6	-3.1	-13.2	-3.8	.8	2.1	-2.1	-9.5	58 I
O 56	5.4	7.1	6.5	6.5	4.5	3.1	-1.0	-5.4	-14.3	-13.0	-9.0	-1.6	.8	3.6	1.9	-5.9	-12.9	-2.4	2.4	3.0	-1.6	56 O
N 54	5.1	6.9	6.5	6.7	5.2	4.2	1.5	-1.7	-5.6	-16.7	-19.3	-6.7	-2.0	3.3	4.0	.7	-7.9	-12.4	-1.3	3.0	3.0	54 N
52	4.7	6.7	6.3	6.8	5.8	5.1	3.3	.9	-1.2	-6.7	-8.8	-21.9	-7.2	1.5	4.3	3.6	-.5	-7.6	-15.4	-1.8	2.6	52
A 50	4.3	6.4	6.2	6.8	6.1	5.8	4.7	2.9	1.6	-1.8	-3.0	-8.3	-11.8	-2.3	3.0	4.3	2.7	-.3	-3.7	-12.0	-3.3	50 A
N 48	3.8	6.0	6.0	6.7	6.4	6.2	5.6	4.3	3.6	1.3	.4	-2.0	-5.0	-9.9	-.5	3.2	3.7	2.7	1.7	.0	-5.4	48 N
G 46	3.4	5.7	5.7	6.6	6.5	6.5	6.4	5.4	5.1	3.5	2.8	1.5	-.4	-6.6	-8.3	-.1	2.9	3.6	3.6	3.6	2.3	46 G
L 44	2.9	5.3	5.4	6.3	6.5	6.6	6.8	6.2	6.2	5.1	4.6	3.8	2.4	-.4	-6.2	-8.0	-.5	2.5	3.6	4.3	4.6	44 L
E 42	2.5	4.9	5.0	6.0	6.4	6.6	7.1	6.7	7.0	6.3	5.9	5.4	4.4	3.0	.8	-4.3	-8.2	-1.5	1.5	2.9	4.1	42 E
40	2.0	4.4	4.6	5.6	6.1	6.5	7.2	7.0	7.5	7.1	6.8	6.6	5.8	5.1	4.3	2.3	-2.7	-11.3	-5.0	-1.2	1.2	40
I 38	1.4	3.9	4.1	5.2	5.8	6.2	7.1	7.1	7.7	7.6	7.4	7.5	6.8	6.5	6.4	5.6	3.3	-1.0	-9.1	-21.0	-7.5	38 I
N 36	.9	3.4	3.6	4.6	5.4	5.8	6.9	7.1	7.7	7.9	7.8	8.0	7.5	7.5	7.6	7.5	6.5	4.6	2.1	-1.2	-6.2	36 N
34	.3	2.9	3.0	4.1	4.9	5.4	6.5	6.8	7.5	7.9	7.9	8.2	7.9	8.1	8.4	8.5	8.2	7.5	6.5	5.2	3.3	34
D 32	-.2	2.3	2.4	3.5	4.4	4.8	6.0	6.4	7.2	7.7	7.8	8.2	8.0	8.3	8.8	9.1	9.1	9.0	8.8	8.3	7.4	32 D
E 30	-.8	1.7	1.8	2.9	3.8	4.2	5.4	5.9	6.7	7.3	7.4	7.9	7.9	8.3	8.8	9.3	9.5	9.7	9.9	9.8	9.5	30 E
G 28	-1.4	1.1	1.2	2.1	3.1	3.5	4.8	5.2	6.0	6.7	6.8	7.4	7.4	8.0	8.6	9.2	9.6	9.9	10.3	10.5	10.5	28 G
R 26	-2.1	.4	.5	1.4	2.4	2.7	4.0	4.5	5.2	6.0	6.1	6.7	6.8	7.4	8.1	8.7	9.3	9.8	10.2	10.5	10.7	26 R
E 24	-2.7	-.2	-.2	.7	1.7	1.9	3.2	3.7	4.4	5.2	5.2	5.8	5.9	6.5	7.2	7.9	8.6	9.2	9.8	10.2	10.5	24 E
E 22	-3.4	-.9	-.9	-.1	.9	1.1	2.4	2.8	3.5	4.2	4.2	4.8	4.8	5.4	6.0	6.7	7.4	8.2	8.9	9.4	9.9	22 E
S 20	-4.1	-1.6	-1.7	-.9	.1	.3	1.6	2.0	2.6	3.3	3.2	3.8	3.7	4.1	4.5	5.0	5.7	6.6	7.4	8.1	8.7	20 S
18	-4.9	-2.4	-2.5	-1.7	-.7	-.5	.8	1.2	1.8	2.5	2.4	2.8	2.7	2.9	2.9	3.0	3.5	4.3	5.1	5.8	6.7	18
16	-5.7	-3.2	-3.4	-2.5	-1.5	-1.3	.0	.4	1.1	1.8	1.6	2.1	1.9	2.0	1.8	1.4	1.2	1.4	1.8	2.3	3.2	16
14	-6.6	-4.1	-4.3	-3.5	-2.4	-2.2	-.8	-.4	.3	1.1	1.0	1.6	1.4	1.5	1.4	1.0	.3	-.4	-1.0	-1.8	-2.1	14
12	-7.7	-5.2	-5.4	-4.5	-3.4	-3.1	-1.7	-1.2	-.4	.4	.5	1.1	1.0	1.4	1.6	1.5	1.2	.7	.1	-.8	-2.2	12
10	-8.9	-6.4	-6.6	-5.7	-4.5	-4.2	-2.7	-2.2	-1.3	-.4	-.2	.5	.5	1.2	1.8	2.1	2.3	2.4	2.5	2.5	2.3	10
8	-10.4	-7.9	-8.1	-7.2	-6.0	-5.6	-4.1	-3.5	-2.5	-1.5	-1.2	-.4	-.3	.7	1.5	2.2	2.8	3.3	3.8	4.2	4.6	8
6	-12.3	-9.9	-10.1	-9.1	-7.9	-7.6	-5.9	-5.3	-4.2	-3.2	-2.8	-1.9	-1.7	-.6	.5	1.4	2.2	2.9	3.7	4.4	5.1	6
4	-12.5	-12.5	-12.5	-12.1	-10.9	-10.4	-8.8	-8.1	-7.0	-5.9	-5.5	-4.5	-4.2	-3.0	-1.8	-.7	.2	1.1	2.0	2.8	3.6	4
2	-10.0	-10.0	-10.0	-10.0	-10.0	-10.0	-10.0	-10.0	-10.0	-10.0	-10.0	-9.7	-9.3	-8.1	-6.8	-5.7	-4.6	-3.7	-2.7	-1.8	-.9	2
0	-10.0	-10.0	-10.0	-10.0	-10.0	-10.0	-10.0	-10.0	-10.0	-10.0	-10.0	-10.0	-10.0	-10.0	-10.0	-10.0	-10.0	-10.0	-10.0	-10.0	-10.0	0
	2	3	4	5	6	7	8	9	10	11	12	13	14	16	18	20	22	24	26	28	30	

FREQUENCY IN MEGAHERTZ

ANTENNA EFFICIENCY

0.0	0.0	0.0	0.0	0.0	0.0	0.0	0.0	0.0	0.0	0.0	0.0	0.0	0.0	0.0	0.0	0.0	0.0	0.0	0.0	0.0
2	3	4	5	6	7	8	9	10	11	12	13	14	16	18	20	22	24	26	28	30

FREQUENCY IN MEGAHERTZ

Table 41. Isotropic Antenna, Output Antenna Pattern

METHOD 13 IONCAP 78.03 PAGE 12

IONCAP 80.01 ANTENNA PACKAGE — ANTENNA PATTERN

FREQUENCY RANGE	ANTENNA TYPE	HEIGHT	LENGTH	ANGLE	AZIMUTH	EX(1)	EX(2)	EX(3)	EX(4)	CONDUCT.	DIELECT.
1.0 TO 30.0	ISOT ROPE	0.000	0.000	0.000	0.000	5.000	0.000	0.000	0.000	.001	4.000

ELEVATION ANGLE IN DEGREES	2	3	4	5	6	7	8	9	10	11	12	13	14	16	18	20	22	24	26	28	30	
90	5.0	5.0	5.0	5.0	5.0	5.0	5.0	5.0	5.0	5.0	5.0	5.0	5.0	5.0	5.0	5.0	5.0	5.0	5.0	5.0	5.0	90
88	5.0	5.0	5.0	5.0	5.0	5.0	5.0	5.0	5.0	5.0	5.0	5.0	5.0	5.0	5.0	5.0	5.0	5.0	5.0	5.0	5.0	88
86	5.0	5.0	5.0	5.0	5.0	5.0	5.0	5.0	5.0	5.0	5.0	5.0	5.0	5.0	5.0	5.0	5.0	5.0	5.0	5.0	5.0	86
84	5.0	5.0	5.0	5.0	5.0	5.0	5.0	5.0	5.0	5.0	5.0	5.0	5.0	5.0	5.0	5.0	5.0	5.0	5.0	5.0	5.0	84
82	5.0	5.0	5.0	5.0	5.0	5.0	5.0	5.0	5.0	5.0	5.0	5.0	5.0	5.0	5.0	5.0	5.0	5.0	5.0	5.0	5.0	82
80	5.0	5.0	5.0	5.0	5.0	5.0	5.0	5.0	5.0	5.0	5.0	5.0	5.0	5.0	5.0	5.0	5.0	5.0	5.0	5.0	5.0	80
78	5.0	5.0	5.0	5.0	5.0	5.0	5.0	5.0	5.0	5.0	5.0	5.0	5.0	5.0	5.0	5.0	5.0	5.0	5.0	5.0	5.0	78
76	5.0	5.0	5.0	5.0	5.0	5.0	5.0	5.0	5.0	5.0	5.0	5.0	5.0	5.0	5.0	5.0	5.0	5.0	5.0	5.0	5.0	76
74	5.0	5.0	5.0	5.0	5.0	5.0	5.0	5.0	5.0	5.0	5.0	5.0	5.0	5.0	5.0	5.0	5.0	5.0	5.0	5.0	5.0	74
72	5.0	5.0	5.0	5.0	5.0	5.0	5.0	5.0	5.0	5.0	5.0	5.0	5.0	5.0	5.0	5.0	5.0	5.0	5.0	5.0	5.0	72
70	5.0	5.0	5.0	5.0	5.0	5.0	5.0	5.0	5.0	5.0	5.0	5.0	5.0	5.0	5.0	5.0	5.0	5.0	5.0	5.0	5.0	70
68	5.0	5.0	5.0	5.0	5.0	5.0	5.0	5.0	5.0	5.0	5.0	5.0	5.0	5.0	5.0	5.0	5.0	5.0	5.0	5.0	5.0	68
66	5.0	5.0	5.0	5.0	5.0	5.0	5.0	5.0	5.0	5.0	5.0	5.0	5.0	5.0	5.0	5.0	5.0	5.0	5.0	5.0	5.0	66
64	5.0	5.0	5.0	5.0	5.0	5.0	5.0	5.0	5.0	5.0	5.0	5.0	5.0	5.0	5.0	5.0	5.0	5.0	5.0	5.0	5.0	64
62	5.0	5.0	5.0	5.0	5.0	5.0	5.0	5.0	5.0	5.0	5.0	5.0	5.0	5.0	5.0	5.0	5.0	5.0	5.0	5.0	5.0	62
60	5.0	5.0	5.0	5.0	5.0	5.0	5.0	5.0	5.0	5.0	5.0	5.0	5.0	5.0	5.0	5.0	5.0	5.0	5.0	5.0	5.0	60
58	5.0	5.0	5.0	5.0	5.0	5.0	5.0	5.0	5.0	5.0	5.0	5.0	5.0	5.0	5.0	5.0	5.0	5.0	5.0	5.0	5.0	58
56	5.0	5.0	5.0	5.0	5.0	5.0	5.0	5.0	5.0	5.0	5.0	5.0	5.0	5.0	5.0	5.0	5.0	5.0	5.0	5.0	5.0	56
54	5.0	5.0	5.0	5.0	5.0	5.0	5.0	5.0	5.0	5.0	5.0	5.0	5.0	5.0	5.0	5.0	5.0	5.0	5.0	5.0	5.0	54
52	5.0	5.0	5.0	5.0	5.0	5.0	5.0	5.0	5.0	5.0	5.0	5.0	5.0	5.0	5.0	5.0	5.0	5.0	5.0	5.0	5.0	52
50	5.0	5.0	5.0	5.0	5.0	5.0	5.0	5.0	5.0	5.0	5.0	5.0	5.0	5.0	5.0	5.0	5.0	5.0	5.0	5.0	5.0	50
48	5.0	5.0	5.0	5.0	5.0	5.0	5.0	5.0	5.0	5.0	5.0	5.0	5.0	5.0	5.0	5.0	5.0	5.0	5.0	5.0	5.0	48
46	5.0	5.0	5.0	5.0	5.0	5.0	5.0	5.0	5.0	5.0	5.0	5.0	5.0	5.0	5.0	5.0	5.0	5.0	5.0	5.0	5.0	46
44	5.0	5.0	5.0	5.0	5.0	5.0	5.0	5.0	5.0	5.0	5.0	5.0	5.0	5.0	5.0	5.0	5.0	5.0	5.0	5.0	5.0	44
42	5.0	5.0	5.0	5.0	5.0	5.0	5.0	5.0	5.0	5.0	5.0	5.0	5.0	5.0	5.0	5.0	5.0	5.0	5.0	5.0	5.0	42
40	5.0	5.0	5.0	5.0	5.0	5.0	5.0	5.0	5.0	5.0	5.0	5.0	5.0	5.0	5.0	5.0	5.0	5.0	5.0	5.0	5.0	40
38	5.0	5.0	5.0	5.0	5.0	5.0	5.0	5.0	5.0	5.0	5.0	5.0	5.0	5.0	5.0	5.0	5.0	5.0	5.0	5.0	5.0	38
36	5.0	5.0	5.0	5.0	5.0	5.0	5.0	5.0	5.0	5.0	5.0	5.0	5.0	5.0	5.0	5.0	5.0	5.0	5.0	5.0	5.0	36
34	5.0	5.0	5.0	5.0	5.0	5.0	5.0	5.0	5.0	5.0	5.0	5.0	5.0	5.0	5.0	5.0	5.0	5.0	5.0	5.0	5.0	34
32	5.0	5.0	5.0	5.0	5.0	5.0	5.0	5.0	5.0	5.0	5.0	5.0	5.0	5.0	5.0	5.0	5.0	5.0	5.0	5.0	5.0	32
30	5.0	5.0	5.0	5.0	5.0	5.0	5.0	5.0	5.0	5.0	5.0	5.0	5.0	5.0	5.0	5.0	5.0	5.0	5.0	5.0	5.0	30
28	5.0	5.0	5.0	5.0	5.0	5.0	5.0	5.0	5.0	5.0	5.0	5.0	5.0	5.0	5.0	5.0	5.0	5.0	5.0	5.0	5.0	28
26	5.0	5.0	5.0	5.0	5.0	5.0	5.0	5.0	5.0	5.0	5.0	5.0	5.0	5.0	5.0	5.0	5.0	5.0	5.0	5.0	5.0	26
24	5.0	5.0	5.0	5.0	5.0	5.0	5.0	5.0	5.0	5.0	5.0	5.0	5.0	5.0	5.0	5.0	5.0	5.0	5.0	5.0	5.0	24
22	5.0	5.0	5.0	5.0	5.0	5.0	5.0	5.0	5.0	5.0	5.0	5.0	5.0	5.0	5.0	5.0	5.0	5.0	5.0	5.0	5.0	22
20	5.0	5.0	5.0	5.0	5.0	5.0	5.0	5.0	5.0	5.0	5.0	5.0	5.0	5.0	5.0	5.0	5.0	5.0	5.0	5.0	5.0	20
18	5.0	5.0	5.0	5.0	5.0	5.0	5.0	5.0	5.0	5.0	5.0	5.0	5.0	5.0	5.0	5.0	5.0	5.0	5.0	5.0	5.0	18
16	5.0	5.0	5.0	5.0	5.0	5.0	5.0	5.0	5.0	5.0	5.0	5.0	5.0	5.0	5.0	5.0	5.0	5.0	5.0	5.0	5.0	16
14	5.0	5.0	5.0	5.0	5.0	5.0	5.0	5.0	5.0	5.0	5.0	5.0	5.0	5.0	5.0	5.0	5.0	5.0	5.0	5.0	5.0	14
12	5.0	5.0	5.0	5.0	5.0	5.0	5.0	5.0	5.0	5.0	5.0	5.0	5.0	5.0	5.0	5.0	5.0	5.0	5.0	5.0	5.0	12
10	5.0	5.0	5.0	5.0	5.0	5.0	5.0	5.0	5.0	5.0	5.0	5.0	5.0	5.0	5.0	5.0	5.0	5.0	5.0	5.0	5.0	10
8	5.0	5.0	5.0	5.0	5.0	5.0	5.0	5.0	5.0	5.0	5.0	5.0	5.0	5.0	5.0	5.0	5.0	5.0	5.0	5.0	5.0	8
6	5.0	5.0	5.0	5.0	5.0	5.0	5.0	5.0	5.0	5.0	5.0	5.0	5.0	5.0	5.0	5.0	5.0	5.0	5.0	5.0	5.0	6
4	5.0	5.0	5.0	5.0	5.0	5.0	5.0	5.0	5.0	5.0	5.0	5.0	5.0	5.0	5.0	5.0	5.0	5.0	5.0	5.0	5.0	4
2	5.0	5.0	5.0	5.0	5.0	5.0	5.0	5.0	5.0	5.0	5.0	5.0	5.0	5.0	5.0	5.0	5.0	5.0	5.0	5.0	5.0	2
0	5.0	5.0	5.0	5.0	5.0	5.0	5.0	5.0	5.0	5.0	5.0	5.0	5.0	5.0	5.0	5.0	5.0	5.0	5.0	5.0	5.0	0
	2	3	4	5	6	7	8	9	10	11	12	13	14	16	18	20	22	24	26	28	30	

FREQUENCY IN MEGAHERTZ

ANTENNA EFFICIENCY

0.0	0.0	0.0	0.0	0.0	0.0	0.0	0.0	0.0	0.0	0.0	0.0	0.0	0.0	0.0	0.0	0.0	0.0	0.0	0.0	0.0
2	3	4	5	6	7	8	9	10	11	12	13	14	16	18	20	22	24	26	28	30

FREQUENCY IN MEGAHERTZ

Table 42. Horizontal LPD, Output Antenna Pattern

METHOD 13 IONCAP 78.03 PAGE 13

IONCAP 80.01 ANTENNA PACKAGE ANTENNA PATTERN

FREQUENCY RANGE	ANTENNA TYPE	HEIGHT	LENGTH	ANGLE	AZIMUTH	EX(1)	EX(2)	EX(3)	EX(4)	CONDUCT.	DIELECT.
1.0 TO 30.0	HOR LPD	2.960	33.470	46.000	0.000	0.000	18.000	.870	12.000	.001	4.000

		2	3	4	5	6	7	8	9	10	11	12	13	14	16	18	20	22	24	26	28	30		
	90	-13.1	-5.0	10.8	3.0	2.6	3.0	2.5	1.9	5.6	8.5	1.7	6.3	2.1	-1.4	-3.2	-.2	1.7	2.9	4.9	4.9	4.8	90	
	88	-13.1	-5.0	10.9	3.5	3.0	3.4	2.9	2.4	6.0	8.7	2.1	6.6	2.5	-1.0	-2.9	-.1	1.7	2.9	4.9	4.9	4.8	88	
	86	-13.1	-5.0	10.9	4.0	3.4	3.7	3.3	2.8	6.4	8.9	2.5	6.9	2.8	-.6	-2.6	.1	1.7	2.9	4.9	4.9	4.8	86	
	84	-13.1	-5.0	10.9	4.5	3.8	4.1	3.6	3.3	6.7	9.2	3.0	7.3	3.2	-.2	-2.3	.2	1.7	2.9	4.9	4.9	4.8	84	
	82	-13.1	-5.0	11.0	5.0	4.2	4.4	4.0	3.7	7.1	9.4	3.4	7.6	3.6	.2	-2.1	.3	1.7	2.9	4.9	4.9	4.9	82	
	80	-13.1	-5.0	11.0	5.4	4.6	4.8	4.4	4.2	7.4	9.6	3.8	7.9	4.0	.6	-1.8	.5	1.7	2.9	5.0	5.0	4.9	80	
	78	-13.2	-5.1	11.0	5.9	5.0	5.2	4.8	4.6	7.7	9.9	4.3	8.2	4.4	1.0	-1.5	.6	1.7	2.9	5.0	5.0	4.9	78	
	76	-13.2	-5.1	11.1	6.4	5.5	5.5	5.2	5.1	8.1	10.1	4.7	8.5	4.8	1.4	-1.2	.7	1.7	2.9	5.0	5.0	5.0	76	
	74	-13.2	-5.1	11.1	6.8	5.9	5.9	5.6	5.5	8.4	10.3	5.1	8.8	5.2	1.9	-.9	.8	1.7	2.9	5.0	5.1	5.0	74	
	72	-13.3	-5.1	11.1	7.2	6.3	6.3	6.0	5.9	8.7	10.5	5.6	9.1	5.6	2.3	-.6	1.0	1.7	2.9	5.1	5.1	5.1	72	
E	70	-13.4	-5.2	11.2	7.6	6.7	6.7	6.4	6.3	9.0	10.8	6.0	9.4	6.0	2.7	-.3	1.1	1.7	2.9	5.1	5.2	5.2	70	E
L	68	-13.4	-5.2	11.2	8.0	7.1	7.0	6.8	6.7	9.3	11.0	6.4	9.7	6.3	3.1	-.0	1.2	1.7	3.0	5.1	5.2	5.2	68	L
E	66	-13.5	-5.3	11.2	8.4	7.5	7.4	7.2	7.1	9.6	11.2	6.8	9.9	6.7	3.4	.2	1.3	1.7	3.0	5.1	5.2	5.3	66	E
V	64	-13.6	-5.3	11.2	8.8	7.8	7.8	7.5	7.5	9.9	11.4	7.2	10.2	7.1	3.8	.5	1.5	1.7	3.0	5.2	5.3	5.4	64	V
A	62	-13.7	-5.4	11.2	9.1	8.2	8.1	7.9	7.9	10.1	11.6	7.5	10.4	7.5	4.2	.7	1.6	1.7	3.0	5.2	5.3	5.4	62	A
T	60	-13.8	-5.5	11.2	9.5	8.5	8.4	8.2	8.2	10.4	11.8	7.9	10.7	7.8	4.5	1.0	1.7	1.7	3.0	5.2	5.4	5.5	60	T
I	58	-13.9	-5.6	11.2	9.8	8.9	8.8	8.6	8.6	10.6	11.9	8.2	10.9	8.1	4.9	1.2	1.7	1.7	3.0	5.2	5.4	5.5	58	I
O	56	-14.0	-5.6	11.2	10.1	9.2	9.1	8.9	8.9	10.9	12.1	8.6	11.1	8.5	5.2	1.4	1.8	1.6	3.0	5.2	5.4	5.6	56	O
N	54	-14.2	-5.8	11.1	10.4	9.5	9.4	9.2	9.2	11.1	12.2	8.9	11.3	8.8	5.5	1.6	1.9	1.6	3.0	5.2	5.5	5.6	54	N
	52	-14.3	-5.9	11.1	10.6	9.8	9.7	9.5	9.5	11.3	12.4	9.2	11.5	9.0	5.8	1.8	2.0	1.6	2.9	5.2	5.5	5.7	52	
A	50	-14.5	-6.0	11.0	10.9	10.0	9.9	9.7	9.7	11.4	12.5	9.4	11.6	9.3	6.1	2.0	2.0	1.5	2.9	5.2	5.5	5.7	50	A
N	48	-14.7	-6.1	11.0	11.1	10.3	10.2	10.0	10.0	11.6	12.6	9.7	11.7	9.6	6.3	2.1	2.0	1.4	2.8	5.2	5.5	5.7	48	N
G	46	-14.9	-6.3	10.9	11.3	10.5	10.4	10.2	10.2	11.7	12.6	9.9	11.9	9.8	6.5	2.3	2.0	1.3	2.8	5.1	5.5	5.8	46	G
L	44	-15.1	-6.5	10.8	11.4	10.7	10.6	10.4	10.4	11.8	12.7	10.1	11.9	10.0	6.7	2.4	2.0	1.2	2.7	5.1	5.4	5.7	44	L
E	42	-15.3	-6.7	10.6	11.6	10.8	10.7	10.6	10.5	11.9	12.7	10.2	12.0	10.1	6.9	2.5	2.0	1.1	2.6	5.0	5.4	5.7	42	E
	40	-15.6	-6.9	10.5	11.7	11.0	10.9	10.7	10.6	12.0	12.7	10.4	12.1	10.3	7.0	2.5	2.0	1.0	2.5	4.9	5.3	5.7	40	
I	38	-15.9	-7.1	10.3	11.7	11.1	11.0	10.8	10.7	12.0	12.7	10.5	12.1	10.4	7.2	2.5	1.9	.8	2.3	4.8	5.2	5.6	38	I
N	36	-16.2	-7.4	10.1	11.7	11.1	11.0	10.9	10.8	12.0	12.6	10.5	12.0	10.5	7.2	2.5	1.8	.6	2.2	4.6	5.1	5.5	36	N
	34	-16.5	-7.7	9.9	11.7	11.1	11.0	10.9	10.8	11.9	12.5	10.6	12.0	10.5	7.3	2.5	1.6	.4	2.0	4.5	4.9	5.4	34	
D	32	-16.9	-8.1	9.6	11.7	11.1	11.0	10.9	10.8	11.8	12.4	10.5	11.9	10.5	7.2	2.4	1.5	.2	1.8	4.3	4.7	5.2	32	D
E	30	-17.3	-8.4	9.3	11.6	11.0	11.0	10.8	10.7	11.7	12.2	10.5	11.7	10.4	7.2	2.3	1.3	-.1	1.5	4.0	4.5	5.0	30	E
G	28	-17.8	-8.8	9.0	11.4	10.9	10.8	10.7	10.6	11.5	12.0	10.4	11.5	10.3	7.1	2.1	1.0	-.4	1.2	3.7	4.2	4.7	28	G
R	26	-18.3	-9.3	8.6	11.2	10.7	10.7	10.5	10.4	11.3	11.7	10.2	11.3	10.1	6.9	1.9	.7	-.8	.8	3.4	3.9	4.4	26	R
E	24	-18.8	-9.8	8.1	10.9	10.5	10.4	10.3	10.1	11.0	11.4	9.9	11.0	9.9	6.7	1.6	.3	-1.2	.4	3.0	3.5	4.1	24	E
E	22	-19.5	-10.4	7.6	10.5	10.1	10.1	10.0	9.8	10.6	11.0	9.6	10.6	9.6	6.4	1.2	-.1	-1.7	-.1	2.5	3.1	3.6	22	E
S	20	-20.2	-11.1	7.0	10.1	9.7	9.7	9.6	9.4	10.1	10.5	9.2	10.1	9.2	6.0	.8	-.6	-2.3	-.6	2.0	2.6	3.1	20	S
	18	-21.0	-11.8	6.3	9.6	9.2	9.2	9.1	8.9	9.6	9.9	8.7	9.6	8.7	5.5	.2	-1.2	-2.9	-1.3	1.3	1.9	2.5	18	
	16	-21.9	-12.7	5.4	8.9	8.5	8.6	8.4	8.3	8.9	9.2	8.1	8.9	8.1	4.8	-.4	-1.9	-3.7	-2.1	.6	1.2	1.8	16	
	14	-22.9	-13.7	4.5	8.1	7.7	7.8	7.6	7.5	8.1	8.4	7.3	8.0	7.3	4.1	-1.3	-2.8	-4.7	-3.0	-.3	.3	.9	14	
	12	-22.0	-14.9	3.3	7.0	6.7	6.8	6.7	6.5	7.0	7.3	6.3	7.0	6.4	3.1	-2.3	-3.9	-5.8	-4.1	-1.4	-.8	-.2	12	
	10	-20.4	-16.3	1.9	5.7	5.5	5.5	5.4	5.2	5.8	6.0	5.1	5.7	5.1	1.9	-3.5	-5.2	-7.1	-5.4	-2.8	-2.1	-1.5	10	
	8	-18.5	-18.1	.2	4.1	3.9	3.9	3.8	3.6	4.1	4.4	3.5	4.1	3.5	.3	-5.2	-6.9	-8.9	-7.2	-4.5	-3.8	-3.2	8	
	6	-16.0	-16.0	-2.2	1.9	1.7	1.7	1.6	1.4	1.9	2.1	1.3	1.9	1.3	-1.9	-7.4	-9.1	-11.1	-9.4	-6.8	-6.1	-5.5	6	
	4	-12.5	-12.5	-5.5	-1.4	-1.6	-1.5	-1.6	-1.8	-1.4	-1.2	-1.9	-1.4	-1.9	-5.1	-10.6	-12.4	-12.5	-12.5	-10.1	-9.4	-8.8	4	
	2	-10.0	-10.0	-10.0	-7.2	-7.4	-7.3	-7.4	-7.6	-7.2	-7.0	-7.7	-7.2	-7.6	-10.0	-10.0	-10.0	-10.0	-10.0	-10.0	-10.0	-10.0	2	
	0	-10.0	-10.0	-10.0	-10.0	-10.0	-10.0	-10.0	-10.0	-10.0	-10.0	-10.0	-10.0	-10.0	-10.0	-10.0	-10.0	-10.0	-10.0	-10.0	-10.0	-10.0	0	
		2	3	4	5	6	7	8	9	10	11	12	13	14	16	18	20	22	24	26	28	30		

FREQUENCY IN MEGAHERTZ

ANTENNA EFFICIENCY

0.0	0.0	0.0	0.0	0.0	0.0	0.0	0.0	0.0	0.0	0.0	0.0	0.0	0.0	0.0	0.0	0.0	0.0	0.0	0.0	0.0
2	3	4	5	6	7	8	9	10	11	12	13	14	16	18	20	22	24	26	28	30

FREQUENCY IN MEGAHERTZ

Table 43. Tilted Dipole, Output Antenna Pattern

METHOD 13 IONCAP 78.03 PAGE 14

IONCAP 80.01 ANTENNA PACKAGE ANTENNA PATTERN

FREQUENCY RANGE	ANTENNA TYPE	HEIGHT	LENGTH	ANGLE	AZIMUTH	EX(1)	EX(2)	EX(3)	EX(4)	CONDUCT.	DIELECT.
1.0 TO 30.0	TLT DPOL	-.250	-.500	45.000	0.000	0.000	0.000	0.000	0.000	.001	4.000

		2	3	4	5	6	7	8	9	10	11	12	13	14	16	18	20	22	24	26	28	30		
	90	2.0	1.6	1.3	1.1	1.0	.9	.9	.8	.8	.8	.7	.7	.7	.7	.7	.7	.6	.6	.6	.6	.6	90	
	88	2.0	1.6	1.3	1.1	1.0	.9	.9	.8	.8	.8	.7	.7	.7	.7	.7	.7	.7	.6	.6	.5	.6	88	
	86	2.0	1.6	1.3	1.2	1.0	.9	.9	.8	.8	.8	.8	.7	.7	.7	.7	.7	.7	.7	.7	.6	.6	86	
	84	2.0	1.6	1.4	1.2	1.1	1.0	.9	.9	.8	.8	.8	.8	.7	.7	.7	.7	.7	.7	.7	.7	.7	84	
	82	2.1	1.7	1.4	1.2	1.1	1.0	.9	.9	.9	.8	.8	.8	.8	.8	.7	.7	.7	.7	.7	.7	.7	82	
	80	2.1	1.7	1.4	1.3	1.1	1.0	1.0	.9	.9	.9	.8	.8	.8	.8	.8	.8	.8	.7	.7	.7	.7	80	
	78	2.1	1.8	1.5	1.3	1.2	1.1	1.0	1.0	.9	.9	.9	.9	.9	.8	.8	.8	.8	.8	.8	.8	.8	78	
	76	2.2	1.8	1.5	1.4	1.2	1.2	1.1	1.0	1.0	1.0	.9	.9	.9	.9	.9	.9	.8	.8	.8	.8	.8	76	
	74	2.2	1.9	1.6	1.4	1.3	1.2	1.2	1.1	1.1	1.0	1.0	1.0	1.0	.9	.9	.9	.9	.9	.9	.9	.9	74	
	72	2.3	1.9	1.7	1.5	1.4	1.3	1.2	1.2	1.1	1.1	1.1	1.1	1.0	1.0	1.0	1.0	1.0	1.0	1.0	1.0	.9	72	
E	70	2.4	2.0	1.8	1.6	1.5	1.4	1.3	1.2	1.2	1.2	1.1	1.1	1.1	1.1	1.1	1.1	1.0	1.0	1.0	1.0	1.0	70	E
L	68	2.4	2.1	1.8	1.7	1.5	1.4	1.4	1.3	1.3	1.2	1.2	1.2	1.2	1.2	1.1	1.1	1.1	1.1	1.1	1.1	1.1	68	L
E	66	2.5	2.2	1.9	1.7	1.6	1.5	1.5	1.4	1.4	1.3	1.3	1.3	1.3	1.2	1.2	1.2	1.2	1.2	1.2	1.2	1.2	66	E
V	64	2.6	2.2	2.0	1.8	1.7	1.6	1.5	1.5	1.4	1.4	1.4	1.4	1.3	1.3	1.3	1.3	1.3	1.3	1.3	1.2	1.2	64	V
A	62	2.6	2.3	2.1	1.9	1.8	1.7	1.6	1.6	1.5	1.5	1.5	1.5	1.4	1.4	1.4	1.4	1.4	1.3	1.3	1.3	1.3	62	A
T	60	2.7	2.4	2.2	2.0	1.9	1.8	1.7	1.7	1.6	1.6	1.6	1.5	1.5	1.5	1.5	1.5	1.4	1.4	1.4	1.4	1.4	60	T
I	58	2.8	2.5	2.2	2.1	2.0	1.9	1.8	1.8	1.7	1.7	1.7	1.6	1.6	1.6	1.6	1.5	1.5	1.5	1.5	1.5	1.5	58	I
O	56	2.8	2.5	2.3	2.2	2.0	2.0	1.9	1.8	1.8	1.8	1.7	1.7	1.7	1.7	1.6	1.6	1.6	1.6	1.6	1.6	1.6	56	O
N	54	2.9	2.6	2.4	2.2	2.1	2.0	2.0	1.9	1.9	1.9	1.8	1.8	1.8	1.8	1.7	1.7	1.7	1.7	1.7	1.7	1.7	54	N
	52	2.9	2.7	2.5	2.3	2.2	2.1	2.1	2.0	2.0	1.9	1.9	1.9	1.9	1.8	1.8	1.8	1.8	1.8	1.8	1.8	1.8	52	
A	50	3.0	2.7	2.5	2.4	2.3	2.2	2.1	2.1	2.1	2.0	2.0	2.0	2.0	1.9	1.9	1.9	1.9	1.9	1.9	1.8	1.8	50	A
N	48	3.0	2.7	2.6	2.4	2.3	2.3	2.2	2.2	2.1	2.1	2.1	2.0	2.0	2.0	2.0	2.0	2.0	1.9	1.9	1.9	1.9	48	N
G	46	3.0	2.8	2.6	2.5	2.4	2.3	2.3	2.2	2.2	2.2	2.1	2.1	2.1	2.1	2.1	2.0	2.0	2.0	2.0	2.0	2.0	46	G
L	44	3.0	2.8	2.7	2.5	2.5	2.4	2.3	2.3	2.3	2.2	2.2	2.2	2.2	2.1	2.1	2.1	2.1	2.1	2.1	2.1	2.1	44	L
E	42	3.0	2.8	2.7	2.6	2.5	2.4	2.4	2.3	2.3	2.3	2.3	2.2	2.2	2.2	2.2	2.2	2.1	2.1	2.1	2.1	2.1	42	E
	40	3.0	2.8	2.7	2.6	2.5	2.5	2.4	2.4	2.3	2.3	2.3	2.3	2.3	2.2	2.2	2.2	2.2	2.2	2.2	2.2	2.2	40	
I	38	2.9	2.8	2.7	2.6	2.5	2.5	2.4	2.4	2.4	2.3	2.3	2.3	2.3	2.3	2.2	2.2	2.2	2.2	2.2	2.2	2.2	38	I
N	36	2.9	2.8	2.7	2.6	2.5	2.5	2.4	2.4	2.4	2.3	2.3	2.3	2.3	2.3	2.3	2.2	2.2	2.2	2.2	2.2	2.2	36	N
	34	2.8	2.7	2.6	2.5	2.5	2.4	2.4	2.4	2.3	2.3	2.3	2.3	2.3	2.3	2.2	2.2	2.2	2.2	2.2	2.2	2.2	34	
D	32	2.7	2.6	2.5	2.5	2.4	2.4	2.3	2.3	2.3	2.3	2.3	2.3	2.2	2.2	2.2	2.2	2.2	2.2	2.2	2.2	2.2	32	D
E	30	2.6	2.5	2.4	2.4	2.3	2.3	2.3	2.2	2.2	2.2	2.2	2.2	2.2	2.2	2.1	2.1	2.1	2.1	2.1	2.1	2.1	30	E
G	28	2.4	2.3	2.3	2.2	2.2	2.2	2.1	2.1	2.1	2.1	2.1	2.1	2.1	2.0	2.0	2.0	2.0	2.0	2.0	2.0	2.0	28	G
R	26	2.2	2.1	2.1	2.0	2.0	2.0	2.0	2.0	2.0	1.9	1.9	1.9	1.9	1.9	1.9	1.9	1.9	1.9	1.9	1.9	1.9	26	R
E	24	1.9	1.9	1.8	1.8	1.8	1.8	1.8	1.8	1.7	1.7	1.7	1.7	1.7	1.7	1.7	1.7	1.7	1.7	1.7	1.7	1.7	24	E
E	22	1.6	1.5	1.5	1.5	1.5	1.5	1.5	1.5	1.5	1.5	1.5	1.5	1.5	1.4	1.4	1.4	1.4	1.4	1.4	1.4	1.4	22	E
S	20	1.2	1.2	1.1	1.1	1.1	1.1	1.1	1.1	1.1	1.1	1.1	1.1	1.1	1.1	1.1	1.1	1.1	1.1	1.1	1.1	1.1	20	S
	18	.8	.7	.7	.7	.7	.7	.7	.7	.7	.7	.7	.7	.7	.7	.7	.7	.7	.7	.7	.7	.7	18	
	16	.2	.1	.1	.1	.1	.1	.2	.2	.2	.2	.2	.2	.2	.2	.2	.2	.2	.2	.2	.2	.2	16	
	14	-.5	-.6	-.6	-.6	-.6	-.5	-.5	-.5	-.5	-.5	-.5	-.5	-.5	-.5	-.5	-.5	-.5	-.5	-.5	-.5	-.5	14	
	12	-1.3	-1.5	-1.5	-1.4	-1.4	-1.4	-1.4	-1.4	-1.4	-1.4	-1.4	-1.4	-1.4	-1.3	-1.3	-1.3	-1.3	-1.3	-1.3	-1.3	-1.3	12	
	10	-2.4	-2.6	-2.6	-2.6	-2.5	-2.5	-2.5	-2.5	-2.5	-2.5	-2.5	-2.5	-2.4	-2.4	-2.4	-2.4	-2.4	-2.4	-2.4	-2.4	-2.4	10	
	8	-3.9	-4.0	-4.1	-4.0	-4.0	-4.0	-4.0	-3.9	-3.9	-3.9	-3.9	-3.9	-3.9	-3.9	-3.9	-3.9	-3.9	-3.9	-3.9	-3.9	-3.9	8	
	6	-5.8	-6.1	-6.1	-6.1	-6.0	-6.0	-6.0	-6.0	-5.9	-5.9	-5.9	-5.9	-5.9	-5.9	-5.9	-5.9	-5.9	-5.9	-5.8	-5.8	-5.8	6	
	4	-8.8	-9.1	-9.1	-9.1	-9.1	-9.0	-9.0	-9.0	-9.0	-8.9	-8.9	-8.9	-8.9	-8.9	-8.9	-8.9	-8.9	-8.9	-8.9	-8.9	-8.8	4	
	2	-10.0	-10.0	-10.0	-10.0	-10.0	-10.0	-10.0	-10.0	-10.0	-10.0	-10.0	-10.0	-10.0	-10.0	-10.0	-10.0	-10.0	-10.0	-10.0	-10.0	-10.0	2	
	0	-10.0	-10.0	-10.0	-10.0	-10.0	-10.0	-10.0	-10.0	-10.0	-10.0	-10.0	-10.0	-10.0	-10.0	-10.0	-10.0	-10.0	-10.0	-10.0	-10.0	-10.0	0	
		2	3	4	5	6	7	8	9	10	11	12	13	14	16	18	20	22	24	26	28	30		

FREQUENCY IN MEGAHERTZ

ANTENNA EFFICIENCY

0.0	0.0	0.0	0.0	0.0	0.0	0.0	0.0	0.0	0.0	0.0	0.0	0.0	0.0	0.0	0.0	0.0	0.0	0.0	0.0	0.0
2	3	4	5	6	7	8	9	10	11	12	13	14	16	18	20	22	24	26	28	30

FREQUENCY IN MEGAHERTZ

Table 44. Vertical Half Rhombic, Output Antenna Pattern

METHOD 13 IONCAP 78.03 PAGE 15

IONCAP 80.01 ANTENNA PACKAGE ANTENNA PATTERN

FREQUENCY RANGE	ANTENNA TYPE	HEIGHT	LENGTH	ANGLE	AZIMUTH	EX(1)	EX(2)	EX(3)	EX(4)	CONDUCT.	DIELECT.
1.0 TO 30.0	VER HRHM	0.000	120.000	27.500	0.000	0.000	0.000	0.000	0.000	.001	4.000

	2	3	4	5	6	7	8	9	10	11	12	13	14	16	18	20	22	24	26	28	30	
90	-3.1	-6.7	-11.3	-22.5	-3.8	-4.2	-5.8	-18.8	-14.3	-2.9	-5.3	-7.0	-16.7	-2.7	-9.8	-6.1	-6.7	-9.9	-4.5	-12.7	-3.0	90
88	-3.3	-5.3	-8.4	-23.5	-4.4	-5.1	-3.5	-11.0	-16.7	-4.5	-5.3	-3.4	-11.4	-5.3	-4.3	-10.9	-2.9	-9.1	-7.6	-6.3	-10.7	88
86	-3.7	-3.9	-6.3	-15.2	-6.0	-6.9	-1.9	-6.7	-10.7	-10.0	-6.1	-2.2	-5.0	-21.8	-3.8	-10.4	-5.1	-2.5	-12.5	-4.2	-5.1	86
84	-4.2	-2.7	-4.9	-11.0	-9.3	-8.7	-1.2	-4.8	-6.2	-27.4	-7.5	-3.8	-2.5	-8.5	-8.9	-4.1	-21.2	-4.2	-4.4	-12.8	-2.0	84
82	-4.9	-1.5	-4.0	-3.0	-16.3	-9.7	-1.6	-3.8	-3.1	-8.6	-12.1	-10.1	-1.9	-2.9	-12.9	-3.5	-3.5	-20.1	-4.7	-5.0	-21.2	82
80	-5.6	-.6	-3.5	-5.4	-22.0	-10.3	-3.5	-2.8	-1.8	-4.0	-12.4	-17.3	-4.2	-1.0	-7.1	-6.3	-.9	-4.1	-10.0	-1.8	-2.6	80
78	-6.5	.2	-3.5	-3.1	-11.8	-11.5	-7.5	-2.1	-2.2	-1.3	-5.8	-8.2	-15.0	-2.6	-2.9	-17.4	-4.7	-1.6	-7.2	-9.4	-1.6	78
76	-7.6	.9	-3.6	-1.3	-7.6	-11.9	-17.1	-2.6	-4.0	.2	-3.0	-3.6	-9.9	-10.5	-2.7	-3.3	-14.9	-6.5	-1.9	-4.4	-19.7	76
74	-8.7	1.3	-2.8	.2	-5.0	-8.8	-17.2	-5.0	-6.1	.1	-1.5	-1.1	-2.9	-12.2	-3.7	-.0	-2.3	-10.8	-2.2	.4	-2.9	74
72	-9.7	1.6	-3.6	1.1	-3.0	-5.3	-8.8	-11.6	-7.0	-2.1	-.3	-.9	.2	-5.2	-7.6	-.4	.2	-4.5	-22.4	-4.5	-1.4	72
E 70	-10.4	1.7	-2.9	1.7	-1.1	-2.8	-4.7	-20.2	-8.5	-7.9	-.3	-2.3	1.4	-1.4	-12.7	-9.2	-2.7	-.6	-1.6	-8.5	-5.0	70 E
L 68	-10.5	1.7	-1.8	1.8	.7	-1.5	-1.8	-7.4	-11.4	-18.5	-3.0	-3.1	.1	-.3	-2.1	-7.5	-7.9	.1	1.8	-.9	-10.7	68 L
E 66	-10.1	1.5	-.6	1.4	2.3	-.7	.5	-2.8	-8.2	-8.9	-12.1	-3.9	-4.6	-.4	1.6	-.4	-9.6	-6.3	-1.9	-.0	1.0	66 E
V 64	-9.2	1.1	.6	.6	3.5	-.1	2.0	.1	-3.4	-4.1	-11.5	-8.8	-10.4	-.1	2.9	1.7	-1.7	-5.6	-11.1	-1.1	2.2	64 V
A 62	-8.2	.4	1.5	-.4	4.2	1.0	2.6	2.4	-.6	-.8	-2.9	-12.8	-8.7	-2.3	.6	.8	2.3	1.8	-3.9	-26.0	-10.0	62 A
T 60	-7.1	-.4	2.2	-1.4	4.3	2.5	2.5	4.1	1.5	1.3	1.0	-3.0	-5.3	-15.9	-8.2	.1	3.8	3.2	1.5	.9	-3.7	60 T
I 58	-6.2	-1.4	2.7	-1.3	4.0	3.9	2.0	5.0	3.5	2.4	3.4	1.4	-1.0	-4.8	-8.6	-2.1	.3	1.0	4.2	4.3	1.6	58 I
O 56	-5.4	-2.8	2.9	-1.2	3.2	4.9	1.9	5.0	5.3	3.1	4.7	4.3	2.0	1.7	-3.3	-25.3	-13.2	-.0	3.0	2.3	4.7	56 O
N 54	-4.7	-4.4	2.8	-.1	1.8	5.4	2.9	4.2	6.4	4.3	4.8	6.2	4.4	4.7	1.0	-.3	-4.2	-10.7	-9.4	.8	3.7	54 N
52	-4.1	-6.4	2.4	1.1	-.0	5.3	4.2	3.0	6.5	6.0	4.4	6.8	6.5	6.0	4.3	4.7	.6	-.8	-4.2	-11.0	-9.9	52
A 50	-3.6	-8.7	1.8	1.9	-1.6	4.5	5.2	2.4	5.7	7.1	5.0	6.1	7.9	6.0	7.1	6.6	5.0	5.3	1.3	1.2	-3.4	50 A
N 48	-3.2	-11.0	.9	2.5	-2.0	3.0	5.6	3.2	3.9	7.2	6.4	5.0	7.6	6.4	8.8	6.9	8.2	7.2	6.6	6.3	3.6	48 N
G 46	-2.9	-11.8	-.4	2.6	-1.0	.7	5.2	4.5	2.2	6.1	7.4	5.3	6.0	8.0	8.4	8.1	9.5	8.0	9.6	7.8	8.9	46 G
L 44	-2.7	-10.5	-2.1	2.4	.3	-2.0	4.1	5.2	2.3	3.8	7.1	6.7	4.7	8.8	6.8	9.7	8.4	10.1	9.5	10.1	10.0	44 L
E 42	-2.5	-8.5	-4.5	1.8	1.2	-3.6	1.9	5.0	3.6	1.3	5.4	7.1	5.5	7.6	7.1	9.2	8.3	10.3	9.2	11.1	9.9	42 E
40	-2.4	-6.7	-7.6	.7	1.7	-2.7	-1.4	3.9	4.4	1.3	2.2	6.1	6.6	4.6	8.2	6.4	9.6	7.8	10.7	9.0	11.5	40
I 38	-2.4	-5.2	-12.6	-.9	1.6	-1.0	-5.4	1.5	4.1	2.7	-.7	3.1	6.0	2.9	7.3	5.7	8.2	7.9	8.8	9.7	9.3	38 I
N 36	-2.4	-4.0	-17.4	-3.3	1.0	.2	-5.9	-2.7	2.6	3.3	.4	-1.7	3.3	4.3	3.4	6.9	3.9	8.4	5.7	9.0	8.0	36 N
34	-2.4	-3.0	-12.1	-7.1	-.4	.6	-3.0	-9.6	-.8	2.5	1.9	-2.5	-2.6	4.4	-.6	5.1	4.0	4.3	6.9	3.8	8.2	34
D 32	-2.4	-2.2	-7.6	-14.6	-2.6	.2	-1.0	-7.7	-8.3	-.4	1.7	.2	-5.7	1.3	1.6	-2.1	4.3	-.7	3.9	4.4	1.5	32 D
E 30	-2.5	-1.5	-4.7	-20.9	-5.6	-1.2	-.2	-2.8	-13.0	-7.9	-1.1	.6	-1.1	-9.8	1.2	-4.0	-1.8	1.9	-7.6	1.8	1.3	30 E
G 28	-2.6	-1.0	-2.6	-9.0	-16.2	-4.0	-.7	-.6	-3.4	-13.3	-10.1	-2.5	-.3	-5.0	-6.7	-.1	-7.4	-4.4	-.2	-10.9	-2.7	28 G
R 26	-2.8	-.6	-1.0	-4.2	-14.7	-10.3	-2.7	-.1	.1	-2.1	-8.5	-16.7	-4.1	.7	-5.0	-5.8	1.1	-2.6	-7.9	1.4	-.8	26 R
E 24	-3.0	-.3	.2	-1.2	-5.4	-19.3	-7.4	-1.3	1.1	1.6	.3	-3.6	-11.6	.5	3.0	-2.4	-1.2	4.2	2.4	-2.2	4.6	24 E
E 22	-3.2	-.2	1.1	.8	-1.0	-5.5	-13.6	-4.7	.4	2.8	3.6	2.9	.6	-3.0	4.4	5.5	1.5	3.1	7.2	6.6	3.4	22 E
S 20	-3.5	-.1	1.7	2.3	1.8	-.2	-4.2	-7.6	-2.0	2.2	4.6	5.6	5.5	1.9	2.6	7.4	8.0	5.4	6.2	9.6	10.0	20 S
18	-3.8	-.1	2.1	3.4	3.7	3.1	1.3	-1.7	-3.3	.2	3.8	6.2	7.4	7.2	4.4	6.0	9.6	10.4	8.8	8.4	11.1	18
16	-4.2	-.3	2.3	4.0	5.0	5.2	4.7	3.3	1.2	.0	2.0	5.0	7.3	9.6	9.1	7.1	8.2	11.2	12.4	11.7	10.4	16
14	-4.8	-.6	2.3	4.4	5.8	6.6	6.9	6.5	5.6	4.1	3.0	3.5	5.6	9.6	11.3	11.1	9.5	9.3	11.7	13.5	13.7	14
12	-5.4	-1.1	2.0	4.4	6.2	7.4	8.2	8.5	8.4	7.8	6.9	5.8	5.2	7.6	10.9	12.6	12.7	11.6	10.1	10.8	12.8	12
10	-6.4	-1.9	1.4	4.1	6.1	7.7	8.8	9.6	10.1	10.2	9.9	9.4	8.5	6.9	8.1	10.9	12.8	13.6	13.1	11.4	9.1	10
8	-7.6	-3.0	.4	3.2	5.5	7.3	8.7	9.9	10.7	11.3	11.6	11.6	11.4	10.2	8.2	7.0	8.6	10.9	12.3	12.7	12.1	8
6	-9.4	-4.8	-1.2	1.7	4.1	6.1	7.8	9.2	10.3	11.1	11.8	12.3	12.5	12.5	11.6	9.9	7.0	3.3	2.1	4.6	6.6	6
4	-12.1	-7.5	-3.9	-.9	1.6	3.7	5.5	7.1	8.4	9.4	10.3	11.1	11.6	12.4	12.5	12.2	11.4	10.2	8.8	7.4	6.3	4
2	-11.7	-11.7	-9.1	-6.1	-3.5	-1.3	.6	2.2	3.6	4.8	5.8	6.7	7.4	8.5	9.3	9.6	9.8	9.9	10.0	10.3	10.8	2
0	-11.7	-11.7	-11.7	-11.7	-11.7	-11.7	-11.7	-11.7	-11.7	-11.7	-11.7	-11.7	-11.7	-11.7	-11.7	-11.7	-11.7	-11.7	-11.7	-11.7	-11.7	0
	2	3	4	5	6	7	8	9	10	11	12	13	14	16	18	20	22	24	26	28	30	

FREQUENCY IN MEGAHERTZ

ANTENNA EFFICIENCY

-1.7	-1.7	-1.7	-1.7	-1.7	-1.7	-1.7	-1.7	-1.7	-1.7	-1.7	-1.7	-1.7	-1.7	-1.7	-1.7	-1.7	-1.7	-1.7	-1.7	-1.7
2	3	4	5	6	7	8	9	10	11	12	13	14	16	18	20	22	24	26	28	30

FREQUENCY IN MEGAHERTZ

Table 45. Horizontal Double Rhombic, Output Antenna Pattern

METHOD 13 IONCAP 78.03 PAGE 16

IONCAP 80.01 ANTENNA PACKAGE ANTENNA PATTERN

FREQUENCY RANGE	ANTENNA TYPE	HEIGHT	LENGTH	ANGLE	AZIMUTH	EX(1)	EX(2)	EX(3)	EX(4)	CONDUCT.	DIELECT.
1.0 TO 30.0	HORZ DRHM	62.000	150.000	0.000	0.000	25.500	17.500	214.800	62.000	.001	4.000

		2	3	4	5	6	7	8	9	10	11	12	13	14	16	18	20	22	24	26	28	30		
	90	-37.3	-1.2	-37.3	1.0	-37.3	-26.5	-37.3	3.8	-37.3	-2.7	-37.3	4.4	-37.3	-29.7	-37.3	-29.7	-34.2	-36.0	-28.0	-37.3	-23.8	90	
	88	-20.0	-6.2	-12.3	1.2	-10.1	-7.5	-2.3	.0	-17.0	4.3	-6.4	-23.6	-2.7	-7.9	4.3	-4.2	-2.2	-.7	-18.2	5.7	1.6	88	
	86	-14.2	-24.0	-3.8	-.5	-21.6	-3.6	2.5	-19.7	-.3	-1.0	-18.0	-7.4	2.9	3.9	-7.8	3.8	-3.1	-13.9	-1.6	-7.1	-20.1	86	
	84	-11.1	-9.1	1.0	-4.4	-3.3	-5.3	.2	-14.2	3.0	-23.1	-3.0	-1.9	-11.9	2.1	-2.0	-34.0	-17.2	-4.4	-2.7	-3.4	5.7	84	
	82	-9.3	-3.2	3.8	-12.3	4.4	-15.4	-24.7	-7.0	-1.3	-4.4	-2.4	-3.9	-8.0	-28.5	-3.4	2.4	-1.6	-19.0	1.2	2.4	-11.0	82	
	80	-8.5	-.6	5.3	-37.3	7.7	-16.6	.8	2.2	-29.7	6.7	-20.2	1.5	-2.9	4.9	1.5	-19.3	-5.8	-8.4	-4.4	-1.0	-17.8	80	
	78	-8.5	.2	5.5	-33.5	8.2	-19.8	2.3	1.7	-21.1	7.1	-16.8	3.5	-5.3	4.9	3.7	-10.2	-8.1	-3.4	-12.1	.5	-5.9	78	
	76	-9.5	-.2	4.2	-16.6	5.2	-7.4	-3.5	-31.5	-6.7	-3.2	1.8	-13.4	3.4	-6.7	-21.0	-12.3	-.2	4.3	-3.5	-1.9	-.4	76	
	74	-12.3	-2.0	.9	-7.3	1.0	1.9	-21.0	2.8	-1.8	-11.2	4.9	-12.1	4.1	-8.9	2.7	.4	-2.9	-5.8	-.5	-11.0	-15.5	74	
	72	-20.5	-5.9	-8.2	-2.8	-11.2	5.8	-13.5	4.3	-7.6	-4.3	-2.9	2.9	-20.9	-.7	-1.5	-6.4	-5.3	4.8	1.9	-19.9	-.3	72	
E	70	-18.8	-15.0	-8.1	-.6	-23.6	6.4	-8.0	-3.5	-6.5	4.3	-13.2	2.4	-.2	1.1	-12.2	-2.1	5.1	-2.3	-4.4	.8	-.0	70	E
L	68	-8.2	-16.7	.7	.1	-11.6	3.7	1.3	-10.1	.7	-.4	-2.4	-11.4	8.9	1.4	-6.1	6.4	2.5	-9.8	-5.5	-3.2	-4.4	68	L
E	66	-2.8	-7.7	3.8	-.8	.5	-4.2	3.5	-27.8	-2.5	-4.3	6.1	-25.6	4.9	-19.5	-20.5	-16.5	.3	.7	-10.5	4.9	5.2	66	E
V	64	1.1	-4.8	4.5	-4.2	5.4	-36.4	2.0	3.9	-18.7	1.1	-.6	-1.5	-29.2	-3.0	5.5	-4.0	4.4	-5.0	-9.8	-16.2	-1.3	64	V
A	62	4.0	-4.2	3.3	-18.1	7.1	-12.8	-2.4	9.3	-22.4	-5.8	2.8	3.2	-8.4	5.2	-1.0	-9.6	-26.5	2.8	6.6	-23.0	-7.5	62	A
T	60	6.5	-5.4	-.6	-5.9	6.1	2.4	-12.6	9.1	4.1	-21.6	5.3	-15.0	-.4	.6	.7	3.1	-7.7	4.4	1.6	-1.9	-16.6	60	T
I	58	8.5	-8.8	-12.9	.9	2.2	8.6	-29.9	4.2	11.1	-16.8	-6.1	6.3	-7.5	-15.5	9.2	-5.7	-9.1	-10.9	2.3	.7	2.6	58	I
O	56	10.2	-17.6	-5.9	3.5	-7.4	10.9	-4.1	-7.2	11.8	4.3	-19.7	3.5	.5	4.9	2.7	-1.2	6.1	-8.1	-7.1	6.4	3.9	56	O
N	54	11.6	-18.6	.6	3.3	-12.2	10.1	6.1	-24.1	7.4	10.8	-4.9	-22.4	4.3	4.2	-12.7	8.7	2.0	-3.8	-6.4	2.7	.8	54	N
	52	12.8	-9.2	2.6	-.3	-4.1	5.6	10.8	-7.9	-3.9	11.1	4.1	-4.6	-7.5	-2.4	-.7	5.3	4.9	.4	-.2	-5.5	-.2	52	
A	50	13.9	-4.7	1.9	-17.2	-1.1	-10.9	11.7	2.8	-11.3	5.6	8.7	5.4	-4.9	-.0	1.3	.9	1.0	7.5	1.2	-4.8	3.7	50	A
N	48	14.7	-.9	-2.0	-1.4	-.2	-.8	8.6	8.8	-1.3	-5.1	7.5	5.1	8.6	-8.1	1.3	1.0	2.0	8.6	1.2	-1.1	1.1	48	N
G	46	15.3	2.9	-17.9	4.0	-3.3	1.6	-4.5	10.6	2.5	.3	.4	4.7	9.8	-2.9	4.5	-11.0	5.6	2.8	6.3	10.0	-16.1	46	G
L	44	15.8	6.5	-3.3	5.1	-17.8	-1.1	2.7	7.3	6.4	6.3	1.1	1.5	3.6	10.3	-2.6	.1	-4.0	1.1	7.9	1.1	11.9	44	L
E	42	16.2	9.6	2.5	2.7	.6	-5.8	6.1	-10.1	7.7	5.6	8.8	2.0	-.6	13.9	-1.3	3.1	-6.3	-6.8	7.3	4.8	7.0	42	E
	40	16.4	12.2	4.7	-9.4	5.1	-16.9	3.3	6.6	.8	3.9	10.4	10.0	2.4	9.9	9.3	6.7	-5.4	-2.2	-23.0	12.8	-.9	40	
I	38	16.5	14.3	5.0	1.1	5.2	-2.2	-5.3	8.3	3.1	2.1	5.4	12.9	10.7	1.0	13.0	6.1	8.6	-18.8	-1.1	-10.8	13.3	38	I
N	36	16.4	16.0	4.9	8.0	-1.4	4.1	-13.6	3.8	9.3	-2.0	-.5	9.3	14.1	2.4	10.9	6.7	13.2	5.0	-4.7	-3.1	3.7	36	N
	34	16.2	17.4	7.2	10.7	.4	4.6	-2.3	-8.4	7.6	8.6	-4.8	-1.3	11.0	11.8	7.3	11.2	5.3	15.5	2.1	2.9	-5.7	34	
D	32	15.9	18.4	11.2	11.2	10.1	-4.8	3.2	-7.9	-1.7	8.7	7.2	-4.3	-.2	14.4	4.6	13.5	6.2	10.0	15.5	9.2	3.2	32	D
E	30	15.4	19.1	14.8	9.6	13.9	5.7	1.1	-1.0	-6.4	1.0	8.3	5.8	-3.0	9.3	12.4	10.6	15.4	-.6	10.2	14.4	14.6	30	E
G	28	14.8	19.5	17.5	7.8	15.1	13.6	-.1	.6	-5.1	-4.5	.8	6.8	4.4	-.6	10.7	8.0	16.4	16.0	-.8	6.5	13.1	28	G
R	26	14.1	19.7	19.5	11.8	13.8	16.9	12.6	-3.6	-2.2	-5.7	-2.7	-1.7	3.9	-1.4	1.3	8.5	5.0	19.6	17.1	1.2	-7.0	26	R
E	24	13.3	19.6	20.8	16.6	10.0	17.5	17.6	12.3	-2.1	-6.8	-5.4	-1.2	-3.8	-2.9	.9	-.2	3.4	6.1	21.3	19.6	3.3	24	E
E	22	12.4	19.3	21.7	19.9	11.8	15.2	19.3	18.3	13.2	2.5	-18.5	-6.5	-.7	-3.8	-6.4	2.5	4.2	-18.3	4.3	21.8	22.9	22	E
S	20	11.3	18.8	22.2	22.1	18.0	10.1	18.0	20.5	19.3	15.2	7.8	-5.4	-8.9	1.5	5.1	1.1	3.3	9.7	6.3	-.2	19.7	20	S
	18	10.1	18.1	22.2	23.5	21.9	16.2	12.3	19.3	21.4	20.7	17.8	13.0	5.4	-3.1	5.4	11.5	6.5	3.6	12.3	14.5	-16.1	18	
	16	8.7	17.2	22.0	24.2	24.3	22.0	15.8	12.9	19.6	22.0	22.0	20.5	17.6	6.2	-1.0	9.3	16.0	12.6	3.2	10.9	18.3	16	
	14	7.2	16.1	21.4	24.4	25.7	25.3	22.9	17.6	11.8	18.4	21.8	22.9	22.6	19.0	9.5	-.6	10.7	18.8	18.0	5.6	4.0	14	
	12	5.5	14.7	20.4	24.1	26.2	27.0	26.6	24.8	21.2	14.7	14.2	19.5	22.2	23.5	21.3	13.9	-1.9	5.9	18.4	20.8	14.3	12	
	10	3.6	13.0	19.1	23.3	26.0	27.7	28.4	28.3	27.2	25.1	21.7	15.4	12.8	20.9	23.8	23.0	17.3	-.9	11.8	4.2	16.8	10	
	8	1.3	11.0	17.4	21.9	25.2	27.4	28.9	29.7	29.8	29.5	28.5	27.1	24.9	17.8	13.7	20.6	21.9	17.5	7.4	20.8	22.2	8	
	6	-1.4	8.4	15.0	19.8	23.4	26.1	28.1	29.4	30.3	30.8	31.0	30.8	30.3	28.8	26.2	21.7	12.4	7.9	8.4	9.4	21.2	6	
	4	-5.1	4.8	11.6	16.6	20.4	23.4	25.7	27.5	28.8	29.8	30.5	30.9	31.2	31.4	31.2	30.6	29.2	26.3	20.6	4.3	11.2	4	
	2	-11.2	-1.2	5.7	10.9	14.8	17.9	20.4	22.4	23.9	25.2	26.1	26.9	27.5	28.5	29.2	29.7	29.7	28.7	25.8	18.3	12.4	2	
	0	-11.7	-11.7	-11.7	-11.7	-11.7	-11.7	-11.7	-11.7	-11.7	-11.7	-11.7	-11.7	-11.7	-11.7	-11.7	-11.7	-11.7	-11.7	-11.7	-11.7	-11.7	0	
		2	3	4	5	6	7	8	9	10	11	12	13	14	16	18	20	22	24	26	28	30		

FREQUENCY IN MEGAHERTZ

ANTENNA EFFICIENCY

2	3	4	5	6	7	8	9	10	11	12	13	14	16	18	20	22	24	26	28	30
-1.7	-1.7	-1.7	-1.7	-1.7	-1.7	-1.7	-1.7	-1.7	-1.7	-1.7	-1.7	-1.7	-1.7	-1.7	-1.7	-1.7	-1.7	-1.7	-1.7	-1.7

FREQUENCY IN MEGAHERTZ

Table 46. Log Periodic Array of Vertical Dipoles, Output Antenna Pattern

METHOD 13 IONCAP 78.03 PAGE 17

IONCAP 80.01 ANTENNA PACKAGE — ANTENNA PATTERN

FREQUENCY RANGE	ANTENNA TYPE	HEIGHT	LENGTH	ANGLE	AZIMUTH	EX(1)	EX(2)	EX(3)	EX(4)	CONDUCT.	DIELECT.
1.0 TO 30.0	VER LPD	3.000	15.000	90.000	0.000	0.000	12.500	.870	12.000	.001	4.000

		2	3	4	5	6	7	8	9	10	11	12	13	14	16	18	20	22	24	26	28	30		
	90	-35.6	-35.6	-35.6	-35.6	-35.6	-35.6	-35.6	-35.6	-35.6	-35.6	-35.6	-35.6	-35.5	-35.6	-35.6	-35.6	-35.5	-35.6	-35.6	-35.6	-35.6	90	
	88	-35.6	-35.6	-35.6	-35.6	-35.6	-30.4	-27.0	-24.6	-23.8	-23.4	-21.4	-22.7	-19.5	-18.4	-17.9	-20.5	-19.9	-20.9	-25.3	-24.1	-26.1	88	
	86	-35.6	-35.6	-35.6	-35.6	-35.4	-24.3	-20.9	-18.5	-17.5	-16.9	-15.1	-16.1	-13.1	-12.0	-11.6	-13.8	-13.4	-14.5	-18.6	-17.6	-19.5	86	
	84	-35.6	-35.6	-35.5	-33.3	-31.8	-20.8	-17.3	-14.8	-13.7	-12.9	-11.2	-12.0	-9.2	-8.1	-7.7	-9.7	-9.4	-10.5	-14.5	-13.7	-15.5	84	
	82	-35.6	-35.6	-33.0	-30.8	-29.3	-18.2	-14.8	-12.1	-10.9	-10.1	-8.4	-9.0	-6.4	-5.2	-4.9	-6.7	-6.4	-7.6	-11.3	-10.8	-12.6	82	
	80	-35.6	-34.6	-31.1	-28.3	-27.3	-16.2	-12.7	-10.0	-8.7	-7.8	-6.2	-6.7	-4.2	-3.0	-2.7	-4.2	-4.0	-5.2	-8.7	-8.5	-10.3	80	
	78	-35.6	-33.0	-29.5	-27.2	-25.7	-14.6	-11.0	-8.3	-6.9	-5.9	-4.4	-4.7	-2.3	-1.2	-.8	-2.2	-1.9	-3.1	-6.4	-6.5	-8.4	78	
	76	-35.6	-31.7	-28.2	-25.8	-24.3	-13.2	-9.6	-6.8	-5.3	-4.2	-2.8	-3.0	-.8	.4	.8	-.4	-.2	-1.3	-4.4	-4.7	-6.8	76	
	74	-35.6	-30.5	-27.0	-24.6	-23.1	-11.9	-8.3	-5.5	-3.9	-2.8	-1.5	-1.5	.6	1.8	2.2	1.2	1.4	.3	-2.6	-3.1	-5.4	74	
	72	-35.2	-29.5	-26.0	-23.6	-22.0	-10.8	-7.1	-4.3	-2.7	-1.5	-.3	-.2	1.8	3.0	3.4	2.7	2.9	1.8	-.8	-1.6	-4.1	72	
E	70	-34.3	-28.7	-25.1	-22.6	-21.0	-9.8	-6.1	-3.2	-1.6	-.4	.7	.9	2.8	4.1	4.5	4.0	4.2	3.2	.8	-.1	-2.8	70	E
L	68	-33.6	-27.9	-24.2	-21.8	-20.1	-8.9	-5.1	-2.2	-.6	.6	1.6	2.0	3.7	5.0	5.5	5.1	5.4	4.4	2.3	1.3	-1.6	68	L
F	66	-32.9	-27.1	-23.5	-21.0	-19.3	-8.0	-4.2	-1.2	.4	1.6	2.5	2.9	4.6	5.8	6.3	6.2	6.5	5.6	3.7	2.7	-.4	66	E
V	64	-32.2	-26.5	-22.8	-20.3	-18.5	-7.2	-3.3	-.3	1.3	2.5	3.3	3.7	5.3	6.6	7.1	7.2	7.5	6.7	5.0	4.0	.8	64	V
A	62	-31.7	-25.9	-22.2	-19.6	-17.8	-6.4	-2.5	.5	2.2	3.3	4.0	4.5	5.9	7.3	7.8	8.0	8.4	7.7	6.3	5.3	2.1	62	A
T	60	-31.1	-25.4	-21.6	-19.0	-17.1	-5.7	-1.7	1.3	3.0	4.1	4.7	5.2	6.5	7.8	8.4	8.8	9.2	8.6	7.5	6.6	3.4	60	T
I	58	-30.7	-24.9	-21.1	-18.4	-16.5	-5.0	-1.0	2.1	3.8	4.9	5.3	5.8	7.1	8.4	9.0	9.5	10.0	9.5	8.6	7.7	4.7	58	I
O	56	-30.2	-24.4	-20.6	-17.8	-15.9	-4.4	-.2	2.9	4.6	5.6	5.9	6.4	7.6	8.8	9.4	10.2	10.7	10.2	9.6	8.8	6.0	56	O
N	54	-29.8	-24.0	-20.1	-17.3	-15.3	-3.7	.4	3.6	5.3	6.3	6.5	7.0	8.0	9.2	9.8	10.7	11.3	10.9	10.5	9.9	7.2	54	N
	52	-29.5	-23.6	-19.7	-16.9	-14.8	-3.1	1.1	4.4	6.1	7.1	7.1	7.6	8.5	9.6	10.2	11.2	11.8	11.5	11.3	10.8	8.3	52	
A	50	-29.1	-23.2	-19.3	-16.4	-14.3	-2.6	1.7	5.1	6.8	7.8	7.7	8.2	8.9	9.9	10.5	11.6	12.2	12.0	12.0	11.6	9.4	50	A
N	48	-28.8	-22.9	-18.9	-16.0	-13.8	-2.1	2.3	5.7	7.5	8.5	8.3	8.7	9.3	10.2	10.7	11.9	12.6	12.5	12.7	12.4	10.4	48	N
G	46	-28.6	-22.6	-18.6	-15.6	-13.4	-1.6	2.9	6.4	8.2	9.2	8.9	9.3	9.8	10.5	10.9	12.2	12.9	12.8	13.2	13.0	11.2	46	G
L	44	-28.3	-22.4	-18.3	-15.2	-13.0	-1.1	3.4	7.0	8.9	9.9	9.6	9.9	10.3	10.8	11.1	12.4	13.1	13.1	13.6	13.5	12.0	44	L
E	42	-28.1	-22.2	-18.1	-15.0	-12.6	-.7	3.9	7.6	9.5	10.5	10.2	10.5	10.8	11.2	11.4	12.6	13.3	13.3	14.0	13.9	12.6	42	E
	40	-28.0	-22.0	-17.8	-14.7	-12.3	-.3	4.4	8.1	10.1	11.2	10.8	11.2	11.3	11.5	11.6	12.8	13.4	13.5	14.2	14.2	13.0	40	
I	38	-27.8	-21.8	-17.6	-14.5	-12.0	.0	4.8	8.6	10.7	11.8	11.4	11.8	11.8	11.9	11.9	13.0	13.5	13.6	14.4	14.5	13.4	38	I
N	36	-27.7	-21.7	-17.5	-14.3	-11.7	.4	5.2	9.1	11.3	12.4	12.0	12.4	12.4	12.4	12.2	13.3	13.7	13.7	14.5	14.6	13.6	36	N
	34	-27.6	-21.6	-17.4	-14.1	-11.5	.6	5.5	9.5	11.7	12.9	12.5	13.0	12.9	12.9	12.6	13.6	13.9	13.8	14.6	14.7	13.8	34	
D	32	-27.6	-21.5	-17.3	-14.0	-11.3	.9	5.8	9.8	12.2	13.4	13.0	13.5	13.4	13.4	13.0	14.0	14.1	13.9	14.8	14.8	13.9	32	D
E	30	-27.5	-21.5	-17.2	-13.9	-11.2	1.0	6.1	10.2	12.6	13.8	13.5	14.0	13.9	13.9	13.4	14.4	14.4	14.2	15.0	14.9	14.0	30	E
G	28	-27.6	-21.5	-17.2	-13.9	-11.1	1.2	6.3	10.4	12.9	14.2	13.9	14.5	14.4	14.3	13.9	14.8	14.9	14.5	15.2	15.1	14.2	28	G
R	26	-27.6	-21.6	-17.2	-13.9	-11.1	1.2	6.4	10.6	13.1	14.5	14.2	14.9	14.8	14.8	14.4	15.3	15.3	14.9	15.6	15.4	14.4	26	R
E	24	-27.7	-21.7	-17.4	-13.9	-11.1	1.3	6.5	10.7	13.3	14.7	14.5	15.2	15.1	15.2	14.8	15.8	15.8	15.4	16.1	15.8	14.8	24	E
E	22	-27.1	-21.9	-17.5	-14.1	-11.2	1.2	6.4	10.8	13.4	14.9	14.6	15.4	15.3	15.4	15.1	16.2	16.2	15.8	16.6	16.3	15.4	22	E
S	20	-26.3	-22.1	-17.7	-14.3	-11.4	1.0	6.3	10.7	13.4	14.9	14.7	15.5	15.5	15.6	15.4	16.5	16.6	16.2	17.1	16.8	15.9	20	S
	18	-25.4	-22.4	-18.1	-14.6	-11.7	.8	6.1	10.6	13.3	14.9	14.7	15.5	15.5	15.7	15.5	16.7	16.8	16.6	17.5	17.3	16.4	18	
	16	-24.4	-22.9	-18.5	-15.0	-12.1	.5	5.8	10.3	13.1	14.7	14.5	15.4	15.4	15.7	15.5	16.8	17.0	16.7	17.7	17.6	16.9	16	
	14	-23.3	-23.3	-19.0	-15.5	-12.6	-.0	5.4	9.8	12.7	14.3	14.1	15.1	15.1	15.4	15.3	16.7	16.9	16.7	17.8	17.7	17.1	14	
	12	-22.0	-22.0	-19.9	-16.2	-13.3	-.7	4.7	9.2	12.1	13.7	13.6	14.5	14.6	15.0	14.9	16.3	16.6	16.5	17.6	17.6	17.1	12	
	10	-20.4	-20.4	-20.4	-17.2	-14.2	-1.6	3.8	8.3	11.2	12.9	12.8	13.8	13.8	14.2	14.2	15.7	16.0	16.0	17.2	17.2	16.7	10	
	8	-18.5	-18.5	-18.5	-18.5	-15.5	-2.9	2.5	7.1	10.0	11.7	11.6	12.6	12.7	13.1	13.1	14.7	15.0	15.0	16.3	16.3	15.9	8	
	6	-16.0	-16.0	-16.0	-16.0	-16.0	-4.8	.7	5.3	8.2	9.9	9.8	10.8	10.9	11.4	11.4	13.0	13.4	13.4	14.7	14.8	14.4	6	
	4	-12.5	-12.5	-12.5	-12.5	-12.5	-7.6	-2.1	2.5	5.4	7.1	7.0	8.0	8.1	8.6	8.7	10.3	10.7	10.7	12.1	12.2	11.8	4	
	2	-10.0	-10.0	-10.0	-10.0	-10.0	-10.0	-7.5	-2.9	.1	1.8	1.7	2.7	2.8	3.3	3.4	5.0	5.4	5.5	6.8	7.0	6.7	2	
	0	-10.0	-10.0	-10.0	-10.0	-10.0	-10.0	-10.0	-10.0	-10.0	-10.0	-10.0	-10.0	-10.0	-10.0	-10.0	-10.0	-10.0	-10.0	-10.0	-10.0	-10.0	0	
		2	3	4	5	6	7	8	9	10	11	12	13	14	15	18	20	22	24	26	28	30		

FREQUENCY IN MEGAHERTZ

ANTENNA EFFICIENCY

0.0	0.0	0.0	0.0	0.0	0.0	0.0	0.0	0.0	0.0	0.0	0.0	0.0	0.0	0.0	0.0	0.0	0.0	0.0	0.0	0.0
2	3	4	5	6	7	8	9	10	11	12	13	14	15	18	20	22	24	26	28	30

FREQUENCY IN MEGAHERTZ

Table 47. General Purpose Subroutines for the Antenna Calculations

SUBROUTINE	FUNCTION
SETCOM	To assure that all common blocks are the correct length
AERIAL	To process antenna INPUT data
GETANT	To generate an antenna pattern
OUTANT	To put an antenna pattern on an output file
GAIN	Main antenna gain subroutine
FRESNL	To calculate the Fresnel reflection factors
ANTAB	To read an antenna pattern from an input file
GRDLOS	To calculate the ground loss (needed by the prediction program)
ANTWAV	To adjust the nulls in the antenna pattern
VEFF	To calculate the efficiency of a vertical monopole
CISI	To calculate the sine and cosine integrals
RWIRE	To calculate the radiation resistance of a bent wire
RVDPOL	To calculate the radiation resistance of a dipole

Table 48. Antenna Subroutines

INPUT NO.	SUBROUTINE	ANTENNA	INPUT TABLE	THEORY SECTION	EQUATIONS
1	HRHOM	Horizontal Rhombic	6	6	196
2	VMON	Vertical Monopole	7	4	66 to 69
3	HDPOL	Horizontal Dipole	8	5	122
4	HYAGI	Horizontal Yagi	9	5	129, 130
5	VDPOL	Vertical Dipole	10	5	127
6	HCURT	Horizontal Curtain	11	5	131 to 134
7	SLPVEE	Sloping Vee	12	6	174 to 186
8	INVTL	Inverted L	13	4	96 to 103
9	SLPRHM	Sloping Rhombic	14	6	191 to 195
10	INLRH	Interlaced Rhombic	15	6	196 to 198
11	SLPWIR	Sloping Wire (unterminated)	16	4	77 to 83
12	ISOTRP	Isotropic Antenna	17	7.1	210 to 212
13	HLPD	Horizontal Log Periodic Dipole Array	18	5	146 to 157
14	TDPOLE	Tilted Dipole	19	5	113 to 121
15	VHRHOM	Vertical Half Rhombic	20	6	206 to 209
16	HDRHOM	Horizontal Double Rhombic	21	6	199 to 203
17	VMGS	Vertical Monopole with Ground Screen	22	4	--
18	ANTIN	Antenna Read in From an Input File	23	-	--
19	VLPM	Log Periodic Array of Vertical Monopoles	24	4	--
20	TERWIR	Sloping Wire (terminated)	25	6	171 to 173
22	VLPV	Log Periodic Array of Vertical Dipoles	26	5	158 to 163
23	STVLPD	Stacked Array of Vertical LPA's	27, 28	5	164 to 167
25	EFLOOP	Array of Vertical Loops	29	7.2	--

FORM **NTIA-29**
(4-80)

U.S. DEPARTMENT OF COMMERCE
NAT'L. TELECOMMUNICATIONS AND INFORMATION ADMINISTRATION

BIBLIOGRAPHIC DATA SHEET

	1. PUBLICATION NO.	2. Gov't Accession No.	3. Recipient's Accession No.
	NTIA Report 83-136		

4. TITLE AND SUBTITLE

Computation of Linear Communication Antennas

5. Publication Date

October 1983

6. Performing Organization Code

DoC/NTIA

7. AUTHOR(S)

John L. Lloyd

8. PERFORMING ORGANIZATION NAME AND ADDRESS

U.S. Department of Commerce
National Telecommunications and Information Admin.
Institute for Telecommunication Sciences
Boulder, Colorado 80303

9. Project/Task/Work Unit No.

10. Contract/Grant No.

11. Sponsoring Organization Name and Address

Commander
USA/CEEIA
ATTN: CCC-CED-PED
Ft. Huachuca, Arizona 85613

12. Type of Report and Period Covered

13.

14. SUPPLEMENTARY NOTES

15. ABSTRACT *(A 200-word or less factual summary of most significant information. If document includes a significant bibliography or literature survey, mention it here.)*

This report contains a consolidation of practical engineering equations for linear communication antennas suitable for use in the prediction and analysis of the system performance of high frequency communication equipment. The theoretical background and the nature of the approximations are discussed. Complete equations are provided. Examples of the computations are given for each type of antenna.

16. Key Words *(Alphabetical order, separated by semicolons)*

17. AVAILABILITY STATEMENT	18. Security Class. *(This report)*	20. Number of pages
☒ UNLIMITED.	Unclassified	
	19. Security Class. *(This page)*	**21. Price:**
☐ FOR OFFICIAL DISTRIBUTION.	Unclassified	

☆U.S. Government Printing Office: 1980—678-495/529